

Type II Topoisomerases: Repurposing Old Enzymes for New Drugs

By

Jessica Anne Collins

Dissertation

Submitted to the Faculty of the  
Graduate School of Vanderbilt University  
in partial fulfillment of the requirements

for the degree of

DOCTOR OF PHILOSOPHY

in

Biochemistry

May 10, 2024

Nashville, Tennessee

Approved:

James Dewar, Ph.D.

Martin Egli, Ph.D.

Emily Hodges, Ph.D.

Katherine Friedman, Ph.D.

Neil Osheroff, Ph.D.

Copyright © 2024 Jessica Anne Collins  
All Rights Reserved

In loving memory of my grandmother, Margaret Anne Roberts, who filled my mind with curiosity,  
my days with creativity, and my cup with coffee.

## ACKNOWLEDGMENTS

As I prepare to take my final bow under the academic “big top,” I am filled with gratitude for the accomplished performers who have made this circus of a Ph.D. journey possible.

First and foremost, I extend my deepest appreciation to the Ringmaster Extraordinaire, Dr. Neil Osheroff. His expert guidance and mentorship have not only directed the show but also kept the lions (also known as graduate students) well-fed. Thank you for instilling a deep sense of curiosity and passion for scientific inquiry in me. Your dedication to my growth and development as a scholar has been unwavering, and I am endlessly grateful for your patience, encouragement, and belief in me, especially when my confidence faltered.

Thank you to my dissertation committee, the Circus Fortune Tellers. Each member of the committee has contributed a unique perspective to my research. Your insightful feedback and encouragement have provided unparalleled clarity and foresight to guide my doctoral journey.

A heartfelt thank you to Jo Ann Byl, the Circus Juggler, a scientific mentor, and dear friend. Your unrelenting support and guidance have been a safety net, ensuring that I always landed on my feet.

To my fellow Circus Performers – Alexandria, Esha, Jeffrey, Soziema, Jill, Samika, and Chelsea – your camaraderie and collaboration have transformed the laboratory into a vibrant community, filled with laughter, learning, and loads of Jeni’s ice cream.

I am so grateful for my friends, the Circus Acrobats, who have filled my stomach with belly-laughs and my days with unforgettable memories. You have lifted my spirits and provided a welcome respite from the rigors of research. Thank you for choosing to take a front row seat in this journey with me. I hope you brought popcorn.

I owe an immeasurable debt of gratitude to my parents, the Circus Contortionists, who have displayed enormous flexibility to support me throughout my Ph.D. performance, no matter the twists and bends along the way. From the earliest days of my academic pursuits to the culmination of this doctoral journey, you have been my greatest cheerleaders. Your sacrifices,

guidance, and unconditional love have laid the foundation for my success, and for that, I am eternally grateful.

And to Skyler, my Circus Clown, your boundless love and unflappable reassurance have kept me balanced and focused as I walk the tightrope of academia. You have infused every step of this journey with positivity, enthusiasm, and a sense of adventure. No matter the number of plates to spin or fiery hoops to jump through, I know I can overcome any obstacle with you by my side. I love you!

Together, you have all made this circus of a dissertation journey a spectacle to behold, and for that, I am forever grateful.

Above all else, I thank God for his generous blessings. Before I even stepped foot in Nashville, you orchestrated a beautiful plan for my life at Vanderbilt and in this city. Thank you for guiding me every step, moment, and breath of my Ph.D. journey. Your holiness and wonder have been my constant companion, and I am thoroughly humbled by Your kindness, faithfulness, and blessings. In my deepest failures, your grace has been revealed all the more. I pray that this degree will honor you and reveal your heavenly kingdom on earth.

## TABLE OF CONTENTS

	Page
LIST OF FIGURES.....	x
LIST OF ABBREVIATIONS/NOMENCLATURE .....	xiv
I. INTRODUCTION.....	1
DNA Topology.....	1
Topoisomerases .....	3
Type II Topoisomerases .....	5
<i>Structure</i> .....	5
<i>Catalytic cycle</i> .....	8
<i>Human type II topoisomerases</i> .....	10
<i>Bacterial type II topoisomerases</i> .....	11
Type II Topoisomerases as Drug Targets .....	14
<i>Anticancer therapies</i> .....	17
<i>Antibacterial drugs</i> .....	22
Target-Mediated Fluoroquinolone Resistance.....	26
<i>Fluoroquinolone targeting</i> .....	27
<i>Interactions with gyrase and topoisomerase IV through a water-metal ion bridge</i> .....	28
<i>Clinical impact of fluoroquinolone resistance</i> .....	31
Overcoming Fluoroquinolone Resistance .....	32
<i>Novel bacterial topoisomerase inhibitors, M. tuberculosis gyrase inhibitors, and triazaacenaphthylenes</i> .....	33
<i>Spiropyrimidinetriones</i> .....	37
Scope of the Dissertation .....	40
II. METHODS .....	43
Materials.....	43

<i>DNA substrates</i> .....	43
<i>Drugs, preclinical compounds, and chemicals</i> .....	43
Human Type II Topoisomerases .....	44
<i>Enzymes</i> .....	44
<i>Topoisomerase II-mediated DNA cleavage</i> .....	44
<i>Persistence of topoisomerase II-DNA cleavage complexes</i> .....	45
<i>Topoisomerase II-mediated DNA ligation</i> .....	46
Bacterial Type II Topoisomerases.....	47
<i>Enzymes</i> .....	47
<i>Gyrase-catalyzed DNA supercoiling</i> .....	48
<i>Topoisomerase IV-catalyzed DNA decatenation</i> .....	49
<i>Gyrase/topoisomerase IV-mediated DNA cleavage</i> .....	49
<i>Persistence of gyrase/topoisomerase IV-cleaved DNA complexes</i> .....	51
<i>Gyrase/topoisomerase IV-mediated DNA ligation</i> .....	52
III. 1,2-NAPHTHOQUINONE AS A POISON OF HUMAN TYPE II TOPOISOMERASES.....	53
Introduction.....	53
Results .....	56
<i>1,2-Naphthoquinone is a poison of human type II topoisomerases</i> .....	56
<i>Effects of ATP on the enhancement of double-stranded DNA cleavage induced by 1,2 naphthoquinone</i> .....	62
<i>1,2-Naphthoquinone is a covalent poison of human topoisomerase II<math>\alpha</math></i> .....	65
<i>1,2-Naphthoquinone displays characteristics of a covalent poison against human topoisomerase II<math>\beta</math></i> .....	67
Discussion .....	71
IV. TARGET-MEDIATED FLUOROQUINOLONE RESISTANCE IN <i>NEISSERIA GONORROHEAE</i> : ACTIONS OF CIPROFLOXACIN AGAINST GYRASE AND TOPOISOMERASE IV .....	74
Introduction.....	74
Results and Discussion .....	75

	<i>Gyrase-mediated fluoroquinolone resistance</i> .....	75
	<i>Use of the water-metal ion bridge to promote fluoroquinolone interactions in N. gonorrhoeae gyrase.</i> .....	81
	<i>Topoisomerase IV-mediated fluoroquinolone resistance</i> .....	85
V.	ACTIONS OF A NOVEL BACTERIAL TOPOISOMERASE INHIBITOR AGAINST <i>NEISSERIA GONORRHOEAE</i> GYRASE AND TOPOISOMERASE IV: ENHANCEMENT OF DOUBLE-STRANDED DNA BREAKS .....	90
	Introduction.....	90
	Results .....	91
	<i>OSUAB-185 induces double-stranded DNA cleavage mediated by N. gonorrhoeae topoisomerase IV</i> .....	91
	<i>Stability of single- and double-stranded DNA breaks induced by OSUAB-185</i> ...	99
	<i>Effects of OSUAB-185 on fluoroquinolone-resistant N. gonorrhoeae gyrase and topoisomerase IV</i> .....	102
	<i>Effects of OSUAB-185 on gyrase and topoisomerase IV from E. coli and S. aureus</i> .....	102
	<i>Effects of OSUAB-185 on human topoisomerase II<math>\alpha</math></i> .....	105
	Discussion .....	105
VI.	ACTIONS OF SPIROPYRIMIDINTRIONES AGAINST <i>NEISSERIA GONORRHOEAE</i> TYPE II TOPOISOMERASES .....	109
	Introduction.....	109
	<i>Effects of SPTs on the catalytic and DNA cleavage activities of N. gonorrhoeae gyrase and topoisomerase IV</i> .....	110
	<i>Stability of double-stranded DNA breaks induced by zoliflodacin</i> .....	113
	<i>Activities of zoliflodacin against fluoroquinolone-resistant N. gonorrhoeae gyrase</i> .....	116
	<i>Effects of SPTs on gyrase and topoisomerase IV from B. anthracis and E. coli</i>	119
VII.	CONCLUSIONS AND IMPLICATIONS .....	121
	Overcoming Fluoroquinolone Resistance .....	121



Future Studies .....	126
REFERENCES.....	129

## LIST OF FIGURES

	Page
Figure 1.1. DNA topology. ....	2
Figure 1.2. DNA topoisomerases and topology. ....	4
Figure 1.3. Domain structure of type II topoisomerases. ....	7
Figure 1.4. Catalytic cycle of type II topoisomerases. ....	9
Figure 1.5. Topological problems resolved by gyrase and topoisomerase IV during DNA replication and transcription. ....	13
Figure 1.6. Cellular death induced by type II topoisomerase-targeted drugs. ....	15
Figure 1.7. Anticancer and cardioprotective therapies targeted by human topoisomerase II $\alpha$ and II $\beta$ . ....	18
Figure 1.8. Structures of bacterial type II topoisomerase inhibitors. ....	23
Figure 1.9. Structures of fluoroquinolone gyrase/topoisomerase IV poisons. ....	25
Figure 1.10. Schematic of the water-metal ion bridge that mediates interactions between fluoroquinolones and bacterial type II topoisomerases. ....	30
Figure 1.11. Novel bacterial topoisomerase inhibitors (NBTI), <i>M. tuberculosis</i> gyrase inhibitor (MGI), and triazaacenaphthylene structures. ....	34
Figure 1.12. Spiropyrimidinetrione (SPT) structures. ....	38
Figure 3.1. Naphthoquinones. ....	54
Figure 3.2. 1,2-Naphthoquinone and 1,4-naphthoquinone enhance DNA cleavage mediated by human topoisomerase II $\alpha$ and II $\beta$ . ....	57
Figure 3.3. Effects of naphthoquinone derivatives on DNA cleavage mediated by human type II topoisomerases. ....	58
Figure 3.4. DNA cleavage induced by 1,2-naphthoquinone is mediated by human topoisomerase II $\alpha$ and II $\beta$ . ....	60
Figure 3.5. Establishment of DNA cleavage/ligation equilibria induced by 1,2-naphthoquinone with human topoisomerase II $\alpha$ or II $\beta$ . ....	61

Figure 3.6. Effects of ATP on the enhancement of double-stranded DNA cleavage induced by 1,2-naphthoquinone with human topoisomerase II $\alpha$ or II $\beta$ .	63
Figure 3.7. Effects of sulfhydryl and reducing agents on topoisomerase II $\alpha$ -mediated double-stranded DNA cleavage induced by 1,2-naphthoquinone.	66
Figure 3.8. Effects of 1,2-naphthoquinone on the persistence and ligation of DNA cleavage complexes generated by human topoisomerase II $\alpha$ .	68
Figure 3.9. 1,2-Naphthoquinone inactivates human topoisomerase II $\alpha$ when incubated with the enzyme prior to the addition of DNA.	69
Figure 3.10. 1,2-Naphthoquinone induces minimal DNA cleavage mediated by the catalytic core of human topoisomerase II $\alpha$ .	70
Figure 3.11. Effects of sulfhydryl and reducing agents on topoisomerase II $\beta$ -mediated double-stranded DNA cleavage induced by 1,2-naphthoquinone.	72
Figure 4.1. Schematic of the water-metal ion bridge that mediates interactions between ciprofloxacin and <i>N. gonorrhoeae</i> gyrase and topoisomerase IV.	77
Figure 4.2. Effects of ciprofloxacin on DNA supercoiling catalyzed by WT and mutant <i>N. gonorrhoeae</i> gyrase.	78
Figure 4.3. Effects of ciprofloxacin on DNA cleavage mediated by WT and mutant <i>N. gonorrhoeae</i> gyrase.	80
Figure 4.4. Effects of 8-methyl-2,4-quinazolinedione on the DNA supercoiling activities of GyrA <sup>S91F/D95G</sup> <i>N. gonorrhoeae</i> gyrase.	82
Figure 4.5. Effects of 8-methyl-2,4-quinazolinedione on the DNA cleavage activities of WT and GyrA <sup>S91F/D95G</sup> gyrase.	84
Figure 4.6. Effects of ciprofloxacin on the DNA decatenation activities of WT and mutant <i>N. gonorrhoeae</i> topoisomerase IV.	86
Figure 4.7. Effects of ciprofloxacin on the DNA cleavage activities of WT and mutant <i>N. gonorrhoeae</i> topoisomerase IV.	87
Figure 5.1. OSUAB-185 enhances DNA cleavage mediated by <i>N. gonorrhoeae</i> gyrase and topoisomerase IV.	92
Figure 5.2. DNA cleavage induced by OSUAB-185 is mediated by <i>N. gonorrhoeae</i> gyrase and topoisomerase IV.	94

Figure 5.3. Time courses for DNA cleavage mediated by <i>N. gonorrhoeae</i> gyrase and topoisomerase IV.....	96
Figure 5.4. Ratios of NBTI-induced single-stranded to double-stranded DNA cleavage mediated by <i>N. gonorrhoeae</i> topoisomerase IV are maintained over OSUAB-185 concentrations and reaction time.....	97
Figure 5.5. OSUAB-185 suppresses levels of double-stranded DNA cleavage mediated by <i>N. gonorrhoeae</i> gyrase and increases levels of double-stranded DNA breaks generated by topoisomerase IV.....	98
Figure 5.6. OSUAB-185 induces stable DNA cleavage complexes with <i>N. gonorrhoeae</i> gyrase and topoisomerase IV.....	100
Figure 5.7. OSUAB-185 inhibits DNA ligation mediated by <i>N. gonorrhoeae</i> gyrase and topoisomerase IV.....	101
Figure 5.8. Activity of OSUAB-185 against <i>N. gonorrhoeae</i> gyrase and topoisomerase IV that contain fluoroquinolone-resistance mutations.....	103
Figure 5.9. OSUAB-185 induces double-stranded DNA breaks mediated by gyrase and topoisomerase IV from <i>E. coli</i> and <i>S. aureus</i> .....	104
Figure 5.10. Effects of OSUAB-185 on DNA cleavage mediated by human topoisomerase II $\alpha$ . .....	106
Figure 6.1. Effects of zoliflodacin and H3D-005722 on DNA supercoiling and DNA decatenation catalyzed by <i>N. gonorrhoeae</i> gyrase and topoisomerase IV, respectively.....	111
Figure 6.2. Effects of zoliflodacin and H3D-005722 on DNA scission mediated by <i>N. gonorrhoeae</i> gyrase and topoisomerase IV.....	112
Figure 6.3. Effects of zoliflodacin on the persistence of DNA cleavage complexes formed by <i>N. gonorrhoeae</i> gyrase and topoisomerase IV. ....	114
Figure 6.4. Effects of zoliflodacin on DNA religation mediated by <i>N. gonorrhoeae</i> gyrase and topoisomerase IV.....	115
Figure 6.5. Effects of zoliflodacin on DNA supercoiling catalyzed by WT and fluoroquinolone-resistant <i>N. gonorrhoeae</i> gyrase.....	117
Figure 6.6. Effects of zoliflodacin on DNA cleavage mediated by WT and fluoroquinolone-resistant <i>N. gonorrhoeae</i> gyrase. ....	118

Figure 6.7. Effects of zoliflodacin on single-stranded and double-stranded DNA scission mediated by gyrase and topoisomerase IV from *N. gonorrhoeae*, *E. coli*, and *B. anthracis*..... 120

## LIST OF ABBREVIATIONS/NOMENCLATURE

(-)SC	negatively supercoiled
(+)SC	positively supercoiled
ADP	adenosine diphosphate
AML	acute myeloid leukemia
APL	acute promyelocytic leukemia
Asp	aspartic acid
ATP	adenosine triphosphate
BSA	bovine serum albumin
CDC	Centers for Disease Control and Prevention
DMSO	dimethyl sulfoxide
DNA	deoxyribonucleic acid
DS	double-stranded
DTT	dithiothreitol
E	glutamate
EDTA	ethylenediaminetetraacetic acid
F	phenylalanine
FDA	Food and Drug Administration
G	glycine
GHKL	gyrase, hsp90, histidine kinase, mutL
Glu	glutamic acid
hTII $\alpha$	human topoisomerase II $\alpha$
hTII $\beta$	human topoisomerase II $\beta$
Lin	linear
MGI	<i>Mycobacterium tuberculosis</i> gyrase inhibitor
MLL	mixed lineage leukemia
N	asparagine
NBTI	novel bacterial topoisomerase inhibitor
Nick	nicked
PML	promyelocytic leukemia
RARA	retinoic acid receptor $\alpha$
Relax	relaxed
SDS	sodium dodecyl sulfate
Ser	serine
SPT	spiropyrimidinetrione
SS	single-stranded
TOPRIM	topoisomerase-primase
WHD	winged-helix domain
WHO	World Health Organization
WT	wild-type
Y	tyrosine

# CHAPTER I

## INTRODUCTION

Parts of this chapter are adapted with permission from my co-author Neil Osheroff and the publisher *ACS Infect. Dis.* 2024, in press. Copyright 2024 Jessica A. Collins and Neil Osheroff.

### DNA Topology

In the time it takes you to read this sentence, your body will have finished growing ~8 million new cells.<sup>1</sup> Each one of those cells contains roughly 2 meters (6.56 feet) of DNA stretched end-to-end.<sup>2</sup> Considering the human body is made up of ~32 trillion cells, ~192 trillion feet or 36.3 billion miles of DNA are stored inside of it.<sup>3</sup> If laid end-to-end, this DNA could stretch from the sun and back 397 times. Astonishingly, all of the DNA in a cell not only fits inside a nucleus 5-10  $\mu\text{M}$  in diameter but also remains accessible for essential cellular processes.<sup>2</sup>

In human cells, DNA is linear and separated into 46 chromosomes.<sup>4</sup> Despite its linear structure, the DNA ends are not free. Rather, they are fixed in space due to the extraordinary length of DNA, its degree of compaction, and its attachment to scaffolding proteins.<sup>5-9</sup> Likewise, most bacteria possess circular chromosomes that prevent DNA ends from freely rotating during helix opening processes.<sup>5-9</sup> Therefore, DNA is considered a closed topological system, and the topological properties of DNA cannot be altered without breaking one or both strands of the double helix.<sup>5, 7, 9</sup> Because DNA is contained in a plectonemically coiled double helix and its ends are fixed in space, cells must overcome both torsional and axial topological barriers in order to replicate and survive.<sup>5-14</sup>

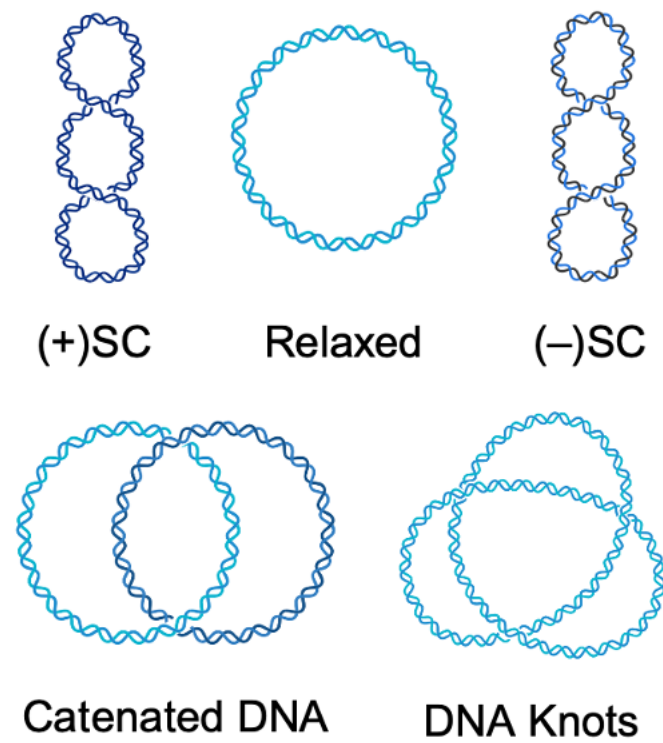


**Figure 1.1. DNA topology.**

In the absence of torsional stress, DNA is considered to be “relaxed” (top middle). Overwinding and underwinding of the double helix drives positive [(+)SC, top left] and negative [(-)SC, top right] DNA supercoiling, respectively. Entanglements between two or more DNA molecules or within a single DNA molecule yield catenated (bottom left) or knotted (bottom right) DNA molecules, respectively. Created with biorender.com.



Torsional stress on the double helix can be problematic for cells. This stress manifests as DNA over- and underwinding and plays a fundamental role in genome maintenance.<sup>9, 15, 16</sup> DNA without torsional stress is known as relaxed, whereas DNA under torsional stress is referred to as supercoiled (Figure 1.1).<sup>5, 7, 9, 15-17</sup> Supercoiling occurs when topological stress drives over- or underwound DNA molecules to wrap around themselves, generating superhelical twists. These superhelical twists create positive (overwound) and negative (underwound) DNA supercoils.<sup>9, 15, 16, 18</sup> In eubacteria and eukaryotes, DNA is globally underwound by ~6%.<sup>19, 20</sup> Negative supercoiling adds energy to the double helix, lowering the threshold for strand melting during DNA replication and transcription.<sup>8, 20-23</sup> Consequently, DNA underwinding facilitates these critical cellular processes. In contrast, the movement of replication forks and transcription complexes along the DNA locally overwinds the genetic material ahead of these complexes.<sup>8, 20-23</sup> Because overwinding makes it more difficult to pull the DNA strands apart, these essential cellular processes are stymied.<sup>8, 20-23</sup> The fixed ends of the DNA pose an additional topological problem for cells. Tangles (formed between two or more DNA molecules) and knots (formed within a single DNA molecule) can arise in the double helix during DNA replication and recombination, respectively.<sup>8, 22, 24</sup> DNA tangles (also referred to as catenanes) can obstruct daughter chromosome separation during cell division.<sup>25, 26</sup> Similarly, if DNA knots are not resolved, they can impede the separation of the double helix and reduce the tensile strength of the genetic material.<sup>26, 27</sup> Persistent knots and tangles threaten cellular survival.

### **Topoisomerases**

To manage the complex topological relationships in DNA, cells express multiple enzymes known as topoisomerases. These ubiquitous enzymes open the topological system by generating transient breaks in the sugar-phosphate backbone of DNA.<sup>20, 28, 29</sup> This strand breakage activity is required for the regulation of superhelical density and the resolution of DNA knots and tangles by topoisomerases (Figure 1.2).<sup>20, 28, 29</sup>

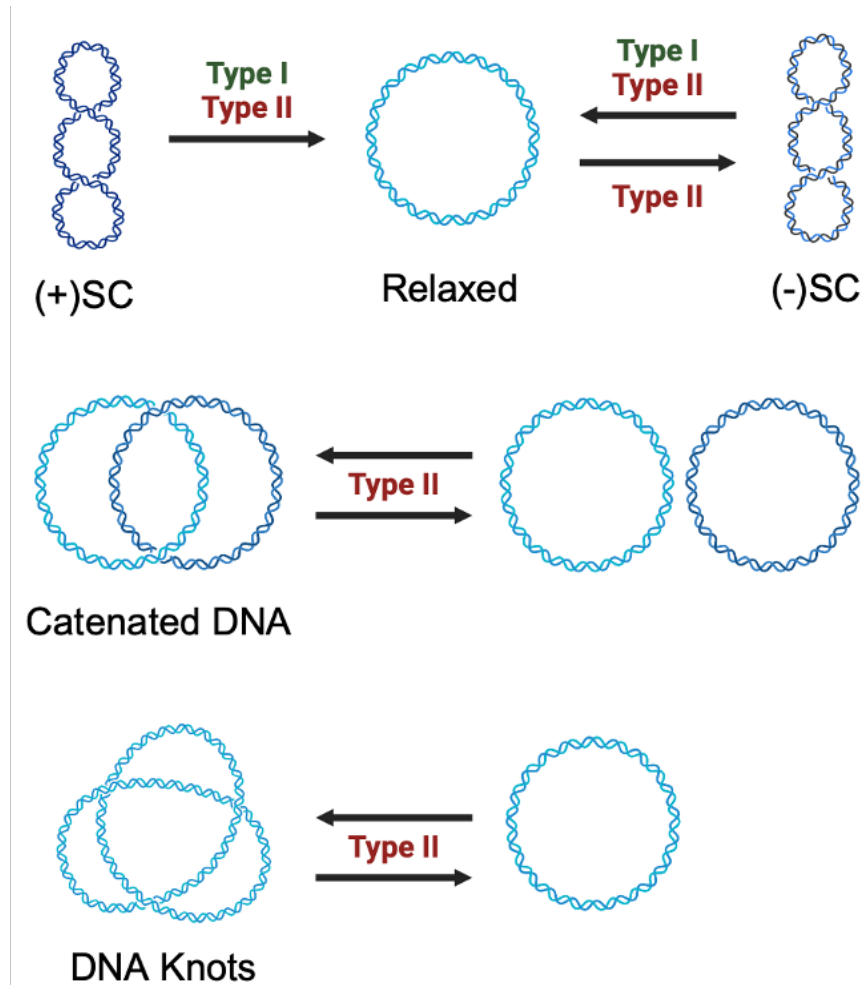


**Figure 1.2. DNA topoisomerases and topology.**

Bacterial and eukaryotic type I and type II topoisomerases can relax positively [(+)SC] and negatively supercoiled [(-)SC] DNA (top). However, only a single type II enzyme, bacterial gyrase, can introduce negative supercoils into relaxed DNA. Type II topoisomerases cleave both strands of the double helix in order to perform the strand passage activities necessary to relax supercoils and resolve intermolecular tangles (catenanes, middle) and knots (bottom). Created with biorender.com.

Topoisomerases are categorized as type I and type II, numbered according to the order in which they were discovered.<sup>30</sup> The first topoisomerase, topoisomerase I (originally identified as the  $\omega$  protein), was discovered in *Escherichia coli* by James C. Wang in 1971.<sup>31</sup> Five years later, Martin Gellert identified the first type II topoisomerase, DNA gyrase, in *E. coli*.<sup>32</sup> Coincidentally, naming the enzymes by order of discovery also coincided with the number of DNA strands cleaved by the enzyme during catalysis: type I topoisomerases cut one DNA strand, while type II topoisomerases cut two DNA strands.<sup>20, 28-30, 33</sup>

In human cells, type I topoisomerases primarily relax negatively and positively supercoiled DNA molecules.<sup>20, 28, 29</sup> However, there is some evidence that type I enzymes can decatenate hemicatenated sister chromatids prior to replication fork convergence.<sup>34, 35</sup> Conversely, type II topoisomerases primarily control levels of DNA supercoiling and remove tangles and knots from the genome.<sup>20, 28, 29</sup>

### **Type II Topoisomerases**

There are two subclasses of type II topoisomerases, type IIA and type IIB. The bacterial type II topoisomerases, gyrase and topoisomerase IV, and eukaryotic type II topoisomerase comprise the type IIA subclass. Type IIB enzymes include topoisomerase VI and topoisomerase VIII, which are primarily found in archaea, plants, and algae.<sup>20, 28-30</sup> This dissertation will focus on type IIA topoisomerases from humans and bacteria.

#### *Structure*

Human type II topoisomerases are homodimers, while bacterial type II topoisomerases are heterotetramers with an A<sub>2</sub>B<sub>2</sub> structure.<sup>36-38</sup> The eukaryotic enzymes are homologous to their bacterial counterparts, and possess a single polypeptide arising from the fusion of the A and B bacterial subunits.<sup>28, 29, 39</sup> In gyrase, these subunits are GyrA and GyrB.<sup>36</sup> The analogous subunits

in topoisomerase IV are ParC and ParE in Gram-negative species (originally named because of chromosomal partitioning defects that accompany mutations in these subunits) and GrIA and GrIB in Gram-positive species (named as “gyrase-like” proteins).<sup>37, 40</sup> For the sake of simplicity, the GyrA/ParC/GrIA subunit will be referred to as the A subunit, and the GyrB/ParE/GrIB subunit will be referred to as the B subunit.

Human and bacterial type II topoisomerases share several structural domains within three regions of the enzyme (Figure 1.3). Using gyrase as a model, the N-terminus is in GyrB, the catalytic core spans GyrA and GyrB, and the C-terminus is in GyrA.<sup>20, 29</sup>

The N-terminal region contains an N-terminal gate, or N-gate, a GHKL (Gyrase, Hsp90, Histidine Kinase, MutL) ATPase domain, and a transducer domain.<sup>20, 29, 38, 41-44</sup> DNA first enters the enzyme through the N-gate.<sup>41, 45, 46</sup> Upon ATP binding, the two ATPase domains dimerize and close the N-gate.<sup>41, 43</sup> The transducer domain relays information between the catalytic core and ATPase domains to facilitate DNA-stimulated ATP hydrolysis.<sup>42, 43, 47</sup>

The catalytic core is composed of two DNA-interaction domains, the WHD (winged-helix domain) and tower domain, and a metal-ion binding domain, the TOPRIM (topoisomerase/primase) domain.<sup>20, 29, 48-51</sup> The WHD mediates DNA binding and contains an active site tyrosine residue required for DNA cleavage.<sup>49-51</sup> The tower domain promotes DNA bending and uses a conserved isoleucine residue to induce a ~150° curve in the genetic material.<sup>49-52</sup> The WHD and tower domain form a DNA gate that undergoes large conformational changes during DNA cleavage and strand passage.<sup>38, 51, 53</sup> The TOPRIM domain chelates divalent metal ions, magnesium (Mg<sup>2+</sup>) *in vivo*, that anchor the DNA and stabilize the cleavage/ligation transition state.<sup>48, 49, 54-56</sup>

The type II topoisomerase C-terminus displays significant variation between species.<sup>20, 29, 57, 58</sup> In gyrase, the C-terminal domain contains a conserved seven-amino acid “GyrA box” motif. The GyrA box facilitates DNA wrapping in a positive supercoil that is inverted upon strand passage.<sup>58-61</sup> Even though topoisomerase IV and human type II enzymes lacks this structural

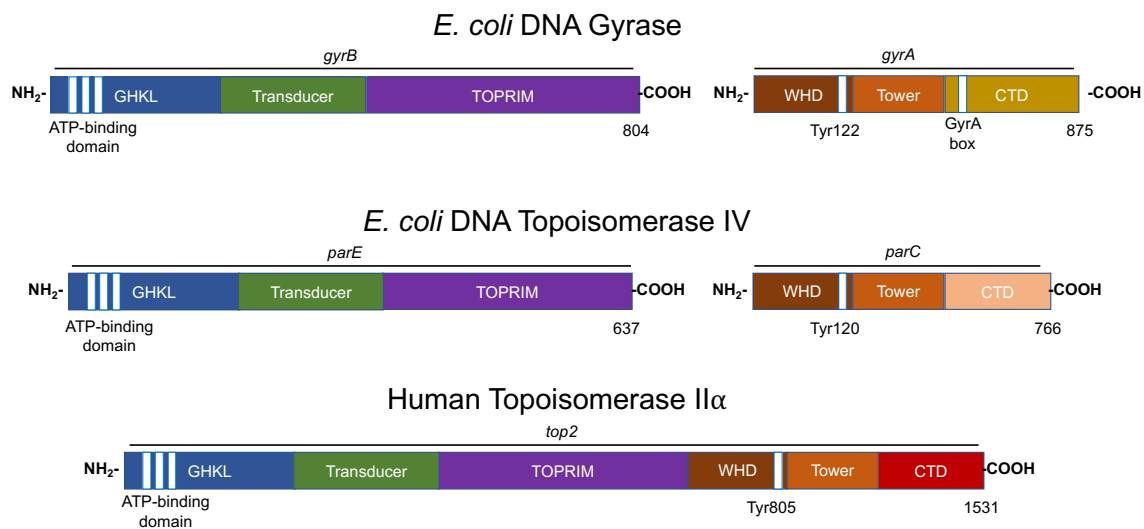


**Figure 1.3. Domain structure of type II topoisomerases.**

The domain structures of bacterial (DNA gyrase and topoisomerase IV) and human type II topoisomerases (topoisomerase II $\alpha$ ) are shown. Homologous regions of the enzymes are indicated by color. The N-terminus contains an N-gate comprised of an ATPase domain (GKHL, blue) and a transducer element (green). The enzyme core carries a divalent metal ion binding site (TOPRIM, purple) and the active site tyrosine residue required for DNA scission (brown). The C-terminus varies between species. For DNA gyrase, the C-terminal domain (CTD, gold) contains a “GyrA box” essential for DNA wrapping, which the CTD of topoisomerase IV (peach) lacks. Furthermore, the CTD of human topoisomerase II $\alpha$  contains nuclear localization signals and phosphorylation sites (red). Created with biorender.com.

element, their C-terminal regions contain basic amino acid residues that facilitate DNA binding and bending.<sup>59-61</sup> Even though the C-terminus of eukaryotic topoisomerase II is intrinsically disordered in the absence of DNA, this region features nuclear localization sequences and post-translational modification sites. It also plays an important role in recognizing DNA supercoil handedness during catalysis.<sup>20, 62-64</sup>

### *Catalytic cycle*

As mentioned previously, type II topoisomerases catalyze a double-stranded DNA passage reaction to regulate the topological state of the genetic material.<sup>9, 20, 28, 29</sup> This reaction can be divided into a number of discrete steps (Figure 1.4). (1) The enzymes bind their DNA substrate(s).<sup>52, 65-69</sup> The first double helix bound at the DNA gate becomes the G-segment. The T-segment is then captured by the N-gate.<sup>43, 52, 69-72</sup> (2) The enzymes select their site of DNA cleavage by their ability to bend the G-segment.<sup>52, 55, 73-75</sup> DNAs that cannot be bent by the enzyme are not cleaved. The ability of type II enzymes to bend DNA does not reflect the intrinsic malleability of the DNA segment, rather it is due to specific interactions between the enzyme and the G-segment.<sup>52, 55, 73, 75</sup> (3) The active site tyrosine residue located in the catalytic core initiates a nucleophilic attack on the opposite strands of the double-helix, resulting in a covalent bond between the 4'-hydroxyl group of the tyrosine and the newly created 5'-terminal phosphate of the DNA backbone.<sup>49, 50, 52, 55, 76</sup> The scissile bonds on the Watson and Crick strands are across the major groove from one another and the cleavage reaction generates 4-base, 5' overhanging cohesive ends.<sup>38, 49, 51, 52, 55, 76</sup> This covalent enzyme-cleaved DNA complex is known as the cleavage complex.<sup>20, 77</sup> The cleavage complex plays two critical roles: It preserves the energy of the DNA sugar-phosphate backbone and preserves genomic integrity while the DNA is cleaved.<sup>9, 38, 55, 78, 79</sup> The enzymes utilize a non-canonical two metal ion mechanism to support the DNA cleavage reaction.<sup>49, 56, 80, 81</sup> As opposed to the canonical two metal ion mechanism, in this

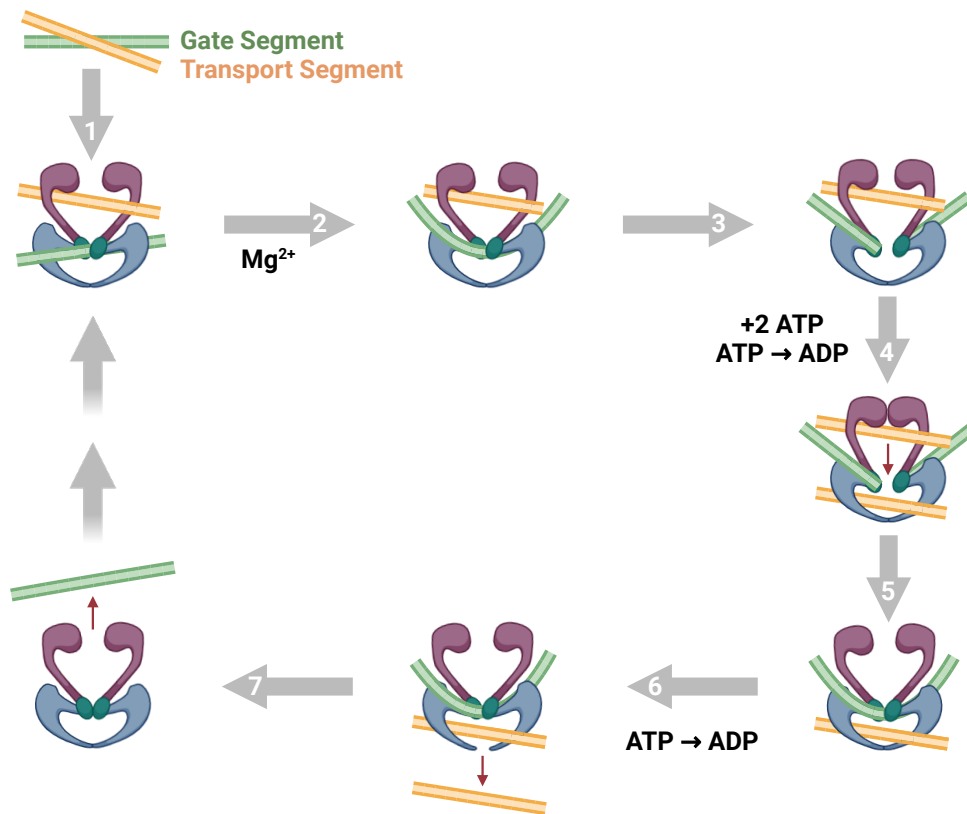


**Figure 1.4. Catalytic cycle of type II topoisomerases.**

The double-stranded DNA passage reaction of type II topoisomerases can be separated into discrete steps: (1) capturing two segments of DNA through the N-gate, the gate, or G-segment (green), and the transport, or T-segment (yellow); (2) bending the G-segment to assess DNA sites for cleavability; (3) cleaving both strands of the G-segment; (4) binding 2 molecules of ATP, which triggers N-gate dimerization, DNA gate opening, and T-segment strand passage through the DNA gate. The rate of the DNA passage step is increased if one of the two ATP molecules is hydrolyzed; (5) closing the DNA gate and religating the G-segment; (6) hydrolyzing the second ATP molecule and releasing the T-segment through the C-gate; (7) initiating enzyme turnover. Created with biorender.com.

scheme, one metal ion stabilizes the transition state and promotes DNA cleavage and religation, while the other metal ion anchors the DNA.<sup>49</sup> (4) Upon ATP binding, the DNA gate formed by cleavage of the G-segment opens, the N-terminal portions of the ATPase domain dimerize, and the T-segment is passed through the open gate.<sup>46, 51, 72, 82-84</sup> The rate of the DNA passage step is increased if one of the two ATP molecules is hydrolyzed.<sup>85</sup> (5) The DNA cleavage reaction is reversed, the covalent bond between the enzyme and the DNA is broken, and the double helix is religated.<sup>51, 82</sup> (6) The second ATP molecule is hydrolyzed,<sup>86</sup> leading to extrusion of the T-segment<sup>51</sup> and (7) enzyme turnover.<sup>87</sup>

### *Human type II topoisomerases*

The first eukaryotic type II topoisomerase, topoisomerase II, was discovered in 1980 and purified from *Saccharomyces cerevisiae* and *Drosophila melanogaster* shortly thereafter.<sup>88-92</sup> Single-celled yeast, insects, and other lower eukaryotes encode a single topoisomerase II enzyme, while vertebrates express two isoforms of topoisomerase II,  $\alpha$  and  $\beta$ .<sup>30, 93</sup> In humans, topoisomerase II $\alpha$  and II $\beta$  are encoded on separate chromosomes (17q21-22 and 3p24, respectively) and possess different molecular masses (170 kDa and 180 kDa, respectively), yet they share ~70% sequence identity.<sup>28, 30, 94-98</sup> Although both isoforms can relax positive and negative supercoils and resolve DNA knots and tangles, their cellular roles and expression patterns vary considerably.<sup>98-102</sup>

Topoisomerase II $\alpha$  is an essential enzyme that plays an important role in DNA replication, chromosome compaction, and genome segregation.<sup>28, 29, 100, 101</sup> Expression of topoisomerase II $\alpha$  is cell cycle dependent; enzyme levels rise in mid-S phase, peak in G2/M phase, and fall upon cell division.<sup>38, 101, 103, 104</sup> The expression of this isoform is inextricably linked to its cellular role. During DNA replication, topoisomerase II $\alpha$  relaxes supercoils, disentangles newly replicated DNA duplexes (precatenanes), and facilitates fork convergence during termination.<sup>100, 105-107</sup> The  $\alpha$



isoform is required for chromosome condensation but its activity is regulated to maintain sister chromatid cohesion.<sup>108-110</sup> During anaphase, topoisomerase II $\alpha$  separates remaining interlinked sister chromosomes, though most DNA tangles are removed during replication.<sup>26, 88, 100, 101, 111</sup> This enzyme also plays a role in transcription.<sup>101, 112, 113</sup>

While topoisomerase II $\beta$  is non-essential at the cellular level, it serves key functions in development and transcription.<sup>98, 114-116</sup> In contrast to topoisomerase II $\alpha$ , the  $\beta$  isoform is expressed throughout the cell cycle and in all cell types, irrespective of proliferation status.<sup>98, 99, 102, 117</sup> Topoisomerase II $\beta$  is required for neuronal differentiation and cortical development in mice.<sup>98, 117-122</sup> In humans, expression of the  $\beta$  isoform is highest in the cerebellum and mutations in this enzyme are associated with autism spectrum disorder, neurodevelopmental delays, and B cell immunodeficiency.<sup>98, 101, 123-125</sup> Although its cellular functions are not well defined, the  $\beta$  isoform is also involved in the transcription of hormonally activated and developmentally regulated genes.<sup>98, 101, 112, 115, 126-128</sup>

### *Bacterial type II topoisomerases*

Gyrase was discovered in 1976 and was the first type II topoisomerase to be described.<sup>32</sup> The enzyme was identified by its activity to convert relaxed closed-circular DNA to negatively supercoiled (i.e., underwound) molecules.<sup>32</sup> Gyrase is found in all bacterial species and is essential for life.<sup>30</sup> For 14 years, gyrase was believed to be the only type II topoisomerase in bacterial cells. However, in 1990, the genes encoding a second type II topoisomerase, topoisomerase IV, were identified from a genetic screen for mutations that impeded chromosome partitioning in *Escherichia coli*.<sup>37</sup> On the basis of sequencing and enzymology studies, topoisomerase IV was determined to be a homolog of gyrase that utilized a similar reaction mechanism (detailed below).<sup>37, 129</sup>

Most bacterial species encode topoisomerase IV in addition to gyrase, and in those species, both enzymes are essential.<sup>30</sup> In contrast, some species such as *Mycobacterium tuberculosis*, *Helicobacter pylori*, and *Treponema pallidum* (the causative agents of tuberculosis, stomach ulcers, and syphilis, respectively) encode only gyrase.<sup>61, 130-133</sup> It appears that in these species, gyrase has also taken over the critical biological functions of topoisomerase IV.<sup>61, 133</sup>

Although the catalytic cycles of gyrase and topoisomerase IV are identical, the two enzymes differ in one critical aspect of their DNA interactions. Gyrase wraps its DNA substrate around the C-terminal domain of its A subunit to form a positive supercoil that is converted to a negative supercoil following strand passage (Figure 1.5).<sup>44, 58, 59, 134</sup> This wrapping mechanism has two major biological effects: 1) the preferred T- and G-segments come from the same DNA molecule and are in close proximity (i.e. within 100-150 base pairs of one another).<sup>65, 135-137</sup> As a consequence of this intramolecular DNA reaction, gyrase primarily modulates the superhelical state of the bacterial chromosome;<sup>61, 138</sup> 2) the handedness of DNA wrapping necessitates that gyrase acts in a unidirectional manner, removing positive supercoils and introducing negative supercoils into relaxed DNA (i.e., DNA that lacks torsional stress).<sup>28, 58, 61, 139</sup>

In contrast to gyrase, the C-terminal domain of topoisomerase IV interacts with DNA but does not wrap the double helix (Figure 1.5).<sup>59-61</sup> The lack of wrapping allows the enzyme to capture T- and G-segments from distal regions of the bacterial chromosome or even from entirely different chromosomes.<sup>61, 68</sup> This enzymatic characteristic has two important biological consequences: 1) topoisomerase IV can carry out strand passage reactions involving intermolecular DNA substrates (i.e., it can unlink tangled chromosomes);<sup>11, 37, 61, 140-142</sup> 2) intramolecular reactions that are performed by the enzyme are driven by the directionality of torsional stress, converting either under- or over-wound DNA substrates into products with less torsional stress.<sup>20, 139, 143, 144</sup>

The differences in the way that gyrase and topoisomerase IV interact with DNA have a profound effect on the biological functions of these two enzymes. Because of its DNA wrapping mechanism, gyrase primarily works ahead of DNA tracking systems, including replication forks

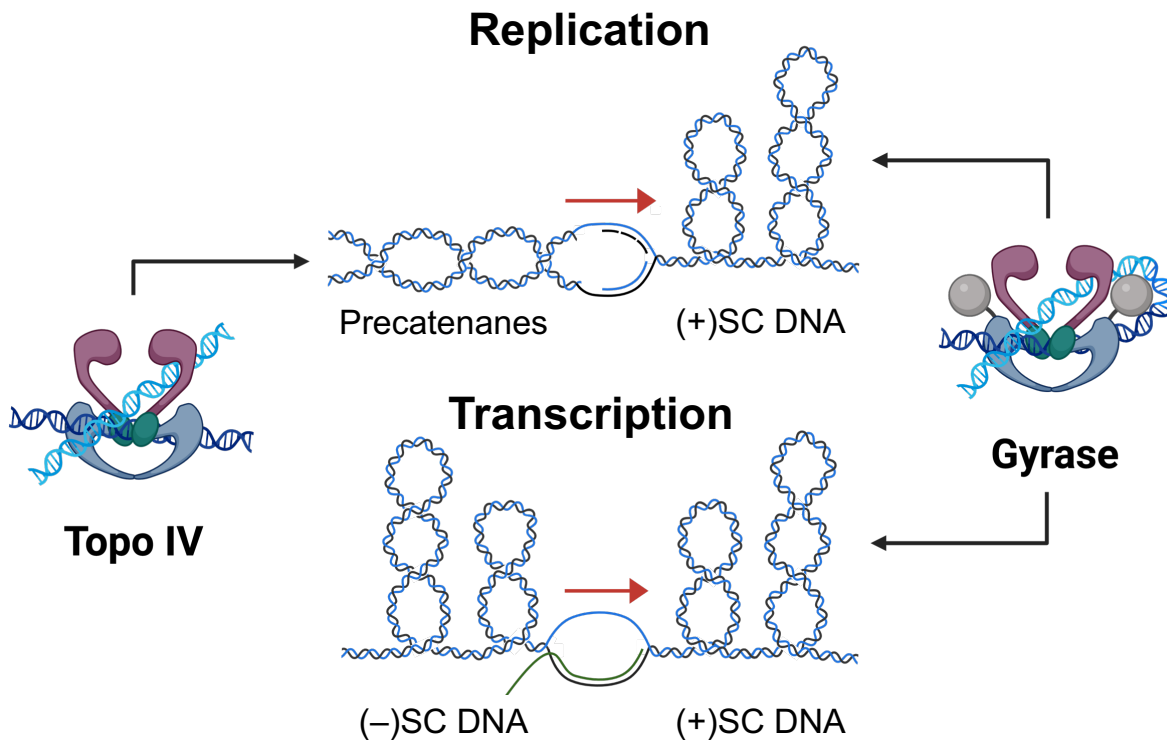


**Figure 1.5. Topological problems resolved by gyrase and topoisomerase IV during DNA replication and transcription.**

The movement of replication forks and transcription complexes along the double helix generates torsional stress ahead of and behind these systems. The positive supercoils [(+)SC] formed in front of DNA tracking machineries pose a physical barrier to progressing complexes. Gyrase (right) uses a DNA wrapping mechanism to rapidly remove these positive supercoils. The precatenanes (two intertwined partially replicated DNA duplexes) that trail replication complexes and are untangled by topoisomerase IV using a canonical strand passage mechanism prior to cell division. The negative supercoils that accumulate behind transcription complexes are most likely removed by the  $\omega$  protein, a type I topoisomerase. Created with biorender.com.

and transcription complexes, to rapidly remove positive supercoils that accumulate as a result of helicases opening the double helix (Figure 1.5).<sup>9, 61, 134, 138, 145</sup> The enzyme also works in conjunction with the  $\omega$  protein (a type I topoisomerase that relaxes negative DNA supercoils), acting as a “supercoiling thermostat” to set the global level of DNA underwinding in the bacterial chromosome.<sup>138, 146-148</sup>

Similar to gyrase, topoisomerase IV can also affect the superhelical state of the bacterial chromosome.<sup>20, 138, 139, 143, 144, 149</sup> While this enzyme can relax negative supercoils formed behind transcription complexes (Figure 1.5), its cellular functions generally involve its interactions with distal portions of the bacterial genome.<sup>61, 68, 138</sup> Topoisomerase IV primarily resolves precatenanes that form behind replication forks (Figure 1.5), unlinks daughter chromosomes during cell division, and removes knots that are formed during recombination events.<sup>11, 140-142, 150</sup>

### **Type II Topoisomerases as Drug Targets**

All eukaryotic and prokaryotic cells encode at least one type II topoisomerase that regulates DNA topology.<sup>20, 28, 29, 79</sup> The type II enzymes are essential for cell viability, and cleavage complexes are held in a critical balance that vastly favors ligation (Figure 1.6). Under normal conditions, enzyme-cut DNA complexes are transient and readily reversible to protect genomic integrity.<sup>20, 29, 77, 101, 104, 151</sup> Perturbation of this delicate balance can be deleterious to cells.

Shortly after their discovery, type II topoisomerases emerged as a valuable target for the development of human medicines. Inhibiting or harnessing the power of these DNA-cleaving topology modulators has resulted in the successful clinical development of numerous anticancer and antibacterial therapies. Drugs that target human and bacterial type II topoisomerases kill cells in two different ways.<sup>77, 79, 151-153</sup>

First, drugs can reduce levels of DNA cleavage by inhibiting the overall catalytic function of human and bacterial type II topoisomerases, which robs the cell of critical enzymatic activities.<sup>77, 151-156</sup> Reduced DNA cleavage and, subsequently, strand passage leads to the

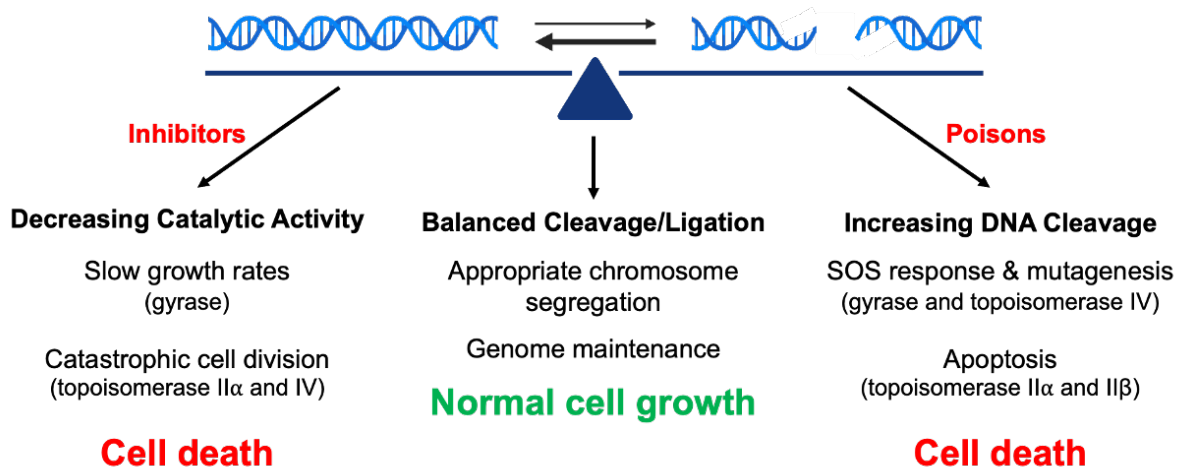


**Figure 1.6. Cellular death induced by type II topoisomerase-targeted drugs.**

Under normal cellular conditions, DNA cleavage complexes generated by type II topoisomerases are short-lived and readily reversible, leading to normal cellular growth (middle). However, topoisomerase poisons and inhibitors shift the balance between DNA cleavage and ligation. Topoisomerase poisons increase levels of enzyme-mediated DNA breaks by stabilizing cleavage complexes. In response to the DNA damage, human and bacterial cells initiate apoptosis or the SOS response, respectively (right). Conversely, topoisomerase inhibitors prevent the type II enzymes from completing their catalytic cycles. This robs the cell of essential enzyme functions. Inhibition of gyrase can stall DNA replication and transcription, which impedes bacterial growth, while inhibition of topoisomerase II $\alpha$  or topoisomerase IV can lead to catastrophic cell division and death. Created with biorender.com.

accumulation of positive supercoils ahead of DNA tracking systems (see Figure 1.5) and profoundly affects ability of cells to synthesize DNA and RNA (Figure 1.6).<sup>77, 151-153, 155, 156</sup> Behind replication machineries and transcription complexes, inhibition of the type II enzymes prevents the untangling of daughter chromosomes (see Figure 1.5), leading to stalled or catastrophic division (Figure 1.6).<sup>77, 151-158</sup> Drugs that act by inhibiting type II topoisomerase catalysis (without increasing levels of DNA scission) are referred to as catalytic inhibitors.<sup>152-156</sup>

Second, drugs can stabilize DNA strand breaks generated as requisite intermediates of the type II topoisomerase catalytic cycle.<sup>77, 155, 156, 159-162</sup> When the accrual of these strand breaks becomes too high, they can induce apoptosis (human cells) or the SOS response (bacterial cells) to trigger cell death pathways (Figure 1.6)<sup>77, 101, 155, 156, 163, 164</sup> Therefore, drugs that stabilize type II topoisomerase-DNA cleavage complexes have the potential to convert these critical enzymes into potent cellular toxins that fragment the genome.<sup>77, 165</sup> Anticancer and antibacterial drugs that act by increasing levels of gyrase/topoisomerase IV-mediated DNA scission are referred to as topoisomerase poisons.<sup>77, 78, 151-156</sup>

Two aspects of topoisomerase poisons require further discussion. Because DNA strand breaks generated by human and bacterial type II topoisomerases are covalently tethered to the enzymes, they can be ligated once the drug has dissociated from the enzyme-DNA complex.<sup>77, 81, 154, 155, 166, 167</sup> However, these stabilized cleavage complexes become more lethal when cellular machines such as replication and transcription complexes attempt to traverse the covalently attached enzymes.<sup>155, 156, 159-161, 164, 168</sup> As these machines approach the cleavage complexes, they often render (by a poorly understood process) the cut DNA non-ligatable by the type II enzymes.<sup>155, 159, 162, 166</sup> This results in persistent DNA breaks that must be resolved by DNA recombination processes and can lead to mutations, chromosomal abnormalities, and if unrepaired, cell death.<sup>155, 156, 162, 165, 169-171</sup>

Furthermore, beyond the formation of DNA breaks, the presence of covalently bound enzymes on the double helix creates roadblocks that inhibit DNA tracking by replication forks and

transcription complexes.<sup>156, 159, 161, 172, 173</sup> Thus, cleavage complexes block essential genomic processes, such as replication and transcription.<sup>155, 156, 159, 160, 164, 168, 172, 173</sup> Finally, because topoisomerase poisons stall the catalytic cycle of type II topoisomerases, they also inhibit the DNA strand passage activities of these essential enzymes. Consequently, in addition to converting type II enzymes into potentially lethal cellular toxins, topoisomerase poisons deprive human and bacterial cells of important enzymatic and genomic functions.<sup>77, 151, 154-156, 162</sup>

### *Anticancer therapies*

Before type II topoisomerases were discovered, therapies targeting the type II enzymes were used, albeit unknowingly, to treat a myriad of cancers.<sup>151, 152, 174-177</sup> Currently, eight topoisomerase II-targeted anticancer drugs are approved for clinical use in the United States, the majority of which are topoisomerase poisons (Figure 1.7).<sup>177, 178</sup> Clinically developed chemotherapies that target the type II enzymes include demethylepipodophyllotoxins (etoposide and teniposide), anthracyclines (daunorubicin, doxorubicin, epirubicin, and idarubicin), anthracenediones (mitoxantrone), and bisdioxopiperazines (dexrazoxane).<sup>77, 176-178</sup> Anthracyclines and demethylepipodophyllotoxins are effective against solid tumors in breast, ovarian, testicular, lung, and brain tissues as well as blood and bone cancers, including leukemia and lymphoma.<sup>152, 176-178</sup> Anthracenediones are used to treat acute myeloid leukemia and multiple sclerosis,<sup>176-180</sup> while bisdioxopiperazines are prescribed to protect against anthracycline-induced cardiotoxicities.<sup>177, 181-186</sup>

Demethylepipodophyllotoxins, anthracyclines, and anthracenediones are classified as interfacial topoisomerase II poisons.<sup>77, 151, 175</sup> As their name suggests, these drugs bind at the enzyme-DNA interface and intercalate into the double helix at the cut scissile bond (one drug molecule per DNA strand).<sup>77, 175, 187</sup> When bound in the cleavage complex, interfacial poisons act

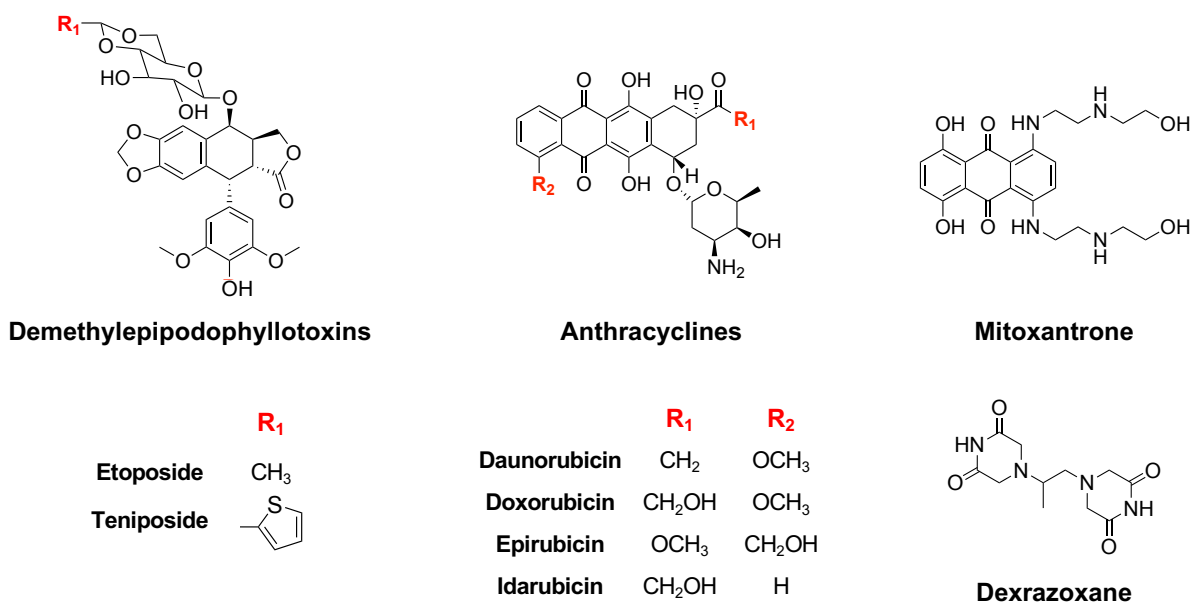


**Figure 1.7. Anticancer and cardioprotective therapies targeted by human topoisomerase II $\alpha$  and II $\beta$ .**

Four classes of human type II topoisomerase-targeted therapies are approved for clinical use in the United States. Demethylepipodophyllotoxins (etoposide and teniposide), anthracyclines (daunorubicin, doxorubicin, epirubicin, and idarubicin), and mitoxantrone are topoisomerase poisons and are used to treat a variety of solid and blood cancers in children and adults. Dexrazoxane is an inhibitor of topoisomerase II that is prescribed to protect against anthracycline-induced cardiomyopathies.



as a “molecular doorstep” to physically block religation of the cleaved DNA and increase levels of DNA scission.<sup>77, 175, 187</sup> All marketed poisons target both human topoisomerase II $\alpha$  and II $\beta$ , albeit some drugs exert stronger effects on one isoform than the other.<sup>77, 175, 178, 188-191</sup>

It is important to note that early topoisomerase II-targeted anticancer therapies were developed and approved for clinical use before their intracellular mechanism of action was defined.<sup>174, 177, 192</sup> The demethylepipodophyllotoxin etoposide is a well-characterized example.<sup>151, 152, 174, 176, 192</sup> The parent compound podophyllotoxin was isolated from the American mandrake, also known as the Himalayan mayapple, which has been used in traditional medicines for centuries.<sup>193, 194</sup> However, it was not until the 1940s that the anticancer activities of podophyllotoxin and its derivatives were evaluated.<sup>192, 195, 196</sup> Subsequent structural optimization to improve antineoplastic activity and reduce toxicity yielded etoposide in 1966 and teniposide in 1967, both of which advanced to human trials.<sup>193, 197, 198</sup> Etoposide was approved by the Food and Drug Administration (FDA) for the treatment of testicular tumors in 1983, only three years after the first eukaryotic type II topoisomerase was discovered.<sup>192</sup> Similarly, the anthracyclines doxorubicin and daunorubicin were isolated from *Streptomyces* soil bacteria in the 1960s and approved for clinical use in 1974 and 1979, respectively.<sup>193, 199-202</sup>

Shortly after the clinical introduction of demethylepipodophyllotoxins and anthracyclines, the oncogenic side effects of topoisomerase II poisons were revealed.<sup>174, 176, 177, 192</sup> As many as 15% of patients previously treated with topoisomerase II-targeted drugs developed therapy-related acute myeloid leukemia (AML), which is characterized by rearrangements in the mixed lineage leukemia (*MLL*) gene at chromosomal band 11q23.<sup>101, 176, 203-206</sup> A current model posits that therapy-related AMLs arise from the erroneous repair of topoisomerase II-mediated chromosomal breaks in a 1-kb breakpoint cluster region (BCR) of the *MLL* gene.<sup>101, 176, 206-208</sup> The illegitimate DNA repair results in translocations and gene fusions that disrupt hematopoiesis and drive oncogenesis.<sup>101, 176, 206, 208-210</sup>

Additional studies indicate that the etiology of therapy-related leukemia is drug specific.<sup>101, 176, 206</sup> For example, treatment of breast cancer and multiple sclerosis by epirubicin and mitoxantrone, respectively, has been shown to correlate with acute promyelocytic leukemia (APL).<sup>211-213</sup> These two therapies give rise to balanced translocations between the promyelocytic leukemia (*PML*) gene on chromosome 15 and the retinoic acid receptor  $\alpha$  (*RARA*) gene on chromosome 17.<sup>176, 212-216</sup> In APL patients, these breakpoints cluster to an 8 bp region of an established mitoxantrone-induced topoisomerase II DNA cleavage site.<sup>215, 212, 213</sup> Even though epirubicin-induced DNA cleavage sites are more dispersed than those induced by mitoxantrone, chromosomal fusions that result in therapy-related APLs are functionally linked to topoisomerase II activity.<sup>176, 206, 211</sup>

As mentioned above, the most clinically relevant topoisomerase II poisons target both human topoisomerase II $\alpha$  and II $\beta$ , but the selectivity of drug targeting to either isoform and the individual roles of  $\alpha$  and  $\beta$  in drug efficacy are not fully understood.<sup>151, 152, 174-177</sup> Some evidence suggests that the  $\alpha$  isoform primarily mediates the antineoplastic activities of topoisomerase poisons, while the  $\beta$  isoform is the major contributor to therapy-related leukemogenic translocations and other cell-type specific side effects.<sup>174, 176, 217-219</sup> Multiple groups have shown that topoisomerase II $\beta$  contributes to etoposide-induced DNA breaks at the *MLL* locus.<sup>207, 208, 220, 221</sup> However, the most recent study also linked topoisomerase II $\alpha$  to etoposide-induced chromosomal breaks at this locus and concludes that the relative abundance of each isoform determines its contribution to oncogenic fusions.<sup>221</sup> In cultured leukemia cell lines, protein levels of  $\alpha$  and  $\beta$  are comparable.<sup>222</sup> However, in primary human haemopoietic stem cells, levels of topoisomerase II $\beta$  mRNA were found to be more than 10-fold higher than those of topoisomerase II $\alpha$ .<sup>206, 223</sup> Other deleterious side effects of topoisomerase II poisons, such as anthracycline-associated cardiotoxicities, have also been attributed to the activity of the  $\beta$  isoform.<sup>116, 186, 207, 224</sup> To this point, deletion of topoisomerase II $\beta$  from murine cardiomyocytes protects against doxorubicin-associated cardiomyopathies by preventing enzyme-mediated DNA breaks and

maintaining mitochondrial homeostasis.<sup>181</sup> To mitigate the clastogenic and cardiotoxic properties of topoisomerase poisons, drug development efforts have focused on selectively targeting topoisomerase II $\alpha$ .<sup>225, 226</sup> Three preclinical compounds with such activity have emerged: NK314, ARN-21934, and most recently, a 7-(3-aminopropoxy)-substituted flavone analogue.<sup>190, 191, 227</sup>

Although most type II topoisomerase-targeted therapies are poisons, catalytic inhibitors of topoisomerase II also have clinical utility.<sup>183-186</sup> Members of the bisdioxopiperazine class, such as dexrazoxane (ICRF-187) and ICRF-193, are examples.<sup>174, 177</sup> Topoisomerase II inhibitors block the enzymes from completing their catalytic cycles without enhancing levels of DNA scission.<sup>77, 174, 177</sup> Bisdioxopiperazines bind to a closed-clamp form of the topoisomerase II-DNA complex at a site distinct from that of ATP.<sup>224, 228, 229</sup> These interactions allow hydrolysis of one ATP molecule but preclude hydrolysis of the second high energy cofactor.<sup>230</sup> Because the enzyme cannot hydrolyze the second high-energy cofactor, the DNA cannot be released, and the enzyme is inactivated.<sup>224, 228-230</sup>

Dexrazoxane is the only topoisomerase II inhibitor in clinical use and is approved for the prevention of cardiomyopathies in patients treated with anthracyclines.<sup>183-186</sup> In pediatric clinical trials, dexrazoxane has been shown to reduce the risk of treatment-related cardiotoxicities and is not associated with the development of secondary leukemias.<sup>231, 232</sup> However, the mechanism of dexrazoxane cardioprotectivity is debated.<sup>233</sup> Two models have been proposed: 1) As a derivative of EDTA, dexrazoxane chelates mitochondrial iron in cardiac tissues to reduce the accumulation of reactive oxygen species in the cell;<sup>234-236</sup> 2) dexrazoxane inhibition of topoisomerase II $\beta$  in cardiomyocytes prevents the formation of drug-stabilized cleavage complexes,<sup>182, 229, 237, 238</sup> which are converted to double-stranded DNA breaks upon proteasomal processing.<sup>126, 239</sup> It is important to note that dexrazoxane is a potent inhibitor of both human type II enzymes but expression of the  $\alpha$  isoform is generally undetectable in non-dividing cardiac cells.<sup>102, 240</sup> Mounting biochemical, cellular, and clinical evidence supports the latter model.<sup>182, 186, 229, 237, 238</sup>

## *Antibacterial drugs*

The first class of bacterial type II topoisomerase-targeted drugs used clinically were the aminocoumarins (Figure 1.8).<sup>151, 153, 241</sup> As with many human type II topoisomerase-targeted drugs, members of this drug class were prescribed to patients before their molecular target was identified.<sup>241, 242</sup> The founding members of the aminocoumarin class are naturally-occurring antibiotics isolated from *Streptomyces* soil bacteria in the 1950s and include novobiocin, coumermycin A<sub>1</sub>, and clorobiocin.<sup>241, 243-246</sup> In 1965, novobiocin was approved for the treatment of *S. aureus* infections, including methicillin-resistant strains.<sup>151, 247, 248</sup> However, just shy of 50 years later, this aminocoumarin was withdrawn by the FDA due to safety and efficacy concerns.<sup>151, 248</sup>

The aminocoumarins are catalytic inhibitors of gyrase and topoisomerase IV.<sup>241, 249-251</sup> Members of this class were initially described as inhibitors of gyrase-catalyzed supercoiling, but this attribution was later clarified, ascribing their bactericidal effects to the competitive inhibition of ATP binding.<sup>36, 242, 249, 252</sup> Numerous structural studies have also described the interactions between the aminocoumarins and the B subunit of the bacterial type II topoisomerases.<sup>250, 253-256</sup> Together, these studies have revealed that the classic aminocoumarins, such as novobiocin, bind to the N-terminal domain of the enzyme at a site that overlaps the ATP-binding site.<sup>250, 253-256</sup> Furthermore, mutations that confer resistance to aminocoumarins reduce the affinity of drug binding.<sup>252, 257, 258</sup> Alterations that diminish drug binding also lower ATP affinity, such that the type II enzymes are unable to carry out their strand passage activities at the same rate, if at all. In either case, bacterial cells die due to slowed bacterial growth and/or catastrophic cell division.<sup>154-158, 242, 249</sup>

Since novobiocin was removed from the market in 2011, no other members of the aminocoumarin class have been approved for human medicine, nor have any other gyrase/topoisomerase IV inhibitors progressed beyond clinical trials.<sup>153, 248, 252</sup> However, efforts to develop bacterial type II topoisomerase inhibitors clinically have persisted.<sup>248</sup> Simocyclinone D8

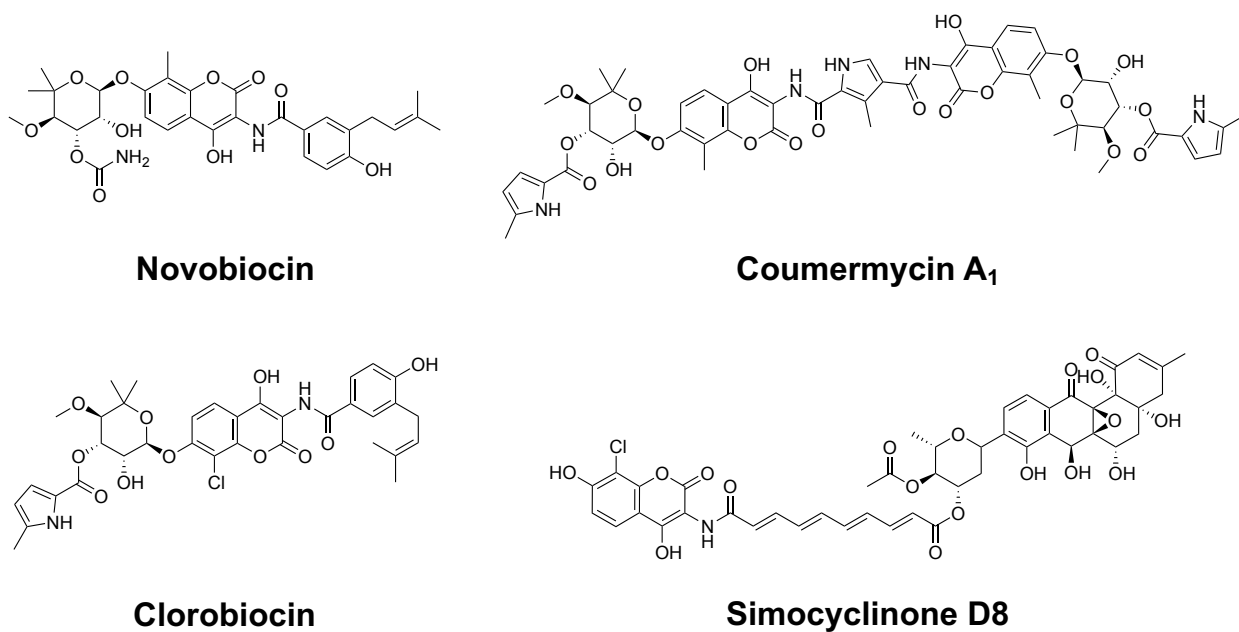


**Figure 1.8. Structures of bacterial type II topoisomerase inhibitors.**

Novobiocin, clorobiocin, and coumermycin A1 are the original members of the aminocoumarin class of gyrase/topoisomerase inhibitors. Novobiocin was the first and only aminocoumarin approved to treat bacterial infections, but it was removed from the market in 2011 due to issues with safety and efficacy. Simocyclinone D8 is a newer bacterial type II inhibitor that uses a different mechanism of action than the three classic aminocoumarins.

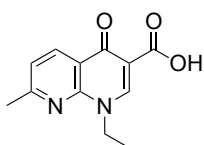
is an established example.<sup>259</sup> This naturally-derived antibiotic binds to the A subunit of gyrase/topoisomerase IV and blocks G-segment DNA binding using a novel mechanism of antibiotic action.<sup>260-263</sup> Due to poor bacterial membrane penetration, this compound is not a viable candidate for antibacterial development.<sup>263</sup> However, knowledge gained from studies on simocyclinone D8 can be used to guide the design and innovation of future anti-infectives.

In contrast to the limited use of gyrase/topoisomerase IV-targeted catalytic inhibitors, the bacterial type II topoisomerases are also the targets of the widely-prescribed fluoroquinolone class of antibacterials.<sup>151, 153-156</sup> Members of this class include drugs such as ciprofloxacin, moxifloxacin, and levofloxacin.<sup>264</sup> Fluoroquinolones are one of the most successful classes of antibacterials introduced into the clinic due to their high oral bioavailability, good tissue distribution, and broad-spectrum activity against Gram-negative, Gram-positive, and atypical (with regard to Gram staining) pathogens.<sup>264-268</sup> This class of antibacterials has been listed by the World Health Organization (WHO) as one of their five “highest priority” critically important antimicrobials for treatments of infections in humans.<sup>267</sup>

Fluoroquinolones are gyrase/topoisomerase IV poisons. Like other topoisomerase poisons, these drugs have two major effects on enzyme activity. First, they enhance levels of gyrase/topoisomerase IV-generated double-stranded DNA breaks by inserting between the 3'- and 5'-termini of the DNA in the cut scissile bonds.<sup>55, 154-156, 167, 266</sup> Bound drugs act as “molecular doorstops” that form a physical barrier to enzyme-mediated DNA ligation.<sup>154-156, 166, 167, 266</sup> Second, because fluoroquinolones stall the catalytic cycle at the DNA cleavage/ligation step, they inhibit the overall catalytic activity of gyrase and topoisomerase IV.<sup>154-156, 158, 167, 266</sup> Either of these drug actions can disrupt cellular functions and lead to bacterial death.<sup>163</sup>

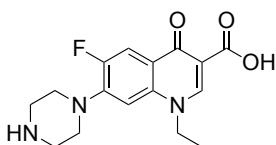
The founding member of the quinolone family, nalidixic acid, was synthesized in 1962 and introduced in the clinic for the treatment of urinary tract infections in 1964 (Figure 1.9).<sup>155, 269-271</sup>

### 1<sup>st</sup> Generation

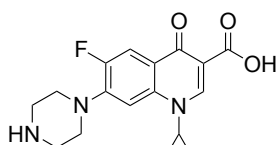


Nalidixic acid

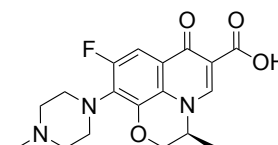
### 2<sup>nd</sup> Generation



Norfloxacin

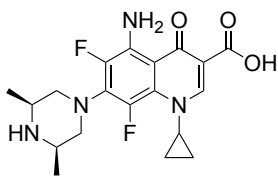


Ciprofloxacin



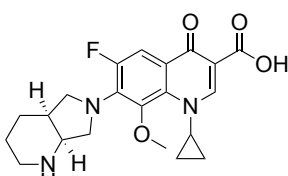
Levofloxacin

### 3<sup>rd</sup> Generation

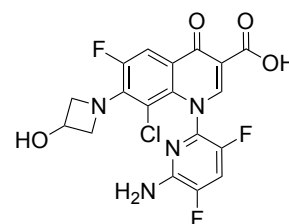


Sparfloxacin

### 4<sup>th</sup> Generation



Moxifloxacin



Delafloxacin

**Figure 1.9. Structures of fluoroquinolone gyrase/topoisomerase IV poisons.**

Nalidixic acid is a first-generation quinolone and founding member of the drug class. It was approved to treat urinary tract infections but was removed from the clinic due to poor pharmacodynamics. The addition of a fluorine atom at the C6 position spurred a new wave of fluoroquinolone drug development. The second-generation drugs, including norfloxacin, ciprofloxacin, and levofloxacin, had better pharmacodynamics and pharmacokinetics than their quinolone precursors and displayed activity against Gram-positive and Gram-negative pathogens. Subsequent third- (sparfloxacin) and fourth-generation (moxifloxacin and delafloxacin) drugs further improved pharmacokinetics/pharmacodynamics and extended antibacterial coverage to atypical bacteria (such as *M. tuberculosis*).

Unfortunately, due to low efficacy and poor tissue distribution, the early quinolones were dropped from clinical use.<sup>264</sup> The critical change that brought quinolones back into clinical relevance was the introduction of a fluorine at the C6 position. The resulting “fluoroquinolones” displayed higher potency and superior pharmacokinetics compared with their quinolone precursors.<sup>155, 156, 264</sup> The first clinically-relevant fluoroquinolone, norfloxacin, was approved for human use in the 1980s.<sup>272, 273</sup> However, due to low serum levels and poor tissue distribution, its therapeutic range was limited to urinary tract infections and some sexually transmitted diseases.<sup>273, 274</sup>

The fluoroquinolone class rose to general medical prominence with the introduction of ciprofloxacin, which was the first family member to display significant activity outside of the urinary tract.<sup>264, 275, 276</sup> Ultimately, due to its high activity against Gram-negative and some Gram-positive infections along with its improved tissue penetration, ciprofloxacin was for many years the most broad-spectrum and efficacious oral antibacterial in clinical use.<sup>155, 264, 275, 276</sup>

Subsequent generations of fluoroquinolones improved pharmacokinetics and extended antibacterial coverage.<sup>155, 264, 276</sup> Examples include levofloxacin and sparfloxacin with expanded coverage against some Gram-positive microbes, such as *Staphylococcus aureus* and *Streptococcus pneumoniae*, respectively, and moxifloxacin with substantial activity against atypical Gram-staining bacteria, such as *M. tuberculosis*.<sup>155, 264, 277</sup> New fluoroquinolones are still being developed. For example, the newest member of this drug class, delafloxacin, was approved for clinical use in 2017.<sup>278</sup> This drug is an anionic fluoroquinolone that is effective against acute skin and skin structure bacterial infections and community-acquired pneumonia.<sup>278</sup>

### **Target-Mediated Fluoroquinolone Resistance**

Bacterial cells that evade fluoroquinolone toxicity do so by one of three resistance mechanisms: 1) increased expression of efflux pumps; 2) uptake of plasmids that express either Qnr proteins that block fluoroquinolones from binding to gyrase and topoisomerase IV or an aminoglycoside acetyltransferase that acetylates and deactivates fluoroquinolones; 3) target-



mediated resistance caused by mutations in gyrase or topoisomerase IV.<sup>154-156, 279</sup> Of the above, target-mediated resistance is the most common and important mechanism for fluoroquinolone resistance in clinical infections.<sup>154, 155, 280, 281</sup>

### *Fluoroquinolone targeting*

On the basis of resistance to nalidixic acid in *E. coli*, gyrase was reported to be the target of quinolone antibacterials in 1977.<sup>282, 283</sup> Following the identification of topoisomerase IV, cellular experiments were carried out to determine the role of this latter type II topoisomerase in quinolone targeting. To this end, *E. coli* strains were engineered that encoded resistance mutations in GyrA, the corresponding alterations in ParC, or mutations in both subunits. Compared to wild-type strains, mutations in GyrA alone conferred ~10-fold resistance in this Gram-negative bacteria, equivalent mutations in ParC alone had no effect on fluoroquinolone potency, and simultaneous mutations in both enzymes conferred ~50-100-fold resistance.<sup>157</sup> Thus, it was concluded that gyrase was the primary and topoisomerase IV was the secondary cytotoxic target of this drug class in bacteria.

The vast majority of later studies employed a genetic approach to determine the primary and secondary target of fluoroquinolones in bacteria.<sup>284-288</sup> The topoisomerase in which the first resistance mutations occurred was declared to be the primary target, and the topoisomerase in which subsequent mutations led to higher levels of resistance was declared to be the secondary target.<sup>157, 284-289</sup> Surprisingly, utilizing this genetic approach, topoisomerase IV, rather than gyrase, was determined to be the primary target for fluoroquinolones in Gram-positive bacteria, such as *S. aureus* and *S. pneumoniae*.<sup>285-287</sup> This finding shifted the fluoroquinolone-targeting paradigm from gyrase being the primary target of fluoroquinolones in all bacteria to gyrase being the primary target in Gram-negative species and topoisomerase IV being the primary target in Gram-positive species.<sup>290</sup> The paradigm was further shifted by subsequent genetic experiments, which reported

that for almost every fluoroquinolone in almost every other species examined (irrespective of Gram stain), gyrase is the primary cellular target.<sup>155</sup> Thus, at present, the targeting of fluoroquinolones needs to be approached on a drug-by-drug and species-by-species basis.<sup>154, 155</sup> One aspect of the paradigm still holds true for most fluoroquinolones. With rare exceptions,<sup>291-293</sup> the targeting of gyrase and topoisomerase IV is not balanced (i.e., there is a primary and secondary target).<sup>154, 155</sup> This unbalanced targeting has profound effects on the evolution of drug resistance; a mutation in a single type II enzyme is often sufficient to cause levels of resistance that allow cells to escape fluoroquinolone treatment or potentially acquire additional mutations (in either the primary or secondary target) that lead to highly resistant strains.<sup>156, 279, 294</sup>

#### *Interactions with gyrase and topoisomerase IV through a water-metal ion bridge*

The understanding of how fluoroquinolones interact with gyrase/topoisomerase IV and the mechanism of target-mediated resistance are inextricably linked. It is well established that mutations in two highly conserved, but non-essential, amino acid residues in the A subunit of gyrase/topoisomerase IV are the primary cause of target-mediated fluoroquinolone resistance.<sup>154, 155, 295-297</sup> The amino acids most frequently associated with this resistance are a serine residue (originally identified as Ser83 in the A subunit of *E. coli* gyrase)<sup>295, 296</sup> and an acidic (originally identified as Asp87)<sup>297</sup> residue four amino acids downstream.<sup>154, 155</sup> Although it had been assumed that these residues played an integral role in mediating fluoroquinolone interactions with the type II enzymes, their specific functions remained an enigma for nearly two decades.

Initial structural studies of moxifloxacin/levofloxacin-induced cleavage complexes with *S. pneumoniae* topoisomerase IV and ciprofloxacin-induced cleavage complexes with *S. aureus* gyrase confirmed the insertion of fluoroquinolones in the scissile bonds of the cleaved DNA and placed the drug in the vicinity of the serine and acidic residues.<sup>55, 298, 299</sup> However, none of the fluoroquinolones were in close enough proximity to interact directly with these amino acids. The

puzzle of how mutations in the serine and acidic residues led to fluoroquinolone resistance began to be solved with the publication of a crystal structure of a moxifloxacin-induced DNA cleavage complex with *Acinetobacter baumannii* topoisomerase IV.<sup>167</sup> This structure contained two fluoroquinolone molecules that were each chelated with a non-catalytic divalent metal ion. Although it had been known for many years that the C3/C4 keto acid of fluoroquinolones chelated divalent metal ions,<sup>300</sup> the function of this interaction was ascribed primarily to effects on drug uptake.<sup>301, 302</sup> In the *A. baumannii* topoisomerase IV structure, the chelated metal ion was coordinated by four water molecules, two of which formed hydrogen bonds with the serine and acidic residues of the type II enzyme (Figure 1.10).<sup>167</sup> This water-metal ion interaction, which has been observed in subsequent structures,<sup>303, 304</sup> was proposed to bridge the fluoroquinolone directly to the residues involved in resistance.

The biological relevance of the proposed “water-metal ion bridge” was ultimately demonstrated through a series of enzymological studies.<sup>154, 155</sup> These experiments showed that: 1) fluoroquinolones require a non-catalytic divalent metal ion in order to increase gyrase-/topoisomerase IV-mediated DNA scission, 2) the range of divalent metal ions that can support fluoroquinolone activity is altered by mutations in the serine and acidic amino acid residues, and 3) the affinity of the chelated metal ion in the cleavage complex is diminished by mutations in these residues.<sup>155, 305-310</sup> These studies also provided strong evidence that the serine and acidic residues anchor the water-metal ion bridge as well as a direct link between fluoroquinolones and target-mediated drug resistance.<sup>155, 305-310</sup>

The water-metal ion bridge has been shown to play a critical role in mediating the actions of fluoroquinolones against gyrase and topoisomerase IV in every species examined to date.<sup>154, 155, 305-310</sup> Although the water-metal ion bridge is the primary conduit between the drug and the type II topoisomerases, its architecture is nuanced and differs from enzyme to enzyme. In some cases, both the serine and the acidic residue are important for bridge formation,

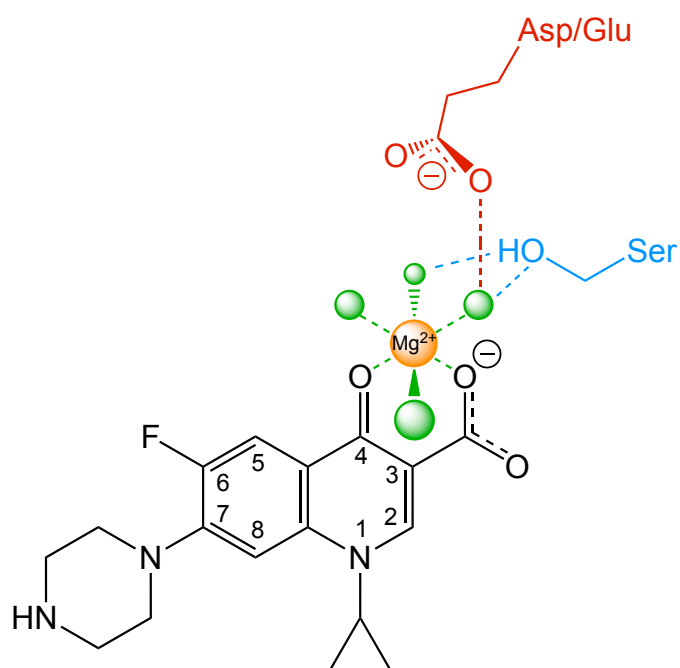


**Figure 1.10. Schematic of the water-metal ion bridge that mediates interactions between fluoroquinolones and bacterial type II topoisomerases.**

For simplicity, only interactions with the protein (and not the DNA) are shown. A non-catalytic divalent metal ion (orange,  $Mg^{2+}$ ) forms an octahedral coordination sphere (green dashed lines) between four water molecules (green) and the C3/C4 keto-acid of ciprofloxacin (black). Two of the water molecules form hydrogen bonds (blue dashed lines) with the serine side chain hydroxyl group (blue), and one water molecule hydrogen bonds (red dashed lines) with the aspartic acid or glutamic acid side chain carboxyl group (red).

<sup>305-307, 310, 311</sup> while in others, only one of the amino acids serves as the primary bridge anchor.<sup>308,</sup>  
<sup>309</sup> For example, the serine residue has been replaced by an alanine residue in *M. tuberculosis*  
gyrase.<sup>312, 313</sup> As a result, the acidic residue is the major anchor for the water-metal ion bridge.<sup>308</sup>  
This finding explains the reduced potency of most fluoroquinolones against this enzyme.<sup>308, 312-</sup>  
<sup>314</sup>

The function of the water-metal ion bridge is dynamic and varies across type II enzymes.<sup>154, 155</sup> In the majority of enzymes examined, the most important role of the bridge is to serve as a vehicle for fluoroquinolone binding, as evidenced by a coordinate loss of catalytic inhibition and DNA cleavage enhancement.<sup>305, 306, 308, 311</sup> However, with some enzymes, disruption of the bridge has little effect on fluoroquinolone binding, as evidenced by sustained catalytic inhibition, but undermines the ability of the drug to enhance DNA cleavage.<sup>307, 311</sup> For the latter, it is assumed that the role of the bridge is to position the fluoroquinolone in the enzyme-DNA complex. In these cases, understanding bridge function provides important insights into fluoroquinolone cytotoxicity. The fact that resistance tracks with the loss of DNA cleavage implies that the mechanism of drug toxicity must also be due to the induction of enzyme-generated double-stranded DNA breaks as opposed to the loss of essential enzyme activities.<sup>154-156, 307, 311</sup>

### *Clinical impact of fluoroquinolone resistance*

Target-mediated resistance caused by mutations in residues that anchor the water-metal ion bridge has profoundly affected fluoroquinolone use in several high-priority infectious diseases.<sup>154-156</sup> Two examples are described below:

First, tuberculosis, which is caused by *M. tuberculosis*, is the second deadliest infectious disease in the world, surpassed only by COVID-19 in 2022.<sup>315</sup> In the same year, tuberculosis caused 1.3 million deaths worldwide, and it is estimated that 1.8 billion people are infected with this pathogen globally.<sup>315, 316</sup> The fluoroquinolones moxifloxacin and levofloxacin have been used

as second-line tuberculosis treatment for individuals who are resistant to or cannot tolerate front-line therapies,<sup>317</sup> or more recently, as a shorter first-line regimen for multidrug-resistant tuberculosis.<sup>318</sup>

Because *M. tuberculosis* encodes only gyrase, it is highly susceptible to target-mediated resistance. To this point, as many as 13% of patients with tuberculosis, who are initially misdiagnosed and treated with fluoroquinolones for at least 10 days, are later found to have fluoroquinolone-resistant tuberculosis.<sup>319</sup>

Second, gonorrhea is a sexually transmitted disease that infects the mucosal epithelium of the genitals, rectum, and throat.<sup>320, 321</sup> More than 82 million new cases are observed worldwide each year.<sup>322</sup> If left untreated, gonorrheal infections can cause severe complications that include pelvic inflammatory disease, infertility, and when disseminated, death.<sup>320, 323</sup> The etiological agent of gonorrhea is the Gram-negative bacterium, *Neisseria gonorrhoeae*.<sup>323</sup>

The fluoroquinolone ciprofloxacin was introduced as frontline treatment for gonorrhea in 1993.<sup>324, 325</sup> However, due to high levels of resistance caused by mutations in the bridge-anchoring amino acids in gyrase and topoisomerase IV, the Centers for Disease Control and Prevention (CDC) removed this drug from gonorrhea treatment guidelines in 2006.<sup>326</sup> In 2021, nearly one-third of clinical *N. gonorrhoeae* isolates in the United States were resistant to ciprofloxacin, and in parts of Asia, this number exceeded 90%.<sup>327</sup>

### **Overcoming Fluoroquinolone Resistance**

To take advantage of gyrase and topoisomerase IV as validated antibacterial targets, efforts have been made to identify new drug classes that interact with the type II enzymes but utilize different amino acid residues for their binding.<sup>299, 303, 328-334</sup> As a result, recent drug discovery programs have led to the development of novel antibacterial classes that target the bacterial type

II topoisomerases.<sup>299, 329-332</sup> Two members from these classes, gepotidacin and zoliflodacin, are advanced clinical candidates that have successfully completed phase III trials.<sup>335-338</sup>

*Novel bacterial topoisomerase inhibitors, M. tuberculosis gyrase inhibitors, and triazaacenaphthylenes*

Novel bacterial topoisomerase inhibitors (NBTIs) were first described as a new class of bacterial type II topoisomerase inhibitors in 2007.<sup>339, 340</sup> The structure of NBTIs is defined by four key elements: a left-hand substituent (LHS), central linker, basic nitrogen, and right-hand substituent (RHS, Figure 1.11).<sup>341, 342</sup> Members of this class can accommodate a variety of modifications to the LHS, central linker, and RHS that still yield activity against gyrase/topoisomerase IV and bacterial cells.<sup>341, 342</sup> However, the basic nitrogen appears to be essential for the anti-topoisomerase and antibacterial activity of this class.<sup>299, 341-345</sup>

Although NBTIs are active against a broad range of Gram-negative and Gram-positive pathogens,<sup>341, 346-350</sup> the parental class generally displays poor activity against the atypical bacterium *M. tuberculosis*. Structural optimization of an NBTI that displayed moderate efficacy against tuberculosis yielded two naphthyridone/aminopiperidine derivatives with high activity against both the disease and *M. tuberculosis* gyrase.<sup>351, 352</sup> Because of this activity, these were designated as *M. tuberculosis* gyrase inhibitors (MGIs, Figure 1.11). Rather than having a broader spectrum of activity, these compounds are more specific to *M. tuberculosis* as compared to the parental class.<sup>352</sup>

Cardiovascular safety concerns, attributed to inhibition of the hERG potassium ion channel, proved to be a major stumbling block to the clinical development of the NBTI class.<sup>343, 353, 354</sup> However, gepotidacin, a compound that combined minimal hERG inhibition with high antibacterial activity, emerged as the premier clinical candidate (discussed in detail below).<sup>355-362</sup>

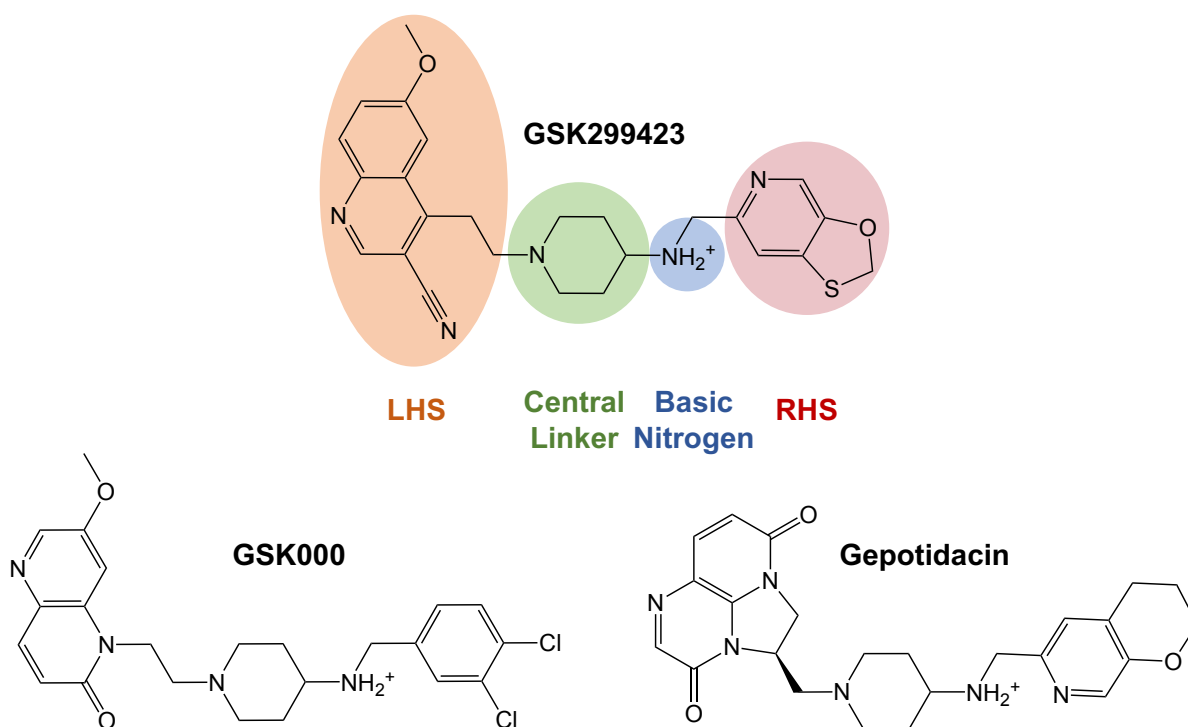


**Figure 1.11. Novel bacterial topoisomerase inhibitors (NBTI), *M. tuberculosis* gyrase inhibitor (MGI), and triazaacenaphthylene structures.**

Members of the NBTI, MGI, and triazaacenaphthylene classes possess a left-hand substituent (LHS, orange), a central linker (green), a basic nitrogen (blue), and a right-hand substituent (RHS, red). While the LHS, central linker, and RHS are amenable to alteration, the basic nitrogen is critical for antibacterial activity. As an example, the structure of GSK299423 (top), an early piperidine-linked NBTI, is shown. GSK000 (bottom left) displays enhanced activity against *M. tuberculosis* gyrase and is a founding member of the MGI class. Gepotidacin (bottom right) is a first-in-class triazaacenaphthylene antibacterial that successfully concluded phase III trials for the treatment of urinary tract infections and uncomplicated urogenital gonorrhea.



The LHS of gepotidacin is a triazaacenaphthylene moiety; hence, this compound is considered to be the founding member of the triazaacenaphthylene class of antibacterials.<sup>363</sup>

Because of the mechanistic similarities between NBTIs, MGIs, and triazaacenaphthylenes, unless there is a reason to be specific, these compounds will be collectively referred to as NBTIs.

In contrast to fluoroquinolones, in which two molecules bind at the active site of gyrase/topoisomerase IV (one at each scissile bond),<sup>55, 167, 299, 303, 304</sup> only a single NBTI molecule binds in the gyrase-DNA complex.<sup>44, 299, 332, 364</sup> Although this is assumed to be the case for topoisomerase IV, structures with this enzyme have yet to be reported. The NBTI LHS sits in a pocket in the DNA on the twofold axis of the complex, midway between the two DNA cleavage sites, and the RHS sits in a pocket on the twofold axis between the two GyrA subunits.<sup>44, 299, 332, 364</sup> One of the most important interactions between gyrase/topoisomerase IV and the NBTI is with an aspartic acid residue (Asp82 in *E. coli* GyrA), which forms a hydrogen bond with the basic nitrogen. NBTIs do not interact directly with the serine or acidic residues that are critical for fluoroquinolone binding.<sup>44, 299, 332, 364</sup> Even though the binding sites of fluoroquinolones and NBTIs do not overlap, it has been demonstrated that both drugs cannot bind to the active site of gyrase/topoisomerase IV simultaneously.<sup>332, 352, 365</sup>

As a result of their binding modality, NBTIs inhibit overall catalytic activity of gyrase and topoisomerase IV and act as topoisomerase poisons.<sup>299, 332, 352, 364-368</sup> However, in contrast to fluoroquinolones, NBTIs enhance primarily single-stranded (as opposed to double-stranded) DNA breaks.<sup>299, 332, 343, 352, 364, 366</sup> Furthermore, in most cases, the binding of NBTIs actually suppresses the ability of gyrase/topoisomerase IV to generate double-stranded DNA breaks.<sup>299, 332, 352, 364, 366</sup> The mechanistic basis for the induction of single-stranded and suppression of double-stranded DNA breaks by NBTIs is not fully understood. However, it is believed that following cleavage of one DNA strand, the NBTI induces sufficient distortion in the active site of bacterial type II topoisomerases that it prevents these enzymes from cleaving the second strand.<sup>44, 299, 352, 364</sup>

Recent results with more structurally diverse NBTIs have challenged the hallmark characteristic of this chemical class (i.e., the generation of single-stranded rather than double-stranded DNA breaks).<sup>364, 367, 369, 370</sup> Some of these compounds induce appreciable levels of double-stranded DNA breaks in addition to single-stranded breaks, although results vary between gyrase and topoisomerase IV from different species. The basis for the enhancement of double-stranded DNA breaks by these NBTIs is an enigma, but it does not appear to be due to the binding of a second NBTI molecule in the active site of the type II enzymes.<sup>367</sup>

Because of the recent emergence of NBTIs as an antibacterial class with clinical potential, relatively little is known about resistance. However, mutations in gyrase/topoisomerase IV that decrease the sensitivity of laboratory strains and clinical isolates to this drug class have been reported.<sup>343, 365, 371-373</sup> A prominent mutation occurs at the aspartic acid residue that has been shown to interact with NBTIs in structural studies.<sup>44, 299, 332</sup> The response of NBTIs to fluoroquinolone resistance mutations varies across compounds and species. Whereas moderate to high levels of resistance are observed in some drug-species combinations, in others, such as MGIs and *M. tuberculosis* gyrase, compounds are more potent and efficacious against enzymes that carry a fluoroquinolone resistance mutation.<sup>351, 352, 365, 366, 373, 374</sup>

As discussed above, a major drawback to fluoroquinolones is their unbalanced targeting of gyrase and topoisomerase IV, which has decreased the effectiveness of this drug class due to the development of clinical resistance.<sup>154, 156, 279, 294</sup> This drawback may be overcome by some members of the NBTI class. For example, the triazaacenaphthylene gepotidacin displays well-balanced, dual targeting against both type II enzymes in *E. coli*.<sup>365, 373, 374</sup> Whereas there is no loss of susceptibility to gepotidacin in strains that contain a resistance mutation in either gyrase or topoisomerase IV, strains that contain a mutation in both type II topoisomerases were found to be more than 100-fold less sensitive to the triazaacenaphthylene.<sup>365, 374</sup> Thus, in at least some species, it appears that gepotidacin (and potentially other NBTIs) may be able to kill bacteria equally well through either gyrase or topoisomerase IV. It is assumed that this well-balanced,

dual-targeting of gyrase and topoisomerase IV will diminish the emergence of resistance and increase the clinical lifespan of gepotidacin and related compounds.

Currently, gepotidacin, a first-in-class triazaacenaphthylene, is the most clinically-advanced non-fluoroquinolone gyrase/topoisomerase IV targeted-antibacterial.<sup>338, 356, 362</sup> Recently, the results of phase III clinical trials for the treatment of uncomplicated urinary tract infections caused primarily by *E. coli* were reported.<sup>338</sup> In these trials, gepotidacin demonstrated statistically significant superiority to an established frontline treatment for uncomplicated urinary tract infections caused by *E. coli* and other uropathogens.<sup>338</sup> Thus, there is a reasonable expectation that gepotidacin will become the first new antibacterial class to treat urinary tract infections in more than two decades. This is especially significant considering the estimates that 50-60% of women will have a urinary tract infection in their lifetime.<sup>375</sup> Beyond its potential use to treat urinary tract infections, gepotidacin was recently evaluated for a second indication. A phase III clinical trial for the treatment of uncomplicated urogenital gonorrhea with the triazaacenaphthylene was concluded in late 2023.<sup>356</sup> This latter study further underscores the clinical potential of gepotidacin. Finally, preclinical studies suggest that gepotidacin may have activity against a variety of biothreat pathogens, including *Francisella tularensis* and *Yersinia pestis*, the etiological pathogens of tularemia and pneumonic plague, respectively.<sup>376-378</sup>

### *Spiropyrimidinetriones*

The most recent class of gyrase/topoisomerase IV-targeted antibacterials in clinical trials is the spiropyrimidinetriones (SPTs, Figure 1.12).<sup>266, 330, 335, 379, 380</sup> SPTs were first identified as inhibitors of gyrase-catalyzed DNA supercoiling in 2014.<sup>381</sup> Subsequently, it was determined that this class also inhibited the catalytic activity of topoisomerase IV and poisoned both type II enzymes.<sup>329</sup>

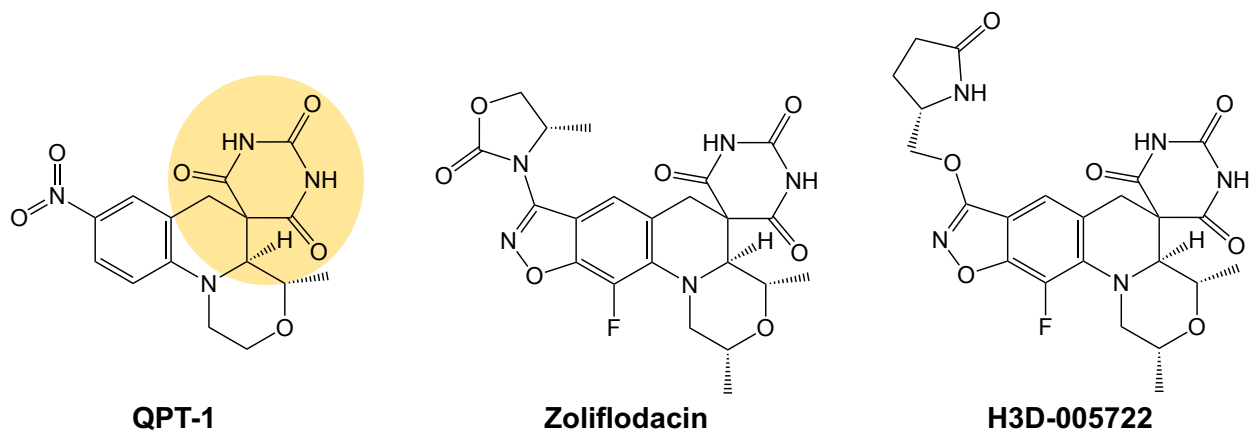


**Figure 1.12. Spiropyrimidinetrone (SPT) structures.**

The SPT class derives its name from the spiropyrimidinetrone group (yellow) that forms critical contacts with gyrase/topoisomerase IV and is essential for antibacterial activity. Optimization of an early progenitor of this class, QPT-1 (left), led to the synthesis of zoliflodacin (middle), which completed phase III trials for the treatment of uncomplicated gonorrhea in late 2023. Current drug development efforts are focused on synthesizing related SPTs with high activity against *M. tuberculosis*, such as H3D-005722 (right).

Structures of gyrase-DNA cleavage complexes formed in the presence of an SPT progenitor (QPT-1),<sup>328</sup> and more recently, the clinical candidate zoliflodacin (AZD0914/ETX0914) have been published.<sup>303, 334</sup> The binding site for SPTs in the complex overlaps those of fluoroquinolones. Like fluoroquinolones, SPTs insert into the cleaved scissile bonds, one molecule on each of the opposite DNA strands.<sup>303, 334</sup> This binding motif is consistent with the fact that SPTs induce gyrase/topoisomerase IV-mediated double-stranded DNA breaks. However, unlike fluoroquinolones, which interact with the GyrA side of the double helix, SPTs mediate their contacts with the enzyme primarily on the opposite, or GyrB side, of the double helix.<sup>303, 334, 382</sup> Asp429 in *N. gonorrhoeae* GyrB (equivalent to Asp426 in *E. coli* GyrB), which is highly conserved across bacteria, appears to be the primary point of contact for SPTs in the enzyme-DNA complex.<sup>303, 334, 382, 383</sup> The interaction between SPTs and GyrB obviates the use of the fluoroquinolone water-metal ion bridge.<sup>303, 329, 334</sup>

The effectiveness of SPTs (zoliflodacin and novel related compounds) against resistant bacteria and type II topoisomerases has been reported.<sup>329, 363, 383-387</sup> Zoliflodacin has displayed potent antibacterial activity against a number of Gram-positive, Gram-negative, atypical, and anaerobic microbes, including laboratory strains and clinical isolates resistant to fluoroquinolones and other antibacterials.<sup>363, 383-386</sup> Furthermore, related SPTs have shown promising activity against drug-resistant strains of *M. tuberculosis* and *S. aureus* in laboratory settings.<sup>388-390</sup> Despite the work in bacterial strains, the biochemical interactions between SPTs and fluoroquinolone-resistant type II topoisomerases have been reported only for gyrase from *N. gonorrhoeae* and *M. tuberculosis*.<sup>329, 387</sup> In the case of *N. gonorrhoeae* gyrase, mutations in residues that anchor the water-metal ion bridge had no effect on the ability of the SPT to inhibit catalytic activity or enhance DNA cleavage.<sup>329</sup> Furthermore, both zoliflodacin and a series of novel SPT analogues either maintained or displayed higher activity against fluoroquinolone-resistant gyrase from *M. tuberculosis*.<sup>387</sup> Although limited in scope, these studies provide optimism that SPTs have the potential to maintain activity against a broad spectrum of fluoroquinolone-resistant infections.

SPT resistance studies have only been performed with zoliflodacin in strains of *N. gonorrhoeae*. These studies indicate that (at least in this species) gyrase is the primary cellular target of zoliflodacin.<sup>382</sup> Reported resistance mutations are located in the TOPRIM domain of the B subunit in Asp429 as well as other amino acid residues that interact (directly or indirectly) with zoliflodacin in structural studies.<sup>334, 382</sup> This finding supports the purported role of these residues in mediating SPT-gyrase interactions.<sup>303, 334</sup>

Even though zoliflodacin displays high activity against purified *N. gonorrhoeae* topoisomerase IV, to date, no cellular mutations in this enzyme have been reported, even in the background of gyrase mutations.<sup>330, 382</sup> Although it is assumed that topoisomerase IV is a secondary target for SPTs in cells that express both type II enzymes, this has yet to be demonstrated. Nonetheless, the unbalanced cellular targeting of zoliflodacin could eventually have clinical consequences.

Today, zoliflodacin is the most clinically advanced SPT and recently completed phase III trials for the treatment of uncomplicated gonorrhea.<sup>335, 337</sup> In this trial, zoliflodacin demonstrated statistical non-inferiority at the urogenital site to a current global standard of care treatment.<sup>337</sup> These results highlight the clinical promise of zoliflodacin to treat this prevalent sexually transmitted disease, especially existing fluoroquinolone-resistant strains. Preclinical studies with related compounds suggest that SPTs may also have potential for the treatment of tuberculosis.<sup>266, 387, 389, 390</sup>

### **Scope of the Dissertation**

Type II topoisomerases are the targets for some of the most highly prescribed anticancer and antibacterial drugs worldwide. Despite their success, the clinical use of these agents has been undermined by off-target effects (anticancer therapy) and target-mediated resistance (antibacterial drugs). Given the clinical utility of type II topoisomerase inhibitors and poisons in cancer and infectious disease treatments, a thorough understanding of how these compounds

interact with enzyme targets is imperative. The goals of this dissertation are to describe the activity of naphthalene derivatives against human topoisomerase II, to define the mechanistic basis for target-mediated fluoroquinolone resistance in *N. gonorrhoeae*, and to characterize the actions of NBTIs and SPTs against wild-type and fluoroquinolone-resistant gyrase and topoisomerase IV.

Chapter I introduces DNA topology, the biological functions of human and bacterial type II topoisomerases, anticancer therapies that target topoisomerase II, gyrase/topoisomerase IV-targeted antibacterial drugs, the biochemical and structural basis of fluoroquinolone resistance, and emerging gyrase/topoisomerase IV-targeted antibacterial drugs. Parts of this section are published in *ACS Infectious Diseases*.<sup>391</sup>

Chapter II details the materials and methods used to accomplish the goals of this dissertation.

Chapter III examines the effects of naphthalene metabolites on human topoisomerase II $\alpha$  and II $\beta$ . Of the five compounds tested, 1,2-naphthoquinone, an environmental pollutant found in diesel exhaust particles, enhanced double-stranded DNA cleavage mediated by both human topoisomerase II $\alpha$  and II $\beta$  but displayed higher activity against the  $\alpha$  isoform. Furthermore, 1,2-naphthoquinone increased type II topoisomerase-mediated DNA cleavage by closing the N-terminal gate of the enzyme. These findings suggest that some of the toxicities associated with 1,2-naphthoquinone may be attributed to its ability to enhance DNA scission mediated by human type II topoisomerases. The results of this study were published in *Chemical Research in Toxicology*.<sup>392</sup>

Chapter IV describes the mechanism of action and resistance of the fluoroquinolone ciprofloxacin against *N. gonorrhoeae* gyrase and topoisomerase IV. Results indicate that ciprofloxacin interacts with gyrase (its primary target) and topoisomerase IV (its secondary target) through a water-metal ion bridge that has been described in other species. Moreover, mutations in amino acid residues that anchor this bridge diminish the susceptibility of the enzymes to the drug, leading to fluoroquinolone resistance. Results further suggest that ciprofloxacin primarily induces its cytotoxic effects by enhancing gyrase-mediated DNA cleavage as opposed to

inhibiting the DNA supercoiling activity of the enzyme. Together, this work links the effects of ciprofloxacin on WT and resistant gyrase to results reported for cellular and clinical studies and provides a mechanistic explanation for the targeting and resistance of fluoroquinolones in *N. gonorrhoeae*. The results of this study were published in *ACS Infectious Diseases*.<sup>311</sup>

Chapter V reports the characterization of gyrase/topoisomerase IV-mediated single-stranded and/or double-stranded DNA breaks induction by OSUAB-185, a dioxane-linked NBTI. OSUAB-185 induced single-stranded and suppressed double-stranded DNA breaks mediated by *N. gonorrhoeae* gyrase. However, the compound stabilized both single- and double-stranded DNA breaks mediated by topoisomerase IV. The induction of double-stranded breaks does not appear to correlate with the binding of a second OSUAB-185 molecule and extends to fluoroquinolone-resistant *N. gonorrhoeae* topoisomerase IV, as well as type II enzymes from other bacteria and humans. These results suggest that some members of this subclass may have alternative binding motifs in the cleavage complex. This work has been published in the *International Journal of Molecular Sciences*.<sup>367</sup>

Chapter VI investigates the interactions of SPTs with gyrase and topoisomerase IV from *N. gonorrhoeae*. Zoliflodacin and H3D-005722, a novel SPT analog, inhibited the catalytic activities of gyrase and topoisomerase IV and enhanced double-stranded DNA scission mediated by the type II enzymes, but both SPTs were more potent against gyrase. Moreover, zoliflodacin displayed high activity against fluoroquinolone-resistant gyrase. Results indicate that the differences in SPT action against *N. gonorrhoeae* gyrase and topoisomerase IV may contribute to their physiological targeting and toxicity. They also imply that SPTs interact with gyrase and topoisomerase IV distinctly within and across bacterial species.

Chapter VII presents the conclusions and implications of the studies described herein and suggests ideas for future research.



## CHAPTER II

### METHODS

#### Materials

##### *DNA substrates*

Negatively supercoiled pBR322 plasmid DNA was prepared from *Escherichia coli* using a Plasmid Mega Kit (Qiagen) according to the manufacturer's protocol. Relaxed pBR322 plasmid was generated by treating negatively supercoiled pBR322 with calf thymus topoisomerase I in 50 mM Tris-HCl (pH 7.5), 50 mM KCl, 10 mM MgCl<sub>2</sub>, 0.5 mM DTT, 0.1 mM EDTA, and 30 µg/mL bovine serum albumin (BSA) for 45 min at 37 °C followed by heat inactivation of topoisomerase I at 75 °C for 10 min.<sup>393</sup> Kinetoplast DNA (kDNA) was isolated from *Crithidia fasciculata* as described by Englund.<sup>394</sup>

##### *Drugs, preclinical compounds, and chemicals*

Etoposide, 1,4-benzoquinone, 1,2-naphthoquinone, 1,4-naphthoquinone, 2-hydroxy-1,4-naphthoquinone, 5-hydroxy-1,4-naphthoquinone, and 5,8-dihydroxy-1,4-naphthoquinone were purchased from Sigma-Aldrich. 1,2-Dihydroxynaphthalene was purchased from TCI. All compounds except 1,4-benzoquinone were stored at 4 °C as 20 mM stock solutions in 100% DMSO. 1,4-Benzoquinone was stored at –20 °C as a 20 mM stock solution in water. In all cases, the activities of compounds in DMSO or water stock solutions were stable for at least 6 months.

Ciprofloxacin was stored at –20 °C as a 40 mM stock solution in 0.1 M NaOH and diluted 5-fold with 10 mM Tris–HCl (pH 7.9) immediately prior to use. 3-Amino-7-[(3S)-3-(aminomethyl)-

1-pyrrolidinyl]-1-cyclopropyl-6-fluoro-8-methyl-2,4(1*H*,3*H*)-quinazolinedione was synthesized using established methods as reported previously and was the gift of Dr. Robert Kerns.<sup>395</sup> For the sake of simplicity, this compound will be termed 8-methyl-2,4-quinazolinedione. It was stored at –20 °C as 20 mM stock solutions in 100% DMSO.

ATP, ascorbic acid, and DTT were purchased Sigma-Aldrich. All other chemicals were analytical reagent grade.

## Human Type II Topoisomerases

### *Enzymes*

Recombinant human wild-type topoisomerase II $\alpha$  and II $\beta$  were expressed in *Saccharomyces cerevisiae* and purified as described previously.<sup>396, 397</sup> The catalytic core of human topoisomerase II $\alpha$  (containing amino acids 431-1193)<sup>50, 395</sup> was expressed in *S. cerevisiae* and purified using a Ni<sup>2+</sup> nitriloacetic acid agarose column as described previously.<sup>42, 398</sup> The enzymes were stored at –80 °C as 1.5 or 7.5 mg/mL stocks in 50 mM Tris-HCl (pH 7.7), 0.1 mM EDTA (pH 8.0), 750 mM KCl, and 40% (v/v) glycerol. For all enzymes, the concentration of dithiothreitol (DTT) remaining from purification was <2  $\mu$ M in final reaction mixtures.

### *Topoisomerase II-mediated DNA cleavage*

DNA cleavage reactions were performed according to the procedure of Fortune and Osheroff.<sup>399</sup> Reactions mixtures contained 10 nM pBR322 and 300 nM wild-type topoisomerase II $\alpha$ , 275 nM wild-type topoisomerase II $\beta$ , or 850 nM topoisomerase II $\alpha$  catalytic core in a total of 20  $\mu$ L of DNA cleavage buffer [10 mM Tris-HCl (pH 7.9), 0.1 mM EDTA (pH 8.0), 100 mM KCl, 5 mM MgCl<sub>2</sub>, 2.5% (w/v) glycerol]. The concentrations of topoisomerase II $\alpha$  and II $\beta$  that were used

yielded equivalent enzyme activities. DNA cleavage reactions were incubated for 6 min at 37 °C before enzyme-DNA cleavage complexes were trapped by adding 2 µL of 4% SDS followed by 2 µL of 250 mM EDTA (pH 8.0). Proteinase K was added (2 µL of a 0.8 mg/mL solution), and reaction mixtures were incubated for 30 min at 45 °C to digest the enzyme. Samples were mixed with 2 µL of agarose loading buffer [60% (w/v) sucrose, 10 mM Tris-HCl (pH 7.9), 0.5% (w/v) bromophenol blue, and 0.5% (w/v) xylene cyanol FF] and heated for 2 min at 45 °C prior to electrophoresis in 1% agarose in 40 mM Tris-acetate (pH 8.3), and 2 mM EDTA (pH 8.0) containing 0.5 µg/mL ethidium bromide. DNA bands were visualized by ultraviolet light and quantified using an Alpha Innotech digital imaging system. Double-stranded DNA cleavage was monitored by the conversion of supercoiled plasmid DNA to linear molecules.

DNA cleavage reactions were performed in the presence of 0-100 µM 1,2-naphthoquinone, 1,4-naphthoquinone, 1,2-dihydroxynaphthalene, 2-hydroxy-1,4-naphthoquinone, 5-hydroxy-1,4-naphthoquinone, 5,8-dihydroxy-1,4-naphthoquinone, etoposide, or 1,4-benzoquinone. Unless stated otherwise, the above compounds were added last to the reaction mixtures. In some cases, reactions contained 1 mM ATP, 2 mM DTT, or 2 mM ascorbic acid. Alternatively, DTT or ascorbic acid were added after the 6 min cleavage reaction, and samples were incubated for an additional 5 min.

#### *Persistence of topoisomerase II-DNA cleavage complexes*

The persistence of topoisomerase II $\alpha$ -DNA cleavage complexes was determined using the procedure of Gentry et al.<sup>400</sup> Initial reactions contained 55 nM pBR322, 2.2 µM wild-type topoisomerase II $\alpha$  (in the absence of compound, in order to raise levels of double-stranded breaks) or 300 nM wild-type topoisomerase II $\alpha$  in the presence of 50 µM 1,2-naphthoquinone or 100 µM etoposide in a total of 20 µL of DNA cleavage buffer. In the reaction that lacked compound, 5 mM MgCl<sub>2</sub> in the cleavage buffer was replaced with 5 mM CaCl<sub>2</sub> to increase baseline levels of

DNA cleavage.<sup>401</sup> To establish a DNA cleavage/ligation equilibrium, reactions were incubated for 6 min at 37 °C and diluted 20-fold with DNA cleavage buffer lacking divalent cation at 37 °C. Samples (20 µL) were removed at times ranging from 0-120 min. DNA cleavage complexes were trapped, and samples were analyzed as discussed under DNA cleavage. Levels of DNA cleavage were set to 100% at time zero, and the persistence of cleavage complexes was determined by the decay of linear reaction product over time.

#### *Topoisomerase II-mediated DNA ligation*

DNA ligation mediated by human topoisomerase II $\alpha$  was monitored as described previously.<sup>393</sup> Initial reactions contained 10 nM pBR322 and 860 nM wild-type topoisomerase II $\alpha$  (no compound, in order to raise levels of double-stranded breaks) or 300 nM wild-type topoisomerase II $\alpha$  (with compound). As described for the DNA cleavage assays, DNA cleavage/ligation equilibria were established for 6 min at 37 °C in the absence or presence of 50 µM 1,2-naphthoquinone or 100 µM etoposide. DNA ligation was initiated by shifting samples from 37 to 0 °C, which allowed enzyme-mediated ligation but prevented new rounds of DNA cleavage from occurring. This resulted in a unidirectional sealing of the cleaved DNA.<sup>42, 402</sup> DNA cleavage complexes were trapped at time points ranging from 0-20 s, and samples were analyzed as discussed under DNA cleavage. Linear DNA cleavage product at time zero was set to 100% to allow direct comparison between the different compounds, and DNA ligation was monitored by the loss of linear DNA.

## Bacterial Type II Topoisomerases

### Enzymes

All proteins were His-tagged. The identities of enzyme constructs were confirmed by DNA sequencing, and all enzymes were stored at  $-80\text{ }^{\circ}\text{C}$ . In all assays, and the stated enzyme concentration reflects that of the holoenzyme ( $A_2B_2$ ).

*Bacillus anthracis* wild-type gyrase (GyrA and GyrB) and topoisomerase IV subunits (GrlA and GrlB) were expressed and purified as described by Dong et al.<sup>42, 403</sup> *B. anthracis* gyrase or topoisomerase IV was used as a 1:2 GyrA:GyrB or GrlA:GrlB mixture, respectively.

*E. coli* wild-type gyrase (GyrA, GyrB) subunits were expressed and purified as described by Chan et al.<sup>303</sup> and *E. coli* wild-type topoisomerase IV (ParC, ParE, gift of Dr. Keir Neumann, NHLBI) subunits were expressed and purified as described by Peng and Marians.<sup>42, 129</sup> *E. coli* gyrase or topoisomerase IV was used as a 1:1 GyrA:GyrB or ParC:ParE mixture, respectively.

*N. gonorrhoeae* wild-type gyrase (GyrA, GyrB) and topoisomerase IV (ParC, ParE) subunits as well as mutant GyrA<sup>S91F</sup> and GyrA<sup>S91F/D95G</sup> gyrase were prepared as described previously.<sup>329, 299, 303</sup> *N. gonorrhoeae* mutant GyrA<sup>D95G</sup> gyrase and mutant ParC<sup>S87N</sup>, ParC<sup>E91G</sup>, and ParC<sup>S87N/E91G</sup> topoisomerase IV were generated using a QuickChange II XL site-directed mutagenesis kit (Agilent Technologies) with custom primers for the desired mutations. Mutant *N. gonorrhoeae* GyrA and ParC subunits were expressed and purified as described by Ashley et al.<sup>139</sup> with the following modifications to optimize protein expression and lysis: 1) GyrA<sup>D95G</sup> was expressed for 2.5 h and ParC<sup>S87N</sup>, ParC<sup>E91G</sup>, and ParC<sup>S87N/E91G</sup> were expressed for 3 h before harvesting, and 2) cells were lysed by sonication using a digital sonifier. *N. gonorrhoeae* gyrase or topoisomerase IV was used as a 1:1 GyrA:GyrB or ParC:ParE mixture, respectively.

*Staphylococcus aureus* wild-type gyrase (GyrA, GyrB) and topoisomerase IV (GrlA and GrlB) subunits were purchased from GenScript and expressed and purified as described

previously.<sup>303, 332</sup> *S. aureus* gyrase or topoisomerase IV was used as a 1:1 GyrA:GyrB or 1:1 GrIA:GrIB mixture, respectively.

#### *Gyrase-catalyzed DNA supercoiling*

DNA supercoiling assays were based on previously published protocols by Aldred et al.<sup>308</sup> Assays contained 15 nM WT or 25 nM mutant (GyrA<sup>S91F</sup>, GyrA<sup>D95G</sup>, or GyrA<sup>S91F/D95G</sup>) *N. gonorrhoeae* gyrase, 5 nM relaxed pBR322, and 1.5 mM ATP in a total volume of 20  $\mu$ L of supercoiling buffer [50 mM Tris-HCl (pH 7.5), 175 mM KCl, 5 mM MgCl<sub>2</sub>, and 50  $\mu$ g/mL BSA]. Assay mixtures were incubated at 37 °C for 20 min with WT and GyrA<sup>D95G</sup>, 25 min with GyrA<sup>S91F/D95G</sup>, or 30 min with GyrA<sup>S91F</sup> *N. gonorrhoeae* gyrase, which represents the minimum time required to completely supercoil the DNA in the absence of drug. Reactions were stopped by the addition of 3  $\mu$ L of stop solution [0.77% SDS and 77.5 mM Na<sub>2</sub>EDTA]. Samples were mixed with 2  $\mu$ L of loading dye [60% sucrose, 10 mM Tris-HCl (pH 7.9), 0.5% bromophenol blue, and 0.5% xylene cyanol FF] and incubated at 45 °C for 2 min before being subjected to electrophoresis on 1% agarose gels in 100 mM Tris-borate (pH 8.3) and 2 mM EDTA. Gels were stained with 1  $\mu$ g/mL ethidium bromide for 20 min, then de-stained with distilled water for 10 min. DNA bands were visualized with medium-range ultraviolet light and quantified using an Alpha Innotech digital imaging system. IC<sub>50</sub> values (the concentration of drug required to inhibit enzyme activity by 50%) were calculated on GraphPad Prism using a non-linear regression analysis with 95% confidence intervals.

For assays that monitored competition between ciprofloxacin and 8-methyl-2,4-quinazolinedione, the fluoroquinolone (0-500  $\mu$ M) and quinazolinedione (50  $\mu$ M) were added simultaneously to reaction mixtures.

### *Topoisomerase IV-catalyzed DNA decatenation*

DNA decatenation assays were based on previously published protocols by Anderson et al.<sup>158</sup> and Aldred et al.<sup>305</sup> Assays contained 10 nM WT, 20 nM ParC<sup>S87N</sup>, 35 nM ParC<sup>E91G</sup>, or 35 nM ParC<sup>S87N/E91G</sup> *N. gonorrhoeae* topoisomerase IV, 5 nM kDNA, and 1 mM ATP in 20  $\mu$ L of 40 mM HEPES-KOH (pH 7.6), 25 mM NaCl, 100 mM KGluc, and 10 mM Mg(OAc)<sub>2</sub>. Assay mixtures were incubated at 37 °C for 10 min with WT, 15 min with ParC<sup>S87N</sup>, and 30 min with ParC<sup>E91G</sup> and ParC<sup>S87N/E91G</sup> *N. gonorrhoeae* topoisomerase IV, which represents the minimum time required to completely decatenate the kDNA in the absence of drug. Reactions were stopped, subjected to electrophoresis, and visualized as described for gyrase-catalyzed DNA supercoiling. IC<sub>50</sub> values were calculated on GraphPad Prism using a non-linear regression analysis with 95% confidence intervals.

### *Gyrase/topoisomerase IV-mediated DNA cleavage*

DNA cleavage reactions were performed according to the procedure of Aldred et al.<sup>305</sup> Reactions were performed in the absence of compound or in the presence of increasing concentrations of fluoroquinolone, NBTI, SPT, or derivatives. For experiments performed with *N. gonorrhoeae* enzymes, assay mixtures contained 10 nM pBR322 and 100 nM WT, 100 nM GyrA<sup>S91F</sup>, 100 nM GyrA<sup>D95G</sup>, or 100 nM GyrA<sup>S91F/D95G</sup> gyrase or 100 nM WT, 200 nM ParC<sup>S87N</sup>, 150 nM ParC<sup>E91G</sup>, or 150 nM ParC<sup>S87N/E91G</sup> topoisomerase IV in a total volume of 20  $\mu$ L of 40 mM Tris-HCl (pH 7.9), 50 mM NaCl, 2.5% (w/v) glycerol, and 10 mM MgCl<sub>2</sub>. The concentration of mutant enzymes employed were normalized to provide the same level of cleavage as the WT enzyme in the presence of 8-methyl-2,4-quinazolidinedione. In some cases, MgCl<sub>2</sub> in the cleavage buffer was replaced with an equivalent concentration of CaCl<sub>2</sub> to increase baseline levels of cleavage.<sup>401</sup> Reactions were incubated at 37 °C for 30 min with WT and mutant (GyrA<sup>S91F</sup>, GyrA<sup>D95G</sup>, and

GyrA<sup>S91F/D95G</sup>) *N. gonorrhoeae* gyrase, 20 min with mutant (ParC<sup>S87N</sup>, ParC<sup>E91G</sup>, and ParC<sup>S87N/E91G</sup>) *N. gonorrhoeae* topoisomerase IV, and 10 min with WT *N. gonorrhoeae* topoisomerase IV.

Unless stated otherwise, assay mixtures for remaining species contained 10 nM pBR322 and 500 nM wild-type *B. anthracis* gyrase, 100 nM wild-type *B. anthracis* topoisomerase IV, 100 nM wild-type *E. coli* gyrase, 20 nM wild-type *E. coli* topoisomerase IV, 100 nM wild-type *S. aureus* gyrase, or 20 nM *S. aureus* topoisomerase IV in a total volume of 20  $\mu$ L of DNA cleavage buffer: 40 mM Tris-HCl (pH 7.9), 50 mM NaCl, 2.5% (w/v) glycerol, and 5 mM or 10 mM MgCl<sub>2</sub> for *E. coli* type II topoisomerases or *B. anthracis* topoisomerase IV, respectively; 50 mM Tris-HCl (pH 7.5), 100 mM K<sub>2</sub>Glu, 5 mM MgCl<sub>2</sub>, 50  $\mu$ g/mL BSA, and 5 mM dithiothreitol (DTT) for *B. anthracis* gyrase and *S. aureus* gyrase; 40 mM Tris-HCl (pH 7.5), 6 mM MgCl<sub>2</sub>, 20 mM NaCl, 50  $\mu$ g/mL BSA, and 10 mM DTT for *S. aureus* topoisomerase IV. Reactions were incubated at 37 °C for 30 min with *B. anthracis* gyrase and *S. aureus* gyrase, 20 min with *E. coli* gyrase, and 10 min with all other enzymes.

Enzyme-DNA cleavage complexes were trapped by adding 2  $\mu$ L of 4% SDS followed by 2  $\mu$ L of 250 mM EDTA (pH 8.0). Proteinase K was added (2  $\mu$ L of a 0.8 mg/mL solution), and reactions mixtures were incubated for 30 min at 45 °C to digest the enzyme. Samples were mixed with 2  $\mu$ L of agarose loading buffer and heated for 2 min at 45 °C prior to electrophoresis in 1% agarose gels in 40 mM Tris-acetate (pH 8.3), and 2 mM EDTA containing 0.5  $\mu$ g/mL ethidium bromide. DNA bands were visualized by mid-range ultraviolet light and quantified using an Alpha Innotech digital imaging system. DNA cleavage was monitored by the conversion of negatively supercoiled plasmid DNA to nicked (single-stranded break) or linear (double-stranded break) molecules. CC<sub>50</sub> values (the concentration of drug that induced 50% maximal DNA cleavage complex formation) were calculated on GraphPad Prism Version 10.0.3 using a non-linear regression analysis with 95% confidence intervals.

For the assay that monitored competition between ciprofloxacin and 8-methyl-2,4-quinazolidinedione with GyrA<sup>S91F/D95G</sup> gyrase, the level of double-stranded DNA cleavage generated



by 500  $\mu\text{M}$  ciprofloxacin in the absence of the quinazolinone was used as a baseline and was subtracted from the cleavage level seen in the presence of both compounds. The amount of double-stranded DNA scission observed in the presence of 50  $\mu\text{M}$  8-methyl-2,4-quinazolinone alone was set to 100% to directly compare the ability of ciprofloxacin to compete with the quinazolinone in the active site of the enzyme. Ciprofloxacin (0-500  $\mu\text{M}$ ) and 8-methyl-2,4-quinazolinone (50  $\mu\text{M}$ ) were added simultaneously to reaction mixtures.  $\text{IC}_{50}$  values were calculated on GraphPad Prism using a non-linear regression analysis with 95% confidence intervals.

#### *Persistence of gyrase/topoisomerase IV-cleaved DNA complexes*

The persistence of gyrase/topoisomerase IV-DNA cleavage complexes was determined as described previously.<sup>305</sup> Cleavage complexes were formed by combining 50 nM pBR322 and 200 nM *N. gonorrhoeae* gyrase or 100 nM *N. gonorrhoeae* topoisomerase IV in the presence of 10  $\mu\text{M}$  OSUAB-185 in a total volume of 20  $\mu\text{L}$  of *N. gonorrhoeae* gyrase/topoisomerase IV DNA cleavage buffer. Parallel control experiments were conducted to assess cleavage complexes formed in the absence of the NBTI by combining 50 nM pBR322 and 500 nM *N. gonorrhoeae* gyrase/topoisomerase IV in 20  $\mu\text{L}$  cleavage buffer. Reactions were incubated at 37 °C until the DNA cleavage/ligation equilibria were reached (30 min with gyrase and 10 min with topoisomerase IV) and diluted 20-fold in DNA cleavage buffer lacking  $\text{Mg}^{2+}$ . Samples (20  $\mu\text{L}$ ) were stopped at time-points ranging from 0-60 min, subjected to electrophoresis, and visualized as described above for DNA cleavage. Nicked and linear DNA cleavage products at time zero were set to 100% to allow direct comparison between different conditions, and the persistence of cleavage complexes were determined by the decay of nicked (single-stranded breaks) or linear (double-stranded breaks) reaction products over time. Cleavage complex stability (half-life,  $t_{1/2}$ )

was calculated on GraphPad Prism using a non-linear regression analysis with 95% confidence intervals.

#### *Gyrase/topoisomerase IV-mediated DNA ligation*

DNA ligation mediated by *N. gonorrhoeae* gyrase and topoisomerase IV was monitored using the procedure of Aldred et al.<sup>305</sup> Initial reactions contained 10 nM pBR322 and 100 nM wild-type *N. gonorrhoeae* gyrase or topoisomerase IV in the absence or presence of 10  $\mu$ M OSUAB-185. To better visualize levels of DNA breaks mediated by gyrase or topoisomerase IV in the absence of the NBTI, 10 mM MgCl<sub>2</sub> was replaced by 10 mM CaCl<sub>2</sub>.<sup>401</sup> DNA cleavage/ligation equilibria were established for 30 min with gyrase and 10 min with topoisomerase IV at 37 °C. DNA ligation was initiated by shifting samples from 37 °C to 65 °C, which allows enzyme-mediated ligation but prevents new rounds of DNA cleavage from occurring.<sup>166</sup> This results in a unidirectional sealing of the cleaved DNA. Reactions were stopped at time points ranging from 0-60 s, subjected to electrophoresis, and visualized as described above for DNA cleavage. Nicked and linear DNA cleavage products at time zero were set to 100% to allow direct comparison between different conditions, and DNA ligation of single- or double-stranded breaks was monitored by the loss of nicked or linear DNA, respectively. The rate of DNA ligation ( $t_{1/2}$ ) was calculated on GraphPad Prism using a non-linear regression analysis with 95% confidence intervals.

## CHAPTER III

### 1,2-NAPHTHOQUINONE AS A POISON OF HUMAN TYPE II TOPOISOMERASES

This chapter is adapted with permission from my co-author Neil Osheroff and the publisher *Chem. Res. Toxicol.* 2021, 34, 1082-1090. Copyright 2021 American Chemical Society.

#### Introduction

Naphthoquinones are secondary metabolites of naphthalene that are found in multiple species of bacteria, fungi, plants, and mammals.<sup>404, 405</sup> These compounds serve important physiological roles in the electron transport chain (ubiquinone and plastoquinone) and in vitamin K synthesis (menadione).<sup>404, 405</sup> Due to their yellow or brown color, naphthoquinones also have been used as pigmentation agents for centuries.<sup>404</sup> In addition, these compounds have been used in a broad range of medicinal applications, including antibiotic, antiviral, antiparasitic, fungicidal, and insecticidal (among others) treatments.<sup>404</sup> Thus, many traditional medicines across the world include naphthoquinone-based components.<sup>404</sup>

Despite the medicinal uses of many naphthoquinones, some members of this family have been associated with negative health outcomes.<sup>404-406</sup> For example, 1,2-naphthoquinone is an electrophilic environmental pollutant found in diesel exhaust particles (Figure 3.1).<sup>406-410</sup> It has been associated with the formation of cataracts and altered pulmonary function in vertebrate animal models.<sup>406, 411, 412</sup> Furthermore, this compound is cytotoxic and genotoxic, impairs mitochondrial function, and promotes an enhanced inflammatory response.<sup>406, 413-417</sup>

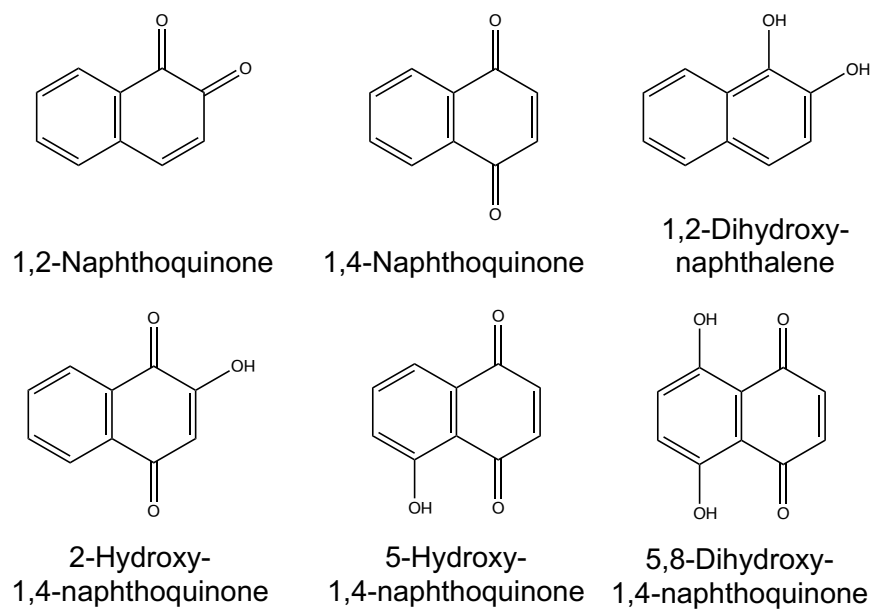


**Figure 3.1. Naphthoquinones.**

Structures of 1,2-naphthoquinone, 1,4-naphthoquinone, and related compounds.

Several quinones and polyphenols (that can be converted to quinones by redox cycling) increase the levels of DNA cleavage mediated by human type II topoisomerases.<sup>418-427</sup> Among these compounds, environmental toxins such as 1,4-benzoquinone (leukemogenic benzene metabolite) and polychlorinated biphenyl (PCB) quinones (toxic metabolites of PCBs) are associated with the formation of human cancers.<sup>420, 421</sup> In contrast, a variety of dietary quinones/polyphenols associated with human health benefits have also been identified as topoisomerase II poisons. Compounds included on this list are (–)-epigallocatechin gallate (EGCG, the active ingredient in green tea), thymoquinone (the active ingredient in *Nigella sativa*, or black seed), curcumin (the primary olfactory and taste component of turmeric), hydroxytyrosol and oleuropein (antioxidants found in olives), and menadione (vitamin K3).<sup>419, 423-426</sup> These natural products display chemoprotective, anti-inflammatory, and antioxidant properties.<sup>418-421, 423-426</sup> Many have been components of traditional and herbal medicines for millennia.<sup>418, 423-426</sup> It has been suggested that at least some of the toxic and medicinal properties of quinones/polyphenols are mediated through interactions with the human type II topoisomerases.<sup>420, 421, 424-426, 428</sup>

Two previous studies characterized interactions between 1,2-naphthoquinone and eukaryotic type II topoisomerases. One examined the effects of the compound on the isolated ATPase domain of human topoisomerase II $\alpha$  and determined that 1,2-naphthoquinone inhibited ATP hydrolysis.<sup>429</sup> However, this study did not examine the effects of the compound on DNA scission. The second study reported that 1,2-naphthoquinone increased DNA cleavage mediated by calf thymus topoisomerase II (a mixture of the  $\alpha$  and  $\beta$  isoforms) but reported no information other than its potency being higher than that of menadione (vitamin K3).<sup>419</sup>

Therefore, to further understand the effects of 1,2-naphthoquinone on the human type II enzymes, we characterized the ability of the compound to act as a topoisomerase II poison. Results indicate that 1,2-naphthoquinone increases levels of double-stranded DNA scission mediated by topoisomerase II $\alpha$  and II $\beta$  but was more potent and efficacious toward the  $\alpha$  isoform. Furthermore, the characteristics of DNA cleavage induced by 1,2-naphthoquinone indicate that

the compound acts as a covalent, rather than an interfacial, poison of the human topoisomerase II $\alpha$ . Although mechanistic studies with topoisomerase II $\beta$  were less conclusive, they also suggest that 1,2-naphthoquinone acts (at least in part) as a covalent poison of the  $\beta$  isoform.

## Results

1,2-Naphthoquinone (see Figure 3.1) is a cytotoxic and genotoxic quinone-based electrophile that is an environmental pollutant found in diesel exhaust particles.<sup>405-410, 413</sup> Several other quinone-based biologically active compounds enhance topoisomerase II-mediated DNA scission.<sup>418-428</sup> Therefore, the effects of 1,2-naphthoquinone on DNA strand breaks generated by human topoisomerase II $\alpha$  and II $\beta$  were examined.

### *1,2-Naphthoquinone is a poison of human type II topoisomerases*

As seen in Figures 3.2 and 3.3, 1,2-naphthoquinone is an efficacious human topoisomerase II poison. The compound generated primarily double-stranded DNA breaks and enhanced levels of enzyme-mediated cleavage more than an order of magnitude compared to baseline values. At 50  $\mu$ M 1,2-naphthoquinone, the compound induced ~25% and ~14% double-stranded DNA cleavage mediated by human topoisomerase II $\alpha$  and II $\beta$ , respectively. By comparison, the same concentration of etoposide induced only ~7% and ~3.5% DNA scission by the two enzyme isoforms.

To assess the effects of carbonyl position and hydroxyl group inclusion on the naphthoquinone ring system, the abilities of 1,4-naphthoquinone, 2-hydroxy-1,4-naphthoquinone, 5-hydroxy-1,4-naphthoquinone, and 5,8-dihydroxy-1,4-naphthoquinone (see Figure 3.1) to induce enzyme-mediated double-stranded DNA cleavage were examined (Figures 3.2 and 3.3). 1,4-Naphthoquinone forms the backbone of vitamin K and the other compounds are used as dyes.<sup>404, 405, 419</sup> Of these naphthoquinone derivatives, only 1,4-naphthoquinone displayed appreciable

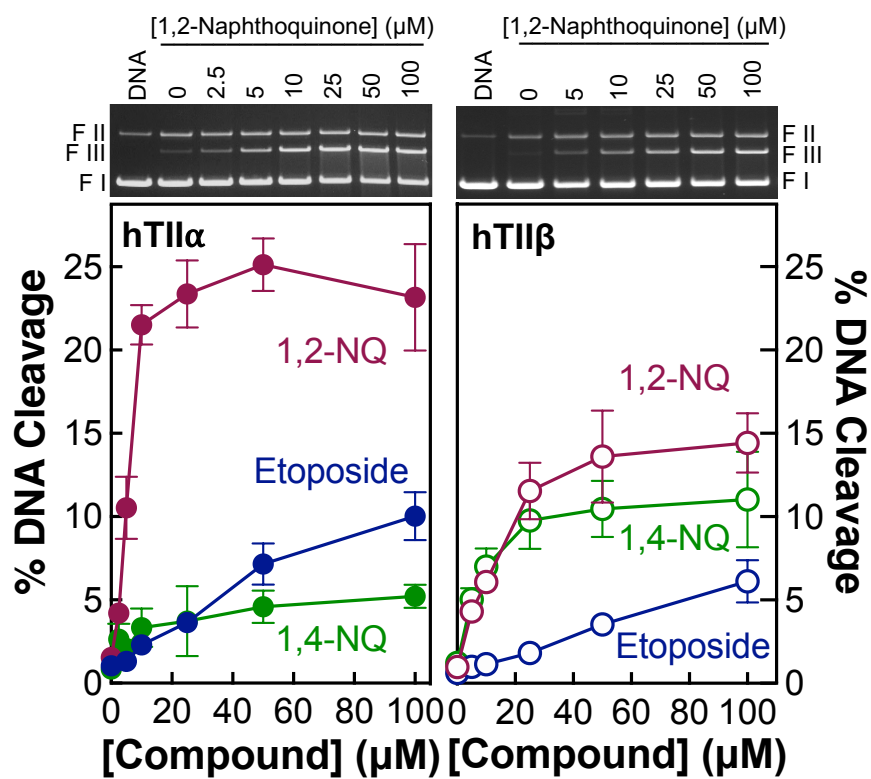


**Figure 3.2. 1,2-Naphthoquinone and 1,4-naphthoquinone enhance DNA cleavage mediated by human topoisomerase II $\alpha$  and II $\beta$ .**

The graphs show the effects of 1,2-naphthoquinone (maroon) and 1,4-naphthoquinone (green) on double-stranded DNA cleavage mediated by human topoisomerase II $\alpha$  (hTII $\alpha$ , left) and II $\beta$  (hTII $\beta$ , right). Results for etoposide (blue) are displayed for comparison. Error bars represent standard deviations (SDs) for at least three independent experiments. Representative gels for DNA cleavage assays with 1,2-naphthoquinone and the respective enzymes are shown above the graphs. Negatively supercoiled DNA (DNA) is shown as a control. The mobilities of negatively supercoiled DNA (form I, FI), nicked circular DNA (form II, FII), and linear DNA (form III, FIII) are indicated.

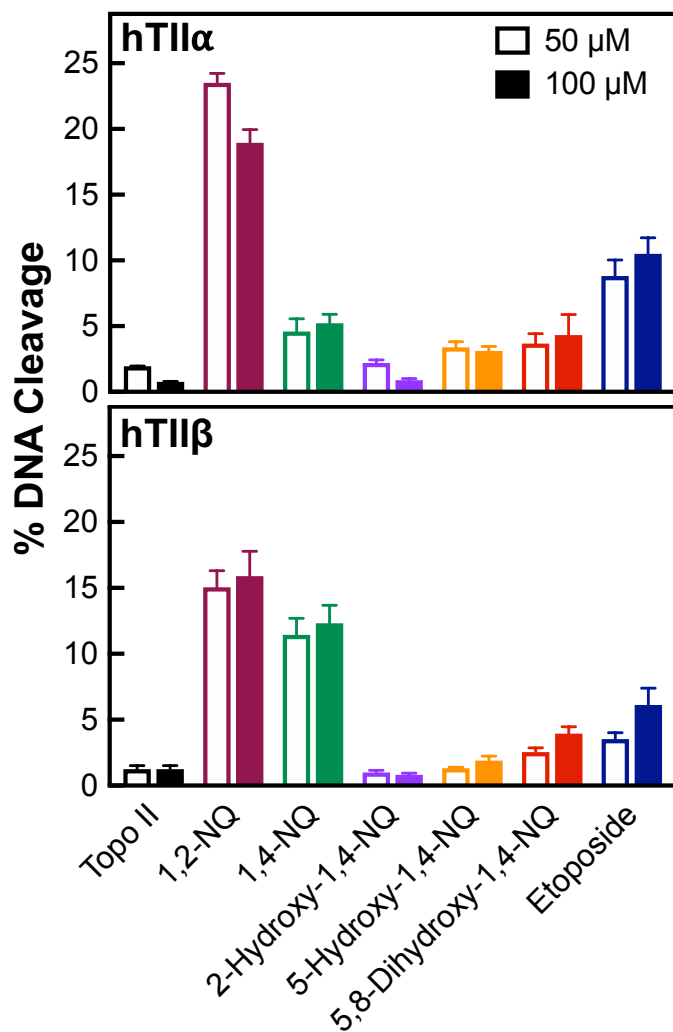


**Figure 3.3. Effects of naphthoquinone derivatives on DNA cleavage mediated by human type II topoisomerases.**

Results are shown for DNA cleavage mediated by human topoisomerase II $\alpha$  (hTII $\alpha$ , top panel) and II $\beta$  (hTII $\beta$ , bottom panel) induced by 50 or 100  $\mu$ M 1,2-naphthoquinone (1,2-NQ, maroon); 1,4-naphthoquinone (1,4-NQ, green); 2-hydroxy-1,4-naphthoquinone (2-hydroxy-1,4-NQ, purple); 5-hydroxy-1,4-naphthoquinone (5-hydroxy-1,4-NQ, orange); and 5,8-dihydroxy-1,4-naphthoquinone (5,8-dihydroxy-1,4-NQ, red). Etoposide (blue) is shown for comparison. Error bars represent SDs for at least three independent experiments.



activity. 1,4-Naphthoquinone induced less DNA cleavage than the 1,2-isomer and displayed a different preference for the two isoforms of topoisomerase II. Whereas 1,2-naphthoquinone was twice as efficacious against topoisomerase II $\alpha$  compared to II $\beta$ , 1,4-naphthoquinone was at least two times more active against the  $\beta$  isoform. The reasons underlying these different preferences are unknown. Therefore, additional studies were carried out to further characterize the effects of 1,2-naphthoquinone on topoisomerase II $\alpha$  and II $\beta$ .

To ensure that DNA cleavage induced by 1,2-naphthoquinone was mediated by the human type II topoisomerases, a series of control experiments were carried out (Figure 3.4). First, the compound failed to induce DNA cleavage in the absence of enzyme. Second, linear and nicked DNA reaction products did not enter the gel unless samples were treated with Proteinase K. This result is consistent with a covalent protein–DNA linkage. Third, the addition of EDTA (which chelates the required active site divalent cations)<sup>54</sup> prior to trapping the cleavage complex with SDS reversed double-stranded DNA cleavage. Similarly, treatment of reaction mixtures with NaCl (which diminishes enzyme–DNA binding) prior to trapping the cleavage complex also lowered the levels of DNA scission. Reversibility of DNA cleavage is a hallmark of the type II enzymes. It is notable that greater salt reversibility was observed with topoisomerase II $\beta$ , which is consistent with previous reports that cleavage complexes formed with the  $\beta$  isoform are less stable than those generated by topoisomerase II $\alpha$ .<sup>430, 431</sup>

As an additional control, time courses of 1,2-naphthoquinone-induced DNA cleavage against topoisomerase II $\alpha$  and II $\beta$  were performed (Figure 3.5). For both enzyme isoforms, the levels of DNA cleavage plateaued within the duration of the 6 min cleavage assay and were followed by a DNA cleavage/ligation equilibrium. These hyperbolic time courses are consistent with topoisomerase II-mediated DNA cleavage. Taken together, control experiments provide strong evidence that the enhanced DNA scission observed in the presence of 1,2-naphthoquinone is mediated by the human type II enzymes.

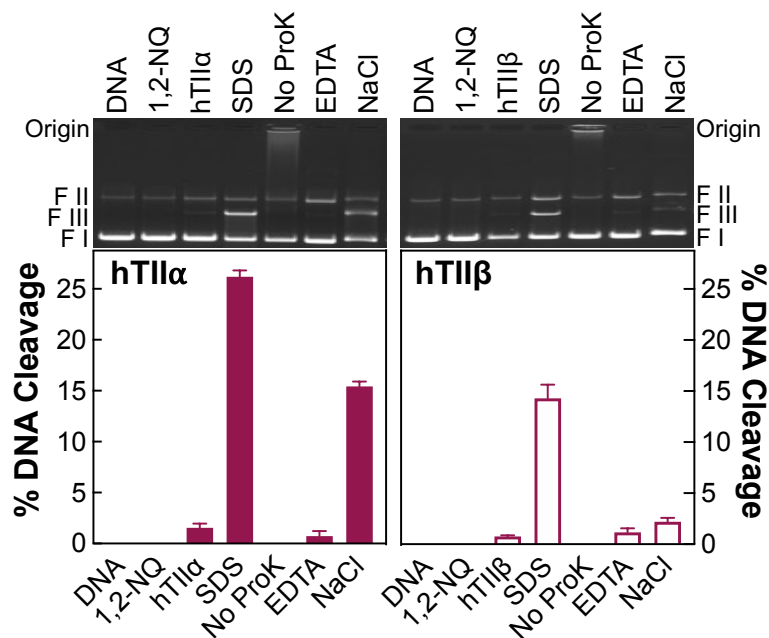


**Figure 3.4. DNA cleavage induced by 1,2-naphthoquinone is mediated by human topoisomerase II $\alpha$  and II $\beta$ .**

Results with topoisomerase II $\alpha$  (hTII $\alpha$ ) are shown at the left and topoisomerase II $\beta$  (hTII $\beta$ ) at the right. The bar graph shows double-stranded DNA cleavage from reactions that contained negatively supercoiled DNA alone (DNA), DNA with 50  $\mu$ M or 100  $\mu$ M 1,2-naphthoquinone (for reactions with hTII $\alpha$  and hTII $\beta$ , respectively) in the absence of enzyme (1,2-NQ), topoisomerase II $\alpha$  or II $\beta$  with DNA in the absence of 1,2-NQ (hTII $\alpha$ , hTII $\beta$ ), or complete reactions that were stopped with SDS prior to the addition of EDTA and Proteinase K (SDS). In other reactions, Proteinase K was omitted (No ProK) or reactions were treated with 22 mM EDTA (EDTA) or 500 mM NaCl (NaCl) for 5 min prior to the addition of SDS and Proteinase K. Error bars represent SDs for at least three independent experiments. A representative gel is shown at the top and DNA positions are as indicated in Figure 3.2.

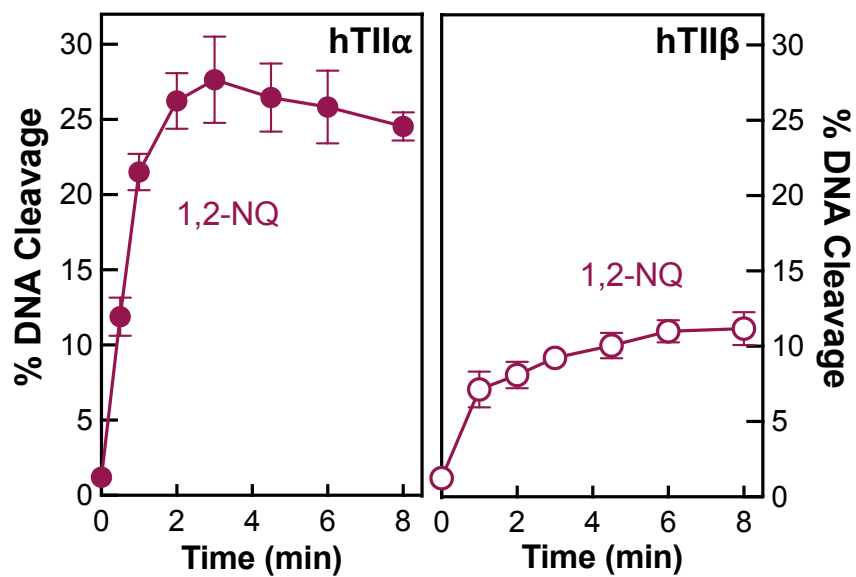


**Figure 3.5. Establishment of DNA cleavage/ligation equilibria induced by 1,2-naphthoquinone with human topoisomerase II $\alpha$  or II $\beta$ .**

The graph displays the time course of DNA cleavage mediated by human topoisomerase II $\alpha$  (hTII $\alpha$ , filled circles, left) and II $\beta$  (hTII $\beta$ , open circles, right) in the presence of 50  $\mu$ M or 100  $\mu$ M 1,2-naphthoquinone (1,2-NQ), respectively. Error bars represent SDs for at least three independent experiments.

### *Effects of ATP on the enhancement of double-stranded DNA cleavage induced by 1,2-naphthoquinone*

Type II topoisomerases do not require ATP for DNA cleavage or ligation (although the high energy cofactor raises baseline levels of DNA scission).<sup>87, 432</sup> However, ATP is required for the enzyme to carry out its complete double-stranded DNA passage reaction.<sup>87, 432</sup> Furthermore, a previous study provided evidence that 1,2-naphthoquinone interacts at the ATP binding site of topoisomerase II $\alpha$  and inhibits ATP hydrolysis (at least in the isolated ATPase domain).<sup>429</sup> Therefore, the effects of the high energy cofactor on 1,2-naphthoquinone-induced DNA cleavage were assessed (note that the other cleavage assays shown in this paper did not contain ATP). As seen in Figure 3.6, similar levels of DNA cleavage were observed in the absence or presence of ATP for both topoisomerase II $\alpha$  and II $\beta$ . Therefore, 1,2-naphthoquinone poisons the human type II topoisomerases under conditions that support the complete catalytic reaction of the enzymes.

### *Covalent vs interfacial topoisomerase II poisons*

Topoisomerase II poisons can be classified as being either interfacial or covalent.<sup>78, 151, 152, 175, 433</sup> Interfacial poisons include anticancer drugs such as etoposide, amsacrine, and mitoxantrone and bind noncovalently at the interface between the enzyme and its DNA substrate.<sup>78, 151, 152, 175, 187</sup> These compounds interact with both the protein and the DNA in the cleavage complex and block ligation by inserting between the 3'-hydroxyl and 5'-phosphate of the cleaved double helix.<sup>78, 151, 152, 175, 187</sup> As a result, most interfacial poisons are strong inhibitors of topoisomerase II-mediated DNA ligation.<sup>78, 151, 152, 175, 187, 402</sup>

In contrast, covalent topoisomerase II poisons, which include a variety of quinone-, polyphenol-, and isothiocyanate-containing compounds,<sup>418-423, 425-428</sup> form protein-adducts via an acylation reaction at cysteine (and potentially other) residues that are outside of the active site of

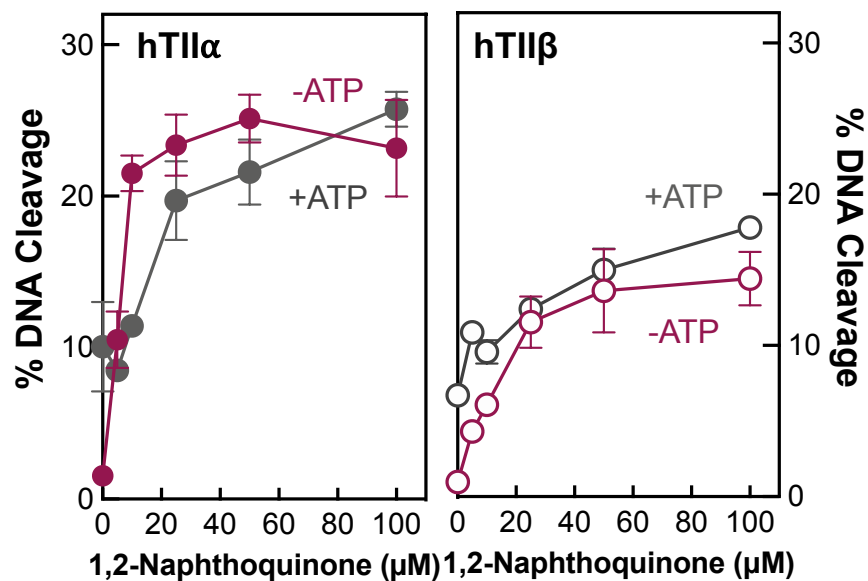


**Figure 3.6. Effects of ATP on the enhancement of double-stranded DNA cleavage induced by 1,2-naphthoquinone with human topoisomerase II $\alpha$  or II $\beta$ .**

Results with topoisomerase II $\alpha$  (hTII $\alpha$ , filled circles) are shown at the left and topoisomerase II $\beta$  (hTII $\beta$ , open circles) at the right. The graphs show the concentration dependence of 1,2-naphthoquinone-induced DNA cleavage in the absence (-ATP, maroon) or presence (+ATP, grey) of 1 mM ATP. Error bars represent SDs for at least three independent experiments.

type II topoisomerases.<sup>78, 434-436</sup> Our understanding of the mechanism by which covalent poisons enhance enzyme-mediated DNA cleavage is less detailed than that described for interfacial poisons. However, covalent poisons appear to act (at least in part) by closing the N-terminal protein gate of topoisomerase II.<sup>421, 437</sup> Because of their covalent attachment to the enzyme, covalent poisons can induce long-lived (i.e. highly persistent) DNA cleavage/ligation equilibria.<sup>431</sup> However, because these compounds do not act by intercalating between the cleaved DNA ends at the scissile bond, they often display a lesser ability to inhibit ligation compared to interfacial poisons that physically block the rejoining of the DNA termini.<sup>425, 426, 438</sup>

Due to the mechanism of action of covalent topoisomerase II poisons, there are a number of additional hallmarks that distinguish compounds in this class from interfacial poisons. First, because the oxidation state of covalent poisons is critical for their adduction chemistry, reducing agents, such as ascorbic acid, prevent their activity against topoisomerase II.<sup>439</sup> Similarly, sulfhydryl reagents, such as DTT, adduct to covalent poisons and inactivate them.<sup>420, 424-428, 438, 439</sup> In contrast, as interfacial poisons are not dependent on redox chemistry for their activity, they are generally unaffected by reducing or sulfhydryl reagents.<sup>420, 428, 438</sup> Second, because covalent poisons close the N-terminal gate of topoisomerase II, they block plasmid DNA from binding to the enzyme.<sup>421, 435, 437</sup> As such, when covalent poisons are incubated with topoisomerase II prior to the addition of DNA, they inhibit, rather than enhance, DNA cleavage.<sup>420, 421, 424-426, 428, 435, 437-440</sup> Interfacial poisons, which act at the active site of the enzyme, induce DNA scission regardless of the order of addition.<sup>175, 419, 421, 438</sup> Finally, because of the reliance of covalent poisons on the N-terminal domain of topoisomerase II, these compounds are unable to induce DNA cleavage with the catalytic core of topoisomerase II $\alpha$  (which lacks both the N-terminal and C-terminal domains of the protein).<sup>439, 441</sup> Due to their interactions at the active site of the enzyme, interfacial poisons maintain their ability to induce scission with the truncated protein.<sup>439, 441</sup>

*1,2-Naphthoquinone is a covalent poison of human topoisomerase II $\alpha$*

To evaluate the mechanism by which 1,2-naphthoquinone poisons human topoisomerase II $\alpha$ , the effects of sulfhydryl and reducing agents on the activity of the compound were determined (Figure 3.7). Similar to the effects of the prototypical covalent poison, 1,4-benzoquinone, on DNA cleavage mediated by human topoisomerase II $\alpha$ , the activity of 1,2-naphthoquinone was abrogated when DTT or ascorbic acid were incubated with the compound prior to inclusion of the quinone in reaction mixtures. It is notable that the effects of DTT on topoisomerase II poisons were observed only when the sulfhydryl reagent reacted with the free compound; once protein adducts were formed, they were not reversed by the addition of DTT.<sup>420, 424-428, 438, 439</sup> Similar to the results seen with 1,4-benzoquinone, the addition of DTT following the establishment of cleavage complexes did not affect the induction of DNA scission by 1,2-naphthoquinone (Figure 3.7). In contrast, DTT and ascorbic acid had little effect on DNA cleavage induced by the interfacial poison etoposide.

Generally, the reduction of quinone-based covalent poisons to their corresponding hydroxyl forms results in a loss of activity.<sup>420, 442</sup> Surprisingly, this was not the case with 1,2-naphthoquinone, as 1,2-dihydroxynaphthalene (see Figure 3.1) displayed high activity against topoisomerase II $\alpha$  (Figure 3.7). However, the activity of the dihydroxy compound was abrogated when DTT or ascorbic acid was added prior to incubation with the enzyme. Moreover, the majority of the activity was retained when 1,2-dihydroxynaphthalene was incubated with DTT after the establishment of DNA cleavage complexes. Because 1,2-dihydroxynaphthalene displays the hallmarks of a covalent poison, the most likely explanation for these results is that the compound readily undergoes redox cycling to the reactive quinone form. This has been reported previously for polyphenolic bioflavonoids and catechins.<sup>422, 423, 428</sup>

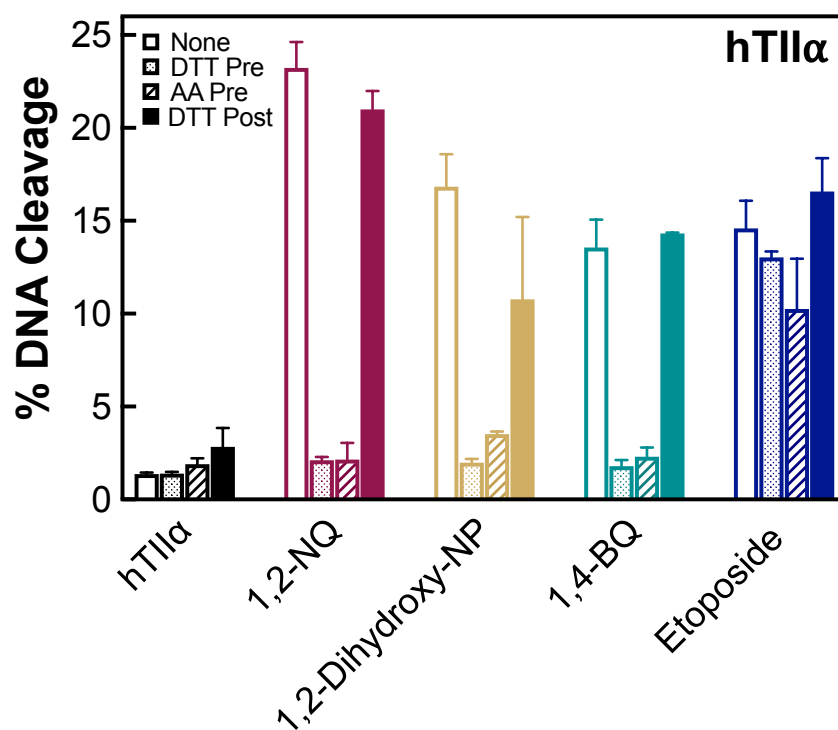


**Figure 3.7. Effects of sulfhydryl and reducing agents on topoisomerase II $\alpha$ -mediated double-stranded DNA cleavage induced by 1,2-naphthoquinone.**

Topoisomerase II $\alpha$ -DNA cleavage reactions were performed in the absence of sulfhydryl/reducing agents (open bars), in the presence of 2 mM DTT (stippled bars) or 2 mM ascorbic acid (AA, diagonal bars) added prior to the start of the 6 min DNA cleavage reaction, or 2 mM DTT added after the 6 min cleavage reaction (filled bars). Results are shown for reactions that contained no compound (hTII $\alpha$ , black), 50  $\mu$ M 1,2-naphthoquinone (1,2-NQ, maroon), 50  $\mu$ M 1,2-dihydroxynaphthalene (1,2-Dihydroxy-NP, gold), 25  $\mu$ M 1,4-benzoquinone (BQ, teal), or 100  $\mu$ M etoposide (blue). 1,4-Benzoquinone and etoposide were included as controls for the effects of the sulfhydryl and reducing agents on a covalent and interfacial topoisomerase II poison, respectively. Error bars represent SDs for at least three independent experiments.



Consistent with the characteristics of a covalent poison, 1,2-naphthoquinone induced topoisomerase II $\alpha$  to form long-lived cleavage complexes (Figure 3.8, left). In the absence of the quinone, cleavage complexes rapidly dissociated following dilution into buffer that lacked divalent metal ion, with a half-life of less than 5 s. In contrast, cleavage complexes formed in the presence of 1,2-naphthoquinone persisted for at least 2 h with no observed decrease in DNA scission. Moreover, 1,2-naphthoquinone inhibited ligation but to a much lesser extent than the interfacial poison etoposide (Figure 3.8, right).

As further evidence that 1,2-naphthoquinone is a covalent poison of topoisomerase II $\alpha$ , incubation of 50  $\mu$ M compound with topoisomerase II $\alpha$  prior to the addition of DNA resulted in a rapid loss of enzyme activity ( $t_{1/2}$  ~80 s) (Figure 3.9). This exposure completely blocked the ability of the enzyme to cleave DNA within 5 min. In a control experiment that lacked the quinone, topoisomerase II $\alpha$  maintained its DNA cleavage activity when incubated in the absence of DNA over the same 5 min period (Figure 3.9, inset).

Finally, the ability of 1,2-naphthoquinone to induce DNA scission was severely impeded when the catalytic core of human topoisomerase II $\alpha$  (which lacks both its N- and C-terminal domains) when used in place of the full-length enzyme (Figure 3.10). Whereas etoposide was still able to induce DNA cleavage with the catalytic core (albeit at lower levels than with the wild-type enzyme), virtually no DNA cleavage was seen in the presence of the quinone. Taken together, the above experiments provide strong evidence that 1,2-naphthoquinone is a covalent poison of human topoisomerase II $\alpha$ .

### *1,2-Naphthoquinone displays characteristics of a covalent poison against human topoisomerase II $\beta$ .*

As observed with topoisomerase II $\alpha$  (see Figure 3.7), DTT abolished the ability of 1,2-

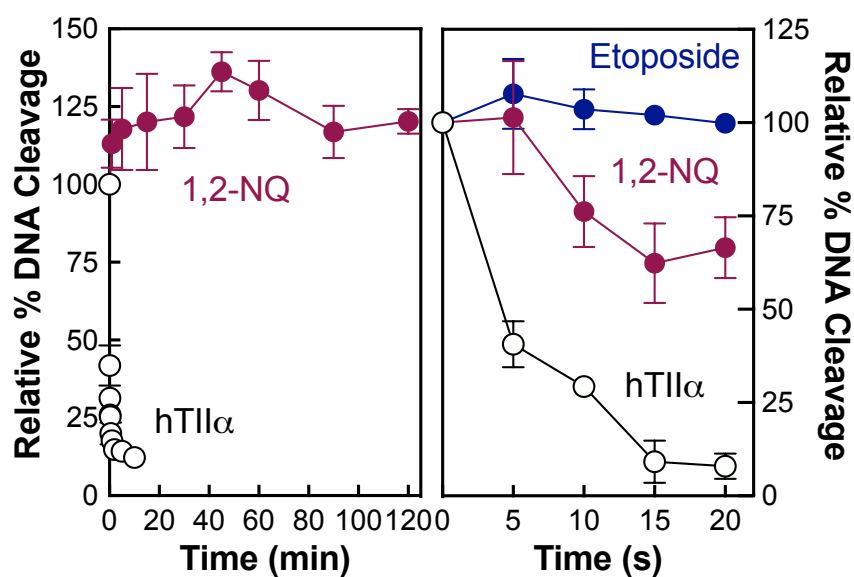


**Figure 3.8. Effects of 1,2-naphthoquinone on the persistence and ligation of DNA cleavage complexes generated by human topoisomerase II $\alpha$ .**

The persistence of topoisomerase II $\alpha$ -DNA cleavage complexes formed in the presence of 1,2-naphthoquinone is shown on the left. DNA cleavage/ligation equilibria were established in the absence (hTII $\alpha$ , black) or presence of 50  $\mu$ M 1,2-naphthoquinone (1,2-NQ, maroon). Persistence assays were initiated by diluting reaction mixtures 20-fold into buffer that lacked divalent cations, and the stability of cleavage complexes was monitored by the loss of double-stranded DNA breaks over time. DNA cleavage at time zero was set to 100%. Error bars represent SDs for at least three independent experiments. The inhibition of topoisomerase II $\alpha$ -mediated DNA ligation by 1,2-naphthoquinone is displayed on the right. DNA cleavage/ligation equilibria were established in the absence (hTII $\alpha$ , black) or presence of 50  $\mu$ M 1,2-naphthoquinone (1,2-NQ, maroon) and ligation was initiated by transferring assays from 37  $^{\circ}$ C to 0  $^{\circ}$ C. Results with 100  $\mu$ M etoposide (blue) are shown for comparison. Double-stranded DNA cleavage levels prior to the induction of ligation were set to 100%. Error bars represent SDs for at least three independent experiments.

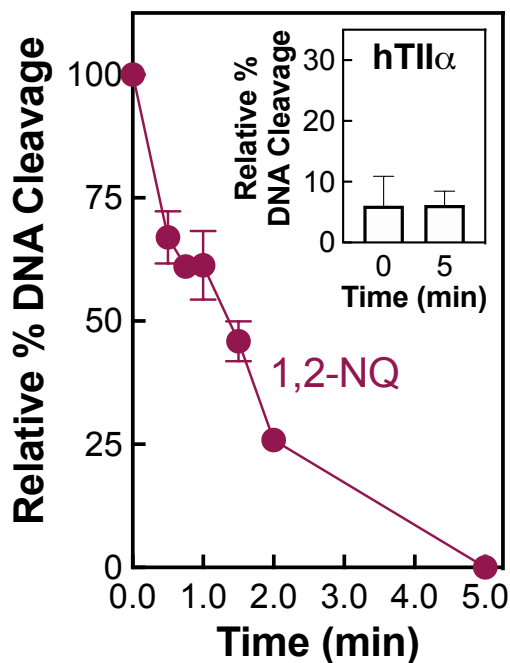


**Figure 3.9. 1,2-Naphthoquinone inactivates human topoisomerase II $\alpha$  when incubated with the enzyme prior to the addition of DNA.**

Double-stranded DNA scission was monitored in the presence of 50  $\mu$ M 1,2-naphthoquinone (maroon). Times indicate the length of incubation of the naphthoquinone with topoisomerase II $\alpha$  prior to the addition of DNA. DNA cleavage levels were calculated relative to those induced when 1,2-naphthoquinone and the enzyme were not incubated prior to reaction initiation. The inset shows a control experiment (hTII $\alpha$ , open black bars) in which the enzyme (in the absence of compound) was incubated for 5 min at 37  $^{\circ}$ C prior to the addition of DNA. Error bars represent SDs for at least three independent experiments.

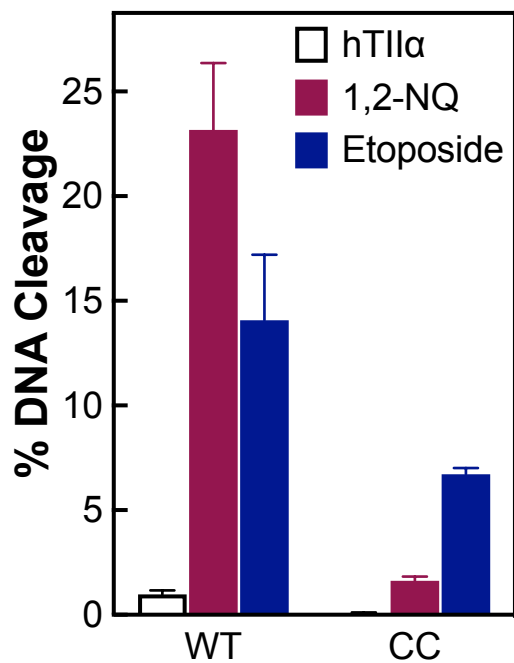


**Figure 3.10. 1,2-Naphthoquinone induces minimal DNA cleavage mediated by the catalytic core of human topoisomerase II $\alpha$ .**

The graph compares double-stranded DNA cleavage levels for wild-type (WT) topoisomerase II $\alpha$  and the catalytic core (CC) of the enzyme (containing residues 431-1193) in the absence (hTII $\alpha$ , open black bars) or presence of 50  $\mu$ M 1,2-naphthoquinone (1,2-NQ, maroon bars). Results with 100  $\mu$ M etoposide (blue bars) are shown for comparison. Error bars represent SDs for at least three independent experiments.

naphthoquinone to induce topoisomerase II $\beta$ -mediated DNA scission when incubated with the quinone prior to cleavage assays but had no effect on the activity of the compound when added after cleavage complexes were established (Figure 3.11). This result establishes that 1,2-naphthoquinone can act as a covalent poison of topoisomerase II $\beta$ . However, further experiments suggest that the compound displays mixed activity against the  $\beta$  isoform. Although DTT, which should adduct the quinone, undercut the activity of the compound, ascorbic acid, which should reduce and maintain the compound in its hydroxyl form, had virtually no effect on DNA cleavage. Indeed, levels of DNA scission induced by 100  $\mu$ M 1,2-naphthoquinone in the presence of 2 mM ascorbic acid were  $\sim$ 90% of those observed in the absence of reducing agent. This result suggests that the hydroxyl form of 1,2-naphthoquinone potentially acts as an interfacial poison of topoisomerase II $\beta$ . Consistent with this hypothesis, 1,2-dihydroxynaphthalene displayed high activity against the  $\beta$  isoform and exhibited responses to the sulfhydryl and reducing agents that were similar to those seen with the quinone.

## Discussion

1,2-Naphthoquinone is an environmental pollutant that has been linked to a variety of health issues in mammalian species and exhibits cytotoxic and genotoxic properties.<sup>405-410, 413</sup> Many environmental and dietary quinones and polyphenols have been shown to act as topoisomerase II poisons.<sup>418-421, 423-426, 428, 436</sup> Several of these environmental quinones/polyphenols have been linked to the formation of human cancers; however, many of the dietary topoisomerase II poisons display chemopreventative properties and have been used extensively in traditional and indigenous medicines to treat a variety of conditions.<sup>404, 420, 421, 424-426, 428, 436</sup> Because of the rich history linking quinones and type II topoisomerases, the effects of 1,2-naphthoquinone on DNA cleavage mediated by human topoisomerase II $\alpha$  and II $\beta$  were examined.

Results indicate that 1,2-naphthoquinone is a topoisomerase II poison with preferential

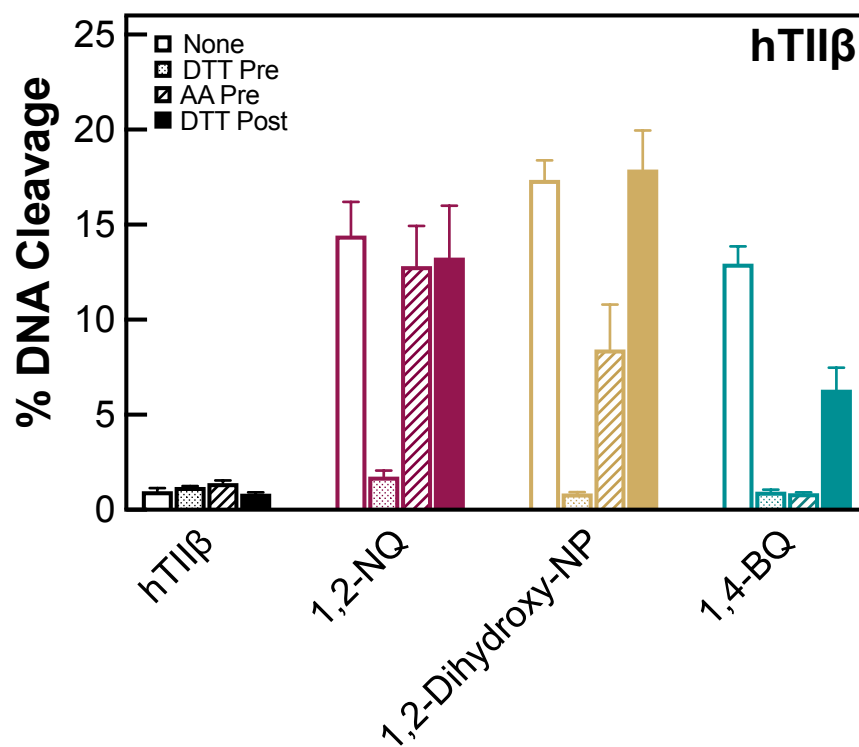


**Figure 3.11. Effects of sulfhydryl and reducing agents on topoisomerase II $\beta$ -mediated double-stranded DNA cleavage induced by 1,2-naphthoquinone.**

Topoisomerase II $\beta$ -DNA cleavage reactions were performed in the absence of sulfhydryl/reducing agents (open bars), in the presence of 2 mM DTT (stippled bars) or 2 mM ascorbic acid (AA, diagonal bars) added prior to the start of the 6 min DNA cleavage reaction, or 2 mM DTT added after the 6 min cleavage reaction (filled bars). Results are shown for reactions that contained no compound (hTII $\beta$ , black), 50  $\mu$ M 1,2-naphthoquinone (1,2-NQ, maroon), 50  $\mu$ M 1,2-dihydroxynaphthalene (1,2-Dihydroxy-NP, gold), or 25  $\mu$ M 1,4-benzoquinone (BQ, teal). 1,4-Benzoquinone was included as a control for the effects of the sulfhydryl and reducing agents on a covalent topoisomerase II poison. Error bars represent SDs for at least three independent experiments.

activity against the  $\alpha$  isoform. Furthermore, although the quinone acts as a covalent poison against both enzyme isoforms, our experiments suggest that the dihydroxy form of 1,2-naphthoquinone (or potentially the parent quinone) may also act as an interfacial poison of topoisomerase II $\beta$ .

In general, topoisomerase II poisons that induce the most stable cleavage complexes are the most damaging to cells.<sup>431</sup> As determined by persistence assays, 1,2-naphthoquinone-induced DNA cleavage complexes, at least with topoisomerase II $\alpha$ , are long-lived and show no degradation over a 2 h time course. Taken together, the above findings suggest that the type II enzymes may be able to mediate some of the effects of the quinone on the human genome.

A previous study demonstrated that 1,2-naphthoquinone inhibited the ability of the isolated N-terminal domain of human topoisomerase II $\alpha$  to hydrolyze ATP.<sup>429</sup> The relationships between the inhibition of ATPase activity and the enhancement of DNA cleavage by 1,2-naphthoquinone are not known and are likely to be complex. Two possibilities exist: a two-site model and a one-site model. In the two-site model, there are two distinct binding sites for the quinone, one that interferes with ATP interactions and another that stabilizes the closed form of the N-terminal clamp (leading to enhanced cleavage). In support of this model, etoposide, a well-characterized interfacial poison, appears to have two binding sites on topoisomerase II: one in the DNA cleavage/ligation active site that stabilizes cleavage complexes and the other in the ATPase domain.<sup>187, 427, 443-445</sup> In the one-site model, the same adduction of the quinone that stabilizes the closed N-terminal domain also alters the ability of the enzyme to interact with ATP. It is likely that considerably more detailed structural and enzymological studies will be necessary to deconvolute the actions of 1,2-naphthoquinone in light of these two models.

In summary, 1,2-naphthoquinone acts as a covalent poison against topoisomerase II $\alpha$  and II $\beta$ . Our findings suggest that some of the genotoxicity and cytotoxicity associated with 1,2-naphthoquinone may be attributed to its ability to induce DNA double-stranded breaks generated by the human type II enzymes.

## CHAPTER IV

### TARGET-MEDIATED FLUOROQUINOLONE RESISTANCE IN *NEISSERIA GONORROHEAE*: ACTIONS OF CIPROFLOXACIN AGAINST GYRASE AND TOPOISOMERASE IV

This chapter is adapted with permission from my co-authors Alexandria A. Oviatt, Pan F. Chan, and Neil Osheroff and the publisher *ACS Infect. Dis.* 2024, in press. Copyright 2024 Jessica A. Collins, Alexandria A. Oviatt, Pan F. Chan, and Neil Osheroff.

#### Introduction

Target-mediated resistance has curtailed the medical utility of fluoroquinolones to treat some bacterial infections since the clinical introduction of this class in the 1960s.<sup>154-156, 266</sup> An important example is *Neisseria gonorrhoeae*, a Gram-negative bacterium that is the etiological agent of gonorrhea.<sup>446</sup> This sexually transmitted disease infects the mucosal epithelium of the genitals, rectum, and throat and causes more than 82 million new cases globally each year.<sup>320, 321</sup> If left untreated, gonorrhea can cause severe complications including pelvic inflammatory disease and infertility, and when disseminated, infections can result in death.<sup>320, 323</sup>

Ciprofloxacin was introduced as frontline treatment for gonorrheal infections in the early 1990s.<sup>324, 325</sup> However, the drug was removed from treatment guidelines for this indication by the Centers for Disease Control and Prevention (CDC) in 2006 due to high levels of resistance.<sup>326</sup> In 2021, nearly 33% of clinical *N. gonorrhoeae* isolates in the United States were resistant to ciprofloxacin compared with 13.3% in 2011 and 0.7% in 2001.<sup>447</sup> As a result of resistance to fluoroquinolones and other antibacterials, gonorrhea is listed as one of five “urgent threats” (the



highest threat level) for resistance by the CDC,<sup>448</sup> and the WHO has warned that drug resistant gonorrhea has the potential to become the third incurable sexually transmitted disease following HIV/AIDS and herpes.<sup>449</sup>

Despite the prevalence and clinical impact of fluoroquinolone-resistant gonorrhea, little is known about the interactions of this drug class with its type II topoisomerase targets from *N. gonorrhoeae*. Therefore, we characterized the effects of ciprofloxacin on the catalytic and DNA cleavage activities of gyrase and topoisomerase IV from this species. Interactions with wild-type (WT) enzymes and with enzymes harboring mutations found in fluoroquinolone-resistant isolates were determined. Results suggest that the enhancement of gyrase-mediated DNA cleavage is the primary mechanism by which ciprofloxacin induces its cytotoxic effects. Furthermore, the *in vitro* effects of mutations in residues that anchor the water-metal ion bridge in gyrase and topoisomerase IV may explain the patterns of enzyme-targeting and clinical resistance to fluoroquinolones in this sexually transmitted disease.

## Results and Discussion

### *Gyrase-mediated fluoroquinolone resistance*

Shortly after fluoroquinolones were approved to treat gonorrhea, cases of drug resistance were reported.<sup>325, 450-454</sup> In laboratory experiments utilizing cultured strains of *N. gonorrhoeae* serially diluted and plated with increasing concentrations of ciprofloxacin, the first spontaneous mutations that exhibited decreased susceptibility to fluoroquinolones were seen in gyrase.<sup>284</sup> This result indicated that gyrase is the primary cellular target for ciprofloxacin and (presumably) other members of this drug class in gonorrhea.<sup>284, 455</sup> Similar results have been reported for resistant isolates from clinical samples.<sup>456-460</sup>

Overwhelmingly, mutations in the GyrA subunit of gyrase were observed at Ser91 and Asp95 in *N. gonorrhoeae*.<sup>461</sup> In laboratory-based genetic studies, the initial mutation event occurs

at Ser91 followed by the acquisition of a second genetic alteration at Asp95 to yield a double mutant.<sup>284</sup> Individual substitution at Asp95 is rarely found.<sup>284, 461, 462</sup> Furthermore, higher MIC (minimum inhibitory concentration) values for ciprofloxacin in laboratory strains and clinical isolates are associated with gyrase that contains mutations in both residues.<sup>284, 457, 458, 460</sup> These findings are reflected in the prevalence of the mutations in patient samples, in which 77.0% of resistant isolates harbor mutations at both Ser91 and Asp95, as opposed to 19.0% at Ser91 and only 2.5% at Asp95 individually.<sup>461</sup> The serine and aspartic acid associated with fluoroquinolone resistance are the residues predicted to anchor the fluoroquinolone-gyrase-water-metal ion bridge shown in Figure 4.1.<sup>154, 155, 167, 303, 304, 461</sup> These findings suggest that *N. gonorrhoeae* gyrase, like other species, relies on the water-metal ion bridge to facilitate interactions with fluoroquinolones.

Despite the importance of gyrase as the primary target of fluoroquinolone treatment in gonorrhea and the role of Ser91 and Asp95 in drug resistance, very little has been reported regarding the interactions of fluoroquinolones with this type II enzyme from *N. gonorrhoeae*. Moreover, the contributions of the individual amino acid residues to bridge function have never been reported, as only the double mutant has been assessed.<sup>329</sup> Therefore, we investigated the effects of ciprofloxacin on the catalytic and DNA cleavage activities of WT gyrase as well as the individual (GyrA<sup>S91F</sup> and GyrA<sup>D95G</sup>) and double (GyrA<sup>S91F/D95G</sup>) mutants associated with fluoroquinolone resistance in cellular studies and clinical isolates.

Initial studies examined the effects of ciprofloxacin on catalytic activity by monitoring DNA supercoiling catalyzed by WT, GyrA<sup>S91F</sup>, GyrA<sup>D95G</sup>, and GyrA<sup>S91F/D95G</sup> *N. gonorrhoeae* gyrase (Figure 4.2). The fluoroquinolone was a potent inhibitor of the WT enzyme with an IC<sub>50</sub> value of 0.39 μM. Despite the fact that mutations at Ser91 are much more prevalent than those at Asp95 in clinical isolates,<sup>461</sup> ciprofloxacin displayed equivalent reductions in potency (~60-fold) against the GyrA<sup>S91F</sup> and GyrA<sup>D95G</sup> mutant enzymes (IC<sub>50</sub> = 24.7 μM and 23.8 μM, respectively). Consistent with cellular results,<sup>284, 458, 461</sup> the GyrA<sup>S91F/D95G</sup> double mutant showed a considerably

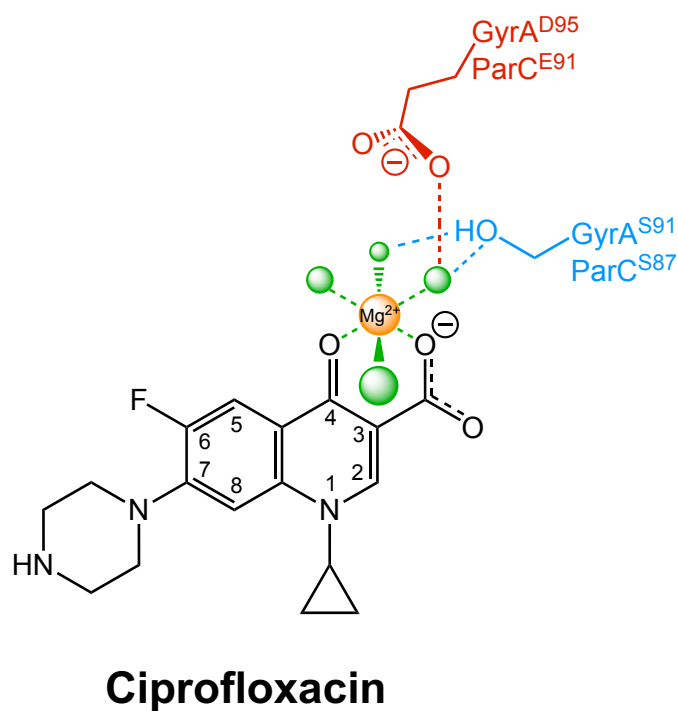


**Figure 4.1. Schematic of the water-metal ion bridge that mediates interactions between ciprofloxacin and *N. gonorrhoeae* gyrase and topoisomerase IV.**

For simplicity, only interactions with the protein (and not the DNA) are shown. A non-catalytic divalent metal ion (orange,  $Mg^{2+}$ ) forms an octahedral coordination sphere (green dashed lines) between four water molecules (green) and the C3/C4 keto-acid of ciprofloxacin (black). Two of the water molecules form hydrogen bonds (blue dashed lines) with the serine side chain hydroxyl group (blue), and one water molecule hydrogen bonds (red dashed lines) with the aspartic acid (GyrA) or glutamic acid (ParC) side chain carboxyl group (red).

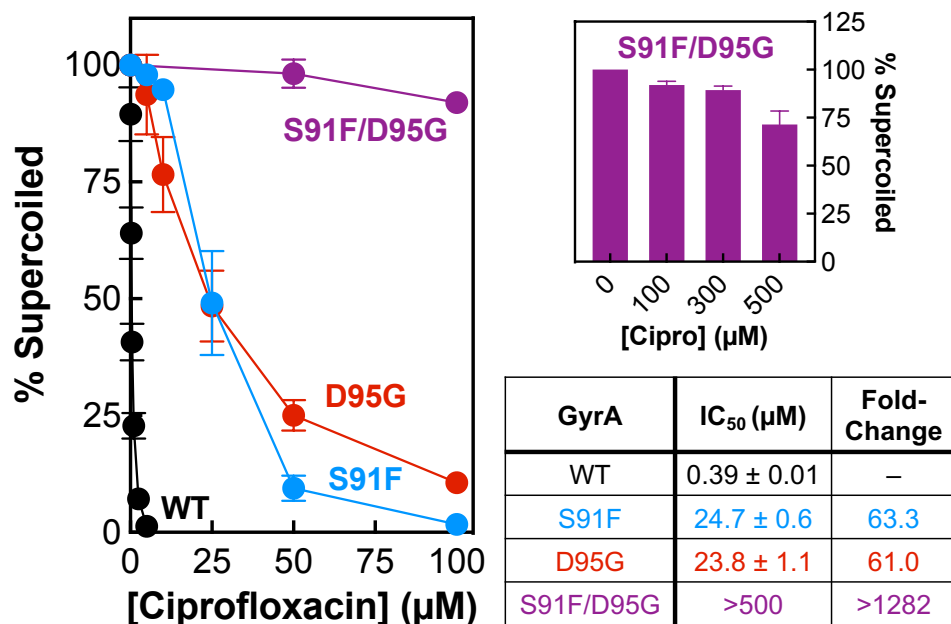


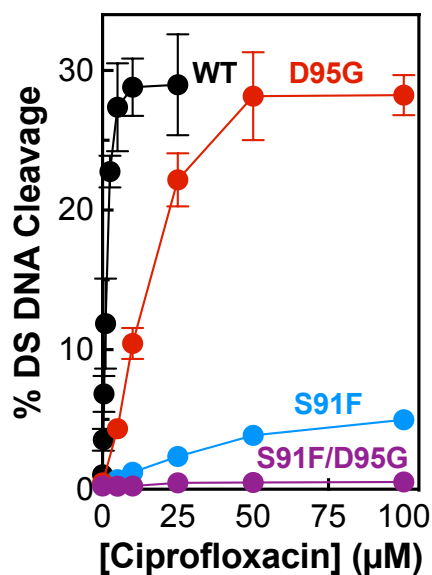
**Figure 4.2. Effects of ciprofloxacin on DNA supercoiling catalyzed by WT and mutant *N. gonorrhoeae* gyrase.**

The abilities of WT (black), GyrA<sup>S91F</sup> (S91F, blue), GyrA<sup>D95G</sup> (D95G, red) and GyrA<sup>S91F/D95G</sup> (S91F/D95G, purple) gyrase to supercoil relaxed plasmid in the presence of ciprofloxacin are shown in the left panel. The righthand panel displays the ability of GyrA<sup>S91F/D95G</sup> gyrase to supercoil relaxed DNA at high ciprofloxacin concentrations (up to 500 μM). Error bars represent the standard deviation of at least 3 independent experiments. The table indicates the corresponding IC<sub>50</sub> values (the drug concentration at which the enzyme activity is inhibited by 50%), including the standard error of the mean, and the fold-change in IC<sub>50</sub> from WT.

reduced susceptibility to ciprofloxacin (Figure 4.2, right). Even at 500  $\mu\text{M}$  drug, less than 30% inhibition of DNA supercoiling was observed.

Considering that GyrA<sup>S91F</sup> and GyrA<sup>D95G</sup> have similar sensitivities to ciprofloxacin in DNA supercoiling assays, it is unclear why individual mutations at Asp95 are rarely observed in resistant isolates, while those at Ser91 occur at high frequencies.<sup>461</sup> Consequently, we compared the effects of ciprofloxacin on DNA cleavage mediated by gyrase harboring the GyrA<sup>S91F</sup> and GyrA<sup>D95G</sup> single mutations to that of WT *N. gonorrhoeae* gyrase (Figures 4.3). In contrast to DNA supercoiling, there was a striking difference between the two mutants in DNA cleavage assays. Ciprofloxacin increased double-stranded DNA scission mediated by GyrA<sup>D95G</sup> to a level comparable to that of WT gyrase (28.2% vs 29.0%, respectively), albeit with an ~10-fold reduction in potency ( $\text{CC}_{50}$  = 13.9  $\mu\text{M}$  vs 1.3  $\mu\text{M}$ , respectively). However, even at 100  $\mu\text{M}$ , ciprofloxacin induced no more than 5.0% DNA cleavage with GyrA<sup>S91F</sup> gyrase with an even greater reduction in potency ( $\text{CC}_{50}$  = 40.0  $\mu\text{M}$ ). These results strongly suggest that ciprofloxacin resistance in *N. gonorrhoeae* cells that carry the GyrA<sup>S91F</sup> mutation tracks with gyrase-mediated DNA cleavage rather than gyrase-catalyzed DNA supercoiling. They further imply that under normal growth conditions, fluoroquinolone-induced cytotoxicity associated with this first-step mutation is caused by the introduction of breaks in the bacterial chromosome as opposed to the loss of gyrase function.

The reduced susceptibility of GyrA<sup>S91F/D95G</sup> to ciprofloxacin was far more dramatic than seen with either of the enzymes carrying the single mutations (Figures 4.3). Even at concentrations as high as 500  $\mu\text{M}$ , the fluoroquinolone induced only 0.53% double-stranded DNA cleavage. This finding is consistent with clinical studies in which the double mutant is considerably more prevalent than the single Ser91 mutant in resistant strains.<sup>461</sup> Although the enhanced resistance associated with the GyrA<sup>S91F/D95G</sup> mutation may be attributed to further loss of DNA scission induced by ciprofloxacin, it is tempting to speculate that the inability of the drug to inhibit



GyrA	CC <sub>50</sub> (µM)	Fold-Change	Max % DSB
WT	1.3 ± 0.1	–	29.0
S91F	40.0 ± 8.2	30.8	5.0
D95G	13.9 ± 1.2	10.7	28.2
S91F/D95G	N/A	N/A	0.53

**Figure 4.3. Effects of ciprofloxacin on DNA cleavage mediated by WT and mutant *N. gonorrhoeae* gyrase.**

The ability of ciprofloxacin to induce double-stranded (DS) DNA cleavage mediated by WT (black), GyrA<sup>S91F</sup> (S91F, blue), GyrA<sup>D95G</sup> (D95G, red), and GyrA<sup>S91F/D95G</sup> (S91F/D95G, purple) gyrase are shown in the top panel. Error bars represent the standard deviation of at least 3 independent experiments. The table at the bottom lists the CC<sub>50</sub> value (the drug concentration at which 50% maximal DS DNA cleavage is reached) for each enzyme, including the standard error of the mean, the fold-change in CC<sub>50</sub> from WT, and the Max % DSB value (maximal percentage of DS DNA breaks) induced at 100 µM ciprofloxacin. Values marked as “N/A” were excluded from additional analyses due to low signal.

DNA supercoiling by the double mutant (see Figure 4.2) may contribute to its reduced susceptibility to fluoroquinolones in cells that harbor this double mutant gyrase.

*Use of the water-metal ion bridge to promote fluoroquinolone interactions in N. gonorrhoeae gyrase.*

Previous studies provide strong evidence that the water-metal ion bridge is the primary conduit between fluoroquinolones and bacterial type II topoisomerases (see Figure 4.1), but that the amino acids that anchor the bridge are utilized differently across species and enzymes.<sup>154, 155, 305-309</sup> The finding that mutations at Ser91 and Asp95 comparably reduce the IC<sub>50</sub> values for inhibition of DNA supercoiling (see Figure 4.2) and also lessen ciprofloxacin potency in DNA cleavage assays (see Figure 4.3) suggest that these two bridge-anchoring residues contribute similarly to the affinity of *N. gonorrhoeae* gyrase for ciprofloxacin. However, the dramatic decrease in drug-induced DNA cleavage by GyrA<sup>S91F</sup> implies that Ser91 (in contrast to Asp95) also plays a role in correctly positioning ciprofloxacin in the active site of the enzyme, such that it stabilizes the cleavage complex.

The reduced effects of ciprofloxacin on GyrA<sup>S91F/D95G</sup> compared to the single mutant enzymes (GyrA<sup>S91F</sup> and GyrA<sup>D95G</sup>) strongly suggest that simultaneous substitution of both bridge-anchoring residues severely diminishes the affinity of the enzyme for the fluoroquinolone. To determine whether this was the case, competition studies that monitored fluoroquinolone interactions at the site of the water-metal ion bridge were performed. To this end, the ability of ciprofloxacin to compete with 8-methyl-2,4-quinazolinedione was assessed (Figure 4.4). Quinazolinediones are similar in structure to fluoroquinolones but lack the C3/C4 keto-acid that is required to chelate the divalent metal ion used in the bridge.<sup>463, 464</sup> Although they share a binding site with fluoroquinolones,<sup>55, 465</sup> 8-methyl-2,4-quinazolinedione and related compounds interact with bacterial type II topoisomerases through their C7 3'-(aminomethyl)pyrrolidinyl moiety,

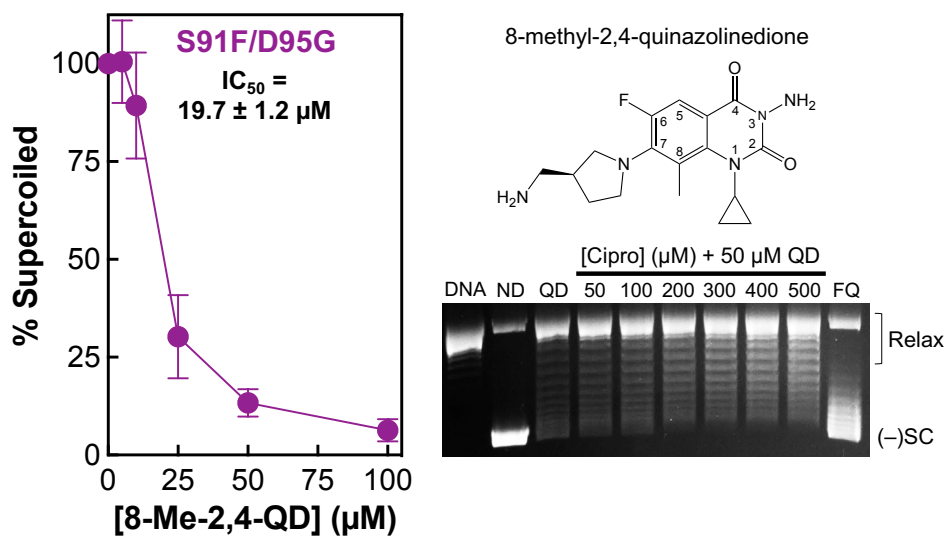


**Figure 4.4. Effects of 8-methyl-2,4-quinazolinone on the DNA supercoiling activities of GyrA<sup>S91F/D95G</sup> *N. gonorrhoeae* gyrase.**

The ability of 8-methyl-2,4-quinazolinone (8-Me-2,4-QD, structure at right) to inhibit DNA supercoiling catalyzed by GyrA<sup>S91F/D95G</sup> gyrase (purple) is shown in the left panel ( $IC_{50} = 19.7 \pm 1.2 \mu M$ ). Error bars represent the standard deviation of at least 3 independent experiments. The ability of 0-500  $\mu M$  ciprofloxacin to compete with 50  $\mu M$  8-methyl-2,4-quinazolinone (QD) for GyrA<sup>S91F/D95G</sup> gyrase during DNA supercoiling is shown in the gel in the right panel. Reaction mixtures contained DNA in the absence of enzyme (DNA) or GyrA<sup>S91F/D95G</sup> gyrase in the absence of compound (ND, no drug), in the presence of either 50  $\mu M$  8-methyl-2,4-quinazolinone (QD) or 500  $\mu M$  ciprofloxacin (FQ) alone, or in the presence of 50  $\mu M$  QD and increasing concentrations of ciprofloxacin (cipro, 50-500  $\mu M$ ). Both drugs were added to reaction mixtures simultaneously. The positions of relaxed (Relax) and negatively supercoiled [(-)SC] plasmid are indicated. The gel is representative of 3 independent experiments.



independent of the water-metal ion bridge.<sup>55, 463, 464, 466, 467</sup> Consequently, quinazolinodiones generally display high activity against fluoroquinolone-resistant type II topoisomerases.<sup>154, 155, 468</sup>

As seen in Figure 4.4, 8-methyl-2,4-quinazolinodione inhibits DNA supercoiling catalyzed by GyrA<sup>S91F/D95G</sup> with an IC<sub>50</sub> of 19.7 μM. Because ciprofloxacin has virtually no effect on supercoiling catalyzed by the GyrA<sup>S91F/D95G</sup> double mutant enzyme (see Figure 4.2), if it effectively competes for enzyme binding with 8-methyl-2,4-quinazolinodione, the fluoroquinolone should overcome the ability of the quinazolinodione to inhibit this enzyme-catalyzed reaction. However, even at concentrations as high as 500 μM, ciprofloxacin displayed little ability to reverse the inhibition of DNA supercoiling at a near saturating concentration of quinazolinodione (see gel in Figure 4.4). This indicates that the affinity of ciprofloxacin for GyrA<sup>S91F/D95G</sup> gyrase is greatly reduced compared to the WT enzyme.

To further study the effects of the double mutation on fluoroquinolone-gyrase interactions, we examined competition between ciprofloxacin and 8-methyl-2,4-quinazolinodione in DNA cleavage assays. As seen in Figure 4.5 (left panel), the quinazolinodione maintained (compared to WT enzyme) a high affinity and high maximal level of DNA cleavage with GyrA<sup>S91F/D95G</sup>. In contrast, ciprofloxacin did not enhance DNA scission at 500 μM with GyrA<sup>S91F/D95G</sup> (Figure 4.5, right, FQ lane). Thus, competition was monitored by the loss of quinazolinodione-induced double-stranded DNA breaks. Although ciprofloxacin was able to compete with 8-methyl-2,4-quinazolinodione, its competition IC<sub>50</sub> value was ~10-fold higher than the CC<sub>50</sub> value of the quinazolinodione against the double mutant enzyme and more than 100 times higher than its CC<sub>50</sub> value against WT gyrase (see Figure 4.3). Taken together, competition studies bolster the conclusion that the loss of the water-metal ion bridge substantially impedes the interactions of ciprofloxacin with GyrA<sup>S91F/D95G</sup>. These results provide an overarching mechanism for the high levels of drug resistance observed in strains that carry gyrase mutations in both Ser91 and Asp95.

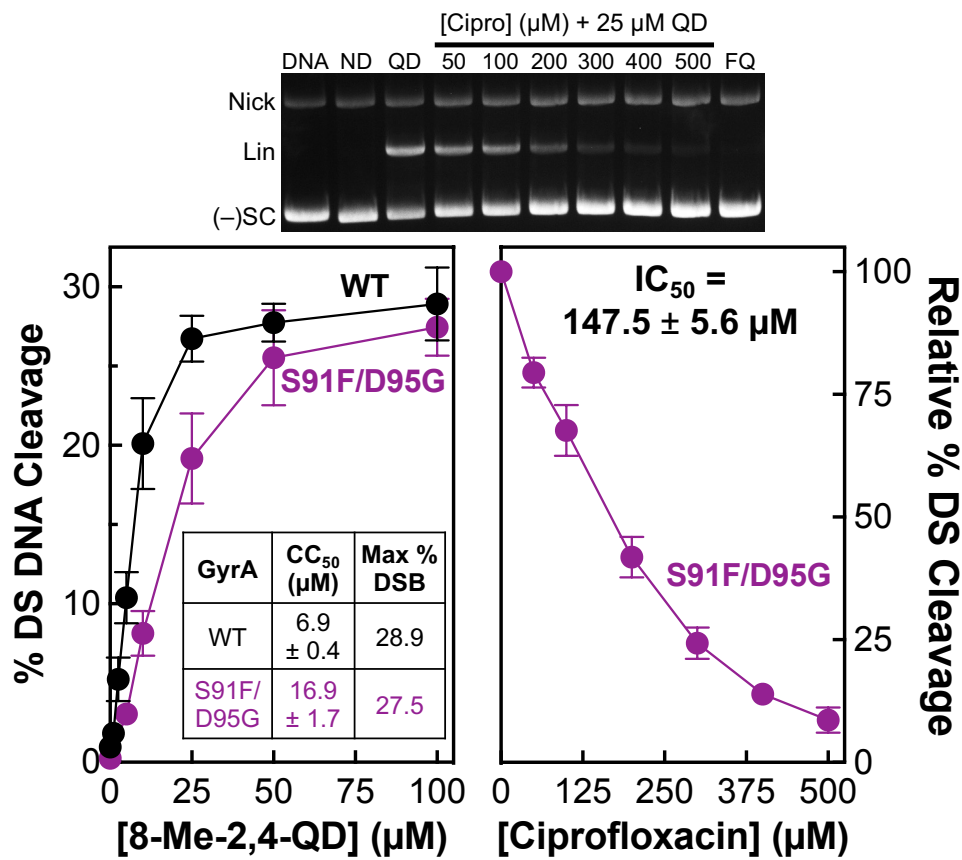


**Figure 4.5. Effects of 8-methyl-2,4-quinazolidione on the DNA cleavage activities of WT and GyrA<sup>S91F/D95G</sup> gyrase.**

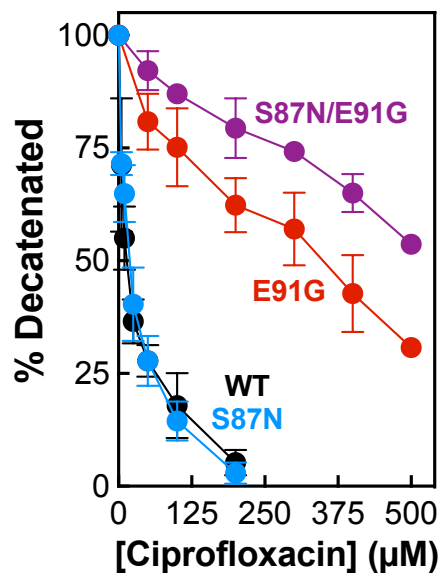
The ability of 8-methyl-2,4-quinazolidione (8-me-2,4-QD) to induce double-stranded (DS) DNA cleavage mediated by WT (black) and GyrA<sup>S91F/D95G</sup> gyrase (S91F/D95G, purple) is shown in the left panel. The inset table shows the corresponding CC<sub>50</sub>, including the standard error of the mean, and Max % DSB values. The ability of 0-500 μM ciprofloxacin (Cipro) to compete with 25 μM 8-methyl-2,4-quinazolidione (QD) for GyrA<sup>S91F/D95G</sup> gyrase-mediated DNA cleavage is shown in the right panel, including the IC<sub>50</sub> value. Both drugs were added to reaction mixtures simultaneously. The relative contribution of the quinazolidione to the total level of DNA cleavage was calculated as follows: (DS DNA cleavage in the presence of the quinazolidione and fluoroquinolone – DS DNA cleavage in the absence of either compound) / (DS DNA cleavage in the presence of 25 μM quinazolidione only). Error bars represent the standard deviation of at least 3 independent experiments. A gel image displaying the competition data quantified in the right panel is shown at the top. Reaction mixtures contained DNA in the absence of enzyme (DNA) or GyrA<sup>S91F/D95G</sup> gyrase in the absence of compound (ND, no drug), in the presence of either 25 μM 8-methyl-2,4-quinazolidione (QD) or 500 μM ciprofloxacin (FQ) alone, or in the presence of 25 μM 8-methyl-2,4-quinazolidione (QD) and increasing concentrations of ciprofloxacin (Cipro, 50-500 μM). The positions of nicked (Nick), linear (Lin), and negatively supercoiled [(-)SC] plasmid are indicated. The gel is representative of 3 independent experiments.

### *Topoisomerase IV-mediated fluoroquinolone resistance*

Although gyrase is the primary cellular target for fluoroquinolones in *N. gonorrhoeae*, laboratory strains and clinical isolates that carry additional mutations in topoisomerase IV display even higher levels of resistance.<sup>284, 456-460, 469-472</sup> These findings indicate that topoisomerase IV is a secondary target for this drug class in *N. gonorrhoeae*.<sup>325, 455</sup> Therefore, we evaluated the effects of ciprofloxacin on WT topoisomerase IV and enzymes that contained the single ParC<sup>S87N</sup> or ParC<sup>E91G</sup> mutation or the double ParC<sup>S87N/E91G</sup> mutation. These substitutions are associated with fluoroquinolone resistance in cellular and clinical studies and occur at the residues predicted to anchor the water-metal ion bridge in *N. gonorrhoeae* topoisomerase IV.<sup>154, 155, 305-309, 462</sup>

Initial experiments examined the effects of ciprofloxacin on topoisomerase IV-catalyzed decatenation (Figure 4.6). The fluoroquinolone was a less potent catalytic inhibitor against WT topoisomerase IV ( $IC_{50} = 13.7 \mu\text{M}$ ) than it was for gyrase ( $IC_{50} = 0.39 \mu\text{M}$ , see Figure 4.2). Furthermore, the mutations in the predicted bridge-anchoring residues had a smaller effect on the susceptibility of topoisomerase IV to ciprofloxacin than observed with gyrase. As compared to WT topoisomerase IV, the ParC<sup>S87N</sup> mutation had virtually no effect on the sensitivity of the enzyme to ciprofloxacin ( $IC_{50} = 16.4 \mu\text{M}$ ). Moreover, the difference in the relative sensitivity between the WT enzyme and ParC<sup>E91G</sup> or ParC<sup>S87N/E91G</sup> was also smaller than observed for the mutations at analogous residues in gyrase (see Figure 4.2).

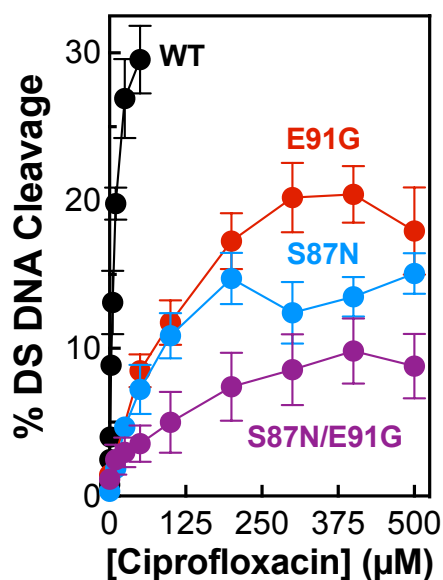
Further experiments investigated the effects of ciprofloxacin on DNA cleavage mediated by WT and mutant *N. gonorrhoeae* topoisomerase IV (Figures 4.7). Once again, the fluoroquinolone appeared to be less potent against WT topoisomerase IV ( $CC_{50} = 7.4 \mu\text{M}$ ) than gyrase ( $CC_{50} = 1.3 \mu\text{M}$ , see Figure 4.3). Levels of DNA scission mediated by WT topoisomerase IV above  $50 \mu\text{M}$  ciprofloxacin were not included in Figure 4.7, as multiple cleavage events per plasmid were observed at higher drug concentrations. Thus, the actual  $CC_{50}$  value is likely to be



ParC	IC <sub>50</sub> (μM)	Fold-Change
WT	13.7 ± 1.4	–
S87N	16.4 ± 1.2	1.2
E91G	301.5 ± 23.8	22.0
S87N/E91G	>500	>37

**Figure 4.6. Effects of ciprofloxacin on the DNA decatenation activities of WT and mutant *N. gonorrhoeae* topoisomerase IV.**

The ability of ciprofloxacin to inhibit decatenation catalyzed by WT (black), ParC<sup>S87N</sup> (S87N, blue), ParC<sup>E91G</sup> (E91G, red), and ParC<sup>S87N/E91G</sup> (S87N/E91G, purple) topoisomerase IV is shown in the top panel. Error bars represent the standard deviations of at least 3 independent experiments. Corresponding IC<sub>50</sub> values, including the standard error of the mean, and the fold-change in IC<sub>50</sub> from WT are indicated in the table at the bottom.



ParC	CC <sub>50</sub> (µM)	Fold-Change	Max % DSB
WT	7.4 ± 1.1	–	30.0
S87N	49.2 ± 7.5	6.6	15.0
E91G	80.0 ± 15.7	10.8	20.4
S87N/E91G	200.7 ± 238.9	27.1	9.8

**Figure 4.7. Effects of ciprofloxacin on the DNA cleavage activities of WT and mutant *N. gonorrhoeae* topoisomerase IV.**

The ability of ciprofloxacin to induce double-stranded (DS) DNA cleavage mediated by WT (black), ParC<sup>S87N</sup> (S87N, blue), ParC<sup>E91G</sup> (E91G, red), and ParC<sup>S87N/E91G</sup> (S87N/E91G, purple) topoisomerase IV is displayed in the top panel. Error bars represent the standard deviations of at least 3 independent experiments. The corresponding CC<sub>50</sub>, including the standard error of the mean, fold-change in CC<sub>50</sub> from WT, and Max % DSB values are indicated in the table at the bottom.

higher than the calculated value. Even though the ParC<sup>S87N</sup> mutation had no effect on the susceptibility of topoisomerase IV to ciprofloxacin in decatenation assays, it affected both the potency (CC<sub>50</sub> = 49.2 μM) and efficacy (Max % DSB = 15.0) of the drug in cleavage assays. Additionally, topoisomerase IV containing the ParC<sup>S87N/E91G</sup> double mutation displayed considerably higher levels of fluoroquinolone-induced cleavage activity (Max % DSB = 9.8) than was seen with gyrase (Max % DSB at 500 μM ciprofloxacin = 0.53).

Taken together, the catalytic and DNA cleavage activities of *N. gonorrhoeae* topoisomerase IV suggest that, similar to gyrase, the mutation at ParC Ser87 affects the positioning of the fluoroquinolone in the active site, reducing its ability to stabilize cleavage complexes. However, unlike results with gyrase, individual mutations at bridge-anchoring residues (ParC<sup>S87N</sup> and ParC<sup>E91G</sup>) had a similar effect on ciprofloxacin sensitivity in DNA cleavage assays. This implies a greater role for the acidic residue in anchoring topoisomerase IV-fluoroquinolone interactions than observed with gyrase.

Unfortunately, the relatively high activity of ciprofloxacin against fluoroquinolone-resistant topoisomerase IV precluded the use of quinazolidinedione competition studies to further analyze the role of the water-metal ion bridge in mediating drug-enzyme interactions. However, as compared with gyrase, the catalytic and DNA cleavage data for WT and mutant topoisomerase IV that harbor residues associated with fluoroquinolone resistance indicate that ciprofloxacin is less potent against topoisomerase IV and that mutations at bridge-anchoring residues have a lesser effect on the sensitivity of the enzyme to ciprofloxacin. Taken together, these findings may explain (at least in part) why topoisomerase IV is the secondary target of fluoroquinolones in *N. gonorrhoeae*.

Finally, the number of clinical studies that report single mutations at either ParC<sup>S87N</sup> or ParC<sup>E91G</sup> in topoisomerase IV is limited, and conclusions are complicated by the fact that these residues are only observed in the background of fluoroquinolone resistance mutations in gyrase.

<sup>456, 458, 460, 470, 472</sup> Thus, further studies will be necessary to draw conclusions regarding the relative

importance of mutations at the two bridge-anchoring residues in *N. gonorrhoeae* topoisomerase IV to clinical resistance.

In summary, fluoroquinolone-resistant *N. gonorrhoeae* is an immediate threat to global health. Unfortunately, little is known about the interactions of fluoroquinolones with gyrase and topoisomerase IV from this species. The work presented above links the effects of ciprofloxacin on gyrase to cellular and clinical studies and provides a mechanistic underpinning for the targeting and resistance of fluoroquinolones in *N. gonorrhoeae*.

## CHAPTER V

### ACTIONS OF A NOVEL BACTERIAL TOPOISOMERASE INHIBITOR AGAINST *NEISSERIA GONORRHOEAE* GYRASE AND TOPOISOMERASE IV: ENHANCEMENT OF DOUBLE-STRANDED DNA BREAKS

This chapter is adapted from *Int. J. Mol. Sci.* 2023, 24, 12107. Copyright 2023 by Soziema E. Dauda, Jessica A. Collins, Jo Ann W. Byl, Yanran Lu, Jack C. Yalowich, Mark J. Mitton-Fry, and Neil Osheroff.

#### Introduction

To address fluoroquinolone resistance, new classes of compounds are under development that also target gyrase/topoisomerase IV but interact with different amino acid residues in the enzymes.<sup>155, 266, 299, 330, 332, 333</sup> As discussed in chapter I, the triazaacenaphthylene gepotidacin is the most clinically advanced member of the novel bacterial topoisomerase inhibitor (NBTIs) class.<sup>155, 266, 336, 338, 358, 361, 362</sup> Results from global phase III clinical trials reported that gepotidacin was a safe and efficacious antibacterial therapy for the treatment of uncomplicated urinary tract infections caused by uropathogens, including *E. coli*.<sup>338, 358, 362, 473</sup> Gepotidacin also successfully completed phase III trials for uncomplicated urogenital gonorrhea (*N. gonorrhoeae*).<sup>336, 361, 474</sup> In contrast to fluoroquinolones, only a single NBTI molecule binds per cleavage complex.<sup>44, 299, 332</sup> The left-hand side of the molecule sits in a pocket in the DNA on the two-fold axis of the complex, midway between the two DNA cleavage sites, and the right-hand side sits in a pocket on the two-fold axis between the two GyrA/ParC subunits.<sup>44, 299, 332</sup> While fluoroquinolones induce gyrase/topoisomerase IV-mediated double-stranded breaks,<sup>154-156, 167, 303,</sup>



<sup>304</sup> a hallmark of NBTIs is the generation of enzyme-mediated single-stranded DNA breaks and the suppression of double-stranded breaks.<sup>332, 352, 366</sup> However, some dioxane-linked amide members of the NBTI class have been shown to induce double-stranded and single-stranded DNA breaks mediated by *Staphylococcus aureus* gyrase.<sup>345</sup>

To further explore the ability of NBTIs to induce double-stranded DNA breaks mediated by bacterial type II topoisomerases, we examined the effects of OSUAB-185 on the DNA cleavage activity of *N. gonorrhoeae* gyrase and topoisomerase IV. Although a member of the NBTI class, the substituents on this dioxane-linked amide NBTI differ considerably from those of canonical members (Figure 5.1). Similar to other NBTIs, OSUAB-185 induced single-stranded and suppressed double-stranded DNA breaks mediated by *N. gonorrhoeae* gyrase. However, in contrast to NBTIs such as GSK126,<sup>366</sup> OSUAB-185 stabilized both single- and double-stranded DNA breaks mediated by topoisomerase IV. It does not appear that the induction of double-stranded breaks is due to the binding of a second NBTI molecule. The ability to induce double-stranded DNA breaks extends to fluoroquinolone-resistant *N. gonorrhoeae* topoisomerase IV, as well as type II enzymes from other species. Together with previous work on the dioxane-linked amide NBTIs,<sup>345</sup> the double-stranded DNA cleavage activity of OSUAB-185 represents a paradigm shift in the hallmark characteristic of NBTIs and suggests that some members of this class may have alternative binding motifs in the cleavage complex.

## Results

*OSUAB-185 induces double-stranded DNA cleavage mediated by N. gonorrhoeae topoisomerase IV*

A previous study demonstrated that some dioxane-linked NBTIs were able to induce double-stranded (in addition to single-stranded) DNA breaks mediated by *S. aureus* gyrase.<sup>345</sup> Therefore, to further explore the ability of this NBTI subclass to induce double-stranded DNA

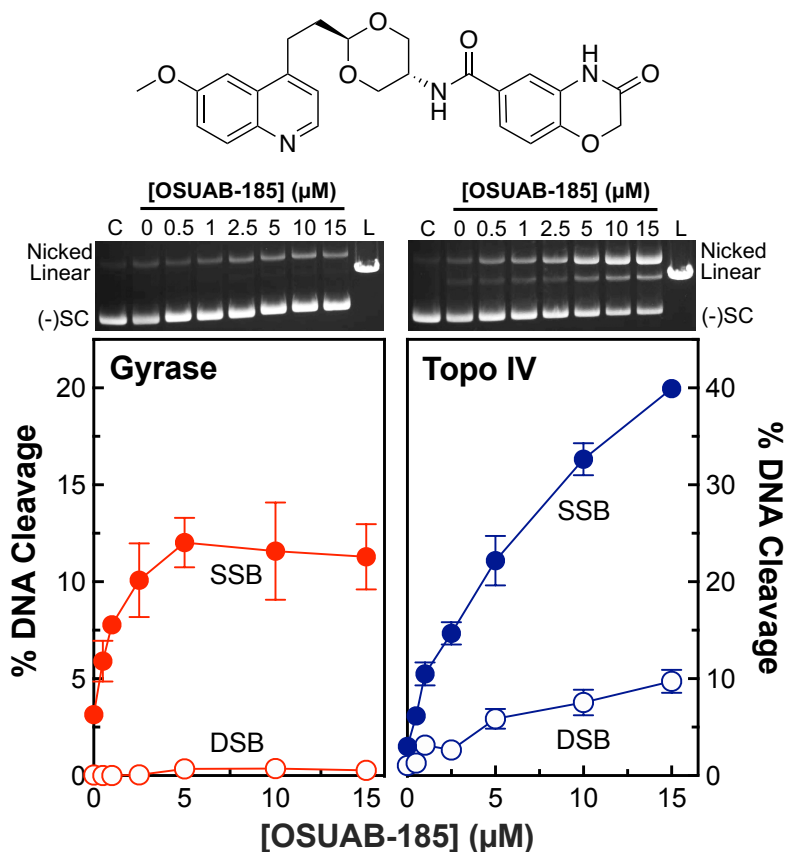


**Figure 5.1. OSUAB-185 enhances DNA cleavage mediated by *N. gonorrhoeae* gyrase and topoisomerase IV.**

The graphs show the effects of OSUAB-185 (top) on single-stranded (SSB, closed circle) and double-stranded (DSB, opened circle) DNA cleavage mediated by *N. gonorrhoeae* gyrase (red, left) and topoisomerase IV (Topo IV, blue, right). Note that the scaling of percent DNA cleavage on the y-axis differs between gyrase and topoisomerase IV. Error bars represent SDs for at least three independent experiments. Representative agarose gels for DNA cleavage assays with gyrase (left) and topoisomerase IV (right) are shown above the graphs. Control DNA (C) in the absence of enzyme and a linear DNA standard (L) are indicated. The positions of negatively supercoiled [(-)SC], nicked, and linear plasmid are shown.

breaks generated by bacterial type II topoisomerases and to address the basis for this activity, we assessed the effects of OSUAB-185 on DNA cleavage mediated by *N. gonorrhoeae* gyrase and topoisomerase IV (Figure 5.1). The NBTI displayed moderate activity against gyrase, increasing single-stranded DNA breaks to ~12.0% at a 5  $\mu$ M compound (compared to a baseline level of ~3.1%) with a  $CC_{50}$  value (concentration of compound required to induce 50% of maximal DNA cleavage) of ~0.9  $\mu$ M. As reported previously for other NBTIs,<sup>332, 352, 366</sup> induction of double-stranded DNA cleavage was not observed. Although OSUAB-185 was less potent against topoisomerase IV ( $CC_{50} \approx 4.8 \mu$ M), it was considerably more efficacious, inducing ~40% single-stranded DNA breaks at a 15  $\mu$ M compound (compared to a baseline level of ~3.0%). Strikingly, OSUAB-185 also increased double-stranded DNA breaks mediated by topoisomerase IV. Approximately 10% double-stranded DNA breaks were observed at a 15  $\mu$ M compound (compared to the baseline level of ~1%) with a  $CC_{50}$  value of ~5.7  $\mu$ M. The increase in double-stranded breaks is contrary to the hallmark of NBTIs, which is the induction of single-stranded DNA breaks by gyrase/topoisomerase IV and the suppression of enzyme-mediated double-stranded DNA breaks.<sup>332, 352, 366</sup>

To ensure that the DNA breaks induced by OSUAB-185 were being generated by gyrase and topoisomerase IV, two controls were carried out (Figure 5.2). First, no single- or double-stranded DNA cleavage was observed in the presence of the 10  $\mu$ M compound in the absence of an enzyme. Second, when DNA cleavage reactions were terminated by the addition of EDTA prior to SDS, DNA cleavage levels dropped for both enzymes. EDTA chelates the required catalytic  $Mg^{2+}$  ion, but only when the DNA is ligated.<sup>54</sup> Therefore, the decrease in cleaved DNA following EDTA treatment is inconsistent with a non-enzymatic reaction. These data provide strong evidence that the DNA breaks observed in the presence of OSUAB-185 were generated by gyrase and topoisomerase IV. It is notable that all of the NBTI-induced double-stranded breaks generated by topoisomerase IV disappeared in the presence of EDTA. This finding suggests that they may be less stable than the single-stranded DNA breaks generated in the presence of the compound.

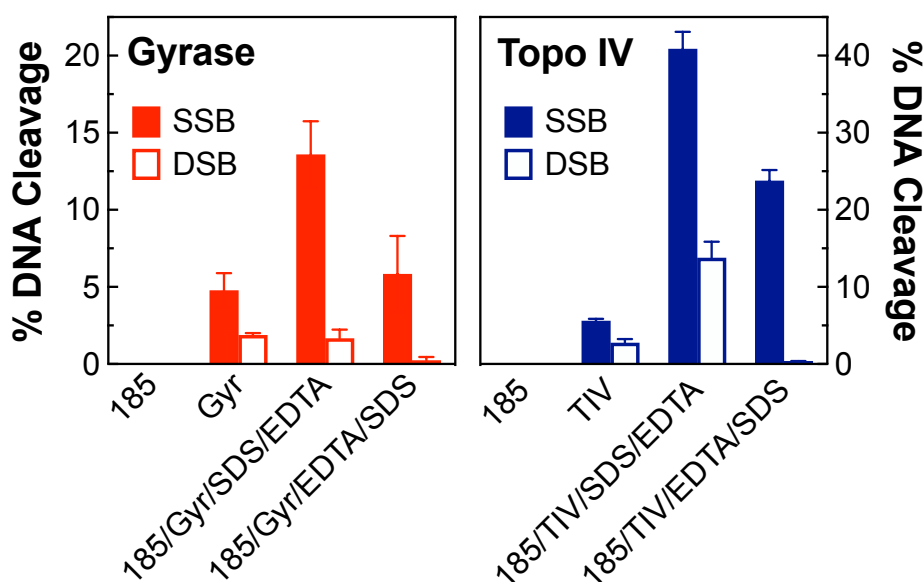


**Figure 5.2. DNA cleavage induced by OSUAB-185 is mediated by *N. gonorrhoeae* gyrase and topoisomerase IV.**

Bar graphs show single-stranded (SSB, filled bars) and double-stranded (DSB, open bars) DNA cleavage mediated by *N. gonorrhoeae* gyrase (red, left) and topoisomerase IV (Topo IV, blue, right). Reactions contained negatively supercoiled DNA, with 10  $\mu$ M OSUAB-185 in the absence of enzyme (185), gyrase (Gyr) or topoisomerase IV (TIV) in the absence of OSUAB-185, or complete reaction mixtures that contained enzyme, DNA, and the NBTI (185/Gyr/SDS/EDTA and 185/TIV/SDS/EDTA). All of these reactions were stopped with SDS prior to the addition of EDTA. Alternatively, reactions that contained enzyme, DNA, and the NBTI were treated with 2  $\mu$ L of 250 mM EDTA for 10 min prior to the addition of SDS (185/Gyr/EDTA/SDS and 185/TIV/EDTA/SDS). Note that the scaling of percent DNA cleavage on the y-axis differs between gyrase and topoisomerase IV and that gyrase reactions contained 200 nM enzyme, which is twice the concentration used in other cleavage assays, to increase baseline levels of DNA cleavage. Error bars represent SDs for at least three independent experiments.

To determine whether the relative levels of topoisomerase IV-mediated double- vs single-stranded DNA breaks change with time, a time course for DNA scission with both enzymes was monitored (Figure 5.3). As with the NBTI titration, no appreciable double-stranded breaks were observed with gyrase (Figure 5.3, left panel). In contrast, double- and single-stranded DNA breaks were observed with topoisomerase IV and appeared to be generated coordinately (Figure 5.3, right panel). To analyze the formation of double-stranded DNA breaks by topoisomerase IV in greater detail, data from the [OSUAB-185] titration (Figure 5.1, as well as NBTI concentrations up to 200  $\mu$ M) and the time course for cleavage (Figure 5.3) were converted to ratios of single-stranded:double-stranded DNA breaks (Figure 5.4, left and right panel, respectively). The single-stranded:double-stranded DNA break ratios remained constant over a wide range of NBTI concentrations and cleavage reaction times. These findings provide further evidence that the single- and double-stranded DNA breaks generated by *N. gonorrhoeae* topoisomerase IV in the presence of OSUAB-185 were generated coordinately. This result argues against a second NBTI molecule entering the active site of topoisomerase IV at higher concentrations of OSUAB-185 or over longer reaction times. It also argues against a change in the binding conformation of the NBTI over time.

As a final demonstration that the induction of topoisomerase IV-mediated double-stranded DNA breaks by OSUAB-185 represents a novel mechanism of action, a titration of the NBTI was carried out in cleavage assays that replaced  $MgCl_2$  with  $CaCl_2$  (Figure 5.5). With some enzymes,  $Ca^{2+}$  dramatically raises baseline levels of single- and double-stranded DNA breaks, which affords a more ready assessment of NBTI effects on DNA cleavage.<sup>306, 352, 366, 401</sup> Similar to previous results with other NBTIs, OSUAB-185 induced single-stranded DNA breaks and suppressed double-stranded breaks mediated by *N. gonorrhoeae* gyrase (Figure 5.5, left panel). However, in marked contrast, the NBTI enhanced both single- and double-stranded DNA cleavage mediated by topoisomerase IV (Figure 5.5, right panel). This finding provides strong evidence that OSUAB-185 induces double-stranded DNA breaks mediated by *N. gonorrhoeae* topoisomerase IV.

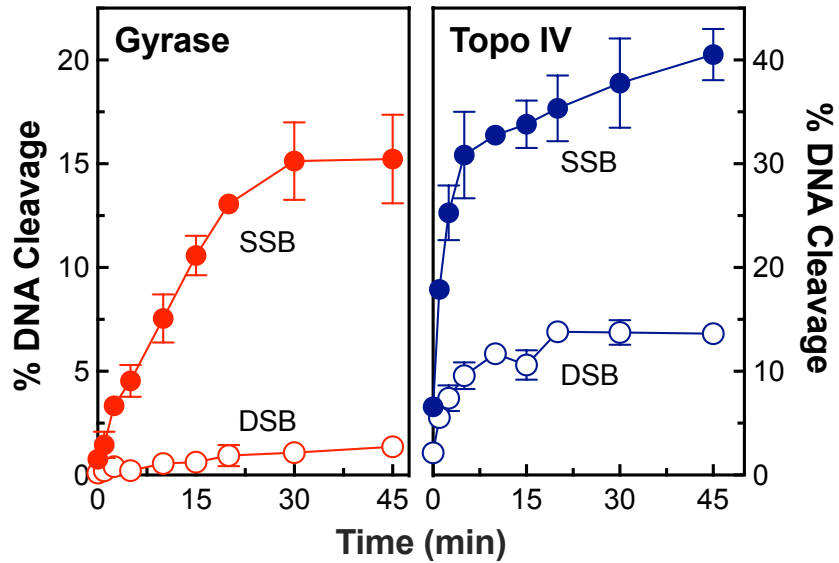


**Figure 5.3. Time courses for DNA cleavage mediated by *N. gonorrhoeae* gyrase and topoisomerase IV.**

Time courses for single-stranded (SSB, closed circle) and double-stranded (DSB, opened circle) DNA cleavage mediated by gyrase (red, left) and topoisomerase IV (Topo IV, blue, right) in the presence of 10  $\mu$ M OSUAB-185 are shown. Error bars represent SDs for at least three independent experiments.

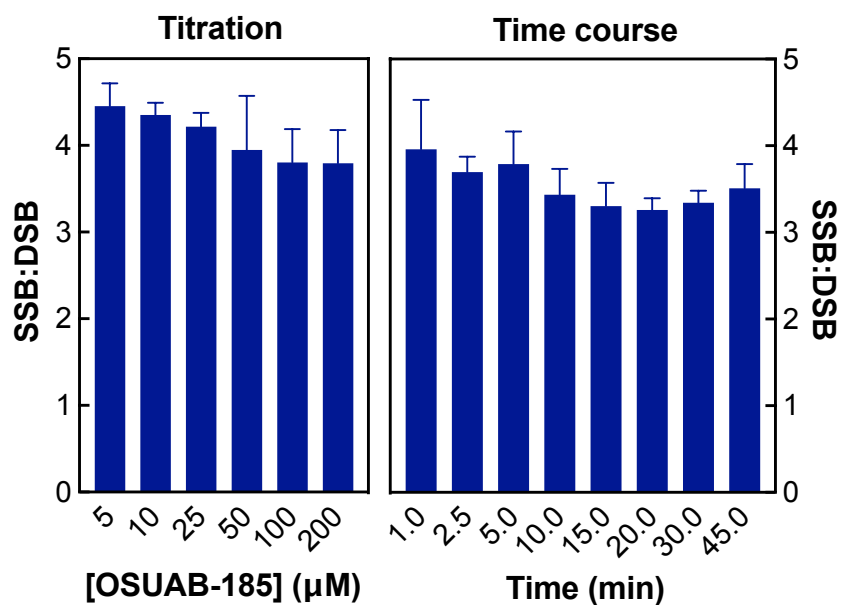


**Figure 5.4. Ratios of NBTI-induced single-stranded to double-stranded DNA cleavage mediated by *N. gonorrhoeae* topoisomerase IV are maintained over OSUAB-185 concentrations and reaction time.**

The ratios of single-stranded to double-stranded (SSB:DSB) DNA breaks over a concentration range of OSUAB-185 (left panel) or a time course of DNA cleavage (right panel) induced by 10 μM NBTI with topoisomerase IV are shown. Error bars represent SDs for at least three independent experiments.

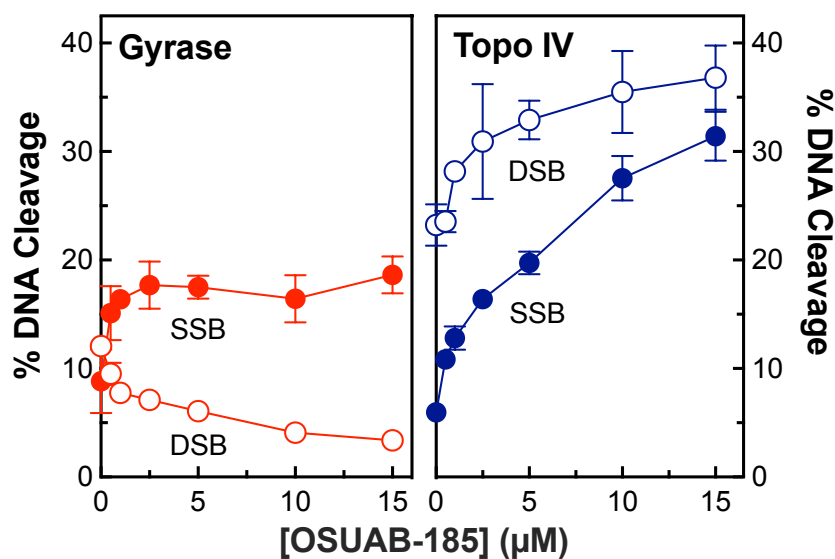


**Figure 5.5. OSUAB-185 suppresses levels of double-stranded DNA cleavage mediated by *N. gonorrhoeae* gyrase and increases levels of double-stranded DNA breaks generated by topoisomerase IV.**

DNA cleavage reactions contained  $\text{CaCl}_2$  in place of  $\text{MgCl}_2$  to raise baseline levels of DNA scission. Graphs show the effects of OSUAB-185 on single-stranded (SSB, closed circle) and double-stranded (DSB, opened circle) DNA cleavage mediated by gyrase (red, left) and topoisomerase IV (Topo IV, blue, right). Error bars represent SDs for at least three independent experiments.



### *Stability of single- and double-stranded DNA breaks induced by OSUAB-185*

Other things being equal, drugs that generate the most stable cleavage complexes appear to be the most lethal in cells.<sup>431</sup> Therefore, two approaches were utilized to assess the effects of OSUAB-185 on the stability of cleavage complexes formed by *N. gonorrhoeae* gyrase and topoisomerase IV. In the first approach, the effects of OSUAB-185 on the persistence of cleavage complexes were determined. In this assay, cleavage complexes were formed in the presence of high concentrations of enzyme and DNA, and the lifetimes of cleavage complexes were monitored following 20-fold dilution into a reaction buffer that lacked the catalytic divalent metal ion. While the shift in condition does not alter the DNA cleavage–ligation equilibrium in established cleavage complexes, complexes that disassociate are unlikely to reform. As seen in Figure 5.6, cleavage complexes formed with gyrase (monitoring single-stranded DNA cleavage, left panel) or topoisomerase IV (monitoring single-stranded DNA cleavage, middle panel, or double-stranded DNA cleavage, right panel) in the absence of the NBTI were highly unstable and rapidly disassociated following dilution. Complexes became considerably more stable in the presence of OSUAB-185. Consistent with the data from Figure 5.3, NBTI-induced double-stranded DNA breaks ( $t_{1/2} \approx 4$  min) were less stable than single-stranded DNA breaks ( $t_{1/2} \approx 8$  min) with topoisomerase IV.

In the second approach, the effects of OSUAB-185 on the rate of gyrase/topoisomerase IV-mediated DNA ligation were monitored by shifting cleavage complexes from 37 °C to 65 °C (a temperature that allows ligation but not cleavage of the DNA).<sup>166</sup> As seen in Figure 5.7, OSUAB-185 had a modest effect on rates of ligation for single-stranded DNA breaks with gyrase (left panel) and topoisomerase IV (middle panel) and double-stranded breaks with topoisomerase IV (right panel). The NBTI generated slightly more stable single-stranded ( $t_{1/2} \approx 35$  s) DNA cleavage complexes than double-stranded ( $t_{1/2} \approx 27$  s) DNA cleavage complexes with topoisomerase IV.

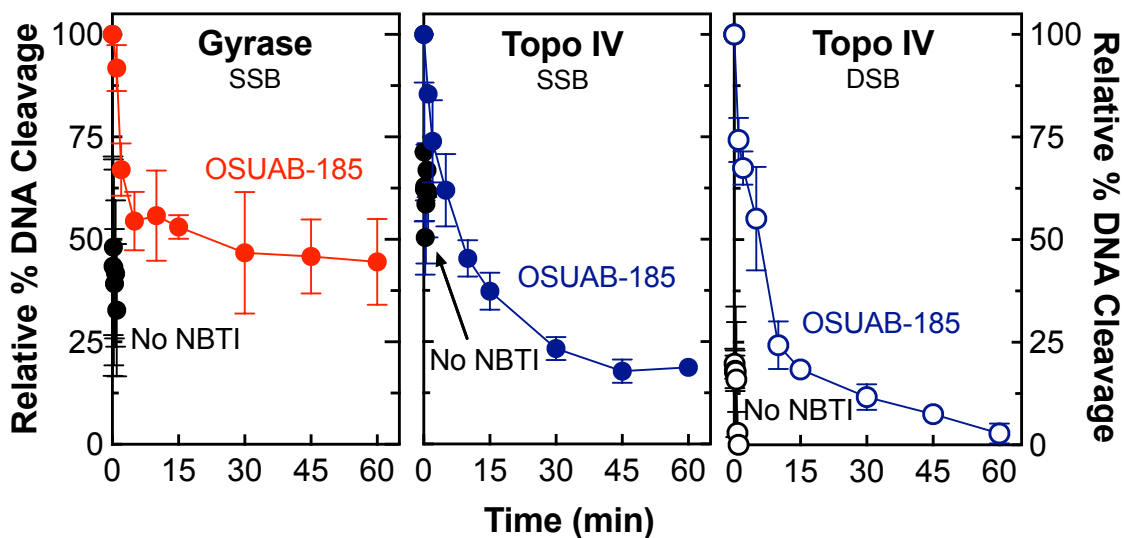


**Figure 5.6. OSUAB-185 induces stable DNA cleavage complexes with *N. gonorrhoeae* gyrase and topoisomerase IV.**

Persistence reactions were allowed to reach cleavage–ligation equilibrium before dilution in reaction buffer that lacked  $MgCl_2$ . The subsequent stability of cleavage complexes was monitored. Persistence of single-stranded DNA (SSB, closed circle) cleavage complexes by gyrase (red, left panel) and topoisomerase IV (blue, middle panel) and double-stranded DNA (DSB, open circle) cleavage complexes by topoisomerase IV (blue, right panel) formed in the presence of 10  $\mu M$  OSUAB-185 are shown. Persistence reactions carried out in the absence of the NBTI (No NBTI) are shown in black (SSB, closed circle; DSB, open circle). DNA cleavage prior to dilution of cleavage complexes was set to 100%. Error bars represent SDs of three independent experiments.

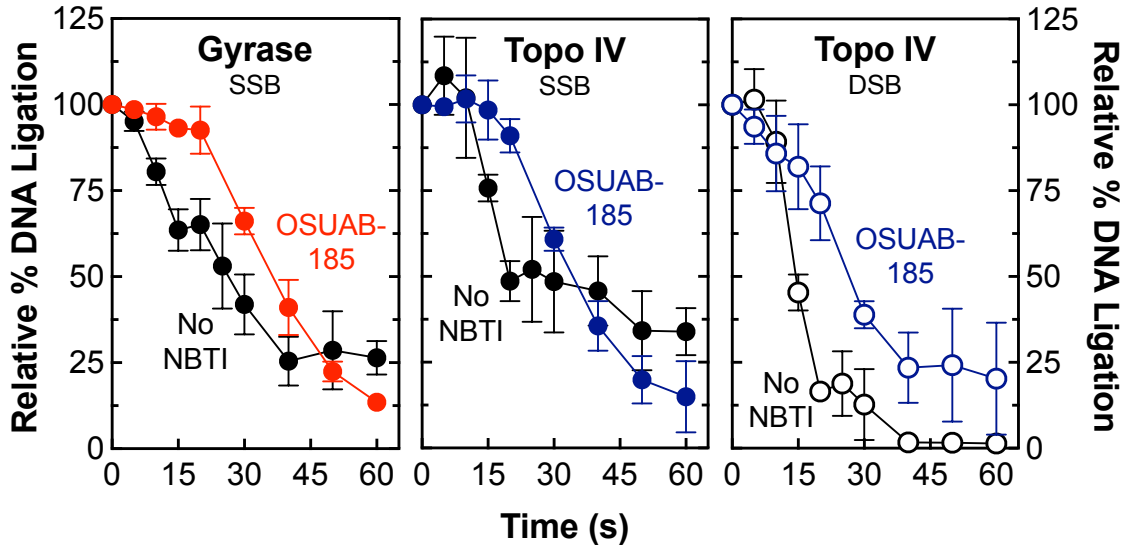


**Figure 5.7. OSUAB-185 inhibits DNA ligation mediated by *N. gonorrhoeae* gyrase and topoisomerase IV.**

Ligation of single-stranded DNA (SSB, closed circle) cleavage complexes by gyrase (red, left panel) and topoisomerase IV (blue, middle panel) and double-stranded DNA (DSB, open circle) cleavage complexes by topoisomerase IV (blue, right panel) formed in the presence of 10  $\mu$ M OSUAB-185 are shown. DNA ligation was also monitored in the absence of the NBTI (black, SSB, closed circle; DSB, open circle). Levels of single- and double-stranded DNA cleavage prior to the induction of ligation were set to 100%. Error bars represent SDs for at least three independent experiments.

#### *Effects of OSUAB-185 on fluoroquinolone-resistant N. gonorrhoeae gyrase and topoisomerase IV*

To determine whether OSUAB-185 is able to overcome fluoroquinolone resistance in *N. gonorrhoeae* type II enzymes, the effects of the NBTI on gyrase that contained GyrA<sup>S91F</sup> and topoisomerase IV that contained ParC<sup>S87N</sup> were examined. These two amino acid substitutions represent the most prevalent fluoroquinolone-resistant mutations in *N. gonorrhoeae* gyrase and topoisomerase IV, respectively (Figure 5.8).<sup>325, 461</sup> Levels of DNA cleavage with GyrA<sup>S91F</sup> gyrase (top left panel) were similar to those obtained with the wild-type enzyme and only single-stranded DNA cleavage was induced by OSUAB-185. However, the NBTI was ~4-fold less potent against the GyrA<sup>S91F</sup> mutant. In contrast, levels of NBTI-induced DNA scission with ParC<sup>S87N</sup> topoisomerase IV (top right panel) were ~3 to 4-fold lower than observed for the wild-type enzyme, and OSUAB-185 maintained its potency. Once again, the NBTI induced single- and double-stranded DNA scission with fluoroquinolone-resistant topoisomerase IV. These findings predict that the NBTI would retain at least some activity against fluoroquinolone-resistant *N. gonorrhoeae* cells harboring common mutations in gyrase/topoisomerase IV. They also suggest that the fluoroquinolone-resistant mutations do not alter the mechanism of action of OSUAB-185 against bacterial type II topoisomerases.

#### *Effects of OSUAB-185 on gyrase and topoisomerase IV from E. coli and S. aureus*

To determine whether OSUAB-185 is able to induce double-stranded DNA breaks with type II topoisomerases from other species (Figure 5.9), the effects of the NBTI on DNA cleavage mediated by gyrase (left panels) and topoisomerase IV (right panels) from *E. coli* (Figure 5.9A) and *S. aureus* (Figure 5.9B) were assessed. Note that the induction of double-stranded DNA breaks by OSUAB-185 and *S. aureus* gyrase has been reported previously.<sup>345</sup> To at least some

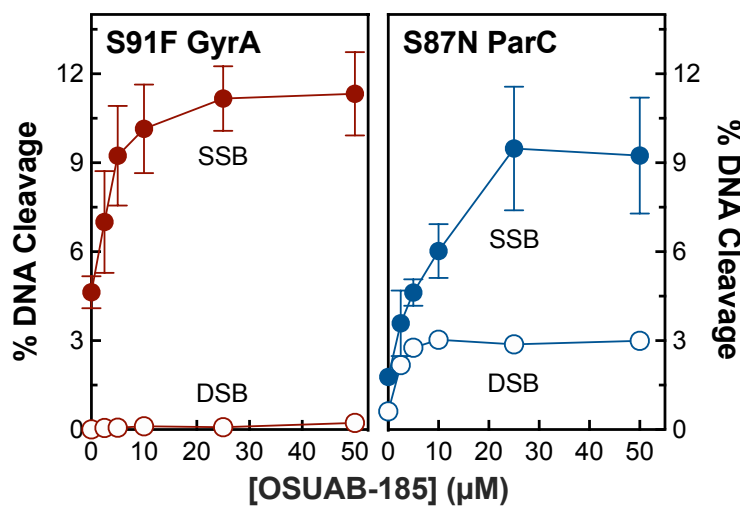


**Figure 5.8. Activity of OSUAB-185 against *N. gonorrhoeae* gyrase and topoisomerase IV that contain fluoroquinolone-resistance mutations.**

The effects of OSUAB-185 on single-stranded (SSB, closed circle) and double-stranded (DSB, open circle) DNA cleavage mediated by fluoroquinolone-resistant GyrA<sup>S91F</sup> gyrase (S91F GyrA; top left, red) and ParC<sup>S87N</sup> topoisomerase IV (S87N ParC; top right, blue) are shown. Error bars represent SDs of three independent experiments. A summary table of DNA cleavage mediated by WT and mutant *N. gonorrhoeae* gyrase and topoisomerase IV is shown at the bottom. CC<sub>50</sub> values are indicated for the enhancement of single-stranded and double-stranded DNA cleavage. Maximal levels of NBTI-induced DNA scission (Max %) are also shown. Significant levels of double-stranded DNA breaks were not observed with WT or GyrA<sup>S91F</sup> gyrase. The ratio of single-stranded to double-stranded DNA breaks (SSB:DSB) were calculated at maximal levels of DNA cleavage for WT and ParC<sup>S87N</sup> topoisomerase IV.

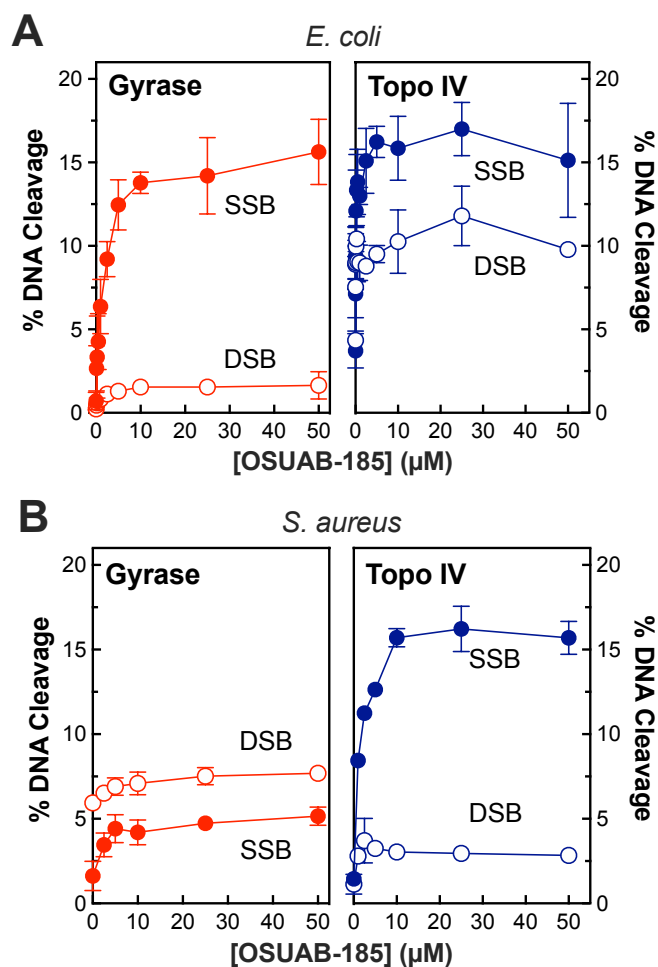


**Figure 5.9. OSUAB-185 induces double-stranded DNA breaks mediated by gyrase and topoisomerase IV from *E. coli* and *S. aureus*.**

The effects of OSUAB-185 on single-stranded (SSB, closed circles) and double-stranded (DSB, open circles) DNA cleavage mediated by gyrase (red, left panels) and topoisomerase IV (blue, right panels) from *E. coli* (A) and *S. aureus* (B) are shown. Error bars represent SDs of three independent experiments.

extent, OSUAB-185 induced double-stranded breaks with all four of the enzymes. Double-stranded DNA breaks were especially prominent with *E. coli* topoisomerase IV. These data indicate that the ability of the NBTI to generate enzyme-mediated double-stranded DNA breaks is not confined to *N. gonorrhoeae* or type II topoisomerase.

#### *Effects of OSUAB-185 on human topoisomerase II $\alpha$*

Very little is known about the interaction of NBTIs with human type II topoisomerases.<sup>344, 475, 476</sup> Therefore, the effects of OSUAB-185 on DNA cleavage mediated by human topoisomerase II $\alpha$  was determined (Figure 5.10). The NBTI displayed reasonable activity against the human type II enzyme, with CC<sub>50</sub> values in the low  $\mu$ M range. In addition, similar to the results with some of the bacterial enzymes, OSUAB-185 induced moderate levels of double-stranded DNA breaks with the human enzyme (maximal levels of cleavage of ~11% and ~8.5% for single- and double-stranded DNA breaks, respectively). This last finding provides further evidence that some members of the NBTI class are capable of generating enzyme-mediated double-stranded DNA breaks.

### **Discussion**

NBTIs are an emerging class of compounds with antibacterial activity. In contrast to fluoroquinolones, a hallmark of most NBTIs is their ability to induce gyrase/topoisomerase IV-mediated single-stranded breaks in DNA and suppress the formation of double-stranded breaks.<sup>332, 352, 366</sup> Together with a previous study, the present work provides strong evidence that select dioxane-linked amide NBTIs are also capable of generating double-stranded DNA breaks mediated by type II topoisomerases from a variety of bacterial species, as well as humans.<sup>345</sup>

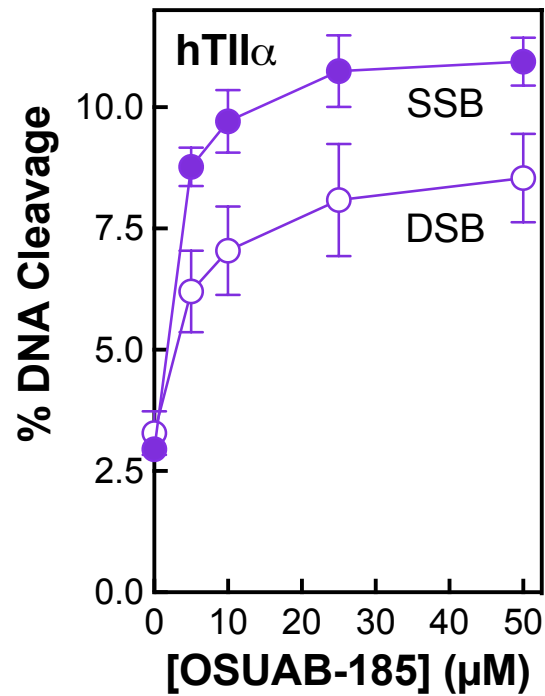


**Figure 5.10. Effects of OSUAB-185 on DNA cleavage mediated by human topoisomerase II $\alpha$ .**

The graph shows the effects of OSUAB-185 on single-stranded (SSB, purple, closed circle) and double-stranded (DSB, purple, open circle) DNA cleavage mediated by human topoisomerase II $\alpha$ . Error bars represent standard error of the mean of two independent experiments.



Fluoroquinolones induce double-stranded DNA breaks because two drug molecules bind in the active site of gyrase and topoisomerase IV, with one molecule stabilizing a cleaved scissile bond on each strand of the double helix.<sup>167, 303, 304</sup> In contrast, only a single NBTI molecule binds in the active site of the bacterial type II topoisomerases, with the molecule binding midway between the two scissile bonds.<sup>44, 299, 332</sup> It is believed that canonical NBTIs stabilize single-stranded and suppress double-stranded DNA breaks by distorting the active site of gyrase/topoisomerase IV in a manner that inhibits ligation of the first strand but does not allow cleavage of the second.<sup>299, 332</sup> It is not known how OSUAB-185 and potentially other dioxane-linked amide NBTIs generate double-stranded breaks. Results from OSUAB-185 titrations (Figures 5.1 and 5.4) and time course experiments (Figures 5.3 and 5.4) strongly suggest that it is not due to the binding of a second molecule of a compound. Potentially, this NBTI has two mutually exclusive binding configurations that distort the active site of the enzyme differently. In the first, the NBTI acts as a canonical member of this class and induces distortion after one strand is cut to inhibit ligation and prevent cleavage of the second strand (thus enhancing single-stranded DNA breaks). In the second, the NBTI acts in a non-canonical manner and only induces the dramatic active site distortion after both DNA strands are cleaved (thus enhancing double-stranded DNA breaks). Future structural studies are needed to determine if this is the case.

The activity of OSUAB-185 against topoisomerase II $\alpha$  suggests that this member of this NBTI subclass might cross over to human systems if used to treat infections. However, our results raise an interesting possibility. The double-stranded DNA breaks generated by human type II topoisomerases during transcription have the potential to trigger secondary leukemias in a small percentage of patients treated with topoisomerase II-targeted anticancer drugs.<sup>78, 176, 208, 212, 477</sup> If a drug was developed that induced only single-stranded DNA breaks with human type II topoisomerases, it is possible that it could overcome the secondary leukemias observed with current drugs. Although OSUAB-185 induced both single- and double-stranded DNA breaks

mediated by human topoisomerase II $\alpha$ , our findings open the door for future work on NBTIs and human type II topoisomerases.

## CHAPTER VI

### ACTIONS OF SPIROPYRIMIDINTRIONES AGAINST *NEISSERIA GONORRHOEAE* TYPE II TOPOISOMERASES

#### Introduction

In response to increasing resistance that undermines the clinical use of fluoroquinolones, a novel class of gyrase/topoisomerase IV-targeted antibacterials with a spiropyrimidinetrione (SPT) pharmacophore have been developed.<sup>330, 478, 479</sup> Zoliflodacin is the leading clinical candidate of this class and recently completed phase III clinical trials for the treatment of uncomplicated gonorrhea.<sup>335, 337</sup> As discussed in chapter I, two SPT molecules bind to the gyrase/topoisomerase IV-DNA complex at the cleaved scissile bond (one molecule per DNA strand). However, zoliflodacin and other SPTs interact with active site residues distinct from those of fluoroquinolones. While zoliflodacin displays activity against gyrase and topoisomerase IV *in vitro*, gyrase appears to be the primary cytotoxic target of the drug in *N. gonorrhoeae* cells.<sup>329, 382</sup>

Despite the advanced clinical develop of zoliflodacin,<sup>335, 337</sup> few studies have assessed the interactions between SPTs and bacterial type II topoisomerases. Therefore, we characterized the actions of zoliflodacin and a related SPT analogue, H3D-005722, on the *in vitro* activities of gyrase and topoisomerase IV from *N. gonorrhoeae*. Results strongly suggest that the disparate activities of SPTs against *N. gonorrhoeae* gyrase and topoisomerase IV contribute to their physiological targeting and toxicity. Furthermore, gyrase-SPT interactions do not appear to be affected by fluoroquinolone-resistance mutations in *N. gonorrhoeae*. Finally, this drug class interacts with gyrase and topoisomerase IV distinctly within and across bacterial species.

## Results and Discussion

### *Effects of SPTs on the catalytic and DNA cleavage activities of N. gonorrhoeae gyrase and topoisomerase IV*

A previous study showed that zoliflodacin inhibited the catalytic activities of gyrase and topoisomerase IV and enhanced double-stranded DNA scission mediated by the type II enzymes.<sup>329</sup> Therefore, to further address the enzymological basis for the activity of zoliflodacin and related SPT analogues against bacterial type II topoisomerases, we assessed the susceptibility of the *N. gonorrhoeae* type II topoisomerases to inhibition of catalysis by zoliflodacin and H3D-005722 (see Figure 1.12), a novel SPT analog optimized for its activity against *M. tuberculosis* gyrase,<sup>387, 389, 390</sup> (Figure 6.1). Both SPTs inhibited DNA supercoiling and DNA decatenation catalyzed by gyrase and topoisomerase IV, respectively, but the drugs were more potent against gyrase with micromolar IC<sub>50</sub> values. Both SPTs were unable to inhibit topoisomerase IV-catalyzed DNA decatenation more than 30% at 200 µM.

In addition to inhibiting catalysis, zoliflodacin and H3D-005722 also enhanced double-stranded DNA scission mediated by *N. gonorrhoeae* gyrase and topoisomerase IV (Figure 6.2). Both SPTs increased levels of double-stranded DNA scission against gyrase with similar dose responses and achieved a maximal percentage of double-stranded DNA breaks (max % DSB) of ~30-33% at 100 µM SPT. In contrast, H3D-005722 induced nearly 3-fold higher levels of double-stranded DNA scission mediated by topoisomerase IV compared with that of zoliflodacin (max % DSB = 32.5 vs 12.1). Although H3D-005722 was selected for its specificity against *M. tuberculosis* and its corresponding gyrase,<sup>387, 389, 390</sup> results from *in vitro* experiments suggest this compound may also possess antimicrobial activity against cultured *N. gonorrhoeae*.

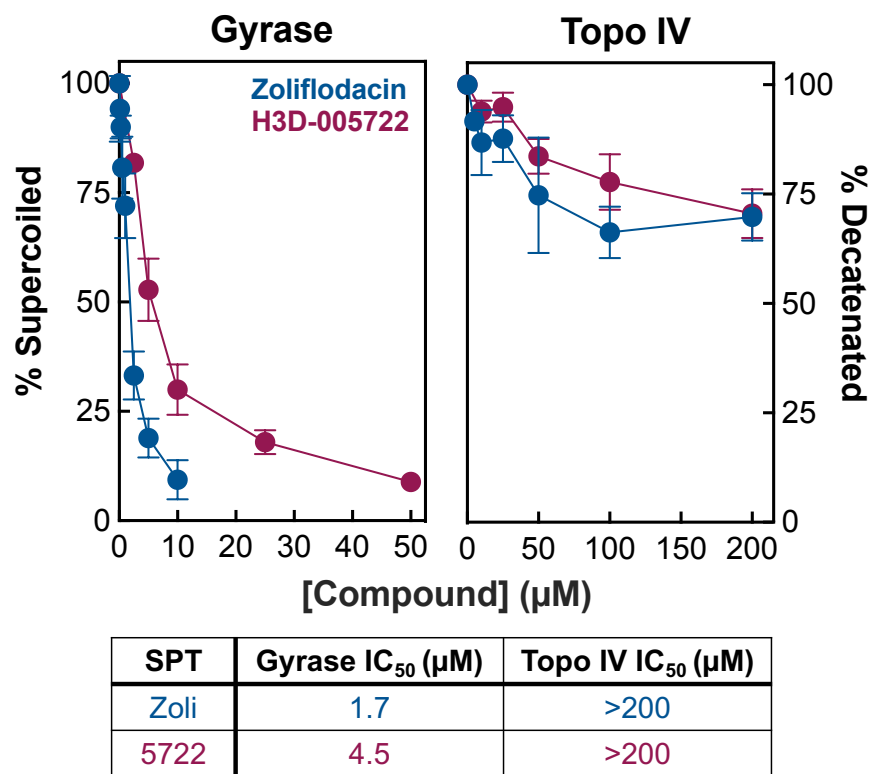


**Figure 6.1. Effects of zoliflodacin and H3D-005722 on DNA supercoiling and DNA decatenation catalyzed by *N. gonorrhoeae* gyrase and topoisomerase IV, respectively.**

The effects of zoliflodacin (Zoli, blue) and H3D-005722 (5722, maroon) on the supercoiling of relaxed DNA by gyrase (left) and on the decatenation of kinetoplast DNA by topoisomerase IV (right) are shown. Error bars represent the standard deviation (SD) of at least 3 independent experiments. The table displays the half maximal inhibitory concentration (IC<sub>50</sub>) for each drug to inhibit the catalytic activity of gyrase or topoisomerase IV.

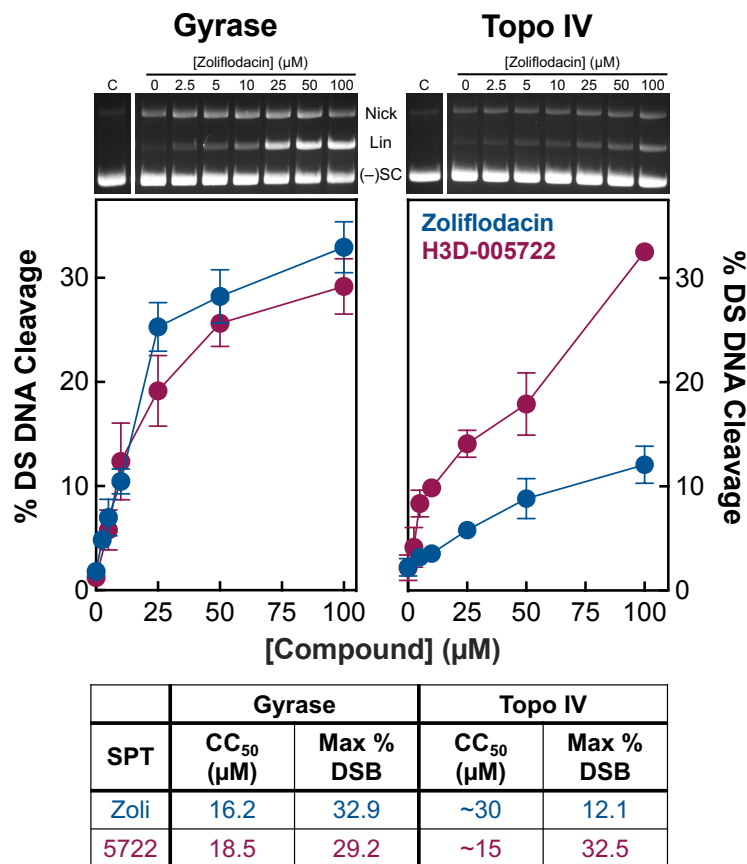


**Figure 6.2. Effects of zoliflodacin and H3D-005722 on DNA scission mediated by *N. gonorrhoeae* gyrase and topoisomerase IV.**

The ability of zoliflodacin (Zoli, blue) and H3D-005722 (5722, maroon) to induce double-stranded (DS) DNA cleavage mediated by gyrase (left) and topoisomerase IV (left) are shown. Error bars represent the standard deviation of at least 3 independent experiments. The table at the bottom lists the CC<sub>50</sub> value (the drug concentration at which 50% maximal DS DNA cleavage is reached) for each enzyme and the Max % DSB value (maximal percentage of DS DNA breaks) induced at 100 μM SPT.

### *Stability of double-stranded DNA breaks induced by zoliflodacin*

A study conducted with human topoisomerase II found that, other things being equal, drugs that generate the most stable cleavage complexes are the most cytotoxic to cells.<sup>431</sup> Therefore, two approaches were employed to investigate the effects of zoliflodacin on the stability of cleavage complexes formed by *N. gonorrhoeae* gyrase and topoisomerase IV. First, the persistence of cleavage complexes in the absence and presence of zoliflodacin was assessed. In the assay, cleavage complexes were formed in the presence of high concentrations of gyrase/topoisomerase IV and DNA, and the lifetimes of cleavage complexes were monitored following 20-fold dilution into a reaction buffer that lacked the catalytic divalent metal ion. While the shift in condition does not alter the DNA cleavage–ligation equilibrium in established cleavage complexes, complexes that disassociate are unlikely to reform. As seen in Figure 6.3, gyrase/topoisomerase IV-DNA cleavage complexes were highly unstable in the absence of drug and rapidly disassociated following dilution ( $t_{1/2} > 5$  s). The stability of these complexes increased considerably in the presence of zoliflodacin. Nevertheless, the gyrase-DNA-SPT complex was ~10 times more stable ( $t_{1/2} \sim 10$  min) than the topoisomerase IV complex ( $t_{1/2} \sim 1$  min),

In the second approach, the effects of zoliflodacin on the rate of gyrase/topoisomerase IV-mediated DNA ligation were monitored. In the assay, cleavage complexes were shifted from 37 °C to 65 °C (a temperature that allows DNA ligation but not DNA cleavage), and the loss of double-stranded DNA breaks was followed. As seen in Figure 6.4, cleavage complexes formed in the absence of the SPT were rapidly religated by gyrase ( $t_{1/2} = 19.8$  s) and topoisomerases IV ( $t_{1/2} = 15$  s). Zoliflodacin had a significant effect on ligation rates for double-stranded DNA breaks with *N. gonorrhoeae* gyrase ( $t_{1/2} > 60$  s) but only modestly affected rates of topoisomerase IV-mediated ligation ( $t_{1/2} = 17$  s). Taken together, these findings suggest that the gyrase-DNA-SPT complex is more stable than the topoisomerase IV complex, which support results from cellular studies that gyrase is the primary cytotoxic target of zoliflodacin in *N. gonorrhoeae*.<sup>381, 382</sup>

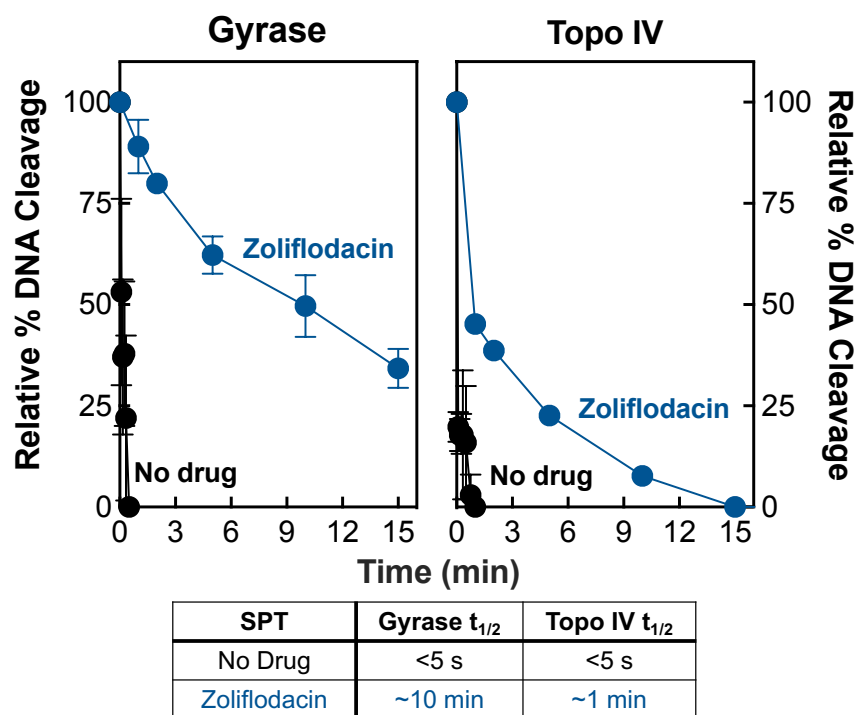


**Figure 6.3. Effects of zoliflodacin on the persistence of DNA cleavage complexes formed by *N. gonorrhoeae* gyrase and topoisomerase IV.**

Reactions were allowed to reach cleavage–ligation equilibrium before dilution in reaction buffer that lacked MgCl<sub>2</sub>. The subsequent stability of cleavage complexes was monitored. Persistence of double-stranded DNA cleavage complexes mediated by gyrase (left) and topoisomerase IV (right) formed in the presence of 100 μM zoliflodacin (blue) are shown. Persistence assays carried out in the absence of the SPT (No Drug) are shown in black. DNA cleavage prior to dilution of cleavage complexes was set to 100%. Error bars represent SDs of at least 3 independent experiments. The table at the bottom lists the  $t_{1/2}$  value (the time at which a 50% reduction in DS DNA cleavage is reached) for each enzyme.



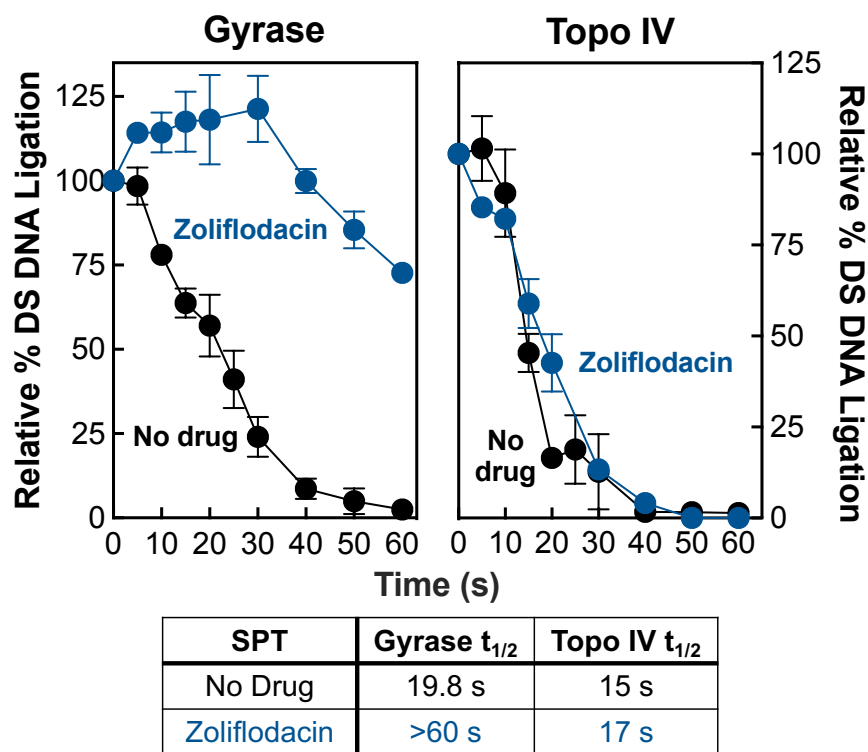


**Figure 6.4. Effects of zoliflodacin on DNA religation mediated by *N. gonorrhoeae* gyrase and topoisomerase IV.**

Ligation of double-stranded DNA cleavage complexes by gyrase (left) and topoisomerase IV (right) formed in the presence of 100  $\mu$ M zoliflodacin are shown. DNA ligation was also monitored in the absence of the SPT (black). Levels of double-stranded DNA cleavage prior to the induction of ligation were set to 100%. Error bars represent SDs of at least 3 independent experiments. The table at the bottom lists the  $t_{1/2}$  value for each enzyme.

### *Activities of zoliflodacin against fluoroquinolone-resistant N. gonorrhoeae gyrase*

Despite the overwhelming need to develop novel antibacterials that overcome target-mediated fluoroquinolone resistance, few studies have reported the interactions of SPTs with fluoroquinolone-resistant type II topoisomerases.<sup>329, 387</sup> Therefore, we investigated the effects of zoliflodacin on the catalytic and DNA cleavage activities of WT gyrase as well as the individual ( $\text{GyrA}^{\text{S91F}}$  and  $\text{GyrA}^{\text{D95G}}$ ) and double ( $\text{GyrA}^{\text{S91F/D95G}}$ ) mutants associated with fluoroquinolone resistance in cellular studies and clinical isolates.

Zoliflodacin was a potent inhibitor of DNA supercoiling catalyzed by WT,  $\text{GyrA}^{\text{S91F}}$ ,  $\text{GyrA}^{\text{D95G}}$ , and  $\text{GyrA}^{\text{S91F/D95G}}$  *N. gonorrhoeae* gyrase (Figure 6.5). The SPT inhibited the WT enzyme with an  $\text{IC}_{50}$  value of 1.5  $\mu\text{M}$ , but the potency dropped 2-3-fold against enzymes harboring fluoroquinolone-resistant mutations ( $\text{IC}_{50}$  = 3.0-4.5  $\mu\text{M}$ ).

We also compared the effects of zoliflodacin on DNA cleavage mediated by WT and fluoroquinolone-resistant gyrase (Figure 6.6). Congruent with results obtained for DNA supercoiling, zoliflodacin displayed similar potency against WT and mutant gyrases ( $\text{CC}_{50}$  Fold-Change = 0.9-1.5). In fact,  $\text{GyrA}^{\text{S91F}}$  and  $\text{GyrA}^{\text{S91F/D95G}}$  gyrase were slightly more sensitive to zoliflodacin ( $\text{CC}_{50}$  = 14.1 and 15.0  $\mu\text{M}$ , respectively) than WT gyrase ( $\text{CC}_{50}$  = 16.2  $\mu\text{M}$ ). However, this small increase in SPT sensitivity was accompanied by a reduction in drug efficacy, as maximal levels of double-stranded DNA breaks fell from 32.9% (WT) to 25.8% ( $\text{GyrA}^{\text{S91F}}$ ) and 23.5% ( $\text{GyrA}^{\text{S91F/D95G}}$ ). Unlike the latter two mutant enzymes,  $\text{GyrA}^{\text{D95G}}$  gyrase enhanced SPT-induced double-stranded DNA cleavage to the same level as WT (max % DSB = ~33%).

Overall, these results provide additional support that SPTs are not cross-resistant with fluoroquinolones and suggest that fluoroquinolone-resistant mutations do not alter the mechanism of action of zoliflodacin against gyrase. The findings further imply that zoliflodacin can overcome fluoroquinolone-resistance in cultured *N. gonorrhoeae* as well as in human gonorrheal infections.

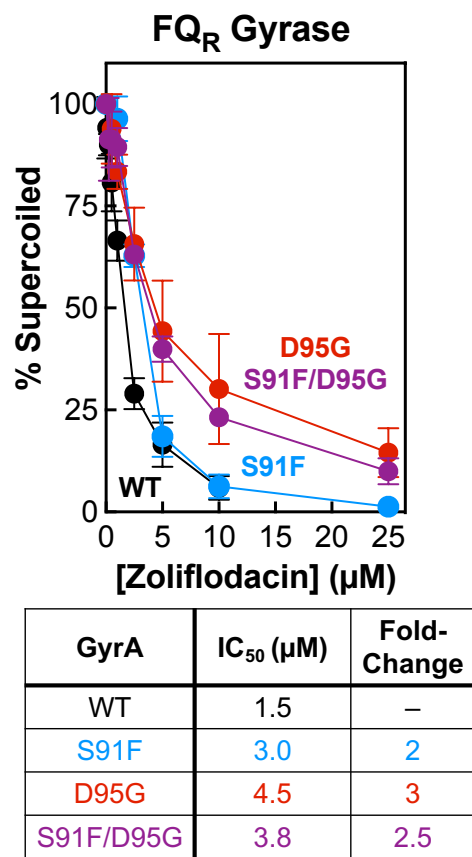
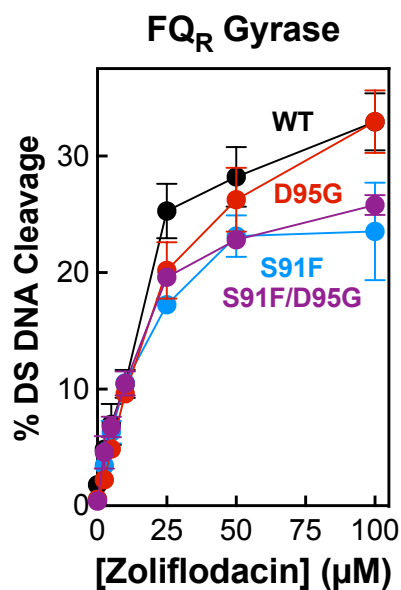


**Figure 6.5. Effects of zoliflodacin on DNA supercoiling catalyzed by WT and fluoroquinolone-resistant *N. gonorrhoeae* gyrase.**

The abilities of WT (black), GyrA<sup>S91F</sup> (S91F, blue), GyrA<sup>D95G</sup> (D95G, red) and GyrA<sup>S91F/D95G</sup> (S91F/D95G, purple) gyrase to supercoil relaxed plasmid in the presence of zoliflodacin are shown in the left panel. Error bars represent the standard deviation of at least 3 independent experiments. The table indicates the corresponding IC<sub>50</sub> values, and the fold-change in IC<sub>50</sub> from WT.



GyrA	CC <sub>50</sub> (µM)	Fold-Change	Max % DSB
WT	16.2	–	32.9
S91F	14.1	0.9	23.5
D95G	24.6	1.5	33.0
S91F/D95G	15.0	0.9	25.8

**Figure 6.6. Effects of zoliflodacin on DNA cleavage mediated by WT and fluoroquinolone-resistant *N. gonorrhoeae* gyrase.**

The ability of zoliflodacin to induce double-stranded (DS) DNA cleavage mediated by WT (black), GyrA<sup>S91F</sup> (S91F, blue), GyrA<sup>D95G</sup> (D95G, red), and GyrA<sup>S91F/D95G</sup> (S91F/D95G, purple) gyrase are shown in the top panel. Error bars represent the standard deviation of at least 3 independent experiments. The table at the bottom lists the CC<sub>50</sub> value for each enzyme, the fold-change in CC<sub>50</sub> from WT, and the Max % DSB value induced at 100 µM SPT.

### *Effects of SPTs on gyrase and topoisomerase IV from B. anthracis and E. coli*

Because fluoroquinolones have been shown to interact with gyrase and topoisomerase IV differently within and across species, we assessed the ability of the SPTs to induce DNA breaks mediated by gyrase and topoisomerase IV from *E. coli* and *B. anthracis* (Figure 6.7).<sup>380, 383</sup> Surprisingly, zoliflodacin induced both single-stranded and double-stranded DNA breaks mediated by gyrase and topoisomerase IV from these species. This result prompted us to consider whether *N. gonorrhoeae* type II topoisomerases mediated single-stranded DNA breaks induced by zoliflodacin. Therefore, single-stranded DNA cleavage induced by the SPT was quantified from the experiments shown in Figure 6.1. The SPT increased levels of single-stranded DNA scission (above baseline) mediated by *N. gonorrhoeae* topoisomerase IV, but not gyrase. In contrast, zoliflodacin induced nearly equivalent levels of single-stranded and double-stranded DNA breaks mediated by *B. anthracis* topoisomerase IV and the type II enzymes from *E. coli*. Only *B. anthracis* gyrase showed a higher susceptibility for SPT-induced single-stranded DNA breaks compared with double-stranded breaks. For this enzyme, single-stranded DNA breaks approached 50% at 100  $\mu$ M SPT, while double-stranded breaks reached ~25% at the same concentration. In summary, both SPT compounds enhanced enzyme-mediated single-stranded and double-stranded DNA scission in these species, but the ratios of single-stranded to double-stranded breaks varied across species and enzyme. These results indicate that SPTs interact with gyrase and topoisomerase IV distinctly within and across bacterial species.

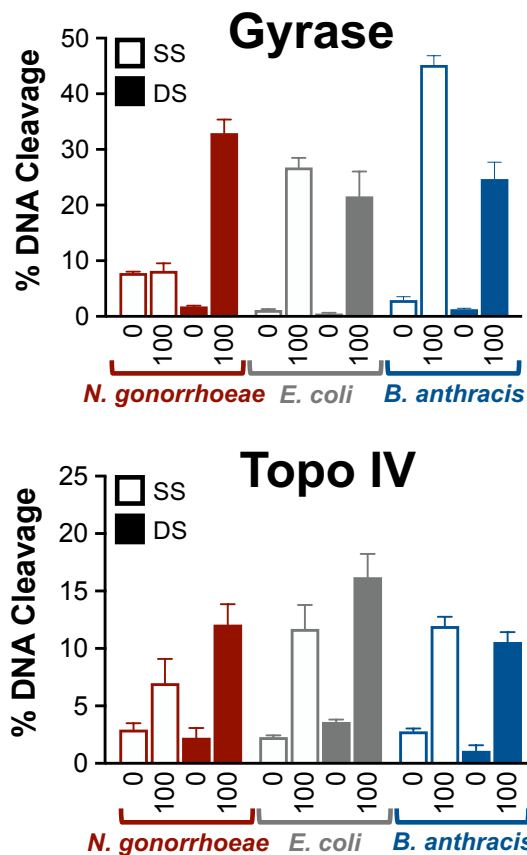


**Figure 6.7. Effects of zoliflodacin on single-stranded and double-stranded DNA scission mediated by gyrase and topoisomerase IV from *N. gonorrhoeae*, *E. coli*, and *B. anthracis*.** Single-stranded (SS, open bar) and double-stranded (DS, closed bar) DNA scission mediated by gyrase (top) and topoisomerase IV (bottom) from *N. gonorrhoeae* (red), *E. coli* (gray), and *B. anthracis* (blue) induced in the absence or presence of 100  $\mu$ M zoliflodacin are shown. Note that the % DNA cleavage scale for topoisomerase IV (bottom) is half of that for gyrase (top). Error bars represent the standard deviation of at least 3 independent experiments.

## CHAPTER VII

### CONCLUSIONS AND IMPLICATIONS

Type II topoisomerases are the targets for many successful anticancer and antibacterial drugs used to treat some of the deadliest diseases in the world. However, the therapeutic efficacy of type II topoisomerase-targeted agents has been compromised. Anticancer drugs that target human topoisomerase II are riddled with off-target toxicities, notably therapy-related leukemias and cardiomyopathies, that curtail their clinical utility. Moreover, the escalating prevalence of drug-resistant bacterial infections has eroded the limited arsenal of gyrase/topoisomerase IV-targeted agents available to combat these diseases. A comprehensive understanding of the actions, resistance mechanisms, and underlying toxicities of drugs that target the type II enzymes is essential in addressing these growing challenges.

This dissertation has sought to define the activities of environmentally and clinically important agents against human and bacterial type II topoisomerases, respectively. In particular, these studies have focused on characterizing the actions of established (fluoroquinolones) and emerging (novel bacterial topoisomerase inhibitors and spiropyrimidinetriones) antibacterial classes that target gyrase and topoisomerase IV.

#### **Overcoming Fluoroquinolone Resistance**

Nearly 1.3 million people died from antimicrobial resistant infections in 2019, and this number is projected to grow to 10 million deaths a year by 2050 unless novel antibacterials are developed.<sup>480, 481</sup> A pathogen of emergent concern is drug-resistant *N. gonorrhoeae*, which is

ranked as one of five “urgent threats” (the highest threat level) by the CDC.<sup>448</sup> This pathogen has been the central focus of the studies reported in this dissertation. As discussed in Chapter I, fluoroquinolones represent a class of critically important broad spectrum antibacterial drugs used to treat a myriad of bacterial infections, such as gonorrhea. However, increasing levels of resistance have curbed their clinical use.<sup>320, 321, 326</sup> As an example, in 2021, ~33% of clinical *N. gonorrhoeae* isolates in the United States were resistant to ciprofloxacin, and in parts of Asia, fluoroquinolone resistance reaches 100%.<sup>447, 482</sup>

The most important and prevalent mechanism of fluoroquinolone resistance is target-mediated and is caused by specific mutations in a highly conserved serine and acidic residue in the A subunit of gyrase and topoisomerase IV.<sup>154-156, 266</sup> Structural and enzymological studies have shown that the serine and acidic residues anchor a “water-metal ion bridge” between the fluoroquinolone and the enzyme.<sup>154, 155, 167, 303, 304</sup> This bridge plays a critical role in mediating the actions of fluoroquinolones against bacterial type II topoisomerases, although its architecture and function varies between species and enzymes. As an example, *M. tuberculosis* gyrase uses the acidic residue alone for fluoroquinolone binding, whereas *E. coli* topoisomerase IV uses both the serine and acidic residues to position the fluoroquinolone in the active site. In either case, resistance mutations disrupt the use and function of the water-metal ion bridge, thereby reducing the sensitivity of the enzyme to the fluoroquinolone.<sup>155, 305-310, 466</sup>

Although the water-metal ion bridge appears to be a universal feature of fluoroquinolone-gyrase/topoisomerase IV interactions, little is known about the utilization of this bridge and its contributions to resistance in *N. gonorrhoeae*. One of the goals of this dissertation has been to describe the actions and resistance mechanisms of the established fluoroquinolone class of antibacterials against gyrase and topoisomerase IV.

Chapter IV reports the utilization and function of the water-metal ion bridge in *N. gonorrhoeae* and highlights the mechanistic basis for target-mediated fluoroquinolone resistance



in this species. For *N. gonorrhoeae* gyrase, both the serine and acidic residues anchor the bridge, which contributes to fluoroquinolone binding and positioning. Fluoroquinolone-topoisomerase IV interactions are less clear, but results suggest that the acidic residue primarily functions to position ciprofloxacin in the active site. These results underscore the critical role of the water-metal ion bridge in mediating fluoroquinolone-topoisomerase interactions and highlight the unique functions of the bridge across species and enzymes.

Furthermore, gyrase-mediated fluoroquinolone resistance in *N. gonorrhoeae* correlates with the loss of DNA cleavage rather than catalytic function. This result implies that the mechanism of drug toxicity is linked to the induction of enzyme-generated double-stranded DNA breaks rather than the loss of essential enzyme activities.

Consistent with genetic and cellular studies in which gyrase is the primary and topoisomerase IV is the secondary target of fluoroquinolones, ciprofloxacin is more potent against gyrase than topoisomerase IV in *N. gonorrhoeae*. These *in vitro* results explain (at least in part) the intrinsic differences in fluoroquinolone activity and targeting to the type II enzymes in this species. The fact that a single mutation in gyrase is sufficient to cause levels of resistance that allow cells to escape fluoroquinolone treatment or potentially acquire additional mutations (in either the primary or secondary target) that lead to highly resistant strains emphasizes the potential clinical consequences of unbalanced gyrase/topoisomerase IV targeting.<sup>156, 279, 294</sup>

Beyond defining the utilization of the water-metal ion bridge and basis for fluoroquinolone resistance in *N. gonorrhoeae*, another focus of this dissertation has been to characterize the actions of two emerging classes of antibacterials that target gyrase and topoisomerases: novel bacterial topoisomerase inhibitors (NBTIs) and spiropyrimidinetriones (SPTs).<sup>299, 330</sup> Both classes enhance levels of DNA breaks and inhibit the catalytic activities of gyrase and topoisomerase IV.<sup>329, 332</sup> However, SPTs enhance both single- and double-stranded DNA cleavage, while NBTIs primarily stabilize single-stranded DNA breaks and suppress double-stranded DNA scission.<sup>329.</sup>

<sup>332, 352</sup> Unlike fluoroquinolones, SPTs and NBTIs do not mediate their interactions with the type II enzymes using the water-metal ion bridge and have the potential to overcome fluoroquinolone-resistant infections.<sup>329, 363, 382, 383</sup>

Chapter V describes the actions of a dioxane-linked NBTI, OSUAB-185. As mentioned above, a hallmark characteristic of NBTIs is the induction of single-stranded and suppression of double-stranded DNA breaks.<sup>299, 332, 352</sup> However, results from this study have challenged this paradigm.

As anticipated, OSUAB-185 induces single-stranded and suppresses double-stranded DNA breaks mediated by *N. gonorrhoeae* gyrase. However, the compound stabilizes both single- and double-stranded DNA breaks mediated by topoisomerase IV. The induction of double-stranded breaks does not appear to correlate with the binding of a second OSUAB-185 molecule and extends to fluoroquinolone-resistant *N. gonorrhoeae* topoisomerase IV, as well as type II enzymes from other bacteria and humans. Results further suggest that some NBTIs may have alternative binding motifs in the cleavage complex. Recent reports of the induction of single-stranded and double-stranded DNA scission by other structurally diverse NBTIs offers additional support to this hypothesis.<sup>369</sup>

Although the activity of OSUAB-185 against human topoisomerase II $\alpha$  abridges its clinical potential, it is important to note that OSUAB-185 maintains some activity against fluoroquinolone-resistant type II enzymes, highlighting the potential for other members of this class to overcome resistance. Gepotidacin, a triazaacenaphthylene NBTI that successfully completed phase III trials for urinary tract and gonorrheal infections,<sup>338, 474</sup> is one such example. This drug displayed well-balanced, dual-targeting of the *E. coli* type II topoisomerases.<sup>338, 365</sup> It is assumed that this well-balanced, dual-targeting of gyrase and topoisomerase IV will taper the emergence of resistance and increase the clinical lifespan of gepotidacin and related compounds.

Chapter VI examines the activities of zoliflodacin, an SPT that recently completed phase III trials for uncomplicated gonorrhea,<sup>335, 337</sup> and H3D-005722, a novel SPT analogue,<sup>387, 389</sup> against the gyrase and topoisomerase IV from the pathogenic agent of gonorrhea, *N. gonorrhoeae*. Like fluoroquinolones, SPT targeting of gyrase and topoisomerase IV in *N. gonorrhoeae* appears to be unbalanced. Genetic studies indicate that gyrase is the primary target of zoliflodacin in this species, and topoisomerase IV is assumed to be the secondary target.<sup>382</sup> The *in vitro* experiments presented herein support the findings from cellular studies that gyrase is the primary cytotoxic target of zoliflodacin in *N. gonorrhoeae*. First, zoliflodacin and H3D-005722 are more potent inhibitors of gyrase-catalyzed DNA supercoiling and enhancers of gyrase-mediated DNA cleavage than the corresponding DNA reactions catalyzed/mediated by topoisomerase IV. Second, gyrase-DNA-SPT cleavage complexes are intrinsically more stable than topoisomerase IV complexes. Taken together, these results strongly suggest that the activity of SPTs against gyrase and topoisomerase IV influence the targeting and toxicity of this class in cells.

Zoliflodacin is also a potent inhibitor of catalysis and enhancer of DNA cleavage with fluoroquinolone-resistant gyrase. At present, the relative contributions of DNA cleavage enhancement and catalytic inhibition to SPT-induced cell death are poorly understood. Studies with fluoroquinolone-resistant topoisomerase IV mutants are still ongoing but are expected to provide additional insight on the ability of SPTs to overcome fluoroquinolone resistance in *N. gonorrhoeae*.

The studies presented in chapters IV, V, and VI present a unique perspective on fluoroquinolone resistance and the strategies to address it. Together, these biochemical results support three main points: 1) fluoroquinolone cytotoxicity in *N. gonorrhoeae* is linked to the induction of gyrase-generated breaks in the bacterial chromosome as opposed to the loss of gyrase catalytic activity; 2) members of the NBTI class have the potential to overcome resistance

through well-balanced dual targeting of gyrase and topoisomerase IV; 3) zoliflodacin maintains high activity against fluoroquinolone-resistant type II topoisomerases in *N. gonorrhoeae*. These conclusions underscore the clinical promise of emerging gyrase/topoisomerase IV-targeted antibacterials that overcome target-mediated fluoroquinolone resistance.

### Future Studies

Future studies will be needed to investigate the translatability of biochemical results to cellular systems. First, differing levels of gyrase and topoisomerase IV protein across bacterial growth stages may account, in part, for incongruencies between the genetic and *in vitro* studies. Experiments to determine cellular concentrations of gyrase and topoisomerase IV during lag- and log-phase *N. gonorrhoeae* growth are critical for understanding drug action and targeting in cellular environments. For example, high cellular concentrations of gyrase (compared with topoisomerase IV) would promote drug poisoning of gyrase due to its relative abundance irrespective of intrinsic drug-enzyme interactions.

Second, although it is generally accepted that compounds that produce the highest levels of DNA cleavage *in vitro* will interact similarly *in cellulo*, this has not been tested empirically. To establish the relationship between genetic, biochemical, and cellular data, levels of drug-induced cleavage complexes in cultured strains of WT and fluoroquinolone-resistant *N. gonorrhoeae* will need to be quantified using an *In vivo* Complex of Enzyme (ICE) bioassay modified for bacterial cells.<sup>483</sup> Monitoring the accumulation of cleavage complexes generated by gyrase and topoisomerase IV at different drug concentrations and across time in cultured *N. gonorrhoeae* provides a cellular link to established biochemical results.

Third, cellular studies with human type II topoisomerases indicate that under conditions in which two different compounds generate similar levels of DNA scission, drug-induced cleavage complexes that persist the longest are more lethal to cells.<sup>431</sup> This suggests that, at least in human

systems, longer-lived cleavage complexes are more cytotoxic. However, analogous experiments have not been conducted in bacterial systems. Therefore, the relationship between cleavage stability and cytotoxicity should be assessed by simultaneously monitoring cleavage complex persistence and *N. gonorrhoeae* cell viability. Persistence would be monitored using a cellular “wash-out” assay in which drugs are removed from the culture and replaced with drug-free media. The longevity of drug-induced cleavage complexes would be monitored following the resuspension of cells in drug-free media using an ICE bioassay, and the number of viable cells would be quantified using a luminescence-based ATP assay.

Together, these studies could relate biochemical drug activities to their cellular effects in *N. gonorrhoeae*. Furthermore, this work should create an experimental roadmap for determining the cellular abundance of the type II enzymes, assessing levels of drug-induced gyrase/topoisomerase IV cleavage complexes, and linking cleavage complex stability with drug toxicity in bacterial systems.

Beyond bridging the gap between *in vitro* and *in vivo* studies, it is also imperative to characterize the mechanism of SPT resistance and toxicity in *N. gonorrhoeae*. Genetic mutation screens identified three mutations in the TOPRIM (metal ion binding) domain of GyrB subunit of *N. gonorrhoeae* gyrase that confer resistance to zoliflodacin: GyrB<sup>D429N</sup>, GyrB<sup>K450T</sup>, and GyrB<sup>S467N</sup>. The aspartate and basic residues (K/R) are conserved across bacterial species and type II enzymes, while the serine is not conserved.<sup>382</sup> All mutated residues are believed to directly interact with the DNA near the cleavage site, and substitutions in corresponding residues in ParE of topoisomerase IV have not been detected.<sup>382</sup> The clinical significance of these mutations is unknown. However, mutations in GyrB<sup>D429</sup> are anticipated to generate the highest levels of resistance due to the high conservation of this residue across species.<sup>382 382</sup>

Although the studies presented in Chapter VI provide a foundational assessment of the activities of SPTs against WT gyrase and topoisomerase IV, the understanding of how SPT

resistance mutations affect drug activity at the enzyme and cellular level remains incomplete. Therefore, it will be necessary to carry out a comprehensive biochemical characterization of the aforementioned gyrase mutations (GyrB<sup>D429N</sup>, GyrB<sup>K450T</sup>, and GyrB<sup>S467N</sup>) and analogous mutations in topoisomerase IV (ParE<sup>D437N</sup>) on the ability of SPTs to inhibit overall catalytic activity of the type II enzymes in *N. gonorrhoeae*. These studies may not only establish the biochemical basis for target-mediated SPT resistance but may also determine the mechanism of SPT cytotoxicity. Similar to resistance studies conducted with fluoroquinolones in Chapter IV, this work could reveal whether SPT resistance mutations alter drug binding or positioning in the active site and may help address future resistance to SPTs should it arise.

In summary, the studies presented in this dissertation make key contributions to the topoisomerase and antibacterial development fields. Chapter IV establishes the mechanistic basis for target-mediated fluoroquinolone resistance in *N. gonorrhoeae* and ascribes the cytotoxic actions of this drug class to the enhancement of enzyme-mediated DNA scission rather than the loss of enzyme activity. Chapter V challenges a hallmark of the NBTI class and describes aspects of gyrase/topoisomerase IV-mediated double-stranded DNA cleavage induced by dioxane-linked members of this class. Finally, chapter VI provides a biochemical basis for defining the activities of zoliflodacin against fluoroquinolone resistant type II topoisomerase. In particular, this last study lends credence to the ability of SPTs to overcome target-mediated fluoroquinolone resistance and presents zoliflodacin as a strategic replacement for fluoroquinolones in the antibacterial drug arsenal.

## REFERENCES

- (1) Sender, R.; Milo, R. The distribution of cellular turnover in the human body. *Nat. Med.* **2021**, *27* (1), 45-48. DOI: 10.1038/s41591-020-01182-9.
- (2) Alberts, B. *Molecular Biology of the Cell*; Garland Science, Taylor and Francis Group, 2015.
- (3) Hatton, I. A.; Galbraith, E. D.; Merleau, N. S. C.; Miettinen, T. P.; Smith, B. M.; Shander, J. A. The human cell count and size distribution. *Proc. Natl. Acad. Sci. U.S.A.* **2023**, *120* (39), e2303077120. DOI: 10.1073/pnas.2303077120 From NLM Medline.
- (4) Nurk, S.; Koren, S.; Rhie, A.; Rautiainen, M.; Bzikadze, A. V.; Mikheenko, A.; Vollger, M. R.; Altemose, N.; Uralsky, L.; Gershman, A.; Aganezov, S.; Hoyt, S. J.; Diekhans, M.; Logsdon, G. A.; Alonge, M.; Antonarakis, S. E.; Borchers, M.; Bouffard, G. G.; Brooks, S. Y.; Caldas, G. V.; Chen, N. C.; Cheng, H.; Chin, C. S.; Chow, W.; de Lima, L. G.; Dishuck, P. C.; Durbin, R.; Dvorkina, T.; Fiddes, I. T.; Formenti, G.; Fulton, R. S.; Functamman, A.; Garrison, E.; Grady, P. G. S.; Graves-Lindsay, T. A.; Hall, I. M.; Hansen, N. F.; Hartley, G. A.; Haukness, M.; Howe, K.; Hunkapiller, M. W.; Jain, C.; Jain, M.; Jarvis, E. D.; Kerpedjiev, P.; Kirsche, M.; Kolmogorov, M.; Korf, J.; Kremitzki, M.; Li, H.; Maduro, V. V.; Marschall, T.; McCartney, A. M.; McDaniel, J.; Miller, D. E.; Mullikin, J. C.; Myers, E. W.; Olson, N. D.; Paten, B.; Peluso, P.; Pevzner, P. A.; Porubsky, D.; Potapova, T.; Rogae, E. I.; Rosenfeld, J. A.; Salzberg, S. L.; Schneider, V. A.; Sedlazeck, F. J.; Shafin, K.; Shew, C. J.; Shumate, A.; Sims, Y.; Smit, A. F. A.; Soto, D. C.; Sovic, I.; Storer, J. M.; Streets, A.; Sullivan, B. A.; Thibaud-Nissen, F.; Torrance, J.; Wagner, J.; Walenz, B. P.; Wenger, A.; Wood, J. M. D.; Xiao, C.; Yan, S. M.; Young, A. C.; Zarate, S.; Surti, U.; McCoy, R. C.; Dennis, M. Y.; Alexandrov, I. A.; Gerton, J. L.; O'Neill, R. J.; Timp, W.; Zook, J. M.; Schatz, M. C.; Eichler, E. E.; Miga, K. H.; Phillippy, A. M. The complete sequence of a human genome. *Science* **2022**, *376* (6588), 44-53. DOI: 10.1126/science.abj6987.
- (5) Bates, A. D.; Maxwell, A. *DNA Topology*; Oxford University Press, 2005.
- (6) Espeli, O.; Marians, K. J. Untangling intracellular DNA topology. *Mol. Microbiol.* **2004**, *52* (4), 925-931. DOI: 10.1111/j.1365-2958.2004.04047.x.
- (7) Buck, D. DNA topology. In *Proceedings of Symposia in Applied Mathematics: Applications of Knot Theory*, Buck, D., Flapan, E. Eds.; Vol. 66; American Mathematical Society, 2009; pp 47-80.
- (8) Seol, Y.; Neuman, K. C. The dynamic interplay between DNA topoisomerases and DNA topology. *Biophys. Rev.* **2016**, *8* (Suppl 1), 101-111. DOI: 10.1007/s12551-016-0240-8.
- (9) Ashley, R. E.; Osheroff, N. Regulation of DNA by topoisomerases: mathematics at the molecular level. In *Knots, Low-Dimensional Topology and Applications*, Adams, C., McA. Gordon, C., Jones, V., Kauffman, L., Lambropoulou, S., Millet, K., Przytycki, J., Ricca, R., Sazdanovic, R. Eds.; Springer Proceedings in Mathematics & Statistics, Springer Nature, 2019; pp 411-433.
- (10) Vologodskii, A. V.; Cozzarelli, N. R. Conformational and thermodynamic properties of supercoiled DNA. *Annu. Rev. Biophys. Biomol. Struct.* **1994**, *23*, 609-643. DOI: 10.1146/annurev.bb.23.060194.003141.
- (11) Liu, Z.; Deibler, R. W.; Chan, H. S.; Zechiedrich, L. The why and how of DNA unlinking. *Nucleic Acids Res.* **2009**, *37* (3), 661-671. DOI: 10.1093/nar/gkp041.
- (12) Vos, S. M.; Tretter, E. M.; Schmidt, B. H.; Berger, J. M. All tangled up: how cells direct, manage and exploit topoisomerase function. *Nat. Rev. Mol. Cell Biol.* **2011**, *12* (12), 827-841. DOI: 10.1038/nrm3228.
- (13) Timsit, Y. Local sensing of global DNA topology: from crossover geometry to type II topoisomerase processivity. *Nucleic Acids Res.* **2011**, *39* (20), 8665-8676. DOI: 10.1093/nar/gkr556.

- (14) Finzi, L.; Olson, W. K. The emerging role of DNA supercoiling as a dynamic player in genomic structure and function. *Biophysical Reviews* **2016**, *8* (Suppl 1), 1-3. DOI: 10.1007/s12551-016-0214-x.
- (15) Bauer, W. R.; Crick, F. H.; White, J. H. Supercoiled DNA. *Sci Am* **1980**, *243* (1), 100-113.
- (16) Boles, T. C.; White, J. H.; Cozzarelli, N. R. Structure of plectonemically supercoiled DNA. *J. Mol. Biol.* **1990**, *213* (4), 931-951. DOI: 10.1016/S0022-2836(05)80272-4.
- (17) Baranello, L.; Levens, D.; Gupta, A.; Kouzine, F. The importance of being supercoiled: how DNA mechanics regulate dynamic processes. *Biochim. Biophys. Acta* **2012**, *1819* (7), 632-638. DOI: 10.1016/j.bbagr.2011.12.007.
- (18) van Loenhout, M. T.; de Grunt, M. V.; Dekker, C. Dynamics of DNA supercoils. *Science* **2012**, *338* (6103), 94-97. DOI: 10.1126/science.1225810.
- (19) Lal, A.; Dhar, A.; Trostel, A.; Kouzine, F.; Seshasayee, A. S.; Adhya, S. Genome scale patterns of supercoiling in a bacterial chromosome. *Nat. Commun.* **2016**, *7*, 11055. DOI: 10.1038/ncomms11055.
- (20) Jian, J. Y.; Osheroff, N. Telling your right hand from your left: the effects of DNA supercoil handedness on the actions of type II topoisomerases. *Int. J. Mol. Sci.* **2023**, *24* (13). DOI: 10.3390/ijms241311199.
- (21) Liu, L. F.; Wang, J. C. Supercoiling of the DNA template during transcription. *Proc. Natl. Acad. Sci. U.S.A.* **1987**, *84* (20), 7024-7027.
- (22) Schwartzman, J. B.; Stasiak, A. A topological view of the replicon. *EMBO Rep.* **2004**, *5* (3), 256-261.
- (23) Dorman, C. J.; Dorman, M. J. DNA supercoiling is a fundamental regulatory principle in the control of bacterial gene expression. *Biophys. Rev.* **2016**, *8* (Suppl 1), 89-100. DOI: 10.1007/s12551-016-0238-2.
- (24) Deweese, J. E.; Osheroff, M. A.; Osheroff, N. DNA topology and topoisomerases: teaching a "knotty" subject. *Biochem. Mol. Biol. Educ.* **2008**, *37* (1), 2-10. DOI: 10.1002/bmb.20244.
- (25) Sundin, O.; Varshavsky, A. Arrest of segregation leads to accumulation of highly intertwined catenated dimers: dissection of the final stages of SV40 DNA replication. *Cell* **1981**, *25* (3), 659-669. DOI: 10.1016/0092-8674(81)90173-2.
- (26) Akimitsu, N.; Adachi, N.; Hirai, H.; Hossain, M. S.; Hamamoto, H.; Kobayashi, M.; Aratani, Y.; Koyama, H.; Sekimizu, K. Enforced cytokinesis without complete nuclear division in embryonic cells depleting the activity of DNA topoisomerase II $\alpha$ . *Genes Cells* **2003**, *8* (4), 393-402. DOI: 10.1046/j.1365-2443.2003.00643.x.
- (27) Arai, Y.; Yasuda, R.; Akashi, K.; Harada, Y.; Miyata, H.; Kinoshita, K., Jr.; Itoh, H. Tying a molecular knot with optical tweezers. *Nature* **1999**, *399* (6735), 446-448. DOI: 10.1038/20894.
- (28) Bush, N. G.; Evans-Roberts, K.; Maxwell, A. DNA topoisomerases. *EcoSal Plus* **2015**, *6* (2). DOI: 10.1128/ecosalplus.ESP-0010-2014.
- (29) McKie, S. J.; Neuman, K. C.; Maxwell, A. DNA topoisomerases: advances in understanding of cellular roles and multi-protein complexes via structure-function analysis. *Bioessays* **2021**, *43*, 2000286. DOI: 10.1002/bies.202000286.
- (30) Forterre, P.; Gribaldo, S.; Gabelle, D.; Serre, M. C. Origin and evolution of DNA topoisomerases. *Biochimie* **2007**, *89* (4), 427-446. DOI: 10.1016/j.biochi.2006.12.009.
- (31) Wang, J. C. Interaction between DNA and an *Escherichia coli* protein omega. *J. Mol. Biol.* **1971**, *55* (3), 523-533. DOI: 10.1016/0022-2836(71)90334-2.
- (32) Gellert, M.; Mizuuchi, K.; O'Dea, M. H.; Nash, H. A. DNA gyrase: an enzyme that introduces superhelical turns into DNA. *Proc. Natl. Acad. Sci. U.S.A.* **1976**, *73*, 3872-3876. DOI: 10.1073/pnas.73.11.3872.
- (33) Mizuuchi, K.; Fisher, L. M.; O'Dea, M. H.; Gellert, M. DNA gyrase action involves the introduction of transient double-strand breaks into DNA. *Proc. Natl. Acad. Sci. U.S.A.* **1980**, *77* (4), 1847-1851. DOI: 10.1073/pnas.77.4.1847.



- (34) Bermejo, R.; Doksani, Y.; Capra, T.; Katou, Y. M.; Tanaka, H.; Shirahige, K.; Foiani, M. Top1- and Top2-mediated topological transitions at replication forks ensure fork progression and stability and prevent DNA damage checkpoint activation. *Genes Dev.* **2007**, *21* (15), 1921-1936. DOI: 10.1101/gad.432107.
- (35) Suski, C.; Marians, K. J. Resolution of converging replication forks by RecQ and topoisomerase III. *Mol. Cell* **2008**, *30* (6), 779-789. DOI: 10.1016/j.molcel.2008.04.020.
- (36) Mizuuchi, K.; O'Dea, M. H.; Gellert, M. DNA gyrase: subunit structure and ATPase activity of the purified enzyme. *Proc. Natl. Acad. Sci. U.S.A.* **1978**, *75*, 5960-5963. DOI: 10.1073/pnas.75.12.5960.
- (37) Kato, J.; Nishimura, Y.; Imamura, R.; Niki, H.; Hiraga, S.; Suzuki, H. New topoisomerase essential for chromosome segregation in *E. coli*. *Cell* **1990**, *63* (2), 393-404. DOI: 10.1016/0092-8674(90)90172-b.
- (38) Chen, S. H.; Chan, N. L.; Hsieh, T. S. New mechanistic and functional insights into DNA topoisomerases. *Annu. Rev. Biochem.* **2013**, *82*, 139-170. DOI: 10.1146/annurev-biochem-061809-100002.
- (39) Lynn, R.; Giaever, G.; Swanberg, S. L.; Wang, J. C. Tandem regions of yeast DNA topoisomerase II share homology with different subunits of bacterial gyrase. *Science* **1986**, *233* (4764), 647-649. DOI: 10.1126/science.3014661.
- (40) Ferrero, L.; Cameron, B.; Manse, B.; Lagneaux, D.; Crouzet, J.; Famechon, A.; Blanche, F. Cloning and primary structure of *Staphylococcus aureus* DNA topoisomerase IV: a primary target of fluoroquinolones. *Mol. Microbiol.* **1994**, *13* (4), 641-653. DOI: 10.1111/j.1365-2958.1994.tb00458.x.
- (41) Wigley, D. B.; Davies, G. J.; Dodson, E. J.; Maxwell, A.; Dodson, G. Crystal structure of an N-terminal fragment of the DNA gyrase B protein. *Nature* **1991**, *351* (6328), 624-629. DOI: 10.1038/351624a0.
- (42) Oestergaard, V. H.; Bjergbaek, L.; Skouboe, C.; Giangiacomo, L.; Knudsen, B. R.; Andersen, A. H. The transducer domain is important for clamp operation in human DNA topoisomerase II $\alpha$ . *J. Biol. Chem.* **2004**, *279* (3), 1684-1691.
- (43) Schmidt, B. H.; Osheroff, N.; Berger, J. M. Structure of a topoisomerase II-DNA-nucleotide complex reveals a new control mechanism for ATPase activity. *Nat. Struct. Mol. Biol.* **2012**, *19* (11), 1147-1154. DOI: 10.1038/nsmb.2388.
- (44) Vanden Broeck, A.; Lotz, C.; Ortiz, J.; Lamour, V. Cryo-EM structure of the complete *E. coli* DNA gyrase nucleoprotein complex. *Nat. Commun.* **2019**, *10*. DOI: 10.1038/s41467-019-12914-y.
- (45) Laponogov, I.; Veselkov, D. A.; Crevel, I. M.; Pan, X. S.; Fisher, L. M.; Sanderson, M. R. Structure of an 'open' clamp type II topoisomerase-DNA complex provides a mechanism for DNA capture and transport. *Nucleic Acids Res.* **2013**, *41* (21), 9911-9923. DOI: 10.1093/nar/gkt749.
- (46) Hartmann, S.; Gubaev, A.; Klostermeier, D. Binding and hydrolysis of a single ATP is sufficient for N-gate closure and DNA supercoiling by gyrase. *J. Mol. Biol.* **2017**, *429* (23), 3717-3729. DOI: 10.1016/j.jmb.2017.10.005.
- (47) Bjergbaek, L.; Kingma, P.; Nielsen, I. S.; Wang, Y.; Westergaard, O.; Osheroff, N.; Andersen, A. H. Communication between the ATPase and cleavage/religation domains of human topoisomerase II $\alpha$ . *J. Biol. Chem.* **2000**, *275* (17), 13041-13048. DOI: 10.1074/jbc.275.17.13041.
- (48) Aravind, L.; Leipe, D. D.; Koonin, E. V. Toprim--a conserved catalytic domain in type IA and II topoisomerases, DnaG-type primases, OLD family nucleases and RecR proteins. *Nucleic Acids Res.* **1998**, *26* (18), 4205-4213. DOI: 10.1093/nar/26.18.4205.
- (49) Schmidt, B. H.; Burgin, A. B.; Deweese, J. E.; Osheroff, N.; Berger, J. M. A novel and unified two-metal mechanism for DNA cleavage by type II and IA topoisomerases. *Nature* **2010**, *465* (7298), 641-644. DOI: 10.1038/nature08974.

- (50) Wendorff, T. J.; Schmidt, B. H.; Heslop, P.; Austin, C. A.; Berger, J. M. The structure of DNA-bound human topoisomerase II $\alpha$ : conformational mechanisms for coordinating inter-subunit interactions with DNA cleavage. *J. Mol. Biol.* **2012**, *424* (3-4), 109-124. DOI: S0022-2836(12)00581-5 [pii] 10.1016/j.jmb.2012.07.014.
- (51) Chen, S. F.; Huang, N. L.; Lin, J. H.; Wu, C. C.; Wang, Y. R.; Yu, Y. J.; Gilson, M. K.; Chan, N. L. Structural insights into the gating of DNA passage by the topoisomerase II DNA-gate. *Nat. Commun.* **2018**, *9* (1), 3085. DOI: 10.1038/s41467-018-05406-y.
- (52) Dong, K. C.; Berger, J. M. Structural basis for gate-DNA recognition and bending by type IIA topoisomerases. *Nature* **2007**, *450* (7173), 1201-1205. DOI: 10.1038/nature06396.
- (53) Vidmar, V.; Vayssieres, M.; Lamour, V. What's on the other side of the gate: a structural perspective on DNA gate opening of type IA and IIA DNA topoisomerases. *Int. J. Mol. Sci.* **2023**, *24* (4). DOI: 10.3390/ijms24043986.
- (54) Osheroff, N. Role of the divalent cation in topoisomerase II mediated reactions. *Biochemistry* **1987**, *26* (20), 6402-6406.
- (55) Laponogov, I.; Pan, X. S.; Veselkov, D. A.; McAuley, K. E.; Fisher, L. M.; Sanderson, M. R. Structural basis of gate-DNA breakage and resealing by type II topoisomerases. *PLoS One* **2010**, *5* (6). DOI: 10.1371/journal.pone.0011338.
- (56) Deweese, J. E.; Osheroff, N. The use of divalent metal ions by type II topoisomerases. *Metallomics* **2010**, *2* (7), 450-459.
- (57) Dickey, J. S.; Osheroff, N. Impact of the C-terminal domain of topoisomerase II $\alpha$  on the DNA cleavage activity of the human enzyme. *Biochemistry* **2005**, *44* (34), 11546-11554.
- (58) Kramlinger, V. M.; Hiasa, H. The "GyrA-box" is required for the ability of DNA gyrase to wrap DNA and catalyze the supercoiling reaction. *J. Biol. Chem.* **2006**, *281* (6), 3738-3742. DOI: 10.1074/jbc.M511160200.
- (59) Corbett, K. D.; Shultzaberger, R. K.; Berger, J. M. The C-terminal domain of DNA gyrase A adopts a DNA-bending beta-pinwheel fold. *Proc. Natl. Acad. Sci. U.S.A.* **2004**, *101* (19), 7293-7298. DOI: 10.1073/pnas.0401595101.
- (60) Lanz, M. A.; Klostermeier, D. The GyrA-box determines the geometry of DNA bound to gyrase and couples DNA binding to the nucleotide cycle. *Nucleic Acids Res.* **2012**, *40* (21), 10893-10903. DOI: 10.1093/nar/gks852.
- (61) Hirsch, J.; Klostermeier, D. What makes a type IIA topoisomerase a gyrase or a topo IV? *Nucleic Acids Res.* **2021**, *49* (11), 6027-6042. DOI: 10.1093/nar/gkab270.
- (62) Linka, R. M.; Porter, A. C.; Volkov, A.; Mielke, C.; Boege, F.; Christensen, M. O. C-terminal regions of topoisomerase II $\alpha$  and II $\beta$  determine isoform-specific functioning of the enzymes *in vivo*. *Nucleic Acids Res.* **2007**, *35* (11), 3810-3822. DOI: 10.1093/nar/gkm102.
- (63) Antoniou-Kourounioti, M.; Mimmack, M. L.; Porter, A. C. G.; Farr, C. J. The impact of the C-terminal region on the interaction of topoisomerase II $\alpha$  with mitotic chromatin. *Int. J. Mol. Sci.* **2019**, *20* (5). DOI: 10.3390/ijms20051238.
- (64) Vanden Broeck, A.; Lotz, C.; Drillien, R.; Haas, L.; Bedez, C.; Lamour, V. Structural basis for allosteric regulation of human topoisomerase II $\alpha$ . *Nat. Commun.* **2021**, *12* (1), 2962. DOI: 10.1038/s41467-021-23136-6.
- (65) Morrison, A.; Cozzarelli, N. R. Contacts between DNA gyrase and its binding site on DNA: features of symmetry and asymmetry revealed by protection from nucleases. *Proc. Natl. Acad. Sci. U.S.A.* **1981**, *78* (3), 1416-1420. DOI: 10.1073/pnas.78.3.1416.
- (66) Kirchhausen, T.; Wang, J. C.; Harrison, S. C. DNA gyrase and its complexes with DNA: direct observation by electron microscopy. *Cell* **1985**, *41* (3), 933-943. DOI: 10.1016/s0092-8674(85)80074-x.
- (67) Corbett, K. D.; Schoeffler, A. J.; Thomsen, N. D.; Berger, J. M. The structural basis for substrate specificity in DNA topoisomerase IV. *J. Mol. Biol.* **2005**, *351* (3), 545-561. DOI: 10.1016/j.jmb.2005.06.029.

- (68) Kumar, R.; Riley, J. E.; Parry, D.; Bates, A. D.; Nagaraja, V. Binding of two DNA molecules by type II topoisomerases for decatenation. *Nucleic Acids Res.* **2012**, *40* (21), 10904-10915. DOI: 10.1093/nar/gks843.
- (69) Laponogov, I.; Pan, X. S.; Veselkov, D. A.; Skamrova, G. B.; Umrekar, T. R.; Fisher, L. M.; Sanderson, M. R. Trapping of the transport-segment DNA by the ATPase domains of a type II topoisomerase. *Nat. Commun.* **2018**, *9* (1), 2579. DOI: 10.1038/s41467-018-05005-x.
- (70) Roca, J.; Wang, J. C. The capture of a DNA double helix by an ATP-dependent protein clamp: a key step in DNA transport by type II DNA topoisomerases. *Cell* **1992**, *71* (5), 833-840. DOI: 10.1016/0092-8674(92)90558-t.
- (71) Williams, N. L.; Howells, A. J.; Maxwell, A. Locking the ATP-operated clamp of DNA gyrase: probing the mechanism of strand passage. *J. Mol. Biol.* **2001**, *306* (5), 969-984. DOI: 10.1006/jmbi.2001.4468.
- (72) Gubaev, A.; Klostermeier, D. DNA-induced narrowing of the gyrase N-gate coordinates T-segment capture and strand passage. *Proc. Natl. Acad. Sci. U.S.A.* **2011**, *108* (34), 14085-14090. DOI: 10.1073/pnas.1102100108.
- (73) Jang, Y.; Son, H.; Lee, S. W.; Hwang, W.; Jung, S. R.; Byl, J. A. W.; Osheroff, N.; Lee, S. Selection of DNA cleavage sites by topoisomerase II results from enzyme-induced flexibility of DNA. *Cell Chem. Biol.* **2019**, *26* (4), 502-511. DOI: 10.1016/j.chembiol.2018.12.003.
- (74) Lee, S.; Jung, S. R.; Heo, K.; Byl, J. A.; Deweese, J. E.; Osheroff, N.; Hohng, S. DNA cleavage and opening reactions of human topoisomerase II $\alpha$  are regulated via Mg<sup>2+</sup>-mediated dynamic bending of gate-DNA. *Proc. Natl. Acad. Sci. U.S.A.* **2012**, *109* (8), 2925-2930. DOI: 1115704109 [pii] 10.1073/pnas.1115704109.
- (75) Lee, I.; Dong, K. C.; Berger, J. M. The role of DNA bending in type IIA topoisomerase function. *Nucleic Acids Res.* **2013**, *41* (10), 5444-5456. DOI: 10.1093/nar/gkt238.
- (76) Sander, M.; Hsieh, T. Double strand DNA cleavage by type II DNA topoisomerase from *Drosophila melanogaster*. *J. Biol. Chem.* **1983**, *258* (13), 8421-8428.
- (77) Vann, K. R.; Oviatt, A. A.; Osheroff, N. Topoisomerase II poisons: converting essential enzymes into molecular scissors. *Biochemistry* **2021**, *60* (21), 1630-1641. DOI: 10.1021/acs.biochem.1c00240.
- (78) Deweese, J. E.; Osheroff, N. The DNA cleavage reaction of topoisomerase II: wolf in sheep's clothing. *Nucleic Acids Res.* **2009**, *37* (3), 738-749. DOI: 10.1093/nar/gkn937.
- (79) Dalvie, E. D.; Osheroff, N. DNA topoisomerases: type II. In *Encyclopedia of Biological Chemistry*, 3rd ed.; Jez, J., Allewell, N. M., Blakenship, R. E., Chapman, K. D., Cooper, A. J. L., Maresca, T. J., Pandey, S., Zaher, H. Eds.; Academic Press, 2021; Vol. 3, pp 479-486. DOI: 10.1016/B978-0-12-809633-8.21378-2.
- (80) Pitts, S. L.; Liou, G. F.; Mitchenall, L. A.; Burgin, A. B.; Maxwell, A.; Neuman, K. C.; Osheroff, N. Use of divalent metal ions in the DNA cleavage reaction of topoisomerase IV. *Nucleic Acids Res.* **2011**, *39* (11), 4808-4817. DOI: 10.1093/nar/gkr018.
- (81) Noble, C. G.; Maxwell, A. The role of GyrB in the DNA cleavage-religation reaction of DNA gyrase: a proposed two metal-ion mechanism. *J. Mol. Biol.* **2002**, *318* (2), 361-371. DOI: 10.1016/S0022-2836(02)00049-9.
- (82) Roca, J.; Berger, J. M.; Harrison, S. C.; Wang, J. C. DNA transport by a type II topoisomerase: direct evidence for a two-gate mechanism. *Proc. Natl. Acad. Sci. U.S.A.* **1996**, *93* (9), 4057-4062. DOI: 10.1073/pnas.93.9.4057.
- (83) Williams, N. L.; Maxwell, A. Probing the two-gate mechanism of DNA gyrase using cysteine cross-linking. *Biochemistry* **1999**, *38* (41), 13502-13511. DOI: 10.1021/bi9912488.
- (84) Corbett, K. D.; Berger, J. M. Structure of the topoisomerase VI-B subunit: implications for type II topoisomerase mechanism and evolution. *EMBO J.* **2003**, *22* (1), 151-163. DOI: 10.1093/emboj/cdg008.

- (85) Harkins, T. T.; Lewis, T. J.; Lindsley, J. E. Pre-steady-state analysis of ATP hydrolysis by *Saccharomyces cerevisiae* DNA topoisomerase II. 2. Kinetic mechanism for the sequential hydrolysis of two ATP. *Biochemistry* **1998**, *37* (20), 7299-7312. DOI: 10.1021/bi9729108.
- (86) Baird, C. L.; Gordon, M. S.; Andrenyak, D. M.; Marecek, J. F.; Lindsley, J. E. The ATPase reaction cycle of yeast DNA topoisomerase II. Slow rates of ATP resynthesis and P(i) release. *J. Biol. Chem.* **2001**, *276* (30), 27893-27898. DOI: 10.1074/jbc.M102544200.
- (87) Osheroff, N. Eukaryotic topoisomerase II. Characterization of enzyme turnover. *J. Biol. Chem.* **1986**, *261*, 9944-9950.
- (88) Baldi, M. I.; Benedetti, P.; Mattoccia, E.; Tocchini-Valentini, G. P. In vitro catenation and decatenation of DNA and a novel eucaryotic ATP-dependent topoisomerase. *Cell* **1980**, *20* (2), 461-467. DOI: 10.1016/0092-8674(80)90632-7.
- (89) Hsieh, T.; Brutlag, D. ATP-dependent DNA topoisomerase from *D. melanogaster* reversibly catenates duplex DNA rings. *Cell* **1980**, *21* (1), 115-125. DOI: 10.1016/0092-8674(80)90119-1.
- (90) Miller, K. G.; Liu, L. F.; Englund, P. T. A homogeneous type II DNA topoisomerase from HeLa cell nuclei. *J. Biol. Chem.* **1981**, *256* (17), 9334-9339.
- (91) Shelton, E. R.; Osheroff, N.; Brutlag, D. L. DNA topoisomerase II from *Drosophila melanogaster*. Purification and physical characterization. *J. Biol. Chem.* **1983**, *258* (15), 9530-9535.
- (92) Goto, T.; Laipis, P.; Wang, J. C. The purification and characterization of DNA topoisomerases I and II of the yeast *Saccharomyces cerevisiae*. *J. Biol. Chem.* **1984**, *259* (16), 10422-10429.
- (93) Drake, F. H.; Zimmerman, J. P.; McCabe, F. L.; Bartus, H. F.; Per, S. R.; Sullivan, D. M.; Ross, W. E.; Mattern, M. R.; Johnson, R. K.; Croke, S. T. Purification of topoisomerase II from amsacrine-resistant P388 leukemia cells. Evidence for two forms of the enzyme. *J. Biol. Chem.* **1987**, *262* (34), 16739-16747.
- (94) Tsai-Pflugfelder, M.; Liu, L. F.; Liu, A. A.; Tewey, K. M.; Whang-Peng, J.; Knutsen, T.; Huebner, K.; Croce, C. M.; Wang, J. C. Cloning and sequencing of cDNA encoding human DNA topoisomerase II and localization of the gene to chromosome region 17q21-22. *Proc. Natl. Acad. Sci. U.S.A.* **1988**, *85* (19), 7177-7181.
- (95) Drake, F. H.; Hofmann, G. A.; Bartus, H. F.; Mattern, M. R.; Croke, S. T.; Mirabelli, C. K. Biochemical and pharmacological properties of p170 and p180 forms of topoisomerase II. *Biochemistry* **1989**, *28* (20), 8154-8160.
- (96) Jenkins, J. R.; Ayton, P.; Jones, T.; Davies, S. L.; Simmons, D. L.; Harris, A. L.; Sheer, D.; Hickson, I. D. Isolation of cDNA clones encoding the  $\beta$  isozyme of human DNA topoisomerase II and localisation of the gene to chromosome 3p24. *Nucleic Acids Res.* **1992**, *20* (21), 5587-5592.
- (97) Tan, K. B.; Dorman, T. E.; Falls, K. M.; Chung, T. D.; Mirabelli, C. K.; Croke, S. T.; Mao, J. Topoisomerase II $\alpha$  and topoisomerase II $\beta$  genes: characterization and mapping to human chromosomes 17 and 3, respectively. *Cancer Res.* **1992**, *52* (1), 231-234.
- (98) Austin, C. A.; Lee, K. C.; Swan, R. L.; Khazeem, M. M.; Manville, C. M.; Cridland, P.; Treumann, A.; Porter, A.; Morris, N. J.; Cowell, I. G. TOP2B: The First Thirty Years. *Int. J. Mol. Sci.* **2018**, *19* (9), 2765. DOI: 10.3390/ijms19092765.
- (99) Woessner, R. D.; Mattern, M. R.; Mirabelli, C. K.; Johnson, R. K.; Drake, F. H. Proliferation- and cell cycle-dependent differences in expression of the 170 kilodalton and 180 kilodalton forms of topoisomerase II in NIH-3T3 cells. *Cell Growth Differ.* **1991**, *2* (4), 209-214.
- (100) Lee, J. H.; Berger, J. M. Cell cycle-dependent control and roles of DNA topoisomerase II. *Genes (Basel)* **2019**, *10* (11). DOI: 10.3390/genes10110859.
- (101) Pommier, Y.; Nussenzweig, A.; Takeda, S.; Austin, C. Human topoisomerases and their roles in genome stability and organization. *Nat. Rev. Mol. Cell Biol.* **2022**, *23* (6), 407-427. DOI: 10.1038/s41580-022-00452-3.

- (102) Capranico, G.; Tinelli, S.; Austin, C. A.; Fisher, M. L.; Zunino, F. Different patterns of gene expression of topoisomerase II isoforms in differentiated tissues during murine development. *Biochim. Biophys. Acta* **1992**, *1132* (1), 43-48. DOI: 10.1016/0167-4781(92)90050-a.
- (103) Grue, P.; Grasser, A.; Sehested, M.; Jensen, P. B.; Uhse, A.; Straub, T.; Ness, W.; Boege, F. Essential mitotic functions of DNA topoisomerase II $\alpha$  are not adopted by topoisomerase II $\beta$  in human H69 cells. *J. Biol. Chem.* **1998**, *273* (50), 33660-33666.
- (104) Pommier, Y.; Sun, Y.; Huang, S. N.; Nitiss, J. L. Roles of eukaryotic topoisomerases in transcription, replication and genomic stability. *Nat. Rev. Mol. Cell Biol.* **2016**, *17* (11), 703-721. DOI: 10.1038/nrm.2016.111.
- (105) Lucas, I.; Germe, T.; Chevrier-Miller, M.; Hyrien, O. Topoisomerase II can unlink replicating DNA by precatenane removal. *EMBO J.* **2001**, *20* (22), 6509-6519. DOI: 10.1093/emboj/20.22.6509.
- (106) Charbin, A.; Bouchoux, C.; Uhlmann, F. Condensin aids sister chromatid decatenation by topoisomerase II. *Nucleic Acids Res.* **2014**, *42* (1), 340-348. DOI: 10.1093/nar/gkt882.
- (107) Heintzman, D. R.; Campos, L. V.; Byl, J. A. W.; Osheroff, N.; Dewar, J. M. Topoisomerase II is crucial for fork convergence during vertebrate replication termination. *Cell Rep.* **2019**, *29* (2), 422-436. DOI: 10.1016/j.celrep.2019.08.097.
- (108) Adachi, Y.; Luke, M.; Laemmli, U. K. Chromosome assembly in vitro: topoisomerase II is required for condensation. *Cell* **1991**, *64* (1), 137-148. DOI: 10.1016/0092-8674(91)90215-k.
- (109) Hirano, T.; Mitchison, T. J. Topoisomerase II does not play a scaffolding role in the organization of mitotic chromosomes assembled in *Xenopus* egg extracts. *J. Cell Biol.* **1993**, *120* (3), 601-612. DOI: 10.1083/jcb.120.3.601.
- (110) Takahashi, N.; Quimbaya, M.; Schubert, V.; Lammens, T.; Vandepoele, K.; Schubert, I.; Matsui, M.; Inze, D.; Berx, G.; De Veylder, L. The MCM-binding protein ETG1 aids sister chromatid cohesion required for postreplicative homologous recombination repair. *PLoS Genet.* **2010**, *6* (1), e1000817. DOI: 10.1371/journal.pgen.1000817.
- (111) Nagasaka, K.; Hossain, M. J.; Roberti, M. J.; Ellenberg, J.; Hirota, T. Sister chromatid resolution is an intrinsic part of chromosome organization in prophase. *Nat. Cell Biol.* **2016**, *18* (6), 692-699. DOI: 10.1038/ncb3353.
- (112) Thakurela, S.; Garding, A.; Jung, J.; Schubeler, D.; Burger, L.; Tiwari, V. K. Gene regulation and priming by topoisomerase II $\alpha$  in embryonic stem cells. *Nat. Commun.* **2013**, *4*, 2478. DOI: 10.1038/ncomms3478.
- (113) Yu, X.; Davenport, J. W.; Urtishak, K. A.; Carillo, M. L.; Gosai, S. J.; Kolaris, C. P.; Byl, J. A. W.; Rappaport, E. F.; Osheroff, N.; Gregory, B. D.; Felix, C. A. Genome-wide TOP2A DNA cleavage is biased toward translocated and highly transcribed loci. *Genome Res.* **2017**, *27* (7), 1238-1249. DOI: 10.1101/gr.211615.116.
- (114) Dereuddre, S.; Frey, S.; Delaporte, C.; Jacquemin-Sablon, A. Cloning and characterization of full-length cDNAs coding for the DNA topoisomerase II $\beta$  from Chinese hamster lung cells sensitive and resistant 9-OH-ellipticine. *Biochim. Biophys. Acta* **1995**, *1264* (2), 178-182. DOI: 10.1016/0167-4781(95)00164-c.
- (115) Ju, B. G.; Lunyak, V. V.; Perissi, V.; Garcia-Bassets, I.; Rose, D. W.; Glass, C. K.; Rosenfeld, M. G. A topoisomerase II $\beta$ -mediated dsDNA break required for regulated transcription. *Science* **2006**, *312* (5781), 1798-1802. DOI: 10.1126/science.1127196.
- (116) Bollimpelli, V. S.; Dholaniya, P. S.; Kondapi, A. K. Topoisomerase II $\beta$  and its role in different biological contexts. *Arch. Biochem. Biophys.* **2017**, *633*, 78-84. DOI: 10.1016/j.abb.2017.06.021.

- (117) Kimura, K.; Saijo, M.; Ui, M.; Enomoto, T. Growth state- and cell cycle-dependent fluctuation in the expression of two forms of DNA topoisomerase II and possible specific modification of the higher molecular weight form in the M phase. *J. Biol. Chem.* **1994**, *269*, 1173-1176.
- (118) Yang, X.; Li, W.; Prescott, E. D.; Burden, S. J.; Wang, J. C. DNA topoisomerase II $\beta$  and neural development. *Science* **2000**, *287* (5450), 131-134. DOI: 10.1126/science.287.5450.131.
- (119) Lyu, Y. L.; Wang, J. C. Aberrant lamination in the cerebral cortex of mouse embryos lacking DNA topoisomerase II $\beta$ . *Proc. Natl. Acad. Sci. U.S.A.* **2003**, *100* (12), 7123-7128. DOI: 10.1073/pnas.1232376100.
- (120) Heng, X.; Le, W. D. The function of DNA topoisomerase II $\beta$  in neuronal development. *Neurosci. Bull.* **2010**, *26* (5), 411-416. DOI: 10.1007/s12264-010-0625-9.
- (121) Tiwari, V. K.; Burger, L.; Nikolettou, V.; Deogracias, R.; Thakurela, S.; Wirbelauer, C.; Kaut, J.; Terranova, R.; Hoerner, L.; Mielke, C.; Boege, F.; Murr, R.; Peters, A. H.; Barde, Y. A.; Schubeler, D. Target genes of topoisomerase II $\beta$  regulate neuronal survival and are defined by their chromatin state. *Proc. Natl. Acad. Sci. U.S.A.* **2012**, *109* (16), E934-943. DOI: 10.1073/pnas.1119798109.
- (122) Stoll, G.; Pietilainen, O. P.; Linder, B.; Suvisaari, J.; Brosi, C.; Hennah, W.; Leppa, V.; Torniainen, M.; Ripatti, S.; Ala-Mello, S.; Plottner, O.; Rehnstrom, K.; Tuulio-Henriksson, A.; Varilo, T.; Tallila, J.; Kristiansson, K.; Isohanni, M.; Kaprio, J.; Eriksson, J. G.; Raitakari, O. T.; Lehtimaki, T.; Jarvelin, M. R.; Salomaa, V.; Hurles, M.; Stefansson, H.; Peltonen, L.; Sullivan, P. F.; Paunio, T.; Lonqvist, J.; Daly, M. J.; Fischer, U.; Freimer, N. B.; Palotie, A. Deletion of TOP3 $\beta$ , a component of FMRP-containing mRNPs, contributes to neurodevelopmental disorders. *Nat. Neurosci.* **2013**, *16* (9), 1228-1237. DOI: 10.1038/nn.3484.
- (123) Lam, C. W.; Yeung, W. L.; Law, C. Y. Global developmental delay and intellectual disability associated with a de novo TOP2B mutation. *Clin. Chim. Acta* **2017**, *469*, 63-68. DOI: 10.1016/j.cca.2017.03.022.
- (124) Broderick, L.; Yost, S.; Li, D.; McGeough, M. D.; Booshehri, L. M.; Guaderrama, M.; Brydges, S. D.; Kucharova, K.; Patel, N. C.; Harr, M.; Hakonarson, H.; Zackai, E.; Cowell, I. G.; Austin, C. A.; Huggle, B.; Gebauer, C.; Zhang, J.; Xu, X.; Wang, J.; Croker, B. A.; Frazer, K. A.; Putnam, C. D.; Hoffman, H. M. Mutations in topoisomerase II $\beta$  result in a B cell immunodeficiency. *Nat. Commun.* **2019**, *10* (1), 3644. DOI: 10.1038/s41467-019-11570-6.
- (125) Hiraide, T.; Watanabe, S.; Matsubayashi, T.; Yanagi, K.; Nakashima, M.; Ogata, T.; Saitsu, H. A de novo TOP2B variant associated with global developmental delay and autism spectrum disorder. *Mol. Genet. Genomic Med.* **2020**, *8* (3), e1145. DOI: 10.1002/mgg3.1145.
- (126) Lyu, Y. L.; Lin, C. P.; Azarova, A. M.; Cai, L.; Wang, J. C.; Liu, L. F. Role of topoisomerase II $\beta$  in the expression of developmentally regulated genes. *Mol. Cell Biol.* **2006**, *26* (21), 7929-7941. DOI: 10.1128/MCB.00617-06.
- (127) King, I. F.; Yandava, C. N.; Mabb, A. M.; Hsiao, J. S.; Huang, H. S.; Pearson, B. L.; Calabrese, J. M.; Starmer, J.; Parker, J. S.; Magnuson, T.; Chamberlain, S. J.; Philpot, B. D.; Zylka, M. J. Topoisomerases facilitate transcription of long genes linked to autism. *Nature* **2013**, *501* (7465), 58-62. DOI: 10.1038/nature12504.
- (128) Cowell, I. G.; Casement, J. W.; Austin, C. A. To break or not to break: the role of TOP2B in transcription. *Int. J. Mol. Sci.* **2023**, *24* (19). DOI: 10.3390/ijms241914806.
- (129) Peng, H.; Mariani, K. J. *Escherichia coli* topoisomerase IV. Purification, characterization, subunit structure, and subunit interactions. *J. Biol. Chem.* **1993**, *268* (32), 24481-24490.
- (130) Tomb, J. F.; White, O.; Kerlavage, A. R.; Clayton, R. A.; Sutton, G. G.; Fleischmann, R. D.; Ketchum, K. A.; Klenk, H. P.; Gill, S.; Dougherty, B. A.; Nelson, K.; Quackenbush, J.; Zhou, L.; Kirkness, E. F.; Peterson, S.; Loftus, B.; Richardson, D.; Dodson, R.; Khalak, H. G.; Glodek, A.; McKenney, K.; Fitzgerald, L. M.; Lee, N.; Adams, M. D.; Hickey, E. K.; Berg,

- D. E.; Gocayne, J. D.; Utterback, T. R.; Peterson, J. D.; Kelley, J. M.; Cotton, M. D.; Weidman, J. M.; Fujii, C.; Bowman, C.; Watthey, L.; Wallin, E.; Hayes, W. S.; Borodovsky, M.; Karp, P. D.; Smith, H. O.; Fraser, C. M.; Venter, J. C. The complete genome sequence of the gastric pathogen *Helicobacter pylori*. *Nature* **1997**, *388* (6642), 539-547. DOI: 10.1038/41483.
- (131) Fraser, C. M.; Norris, S. J.; Weinstock, G. M.; White, O.; Sutton, G. G.; Dodson, R.; Gwinn, M.; Hickey, E. K.; Clayton, R.; Ketchum, K. A.; Sodergren, E.; Hardham, J. M.; McLeod, M. P.; Salzberg, S.; Peterson, J.; Khalak, H.; Richardson, D.; Howell, J. K.; Chidambaram, M.; Utterback, T.; McDonald, L.; Artiach, P.; Bowman, C.; Cotton, M. D.; Fujii, C.; Garland, S.; Hatch, B.; Horst, K.; Roberts, K.; Sandusky, M.; Weidman, J.; Smith, H. O.; Venter, J. C. Complete genome sequence of *Treponema pallidum*, the syphilis spirochete. *Science* **1998**, *281* (5375), 375-388. DOI: 10.1126/science.281.5375.375.
- (132) Cole, S. T.; Brosch, R.; Parkhill, J.; Garnier, T.; Churcher, C.; Harris, D.; Gordon, S. V.; Eiglmeier, K.; Gas, S.; Barry, C. E., 3rd; Tekaiia, F.; Badcock, K.; Basham, D.; Brown, D.; Chillingworth, T.; Connor, R.; Davies, R.; Devlin, K.; Feltwell, T.; Gentles, S.; Hamlin, N.; Holroyd, S.; Hornsby, T.; Jagels, K.; Krogh, A.; McLean, J.; Moule, S.; Murphy, L.; Oliver, K.; Osborne, J.; Quail, M. A.; Rajandream, M. A.; Rogers, J.; Rutter, S.; Seeger, K.; Skelton, J.; Squares, R.; Squares, S.; Sulston, J. E.; Taylor, K.; Whitehead, S.; Barrell, B. G. Deciphering the biology of *Mycobacterium tuberculosis* from the complete genome sequence. *Nature* **1998**, *393* (6685), 537-544. DOI: 10.1038/31159.
- (133) Aubry, A.; Fisher, L. M.; Jarlier, V.; Cambau, E. First functional characterization of a singly expressed bacterial type II topoisomerase: the enzyme from *Mycobacterium tuberculosis*. *Biochem. Biophys. Res. Commun.* **2006**, *348* (1), 158-165. DOI: 10.1016/j.bbrc.2006.07.017.
- (134) Hobson, M. J.; Bryant, Z.; Berger, J. M. Modulated control of DNA supercoiling balance by the DNA-wrapping domain of bacterial gyrase. *Nucleic Acids Res.* **2020**, *48* (4), 2035-2049. DOI: 10.1093/nar/gkz1230.
- (135) Klevan, L.; Wang, J. C. Deoxyribonucleic acid gyrase-deoxyribonucleic acid complex containing 140 base pairs of deoxyribonucleic acid and an alpha 2 beta 2 protein core. *Biochemistry* **1980**, *19* (23), 5229-5234. DOI: 10.1021/bi00564a012.
- (136) Fisher, L. M.; Mizuuchi, K.; O'Dea, M. H.; Ohmori, H.; Gellert, M. Site-specific interaction of DNA gyrase with DNA. *Proc. Natl. Acad. Sci. U.S.A.* **1981**, *78* (7), 4165-4169. DOI: 10.1073/pnas.78.7.4165.
- (137) Kirkegaard, K.; Wang, J. C. Mapping the topography of DNA wrapped around gyrase by nucleolytic and chemical probing of complexes of unique DNA sequences. *Cell* **1981**, *23* (3), 721-729. DOI: 10.1016/0092-8674(81)90435-9.
- (138) Zechiedrich, E. L.; Khodursky, A. B.; Bachellier, S.; Schneider, R.; Chen, D.; Lilley, D. M.; Cozzarelli, N. R. Roles of topoisomerases in maintaining steady-state DNA supercoiling in *Escherichia coli*. *J. Biol. Chem.* **2000**, *275* (11), 8103-8113. DOI: 10.1074/jbc.275.11.8103.
- (139) Ashley, R. E.; Dittmore, A.; McPherson, S. A.; Turnbough, C. L., Jr.; Neuman, K. C.; Osheroff, N. Activities of gyrase and topoisomerase IV on positively supercoiled DNA. *Nucleic Acids Res.* **2017**, *45* (16), 9611-9624. DOI: 10.1093/nar/gkx649.
- (140) Adams, D. E.; Shekhtman, E. M.; Zechiedrich, E. L.; Schmid, M. B.; Cozzarelli, N. R. The role of topoisomerase IV in partitioning bacterial replicons and the structure of catenated intermediates in DNA replication. *Cell* **1992**, *71* (2), 277-288. DOI: 10.1016/0092-8674(92)90356-h.
- (141) Zechiedrich, E. L.; Cozzarelli, N. R. Roles of topoisomerase IV and DNA gyrase in DNA unlinking during replication in *Escherichia coli*. *Genes Dev.* **1995**, *9*, 2859-2869. DOI: 10.1101/gad.9.22.2859.

- (142) Charvin, G.; Bensimon, D.; Croquette, V. Single-molecule study of DNA unlinking by eukaryotic and prokaryotic type-II topoisomerases. *Proc. Natl. Acad. Sci. U.S.A.* **2003**, *100* (17), 9820-9825. DOI: 10.1073/pnas.1631550100.
- (143) Crisona, N. J.; Strick, T. R.; Bensimon, D.; Croquette, V.; Cozzarelli, N. R. Preferential relaxation of positively supercoiled DNA by *E. coli* topoisomerase IV in single-molecule and ensemble measurements. *Genes Dev.* **2000**, *14* (22), 2881-2892. DOI: 10.1101/gad.838900.
- (144) Neuman, K. C.; Charvin, G.; Bensimon, D.; Croquette, V. Mechanisms of chiral discrimination by topoisomerase IV. *Proc. Natl. Acad. Sci. U.S.A.* **2009**, *106* (17), 6986-6991. DOI: 10.1073/pnas.0900574106.
- (145) Gubaev, A.; Klostermeier, D. The mechanism of negative DNA supercoiling: a cascade of DNA-induced conformational changes prepares gyrase for strand passage. *DNA Repair (Amst)* **2014**, *16*, 23-34. DOI: 10.1016/j.dnarep.2014.01.011.
- (146) Drlica, K. Control of bacterial DNA supercoiling. *Mol. Microbiol.* **1992**, *6* (4), 425-433. DOI: 10.1111/j.1365-2958.1992.tb01486.x.
- (147) Higgins, N. P. Species-specific supercoil dynamics of the bacterial nucleoid. *Biophys. Rev.* **2016**, *8* (Suppl 1), 113-121. DOI: 10.1007/s12551-016-0207-9.
- (148) Garcia-Lopez, M.; Megias, D.; Ferrandiz, M. J.; de la Campa, A. G. The balance between gyrase and topoisomerase I activities determines levels of supercoiling, nucleoid compaction, and viability in bacteria. *Front. Microbiol.* **2022**, *13*, 1094692. DOI: 10.3389/fmicb.2022.1094692.
- (149) Zawadzki, P.; Stracy, M.; Ginda, K.; Zawadzka, K.; Lesterlin, C.; Kapanidis, A. N.; Sherratt, D. J. The localization and action of topoisomerase IV in *Escherichia coli* chromosome segregation is coordinated by the SMC complex, MukBEF. *Cell Rep.* **2015**, *13* (11), 2587-2596. DOI: 10.1016/j.celrep.2015.11.034.
- (150) Deibler, R. W.; Rahmati, S.; Zechiedrich, E. L. Topoisomerase IV, alone, unknots DNA in *E. coli*. *Genes Dev.* **2001**, *15* (6), 748-761. DOI: 10.1101/gad.872301.
- (151) Pommier, Y.; Leo, E.; Zhang, H.; Marchand, C. DNA topoisomerases and their poisoning by anticancer and antibacterial drugs. *Chem. Biol.* **2010**, *17* (5), 421-433. DOI: 10.1016/j.chembiol.2010.04.012.
- (152) Pommier, Y. Drugging topoisomerases: lessons and challenges. *ACS Chem. Biol.* **2013**, *8* (1), 82-95. DOI: 10.1021/cb300648v.
- (153) Hiasa, H. DNA topoisomerases as targets for antibacterial agents. In *DNA Topoisomerases*, Drolet, M. Ed.; Methods in Molecular Biology, Vol. 1703; Humana Press, 2018; pp 47-62.
- (154) Aldred, K. J.; Kerns, R. J.; Osheroff, N. Mechanism of quinolone action and resistance. *Biochemistry* **2014**, *53* (10), 1565-1574. DOI: 10.1021/bi5000564.
- (155) Gibson, E. G.; Ashley, R. E.; Kerns, R. J.; Osheroff, N. Fluoroquinolone interactions with bacterial type II topoisomerases and target-mediated drug resistance. In *Antimicrobial Resistance in the 21st Century*, 2nd ed.; Drlica, K., Shlaes, D., Fong, I. W. Eds.; Emerging Infectious Diseases of the 21st Century, Springer Nature, 2018; pp 507-529.
- (156) Bush, N. G.; Diez-Santos, I.; Abbott, L. R.; Maxwell, A. Quinolones: mechanism, lethality and their contributions to antibiotic resistance. *Molecules* **2020**, *25* (23). DOI: 10.3390/molecules25235662.
- (157) Khodursky, A. B.; Zechiedrich, E. L.; Cozzarelli, N. R. Topoisomerase IV is a target of quinolones in *Escherichia coli*. *Proc. Natl. Acad. Sci. U.S.A.* **1995**, *92*, 11801-11805.
- (158) Anderson, V. E.; Gootz, T. D.; Osheroff, N. Topoisomerase IV catalysis and the mechanism of quinolone action. *J. Biol. Chem.* **1998**, *273* (28), 17879-17885. DOI: 10.1074/jbc.273.28.17879.
- (159) Hiasa, H.; Yousef, D. O.; Marians, K. J. DNA strand cleavage is required for replication fork arrest by a frozen topoisomerase-quinolone-DNA ternary complex. *J. Biol. Chem.* **1996**, *271* (42), 26424-26429. DOI: 10.1074/jbc.271.42.26424.



- (160) Pohlhaus, J. R.; Kreuzer, K. N. Norfloxacin-induced DNA gyrase cleavage complexes block *Escherichia coli* replication forks, causing double-stranded breaks in vivo. *Mol. Microbiol.* **2005**, *56* (6), 1416-1429. DOI: 10.1111/j.1365-2958.2005.04638.x.
- (161) Le, T. T.; Wu, M.; Lee, J. H.; Bhatt, N.; Inman, J. T.; Berger, J. M.; Wang, M. D. Etoposide promotes DNA loop trapping and barrier formation by topoisomerase II. *Nat. Chem. Biol.* **2023**, *19* (5), 641-650. DOI: 10.1038/s41589-022-01235-9.
- (162) Nitiss, K. C.; Nitiss, J. L.; Hanakahi, L. A. DNA damage by an essential enzyme: A delicate balance act on the tightrope. *DNA Repair (Amst)* **2019**, *82*, 102639. DOI: 10.1016/j.dnarep.2019.102639.
- (163) Schroder, W.; Goerke, C.; Wolz, C. Opposing effects of aminocoumarins and fluoroquinolones on the SOS response and adaptability in *Staphylococcus aureus*. *J. Antimicrob. Chemother.* **2013**, *68* (3), 529-538. DOI: 10.1093/jac/dks456.
- (164) D'Arpa, P.; Beardmore, C.; Liu, L. F. Involvement of nucleic acid synthesis in cell killing mechanisms of topoisomerase poisons. *Cancer Res.* **1990**, *50* (21), 6919-6924.
- (165) Tamayo, M.; Santiso, R.; Gosalvez, J.; Bou, G.; Fernandez, J. L. Rapid assessment of the effect of ciprofloxacin on chromosomal DNA from *Escherichia coli* using an in situ DNA fragmentation assay. *BMC Microbiol.* **2009**, *9*, 69. DOI: 10.1186/1471-2180-9-69.
- (166) Anderson, V. E.; Zaniewski, R. P.; Kaczmarek, F. S.; Gootz, T. D.; Osheroff, N. Quinolones inhibit DNA religation mediated by *Staphylococcus aureus* topoisomerase IV: changes in drug mechanism across evolutionary boundaries. *J. Biol. Chem.* **1999**, *274*, 35927-35932. DOI: 10.1074/jbc.274.50.35927.
- (167) Wohlkonig, A.; Chan, P. F.; Fosberry, A. P.; Homes, P.; Huang, J.; Kranz, M.; Leydon, V. R.; Miles, T. J.; Pearson, N. D.; Perera, R. L.; Shillings, A. J.; Gwynn, M. N.; Bax, B. D. Structural basis of quinolone inhibition of type IIA topoisomerases and target-mediated resistance. *Nat. Struct. Mol. Biol.* **2010**, *17* (9), 1152-1153. DOI: 10.1038/nsmb.1892.
- (168) Markovits, J.; Pommier, Y.; Kerrigan, D.; Covey, J. M.; Tilchen, E. J.; Kohn, K. W. Topoisomerase II-mediated DNA breaks and cytotoxicity in relation to cell proliferation and the cell cycle in NIH 3T3 fibroblasts and L1210 leukemia cells. *Cancer Res.* **1987**, *47* (8), 2050-2055.
- (169) Cirz, R. T.; O'Neill, B. M.; Hammond, J. A.; Head, S. R.; Romesberg, F. E. Defining the *Pseudomonas aeruginosa* SOS response and its role in the global response to the antibiotic ciprofloxacin. *J. Bacteriol.* **2006**, *188* (20), 7101-7110. DOI: 10.1128/JB.00807-06.
- (170) Lopez, E.; Elez, M.; Matic, I.; Blazquez, J. Antibiotic-mediated recombination: ciprofloxacin stimulates SOS-independent recombination of divergent sequences in *Escherichia coli*. *Mol. Microbiol.* **2007**, *64* (1), 83-93. DOI: 10.1111/j.1365-2958.2007.05642.x.
- (171) Huang, S. N.; Michaels, S. A.; Mitchell, B. B.; Majdalani, N.; Vanden Broeck, A.; Canela, A.; Tse-Dinh, Y. C.; Lamour, V.; Pommier, Y. Exonuclease VII repairs quinolone-induced damage by resolving DNA gyrase cleavage complexes. *Sci. Adv.* **2021**, *7* (10). DOI: 10.1126/sciadv.abe0384.
- (172) Willmott, C. J.; Critchlow, S. E.; Eperon, I. C.; Maxwell, A. The complex of DNA gyrase and quinolone drugs with DNA forms a barrier to transcription by RNA polymerase. *J. Mol. Biol.* **1994**, *242* (4), 351-363. DOI: 10.1006/jmbi.1994.1586.
- (173) Wentzell, L. M.; Maxwell, A. The complex of DNA gyrase and quinolone drugs on DNA forms a barrier to the T7 DNA polymerase replication complex. *J. Mol. Biol.* **2000**, *304* (5), 779-791. DOI: 10.1006/jmbi.2000.4266.
- (174) Nitiss, J. L. Targeting DNA topoisomerase II in cancer chemotherapy. *Nat. Rev. Cancer* **2009**, *9* (5), 338-350. DOI: nrc2607 [pii] 10.1038/nrc2607.
- (175) Pommier, Y.; Marchand, C. Interfacial inhibitors: targeting macromolecular complexes. *Nat. Rev. Drug Discov.* **2012**, *11* (1), 25-36.

- (176) Pendleton, M.; Lindsey, R. H., Jr.; Felix, C. A.; Grimwade, D.; Osheroff, N. Topoisomerase II and leukemia. *Ann. N. Y. Acad. Sci.* **2014**, *1310* (1), 98-110. DOI: 10.1111/nyas.12358.
- (177) Delgado, J. L.; Hsieh, C. M.; Chan, N. L.; Hiasa, H. Topoisomerases as anticancer targets. *Biochem. J.* **2018**, *475* (2), 373-398. DOI: 10.1042/BCJ20160583.
- (178) Yakkala, P. A.; Penumallu, N. R.; Shafi, S.; Kamal, A. Prospects of topoisomerase inhibitors as promising anti-cancer agents. *Pharmaceuticals (Basel)* **2023**, *16* (10). DOI: 10.3390/ph16101456.
- (179) Fox, E. J. Mechanism of action of mitoxantrone. *Neurology* **2004**, *63* (12 Suppl 6), S15-18. DOI: 10.1212/wnl.63.12\_suppl\_6.s15.
- (180) Evison, B. J.; Sleebs, B. E.; Watson, K. G.; Phillips, D. R.; Cutts, S. M. Mitoxantrone, more than just another topoisomerase II poison. *Med. Res. Rev.* **2016**, *36* (2), 248-299. DOI: 10.1002/med.21364.
- (181) Zhang, S.; Liu, X.; Bawa-Khalfe, T.; Lu, L. S.; Lyu, Y. L.; Liu, L. F.; Yeh, E. T. Identification of the molecular basis of doxorubicin-induced cardiotoxicity. *Nat. Med.* **2012**, *18* (11), 1639-1642. DOI: 10.1038/nm.2919.
- (182) Deng, S.; Yan, T.; Jendry, C.; Nemecek, A.; Vincetic, M.; Godtel-Armbrust, U.; Wojnowski, L. Dexrazoxane may prevent doxorubicin-induced DNA damage via depleting both topoisomerase II isoforms. *BMC Cancer* **2014**, *14*, 842. DOI: 10.1186/1471-2407-14-842.
- (183) Cvetkovic, R. S.; Scott, L. J. Dexrazoxane: a review of its use for cardioprotection during anthracycline chemotherapy. *Drugs* **2005**, *65* (7), 1005-1024. DOI: 10.2165/00003495-200565070-00008.
- (184) Hensley, M. L.; Hagerty, K. L.; Kewalramani, T.; Green, D. M.; Meropol, N. J.; Wasserman, T. H.; Cohen, G. I.; Emami, B.; Gradishar, W. J.; Mitchell, R. B.; Thigpen, J. T.; Trotti, A., 3rd; von Hoff, D.; Schuchter, L. M. American Society of Clinical Oncology 2008 clinical practice guideline update: use of chemotherapy and radiation therapy protectants. *J. Clin. Oncol.* **2009**, *27* (1), 127-145. DOI: 10.1200/JCO.2008.17.2627.
- (185) Marinello, J.; Delcuratolo, M.; Capranico, G. Anthracyclines as topoisomerase II poisons: from early studies to new perspectives. *Int. J. Mol. Sci.* **2018**, *19* (11). DOI: 10.3390/ijms19113480.
- (186) Henriksen, P. A. Anthracycline cardiotoxicity: an update on mechanisms, monitoring and prevention. *Heart* **2018**, *104* (12), 971-977. DOI: 10.1136/heartjnl-2017-312103.
- (187) Wu, C. C.; Li, T. K.; Farh, L.; Lin, L. Y.; Lin, T. S.; Yu, Y. J.; Yen, T. J.; Chiang, C. W.; Chan, N. L. Structural basis of type II topoisomerase inhibition by the anticancer drug etoposide. *Science* **2011**, *333* (6041), 459-462. DOI: 10.1126/science.1204117.
- (188) Herzog, C. E.; Holmes, K. A.; Tuschong, L. M.; Ganapathi, R.; Zwelling, L. A. Absence of topoisomerase II $\beta$  in an amsacrine-resistant human leukemia cell line with mutant topoisomerase II $\alpha$ . *Cancer Res.* **1998**, *58* (23), 5298-5300.
- (189) Errington, F.; Willmore, E.; Tilby, M. J.; Li, L.; Li, G.; Li, W.; Baguley, B. C.; Austin, C. A. Murine transgenic cells lacking DNA topoisomerase II $\beta$  are resistant to acridines and mitoxantrone: analysis of cytotoxicity and cleavable complex formation. *Mol. Pharmacol.* **1999**, *56* (6), 1309-1316. DOI: 10.1124/mol.56.6.1309.
- (190) Toyoda, E.; Kagaya, S.; Cowell, I. G.; Kurosawa, A.; Kamoshita, K.; Nishikawa, K.; Iizumi, S.; Koyama, H.; Austin, C. A.; Adachi, N. NK314, a topoisomerase II inhibitor that specifically targets the alpha isoform. *J. Biol. Chem.* **2008**, *283* (35), 23711-23720. DOI: 10.1074/jbc.M803936200.
- (191) Ortega, J. A.; Arencibia, J. M.; Minniti, E.; Byl, J. A. W.; Franco-Ulloa, S.; Borgogno, M.; Genna, V.; Summa, M.; Bertozzi, S. M.; Bertorelli, R.; Armirotti, A.; Minarini, A.; Sissi, C.; Osheroff, N.; De Vivo, M. Novel, potent, and druglike tetrahydroquinazoline inhibitor that is highly selective for human topoisomerase II  $\alpha$  over  $\beta$ . *J. Med. Chem.* **2020**, *63* (21), 12873-12886. DOI: 10.1021/acs.jmedchem.0c00774.

- (192) Hande, K. R. Etoposide: four decades of development of a topoisomerase II inhibitor. *Eur. J. Cancer* **1998**, *34* (10), 1514-1521. DOI: 10.1016/s0959-8049(98)00228-7.
- (193) Hande, K. R. Clinical applications of anticancer drugs targeted to topoisomerase II. *Biochim. Biophys. Acta* **1998**, *1400* (1-3), 173-184. DOI: 10.1016/s0167-4781(98)00134-1.
- (194) Benitez, G.; Leonti, M.; Bock, B.; Vulfsons, S.; Dafni, A. The rise and fall of mandrake in medicine. *J. Ethnopharmacol.* **2023**, *303*, 115874. DOI: 10.1016/j.jep.2022.115874.
- (195) King, L. S.; Sullivan, M. The similarity of the effect of podophyllin and colchicine and their use in the treatment of condylomata acuminata. *Science* **1946**, *104* (2698), 244.
- (196) Greenspan, E. M.; Leiter, J.; Shear, M. J. Effect of alpha-peltatin, beta-peltatin, podophyllotoxin on lymphomas and other transplanted tumors. *J. Natl. Cancer Inst.* **1950**, *10* (6), 1295-1333.
- (197) Felix, W.; Senn, H. J. Clinical study of the new podophyllotoxin derivative, 4'-demethylepipodophyllotoxin 9-(4,6-o-ethylidene- beta-D-glucopyranoside) (NSC-141540; VP-16-213), in solid tumors. *Cancer Chemother. Rep.* **1975**, *59* (4), 737-742.
- (198) Pavone-Macaluso, M.; Caramia, G.; Rizzo, F. P.; Messina, V. Preliminary evaluation of VM-26: a new epipodophyllotoxin derivative, in the treatment of urogenital tumours. *Eur. Urol.* **1975**, *1* (1), 53-56.
- (199) Dimarco, A.; Gaetani, M.; Orezzi, P.; Scarpinato, B. M.; Silvestrini, R.; Soldati, M.; Dasdia, T.; Valentini, L. 'Daunomycin', a new antibiotic of the rhodomycin group. *Nature* **1964**, *201*, 706-707. DOI: 10.1038/201706a0.
- (200) Dimarco, A.; Soldati, M.; Fioretti, A.; Dasdia, T. Activity of daunomycin, a new antitumor antibiotic, on normal and neoplastic cells grown *in vitro*. *Cancer Chemother. Rep.* **1964**, *38*, 39-47.
- (201) Tan, C.; Tasaka, H.; Yu, K. P.; Murphy, M. L.; Karnofsky, D. A. Daunomycin, an antitumor antibiotic, in the treatment of neoplastic disease. Clinical evaluation with special reference to childhood leukemia. *Cancer* **1967**, *20* (3), 333-353. DOI: 10.1002/1097-0142(1967)20:3<333::aid-cnrc2820200302>3.0.co;2-k.
- (202) Arcamone, F.; Cassinelli, G.; Fantini, G.; Grein, A.; Orezzi, P.; Pol, C.; Spalla, C. Adriamycin, 14-hydroxydaunomycin, a new antitumor antibiotic from *S. peuceetius* var. *caesius*. *Biotechnol. Bioeng.* **1969**, *11* (6), 1101-1110. DOI: 10.1002/bit.260110607.
- (203) Pedersen-Bjergaard, J.; Philip, P. Balanced translocations involving chromosome bands 11q23 and 21q22 are highly characteristic of myelodysplasia and leukemia following therapy with cytostatic agents targeting at DNA-topoisomerase II. *Blood* **1991**, *78* (4), 1147-1148.
- (204) Super, H. J.; McCabe, N. R.; Thirman, M. J.; Larson, R. A.; Le Beau, M. M.; Pedersen-Bjergaard, J.; Philip, P.; Diaz, M. O.; Rowley, J. D. Rearrangements of the MLL gene in therapy-related acute myeloid leukemia in patients previously treated with agents targeting DNA-topoisomerase II. *Blood* **1993**, *82* (12), 3705-3711.
- (205) Mauritzson, N.; Albin, M.; Rylander, L.; Billstrom, R.; Ahlgren, T.; Mikoczy, Z.; Bjork, J.; Stromberg, U.; Nilsson, P. G.; Mitelman, F.; Hagmar, L.; Johansson, B. Pooled analysis of clinical and cytogenetic features in treatment-related and de novo adult acute myeloid leukemia and myelodysplastic syndromes based on a consecutive series of 761 patients analyzed 1976-1993 and on 5098 unselected cases reported in the literature 1974-2001. *Leukemia* **2002**, *16* (12), 2366-2378. DOI: 10.1038/sj.leu.2402713.
- (206) Cowell, I. G.; Austin, C. A. DNA fragility at the KMT2A/MLL locus: insights from old and new technologies. *Open Biol.* **2023**, *13* (1), 220232. DOI: 10.1098/rsob.220232.
- (207) Cowell, I. G.; Sondka, Z.; Smith, K.; Lee, K. C.; Manville, C. M.; Sidorczuk-Lesthuruge, M.; Rance, H. A.; Padget, K.; Jackson, G. H.; Adachi, N.; Austin, C. A. Model for MLL translocations in therapy-related leukemia involving topoisomerase II $\beta$ -mediated DNA strand breaks and gene proximity. *Proc. Natl. Acad. Sci. U.S.A.* **2012**, *109* (23), 8989-8994. DOI: 1204406109 [pii]

10.1073/pnas.1204406109.

- (208) Cowell, I. G.; Austin, C. A. Mechanism of generation of therapy related leukemia in response to anti-topoisomerase II agents. *Int. J. Environ. Res. Public Health* **2012**, *9* (6), 2075-2091. DOI: 10.3390/ijerph9062075.
- (209) Cozzio, A.; Passegue, E.; Ayton, P. M.; Karsunky, H.; Cleary, M. L.; Weissman, I. L. Similar MLL-associated leukemias arising from self-renewing stem cells and short-lived myeloid progenitors. *Genes Dev.* **2003**, *17* (24), 3029-3035. DOI: 10.1101/gad.1143403.
- (210) Rowley, J. D.; Olney, H. J. International workshop on the relationship of prior therapy to balanced chromosome aberrations in therapy-related myelodysplastic syndromes and acute leukemia: overview report. *Genes Chromosomes Cancer* **2002**, *33* (4), 331-345. DOI: 10.1002/gcc.10040.
- (211) Mays, A. N.; Osheroff, N.; Xiao, Y.; Wiemels, J. L.; Felix, C. A.; Byl, J. A.; Saravanamuttu, K.; Peniket, A.; Corser, R.; Chang, C.; Hoyle, C.; Parker, A. N.; Hasan, S. K.; Lo-Coco, F.; Solomon, E.; Grimwade, D. Evidence for direct involvement of epirubicin in the formation of chromosomal translocations in t(15;17) therapy-related acute promyelocytic leukemia. *Blood* **2010**, *115* (2), 326-330. DOI: 10.1182/blood-2009-07-235051.
- (212) Joannides, M.; Grimwade, D. Molecular biology of therapy-related leukaemias. *Clin. Transl. Oncol.* **2010**, *12* (1), 8-14. DOI: 10.1007/s12094-010-0460-5.
- (213) Joannides, M.; Mays, A. N.; Mistry, A. R.; Hasan, S. K.; Reiter, A.; Wiemels, J. L.; Felix, C. A.; Coco, F. L.; Osheroff, N.; Solomon, E.; Grimwade, D. Molecular pathogenesis of secondary acute promyelocytic leukemia. *Mediterr. J. Hematol. Infect. Dis.* **2011**, *3* (1), e2011045. DOI: 10.4084/MJHID.2011.045.
- (214) de The, H.; Chomienne, C.; Lanotte, M.; Degos, L.; Dejean, A. The t(15;17) translocation of acute promyelocytic leukaemia fuses the retinoic acid receptor  $\alpha$  gene to a novel transcribed locus. *Nature* **1990**, *347* (6293), 558-561. DOI: 10.1038/347558a0.
- (215) Mistry, A. R.; Felix, C. A.; Whitmarsh, R. J.; Mason, A.; Reiter, A.; Cassinat, B.; Parry, A.; Walz, C.; Wiemels, J. L.; Segal, M. R.; Ades, L.; Blair, I. A.; Osheroff, N.; Peniket, A. J.; Lafage-Pochitaloff, M.; Cross, N. C.; Chomienne, C.; Solomon, E.; Fenaux, P.; Grimwade, D. DNA topoisomerase II in therapy-related acute promyelocytic leukemia. *N. Engl. J. Med.* **2005**, *352* (15), 1529-1538. DOI: 10.1056/NEJMoa042715.
- (216) Hasan, S. K.; Mays, A. N.; Ottone, T.; Ledda, A.; La Nasa, G.; Cattaneo, C.; Borlenghi, E.; Melillo, L.; Montefusco, E.; Cervera, J.; Stephen, C.; Satchi, G.; Lennard, A.; Libura, M.; Byl, J. A.; Osheroff, N.; Amadori, S.; Felix, C. A.; Voso, M. T.; Sperr, W. R.; Esteve, J.; Sanz, M. A.; Grimwade, D.; Lo-Coco, F. Molecular analysis of t(15;17) genomic breakpoints in secondary acute promyelocytic leukemia arising after treatment of multiple sclerosis. *Blood* **2008**, *112* (8), 3383-3390. DOI: 10.1182/blood-2007-10-115600.
- (217) Lyu, Y. L.; Kerrigan, J. E.; Lin, C. P.; Azarova, A. M.; Tsai, Y. C.; Ban, Y.; Liu, L. F. Topoisomerase II $\beta$  mediated DNA double-strand breaks: implications in doxorubicin cardiotoxicity and prevention by dexrazoxane. *Cancer Res.* **2007**, *67* (18), 8839-8846. DOI: 10.1158/0008-5472.CAN-07-1649.
- (218) Cowell, I. G.; Austin, C. A. Mechanism of generation of therapy related leukemia in response to anti-topoisomerase II agents. *Int. J. Environ. Res. Public Health* **2012**, *9* (6), 2075-2091. DOI: 10.3390/ijerph9062075.
- (219) Cowell, I. G.; Sondka, Z.; Smith, K.; Lee, K. C.; Manville, C. M.; Sidorczuk-Lesthuruge, M.; Rance, H. A.; Padget, K.; Jackson, G. H.; Adachi, N.; Austin, C. A. Model for MLL translocations in therapy-related leukemia involving topoisomerase II $\beta$ -mediated DNA strand breaks and gene proximity. *Proc. Natl. Acad. Sci. U. S. A.* **2012**, *109* (23), 8989-8994. DOI: 1204406109 [pii]

10.1073/pnas.1204406109.

- (220) Baranello, L.; Kouzine, F.; Wojtowicz, D.; Cui, K.; Przytycka, T. M.; Zhao, K.; Levens, D. DNA break mapping reveals topoisomerase II activity genome-wide. *Int. J. Mol. Sci.* **2014**, *15* (7), 13111-13122. DOI: 10.3390/ijms150713111.
- (221) Gothe, H. J.; Bouwman, B. A. M.; Gusmao, E. G.; Piccinno, R.; Petrosino, G.; Sayols, S.; Drechsel, O.; Minneker, V.; Josipovic, N.; Mizi, A.; Nielsen, C. F.; Wagner, E. M.; Takeda, S.; Sasanuma, H.; Hudson, D. F.; Kindler, T.; Baranello, L.; Papantonis, A.; Crosetto, N.; Roukos, V. Spatial chromosome folding and active transcription drive DNA fragility and formation of oncogenic *MLL* translocations. *Mol. Cell* **2019**, *75* (2), 267-283 DOI: 10.1016/j.molcel.2019.05.015.
- (222) Padget, K.; Pearson, A. D.; Austin, C. A. Quantitation of DNA topoisomerase II $\alpha$  and  $\beta$  in human leukaemia cells by immunoblotting. *Leukemia* **2000**, *14* (11), 1997-2005. DOI: 10.1038/sj.leu.2401928.
- (223) Adams, D.; Altucci, L.; Antonarakis, S. E.; Ballesteros, J.; Beck, S.; Bird, A.; Bock, C.; Boehm, B.; Campo, E.; Caricasole, A.; Dahl, F.; Dermitzakis, E. T.; Enver, T.; Esteller, M.; Estivill, X.; Ferguson-Smith, A.; Fitzgibbon, J.; Flicek, P.; Giehl, C.; Graf, T.; Grosveld, F.; Guigo, R.; Gut, I.; Helin, K.; Jarvius, J.; Kuppens, R.; Lehrach, H.; Lengauer, T.; Lernmark, A.; Leslie, D.; Loeffler, M.; Macintyre, E.; Mai, A.; Martens, J. H.; Minucci, S.; Ouwehand, W. H.; Pelicci, P. G.; Penderville, H.; Porse, B.; Rakyanc, V.; Reik, W.; Schrappe, M.; Schubeler, D.; Seifert, M.; Siebert, R.; Simmons, D.; Soranzo, N.; Spicuglia, S.; Stratton, M.; Stunnenberg, H. G.; Tanay, A.; Torrents, D.; Valencia, A.; Vellenga, E.; Vingron, M.; Walter, J.; Willcocks, S. BLUEPRINT to decode the epigenetic signature written in blood. *Nat. Biotechnol.* **2012**, *30* (3), 224-226. DOI: 10.1038/nbt.2153.
- (224) Lyu, Y. L.; Kerrigan, J. E.; Lin, C. P.; Azarova, A. M.; Tsai, Y. C.; Ban, Y.; Liu, L. F. Topoisomerase II $\beta$  mediated DNA double-strand breaks: implications in doxorubicin cardiotoxicity and prevention by dexrazoxane. *Cancer Res.* **2007**, *67* (18), 8839-8846. DOI: 10.1158/0008-5472.CAN-07-1649.
- (225) Mariani, A.; Bartoli, A.; Atwal, M.; Lee, K. C.; Austin, C. A.; Rodriguez, R. Differential targeting of human topoisomerase II isoforms with small molecules. *J. Med. Chem.* **2015**, *58* (11), 4851-4856. DOI: 10.1021/acs.jmedchem.5b00473.
- (226) Chen, Y.; Shi, S.; Dai, Y. Research progress of therapeutic drugs for doxorubicin-induced cardiomyopathy. *Biomed. Pharmacother.* **2022**, *156*, 113903. DOI: 10.1016/j.biopha.2022.113903.
- (227) Jeon, K. H.; Park, S.; Shin, J. H.; Jung, A. R.; Hwang, S. Y.; Seo, S. H.; Jo, H.; Na, Y.; Kwon, Y. Synthesis and evaluation of 7-(3-aminopropoxy)-substituted flavone analogue as a topoisomerase II $\alpha$  catalytic inhibitor and its sensitizing effect to enzalutamide in castration-resistant prostate cancer cells. *Eur. J. Med. Chem.* **2023**, *246*, 114999. DOI: 10.1016/j.ejmech.2022.114999.
- (228) Classen, S.; Olland, S.; Berger, J. M. Structure of the topoisomerase II ATPase region and its mechanism of inhibition by the chemotherapeutic agent ICRF-187. *Proc. Natl. Acad. Sci. U.S.A.* **2003**, *100* (19), 10629-10634. DOI: 10.1073/pnas.1832879100.
- (229) Hasinoff, B. B.; Patel, D.; Wu, X. The role of topoisomerase II $\beta$  in the mechanisms of action of the doxorubicin cardioprotective agent dexrazoxane. *Cardiovasc. Toxicol.* **2020**, *20* (3), 312-320. DOI: 10.1007/s12012-019-09554-5.
- (230) Morris, S. K.; Baird, C. L.; Lindsley, J. E. Steady-state and rapid kinetic analysis of topoisomerase II trapped as the closed-clamp intermediate by ICRF-193. *J. Biol. Chem.* **2000**, *275* (4), 2613-2618. DOI: 10.1074/jbc.275.4.2613.
- (231) Lipshultz, S. E.; Rifai, N.; Dalton, V. M.; Levy, D. E.; Silverman, L. B.; Lipsitz, S. R.; Colan, S. D.; Asselin, B. L.; Barr, R. D.; Clavell, L. A.; Hurwitz, C. A.; Moghrabi, A.; Samson, Y.; Schorin, M. A.; Gelber, R. D.; Sallan, S. E. The effect of dexrazoxane on myocardial injury in doxorubicin-treated children with acute lymphoblastic leukemia. *N. Engl. J. Med.* **2004**, *351* (2), 145-153. DOI: 10.1056/NEJMoa035153.

- (232) Seif, A. E.; Walker, D. M.; Li, Y.; Huang, Y. S.; Kavcic, M.; Torp, K.; Bagatell, R.; Fisher, B. T.; Aplenc, R. Dexrazoxane exposure and risk of secondary acute myeloid leukemia in pediatric oncology patients. *Pediatr. Blood Cancer* **2015**, *62* (4), 704-709. DOI: 10.1002/pbc.25043.
- (233) Vejpongsa, P.; Yeh, E. T. Topoisomerase 2 $\beta$ : a promising molecular target for primary prevention of anthracycline-induced cardiotoxicity. *Clin. Pharmacol. Ther.* **2014**, *95* (1), 45-52. DOI: 10.1038/clpt.2013.201.
- (234) Kwok, J. C.; Richardson, D. R. The cardioprotective effect of the iron chelator dexrazoxane (ICRF-187) on anthracycline-mediated cardiotoxicity. *Redox Rep.* **2000**, *5* (6), 317-324. DOI: 10.1179/135100000101535898.
- (235) Lebrecht, D.; Kokkori, A.; Ketelsen, U. P.; Setzer, B.; Walker, U. A. Tissue-specific mtDNA lesions and radical-associated mitochondrial dysfunction in human hearts exposed to doxorubicin. *J. Pathol.* **2005**, *207* (4), 436-444. DOI: 10.1002/path.1863.
- (236) Ichikawa, Y.; Ghanefar, M.; Bayeva, M.; Wu, R.; Khechaduri, A.; Naga Prasad, S. V.; Mutharasan, R. K.; Naik, T. J.; Ardehali, H. Cardiotoxicity of doxorubicin is mediated through mitochondrial iron accumulation. *J. Clin. Invest.* **2014**, *124* (2), 617-630. DOI: 10.1172/JCI72931.
- (237) Vavrova, A.; Jansova, H.; Mackova, E.; Machacek, M.; Haskova, P.; Tichotova, L.; Sterba, M.; Simunek, T. Catalytic inhibitors of topoisomerase II differently modulate the toxicity of anthracyclines in cardiac and cancer cells. *PLoS One* **2013**, *8* (10), e76676. DOI: 10.1371/journal.pone.0076676.
- (238) Jirkovsky, E.; Jirkovska, A.; Bavlovic-Piskackova, H.; Skalicka, V.; Pokorna, Z.; Karabanovich, G.; Kollarova-Brazdova, P.; Kubes, J.; Lencova-Popelova, O.; Mazurova, Y.; Adamcova, M.; Lyon, A. R.; Roh, J.; Simunek, T.; Sterbova-Kovarikova, P.; Sterba, M. Clinically translatable prevention of anthracycline cardiotoxicity by dexrazoxane is mediated by topoisomerase II $\beta$  and not metal chelation. *Circ. Heart Fail.* **2021**, *14* (11), e008209. DOI: 10.1161/CIRCHEARTFAILURE.120.008209.
- (239) Xiao, H.; Mao, Y.; Desai, S. D.; Zhou, N.; Ting, C. Y.; Hwang, J.; Liu, L. F. The topoisomerase II $\beta$  circular clamp arrests transcription and signals a 26S proteasome pathway. *Proc. Natl. Acad. Sci. U.S.A.* **2003**, *100* (6), 3239-3244. DOI: 10.1073/pnas.0736401100.
- (240) Shapiro, A. B.; Austin, C. A. A high-throughput fluorescence anisotropy-based assay for human topoisomerase II beta-catalyzed ATP-dependent supercoiled DNA relaxation. *Anal Biochem* **2014**, *448*, 23-29. DOI: 10.1016/j.ab.2013.11.029.
- (241) Heide, L. New aminocoumarin antibiotics as gyrase inhibitors. *Int. J. Med. Microbiol.* **2014**, *304* (1), 31-36. DOI: 10.1016/j.ijmm.2013.08.013.
- (242) Gellert, M.; O'Dea, M. H.; Itoh, T.; Tomizawa, J. Novobiocin and coumermycin inhibit DNA supercoiling catalyzed by DNA gyrase. *Proc. Natl. Acad. Sci. U.S.A.* **1976**, *73* (12), 4474-4478. DOI: 10.1073/pnas.73.12.4474.
- (243) Harris, D. A.; Reagan, M. A.; Ruger, M.; Wallick, H.; Woodruff, H. B. Discovery and antimicrobial properties of cathomycin, a new antibiotic produced by *Streptomyces spheroides* n. sp. *Antibiot Annu* **1955**, *3*, 909-917.
- (244) Grunberg, E.; Bennett, M. Chemotherapeutic properties of coumermycin A1. *Antimicrob. Agents Chemother.* **1965**, *5*, 786-788.
- (245) Li, S. M.; Heide, L. New aminocoumarin antibiotics from genetically engineered *Streptomyces* strains. *Curr. Med. Chem.* **2005**, *12* (4), 419-427. DOI: 10.2174/0929867053363063.
- (246) Heide, L. The aminocoumarins: biosynthesis and biology. *Nat. Prod. Rep.* **2009**, *26* (10), 1241-1250. DOI: 10.1039/b808333a.
- (247) Colville, J. M.; Gale, H. H.; Cox, F.; Quinn, E. L. Clinical observations on the use of novobiocin in penicillin-resistant staphylococcal septicemia. *Antibiot. Annu.* **1957**, *5*, 920-926.

- (248) Bisacchi, G. S.; Manchester, J. I. A new-class antibacterial-almost. Lessons in drug discovery and development: a critical analysis of more than 50 years of effort toward ATPase inhibitors of DNA gyrase and topoisomerase IV. *ACS Infect. Dis.* **2015**, *1* (1), 4-41. DOI: 10.1021/id500013t.
- (249) Sugino, A.; Higgins, N. P.; Brown, P. O.; Peebles, C. L.; Cozzarelli, N. R. Energy coupling in DNA gyrase and the mechanism of action of novobiocin. *Proc. Natl. Acad. Sci. U.S.A.* **1978**, *75* (10), 4838-4842. DOI: 10.1073/pnas.75.10.4838.
- (250) Lewis, R. J.; Singh, O. M.; Smith, C. V.; Skarzynski, T.; Maxwell, A.; Wonacott, A. J.; Wigley, D. B. The nature of inhibition of DNA gyrase by the coumarins and the cyclothialidines revealed by X-ray crystallography. *EMBO J.* **1996**, *15* (6), 1412-1420.
- (251) Maxwell, A.; Lawson, D. M. The ATP-binding site of type II topoisomerases as a target for antibacterial drugs. *Curr. Top. Med. Chem.* **2003**, *3* (3), 283-303. DOI: 10.2174/1568026033452500.
- (252) Collin, F.; Karkare, S.; Maxwell, A. Exploiting bacterial DNA gyrase as a drug target: current state and perspectives. *Appl. Microbiol. Biotechnol.* **2011**, *92* (3), 479-497. DOI: 10.1007/s00253-011-3557-z.
- (253) Tsai, F. T.; Singh, O. M.; Skarzynski, T.; Wonacott, A. J.; Weston, S.; Tucker, A.; Pauptit, R. A.; Breeze, A. L.; Poyser, J. P.; O'Brien, R.; Ladbury, J. E.; Wigley, D. B. The high-resolution crystal structure of a 24-kDa gyrase B fragment from *E. coli* complexed with one of the most potent coumarin inhibitors, clorobiocin. *Proteins* **1997**, *28* (1), 41-52.
- (254) Lamour, V.; Hoermann, L.; Jeltsch, J. M.; Oudet, P.; Moras, D. An open conformation of the *Thermus thermophilus* gyrase B ATP-binding domain. *J. Biol. Chem.* **2002**, *277* (21), 18947-18953. DOI: 10.1074/jbc.M111740200.
- (255) Lafitte, D.; Lamour, V.; Tsvetkov, P. O.; Makarov, A. A.; Klich, M.; Deprez, P.; Moras, D.; Briand, C.; Gilli, R. DNA gyrase interaction with coumarin-based inhibitors: the role of the hydroxybenzoate isopentenyl moiety and the 5'-methyl group of the noviose. *Biochemistry* **2002**, *41* (23), 7217-7223. DOI: 10.1021/bi0159837.
- (256) Vanden Broeck, A.; McEwen, A. G.; Chebaro, Y.; Potier, N.; Lamour, V. Structural basis for DNA gyrase interaction with coumermycin A1. *J. Med. Chem.* **2019**, *62* (8), 4225-4231. DOI: 10.1021/acs.jmedchem.8b01928.
- (257) Contreras, A.; Maxwell, A. *gyrB* mutations which confer coumarin resistance also affect DNA supercoiling and ATP hydrolysis by *Escherichia coli* DNA gyrase. *Mol. Microbiol.* **1992**, *6* (12), 1617-1624. DOI: 10.1111/j.1365-2958.1992.tb00886.x.
- (258) Gross, C. H.; Parsons, J. D.; Grossman, T. H.; Charifson, P. S.; Bellon, S.; Jernee, J.; Dwyer, M.; Chambers, S. P.; Markland, W.; Botfield, M.; Raybuck, S. A. Active-site residues of *Escherichia coli* DNA gyrase required in coupling ATP hydrolysis to DNA supercoiling and amino acid substitutions leading to novobiocin resistance. *Antimicrob. Agents Chemother.* **2003**, *47* (3), 1037-1046. DOI: 10.1128/AAC.47.3.1037-1046.2003.
- (259) Schimana, J.; Fiedler, H. P.; Groth, I.; Sussmuth, R.; Beil, W.; Walker, M.; Zeeck, A. Simocyclinones, novel cytostatic angucyclinone antibiotics produced by *Streptomyces antibioticus* Tu 6040. I. Taxonomy, fermentation, isolation and biological activities. *J. Antibiot.* **2000**, *53* (8), 779-787. DOI: 10.7164/antibiotics.53.779.
- (260) Flatman, R. H.; Howells, A. J.; Heide, L.; Fiedler, H. P.; Maxwell, A. Simocyclinone D8, an inhibitor of DNA gyrase with a novel mode of action. *Antimicrob. Agents Chemother.* **2005**, *49* (3), 1093-1100. DOI: 10.1128/AAC.49.3.1093-1100.2005.
- (261) Edwards, M. J.; Flatman, R. H.; Mitchenall, L. A.; Stevenson, C. E.; Le, T. B.; Clarke, T. A.; McKay, A. R.; Fiedler, H. P.; Buttner, M. J.; Lawson, D. M.; Maxwell, A. A crystal structure of the bifunctional antibiotic simocyclinone D8, bound to DNA gyrase. *Science* **2009**, *326* (5958), 1415-1418. DOI: 10.1126/science.1179123.
- (262) Hearnshaw, S. J.; Edwards, M. J.; Stevenson, C. E.; Lawson, D. M.; Maxwell, A. A new crystal structure of the bifunctional antibiotic simocyclinone D8 bound to DNA gyrase gives

- fresh insight into the mechanism of inhibition. *J. Mol. Biol.* **2014**, 426 (10), 2023-2033. DOI: 10.1016/j.jmb.2014.02.017.
- (263) Buttner, M. J.; Schafer, M.; Lawson, D. M.; Maxwell, A. Structural insights into simocyclinone as an antibiotic, effector ligand and substrate. *FEMS Microbiol. Rev.* **2018**, 42 (1). DOI: 10.1093/femsre/fux055.
- (264) Pham, T. D. M.; Ziora, Z. M.; Blaskovich, M. A. T. Quinolone antibiotics. *Med. Chem. Commun.* **2019**, 10 (10), 1719-1739. DOI: 10.1039/c9md00120d.
- (265) Centers for Disease Control and Prevention. *Outpatient antibiotic prescriptions — United States, 2017*; U.S. Department of Health and Human Services, Atlanta, GA, 2017.
- (266) Basarab, G. S. Four ways to skin a cat: inhibition of bacterial topoisomerases leading to the clinic. In *Antibacterials: Volume I*, Fisher, J. F., Mobashery, S., Miller, M. J. Eds.; Springer Nature, 2018; pp 165-188.
- (267) *Critically important antimicrobials for human medicine*, Licence: CC BY-NC-SA 3.0 IGO ed.; World Health Organization, 2019.
- (268) Buehrle, D. J.; Wagener, M. M.; Clancy, C. J. Outpatient fluoroquinolone prescription fills in the United States, 2014 to 2020: assessing the impact of Food and Drug Administration safety warnings. *Antimicrob. Agents Chemother.* **2021**, 65 (7), e0015121. DOI: 10.1128/AAC.00151-21.
- (269) Leshner, G. Y.; Froelich, E. J.; Gruett, M. D.; Bailey, J. H.; Brundage, R. P. 1,8-Naphthyridine derivatives. A new class of chemotherapeutic agents. *J. Med. Pharm. Chem.* **1962**, 91, 1063-1065. DOI: 10.1021/jm01240a021.
- (270) Jameson, R. M.; Swinney, J. A clinical trial of the treatment of gram-negative urinary infections with nalidixic acid. *Br. J. Urol.* **1963**, 35, 122-124. DOI: 10.1111/j.1464-410x.1963.tb02603.x.
- (271) Gleckman, R.; Alvarez, S.; Joubert, D. W.; Matthews, S. J. Drug therapy reviews: nalidixic acid. *Am. J. Hosp. Pharm.* **1979**, 36 (8), 1071-1076.
- (272) Ito, A.; Hirai, K.; Inoue, M.; Koga, H.; Suzue, S.; Irikura, T.; Mitsuhashi, S. *In vitro* antibacterial activity of AM-715, a new nalidixic acid analog. *Antimicrob. Agents Chemother.* **1980**, 17 (2), 103-108. DOI: 10.1128/AAC.17.2.103.
- (273) Wise, R. Norfloxacin--a review of pharmacology and tissue penetration. *J. Antimicrob. Chemother.* **1984**, 13 Suppl B, 59-64. DOI: 10.1093/jac/13.suppl\_b.59.
- (274) Wolfson, J. S.; Hooper, D. C. Norfloxacin: a new targeted fluoroquinolone antimicrobial agent. *Ann. Intern. Med.* **1988**, 108 (2), 238-251. DOI: 10.7326/0003-4819-108-2-238.
- (275) Schacht, P.; Arcieri, G.; Branolte, J.; Bruck, H.; Chysky, V.; Griffith, E.; Gruenwaldt, G.; Hullmann, R.; Konopka, C. A.; O'Brien, B.; Rahm, V.; Ryoki, T.; Westwood, A.; Weuta, H. Worldwide clinical data on efficacy and safety of ciprofloxacin. *Infection* **1988**, 16 Suppl 1, S29-43. DOI: 10.1007/BF01650504.
- (276) Emmerson, A. M.; Jones, A. M. The quinolones: decades of development and use. *J. Antimicrob. Chemother.* **2003**, 51 Suppl 1, 13-20. DOI: 10.1093/jac/dkg208.
- (277) Gillespie, S. H. The role of moxifloxacin in tuberculosis therapy. *Eur. Respir. Rev.* **2016**, 25 (139), 19-28. DOI: 10.1183/16000617.0085-2015.
- (278) Turban, A.; Guerin, F.; Dinh, A.; Cattoir, V. Updated review on clinically-relevant properties of delafloxacin. *Antibiotics (Basel)* **2023**, 12 (8). DOI: 10.3390/antibiotics12081241.
- (279) Hooper, D. C.; Jacoby, G. A. Mechanisms of drug resistance: quinolone resistance. *Ann. N.Y. Acad. Sci.* **2015**, 1354, 12-31. DOI: 10.1111/nyas.12830.
- (280) Davies, J.; Davies, D. Origins and evolution of antibiotic resistance. *Microbiol. Mol. Biol. Rev.* **2010**, 74 (3), 417-433. DOI: 10.1128/MMBR.00016-10.
- (281) Munita, J. M.; Arias, C. A. Mechanisms of antibiotic resistance. *Microbiol. Spectr.* **2016**, 4 (2). DOI: 10.1128/microbiolspec.VMBF-0016-2015.



- (282) Gellert, M.; Mizuuchi, K.; O'Dea, M. H.; Itoh, T.; Tomizawa, J. I. Nalidixic acid resistance: a second genetic character involved in DNA gyrase activity. *Proc. Natl. Acad. Sci. U.S.A.* **1977**, *74* (11), 4772-4776. DOI: 10.1073/pnas.74.11.4772.
- (283) Sugino, A.; Peebles, C. L.; Kreuzer, K. N.; Cozzarelli, N. R. Mechanism of action of nalidixic acid: purification of *Escherichia coli* nalA gene product and its relationship to DNA gyrase and a novel nicking-closing enzyme. *Proc. Natl. Acad. Sci. U.S.A.* **1977**, *74* (11), 4767-4771.
- (284) Belland, R. J.; Morrison, S. G.; Ison, C.; Huang, W. M. *Neisseria gonorrhoeae* acquires mutations in analogous regions of gyrA and parC in fluoroquinolone-resistant isolates. *Mol. Microbiol.* **1994**, *14* (2), 371-380. DOI: 10.1111/j.1365-2958.1994.tb01297.x.
- (285) Ferrero, L.; Cameron, B.; Crouzet, J. Analysis of gyrA and grlA mutations in stepwise-selected ciprofloxacin-resistant mutants of *Staphylococcus aureus*. *Antimicrob. Agents Chemother.* **1995**, *39* (7), 1554-1558. DOI: 10.1128/AAC.39.7.1554.
- (286) Pan, X. S.; Ambler, J.; Mehtar, S.; Fisher, L. M. Involvement of topoisomerase IV and DNA gyrase as ciprofloxacin targets in *Streptococcus pneumoniae*. *Antimicrob. Agents Chemother.* **1996**, *40* (10), 2321-2326. DOI: 10.1128/AAC.40.10.2321.
- (287) Fournier, B.; Zhao, X.; Lu, T.; Drlica, K.; Hooper, D. C. Selective targeting of topoisomerase IV and DNA gyrase in *Staphylococcus aureus*: different patterns of quinolone-induced inhibition of DNA synthesis. *Antimicrob. Agents Chemother.* **2000**, *44* (8), 2160-2165. DOI: 10.1128/AAC.44.8.2160-2165.2000.
- (288) Grohs, P.; Podglajen, I.; Gutmann, L. Activities of different fluoroquinolones against *Bacillus anthracis* mutants selected *in vitro* and harboring topoisomerase mutations. *Antimicrob. Agents Chemother.* **2004**, *48* (8), 3024-3027.
- (289) Pan, X.-S.; Fisher, L. M. Targeting of DNA gyrase in *Streptococcus pneumoniae* by sparfloxacin: selective targeting of gyrase or topoisomerase IV by quinolones. *Antimicrob. Agents Chemother.* **1997**, *41*, 471-474. DOI: 10.1128/AAC.41.2.471.
- (290) Cheng, G.; Hao, H.; Dai, M.; Liu, Z.; Yuan, Z. Antibacterial action of quinolones: from target to network. *Eur. J. Med. Chem.* **2013**, *66*, 555-562. DOI: 10.1016/j.ejmech.2013.01.057.
- (291) Pan, X. S.; Fisher, L. M. DNA gyrase and topoisomerase IV are dual targets of clinafloxacin action in *Streptococcus pneumoniae*. *Antimicrob. Agents Chemother.* **1998**, *42* (11), 2810-2816. DOI: 10.1128/AAC.42.11.2810.
- (292) Fisher, L. M.; Gould, K. A.; Pan, X. S.; Patel, S.; Heaton, V. J. Analysis of dual active fluoroquinolones in *Streptococcus pneumoniae*. *J. Antimicrob. Chemother.* **2003**, *52* (2), 312-313. DOI: 10.1093/jac/dkg329.
- (293) Cambau, E.; Matrat, S.; Pan, X. S.; Roth Dit Bettoni, R.; Corbel, C.; Aubry, A.; Lascols, C.; Driot, J. Y.; Fisher, L. M. Target specificity of the new fluoroquinolone besifloxacin in *Streptococcus pneumoniae*, *Staphylococcus aureus* and *Escherichia coli*. *J. Antimicrob. Chemother.* **2009**, *63* (3), 443-450. DOI: 10.1093/jac/dkn528.
- (294) Redgrave, L. S.; Sutton, S. B.; Webber, M. A.; Piddock, L. J. Fluoroquinolone resistance: mechanisms, impact on bacteria, and role in evolutionary success. *Trends Microbiol.* **2014**, *22* (8), 438-445. DOI: 10.1016/j.tim.2014.04.007.
- (295) Yoshida, H.; Kojima, T.; Yamagishi, J.; Nakamura, S. Quinolone-resistant mutations of the gyrA gene of *Escherichia coli*. *Mol. Gen. Genet.* **1988**, *211* (1), 1-7. DOI: 10.1007/BF00338386.
- (296) Cullen, M. E.; Wyke, A. W.; Kuroda, R.; Fisher, L. M. Cloning and characterization of a DNA gyrase A gene from *Escherichia coli* that confers clinical resistance to 4-quinolones. *Antimicrob. Agents Chemother.* **1989**, *33* (6), 886-894. DOI: 10.1128/AAC.33.6.886.
- (297) Heisig, P.; Schedletzky, H.; Falkensteinpaul, H. Mutations in the gyrA gene of a highly fluoroquinolone-resistant clinical isolate of *Escherichia coli*. *Antimicrob. Agents Chemother.* **1993**, *37* (4), 696-701. DOI: 10.1128/Aac.37.4.696.

- (298) Laponogov, I.; Sohi, M. K.; Veselkov, D. A.; Pan, X. S.; Sawhney, R.; Thompson, A. W.; McAuley, K. E.; Fisher, L. M.; Sanderson, M. R. Structural insight into the quinolone-DNA cleavage complex of type IIA topoisomerases. *Nat. Struct. Mol. Biol.* **2009**, *16* (6), 667-669. DOI: 10.1038/nsmb.1604.
- (299) Bax, B. D.; Chan, P. F.; Eggleston, D. S.; Fosberry, A.; Gentry, D. R.; Gorrec, F.; Giordano, I.; Hann, M. M.; Hennessy, A.; Hibbs, M.; Huang, J.; Jones, E.; Jones, J.; Brown, K. K.; Lewis, C. J.; May, E. W.; Saunders, M. R.; Singh, O.; Spitzfaden, C. E.; Shen, C.; Shillings, A.; Theobald, A. J.; Wohlkonig, A.; Pearson, N. D.; Gwynn, M. N. Type IIA topoisomerase inhibition by a new class of antibacterial agents. *Nature* **2010**, *466* (7309), 935-940. DOI: 10.1038/nature09197.
- (300) Palu, G.; Valisena, S.; Ciarrocchi, G.; Gatto, B.; Palumbo, M. Quinolone binding to DNA is mediated by magnesium ions. *Proc. Natl. Acad. Sci. U.S.A.* **1992**, *89* (20), 9671-9675. DOI: 10.1073/pnas.89.20.9671.
- (301) Polk, R. E. Drug-drug interactions with ciprofloxacin and other fluoroquinolones. *Am. J. Med.* **1989**, *87* (5A), 76S-81S. DOI: 10.1016/0002-9343(89)90028-4.
- (302) Turel, I. The interactions of metal ions with quinolone antibacterial agents. *Coordin. Chem. Rev.* **2002**, *232* (1-2), 27-47. DOI: 10.1016/S0010-8545(02)00027-9.
- (303) Chan, P. F.; Srikannathasan, V.; Huang, J.; Cui, H.; Fosberry, A. P.; Gu, M.; Hann, M. M.; Hibbs, M.; Homes, P.; Ingraham, K.; Pizzollo, J.; Shen, C.; Shillings, A. J.; Spitzfaden, C. E.; Tanner, R.; Theobald, A. J.; Stavenger, R. A.; Bax, B. D.; Gwynn, M. N. Structural basis of DNA gyrase inhibition by antibacterial QPT-1, anticancer drug etoposide and moxifloxacin. *Nat. Commun.* **2015**, *6*, 10048. DOI: 10.1038/ncomms10048.
- (304) Blower, T. R.; Williamson, B. H.; Kerns, R. J.; Berger, J. M. Crystal structure and stability of gyrase-fluoroquinolone cleaved complexes from *Mycobacterium tuberculosis*. *Proc. Natl. Acad. Sci. U.S.A.* **2016**, *113* (7), 1706-1713. DOI: 10.1073/pnas.1525047113.
- (305) Aldred, K. J.; McPherson, S. A.; Wang, P.; Kerns, R. J.; Graves, D. E.; Turnbough, C. L.; Osheroff, N. Drug interactions with *Bacillus anthracis* topoisomerase IV: biochemical basis for quinolone action and resistance. *Biochemistry* **2012**, *51* (1), 370-381. DOI: 10.1021/bi2013905.
- (306) Aldred, K. J.; McPherson, S. A.; Turnbough, C. L.; Kerns, R. J.; Osheroff, N. Topoisomerase IV-quinolone interactions are mediated through a water-metal ion bridge: mechanistic basis of quinolone resistance. *Nucleic Acids Res.* **2013**, *41* (8), 4628-4639. DOI: 10.1093/nar/gkt124.
- (307) Aldred, K. J.; Breland, E. J.; Vlčková, V.; Strub, M. P.; Neuman, K. C.; Kerns, R. J.; Osheroff, N. Role of the water-metal ion bridge in mediating interactions between quinolones and *Escherichia coli* topoisomerase IV. *Biochemistry* **2014**, *53* (34), 5558-5567. DOI: 10.1021/bi500682e.
- (308) Aldred, K. J.; Blower, T. R.; Kerns, R. J.; Berger, J. M.; Osheroff, N. Fluoroquinolone interactions with *Mycobacterium tuberculosis* gyrase: enhancing drug activity against wild-type and resistant gyrase. *Proc. Natl. Acad. Sci. U.S.A.* **2016**, *113* (7), 839-846. DOI: 10.1073/pnas.1525055113.
- (309) Ashley, R. E.; Lindsey, R. H., Jr.; McPherson, S. A.; Turnbough, C. L., Jr.; Kerns, R. J.; Osheroff, N. Interactions between quinolones and *Bacillus anthracis* gyrase and the basis of drug resistance. *Biochemistry* **2017**, *56* (32), 4191-4200. DOI: 10.1021/acs.biochem.7b00203.
- (310) Carter, H. E.; Wildman, B.; Schwanz, H. A.; Kerns, R. J.; Aldred, K. J. Role of the water-metal ion bridge in quinolone interactions with *Escherichia coli* gyrase. *Int. J. Mol. Sci.* **2023**, *24* (3). DOI: 10.3390/ijms24032879.
- (311) Collins, J. A.; Oviatt, A. A.; Chan, P. F.; Osheroff, N. Target-mediated fluoroquinolone resistance in *Neisseria gonorrhoeae*: actions of ciprofloxacin against gyrase and topoisomerase IV. *ACS Infect. Dis.* **2024**, in press. DOI: 10.1021/acsinfectdis.4c00041.

- (312) Guillemin, I.; Cambau, E.; Jarlier, V. Sequences of conserved region in the A subunit of DNA gyrase from nine species of the genus *Mycobacterium*: phylogenetic analysis and implication for intrinsic susceptibility to quinolones. *Antimicrob. Agents Chemother.* **1995**, 39 (9), 2145-2149. DOI: 10.1128/AAC.39.9.2145.
- (313) Guillemin, I.; Jarlier, V.; Cambau, E. Correlation between quinolone susceptibility patterns and sequences in the A and B subunits of DNA gyrase in mycobacteria. *Antimicrob. Agents Chemother.* **1998**, 42 (8), 2084-2088. DOI: 10.1128/AAC.42.8.2084.
- (314) Maruri, F.; Sterling, T. R.; Kaiga, A. W.; Blackman, A.; van der Heijden, Y. F.; Mayer, C.; Cambau, E.; Aubry, A. A systematic review of gyrase mutations associated with fluoroquinolone-resistant *Mycobacterium tuberculosis* and a proposed gyrase numbering system. *J. Antimicrob. Chemother.* **2012**, 67 (4), 819-831. DOI: 10.1093/jac/dkr566.
- (315) World Health Organization. *Tuberculosis*. 2023. <https://www.who.int/news-room/fact-sheets/detail/tuberculosis> (accessed 2024 January 12).
- (316) Houben, R. M.; Dodd, P. J. The global burden of latent tuberculosis infection: a re-estimation using mathematical modelling. *PLoS Med.* **2016**, 13 (10), e1002152. DOI: 10.1371/journal.pmed.1002152.
- (317) Falzon, D.; Schunemann, H. J.; Harausz, E.; Gonzalez-Angulo, L.; Lienhardt, C.; Jaramillo, E.; Weyer, K. World Health Organization treatment guidelines for drug-resistant tuberculosis, 2016 update. *Eur. Respir. J.* **2017**, 49 (3). DOI: 10.1183/13993003.02308-2016.
- (318) World Health Organization. *WHO consolidated guidelines on tuberculosis. Module 4: treatment - drug-resistant tuberculosis treatment, 2022 update.*; Licence: CC BY-NC-SA 3.0 IGO; World Health Organization, Geneva, 2022.
- (319) Devasia, R. A.; Blackman, A.; Gebretsadik, T.; Griffin, M.; Shintani, A.; May, C.; Smith, T.; Hooper, N.; Maruri, F.; Warkentin, J.; Mitchel, E.; Sterling, T. R. Fluoroquinolone resistance in *Mycobacterium tuberculosis*: the effect of duration and timing of fluoroquinolone exposure. *Am. J. Respir. Crit. Care Med.* **2009**, 180 (4), 365-370. DOI: 10.1164/rccm.200901-0146OC.
- (320) Quillin, S. J.; Seifert, H. S. *Neisseria gonorrhoeae* host adaptation and pathogenesis. *Nat. Rev. Microbiol.* **2018**, 16 (4), 226-240. DOI: 10.1038/nrmicro.2017.169.
- (321) Web annex 1. Key data at a glance. In *Global progress report on HIV, viral hepatitis and sexually transmitted infections, 2021*, World Health Organization: Geneva, 2021.
- (322) World Health Organization. *Gonorrhoea (Neisseria gonorrhoeae infection)*. World Health Organization: 2023.
- (323) Unemo, M.; Seifert, H. S.; Hook, E. W., 3rd; Hawkes, S.; Ndowa, F.; Dillon, J. R. Gonorrhoea. *Nat. Rev. Dis. Primers* **2019**, 5 (1), 79. DOI: 10.1038/s41572-019-0128-6.
- (324) Moran, J. S.; Levine, W. C. Drugs of choice for the treatment of uncomplicated gonococcal infections. *Clin. Infect. Dis.* **1995**, 20 Suppl 1, 47-65. DOI: 10.1093/clinids/20.supplement\_1.s47.
- (325) Dan, M. The use of fluoroquinolones in gonorrhoea: the increasing problem of resistance. *Expert Opin. Pharmaco.* **2004**, 5 (4), 829-854. DOI: 10.1517/eoph.5.4.829.30157.
- (326) Centers for Disease Control and Prevention. Update to CDC's sexually transmitted diseases treatment guidelines, 2006: fluoroquinolones no longer recommended for treatment of gonococcal infections. *MMWR Morb. Mortal. Wkly. Rep.* **2007**, 56, 332-336.
- (327) National Center for Health Statistics. *Health, United States, 2020-2021: Annual Perspective*. Centers for Disease Control and Prevention: 2023.
- (328) Miller, A. A.; Bundy, G. L.; Mott, J. E.; Skepner, J. E.; Boyle, T. P.; Harris, D. W.; Hromockyj, A. E.; Marotti, K. R.; Zurenko, G. E.; Munzner, J. B.; Sweeney, M. T.; Bammert, G. F.; Hamel, J. C.; Ford, C. W.; Zhong, W. Z.; Graber, D. R.; Martin, G. E.; Han, F.; Dolak, L. A.; Seest, E. P.; Ruble, J. C.; Kamilar, G. M.; Palmer, J. R.; Banitt, L. S.; Hurd, A. R.; Barbachyn, M. R. Discovery and characterization of QPT-1, the progenitor of a new class of bacterial

- topoisomerase inhibitors. *Antimicrob. Agents Chemother.* **2008**, 52 (8), 2806-2812. DOI: 10.1128/AAC.00247-08.
- (329) Kern, G.; Palmer, T.; Ehmann, D. E.; Shapiro, A. B.; Andrews, B.; Basarab, G. S.; Doig, P.; Fan, J.; Gao, N.; Mills, S. D.; Mueller, J.; Sriram, S.; Thresher, J.; Walkup, G. K. Inhibition of *Neisseria gonorrhoeae* type II topoisomerases by the novel spiropyrimidinetrione AZD0914. *J. Biol. Chem.* **2015**, 290 (34), 20984-20994. DOI: 10.1074/jbc.M115.663534.
- (330) Basarab, G. S.; Kern, G. H.; McNulty, J.; Mueller, J. P.; Lawrence, K.; Vishwanathan, K.; Alm, R. A.; Barvian, K.; Doig, P.; Galullo, V.; Gardner, H.; Gowravaram, M.; Huband, M.; Kimzey, A.; Morningstar, M.; Kutschke, A.; Lahiri, S. D.; Perros, M.; Singh, R.; Schuck, V. J.; Tommasi, R.; Walkup, G.; Newman, J. V. Responding to the challenge of untreatable gonorrhea: ETX0914, a first-in-class agent with a distinct mechanism-of-action against bacterial type II topoisomerases. *Sci. Rep.* **2015**, 5, 11827. DOI: 10.1038/srep11827.
- (331) Chan, P. F.; Germe, T.; Bax, B. D.; Huang, J.; Thalji, R. K.; Bacque, E.; Checchia, A.; Chen, D.; Cui, H.; Ding, X.; Ingraham, K.; McCloskey, L.; Raha, K.; Srikannathasan, V.; Maxwell, A.; Stavenger, R. A. Thiophene antibacterials that allosterically stabilize DNA-cleavage complexes with DNA gyrase. *Proc. Natl. Acad. Sci. U.S.A.* **2017**, 114 (22), E4492-E4500. DOI: 10.1073/pnas.1700721114.
- (332) Gibson, E. G.; Bax, B.; Chan, P. F.; Osheroff, N. Mechanistic and structural basis for the actions of the antibacterial gepotidacin against *Staphylococcus aureus* gyrase. *ACS Infect. Dis.* **2019**, 5, 570-581. DOI: 10.1021/acsinfecdis.8b00315.
- (333) Bax, B. D.; Murshudov, G.; Maxwell, A.; Germe, T. DNA topoisomerase inhibitors: trapping a DNA-cleaving machine in motion. *J. Mol. Biol.* **2019**, 431, 3427-3449. DOI: 10.1016/j.jmb.2019.07.008.
- (334) Morgan, H.; Lipka-Lloyd, M.; Warren, A. J.; Hughes, N.; Holmes, J.; Burton, N. P.; Mahenthalingam, E.; Bax, B. D. A 2.8 Å structure of zoliflodacin in a DNA cleavage complex with *Staphylococcus aureus* DNA gyrase. *Int. J. Mol. Sci.* **2023**, 24 (2). DOI: 10.3390/ijms24021634.
- (335) Global Antibiotics Research and Development Partnership. A multi-center, randomized, open-label, non inferiority trial to evaluate the efficacy and safety of a single, oral dose of zoliflodacin compared to a combination of a single intramuscular dose of ceftriaxone and a single oral dose of azithromycin in the treatment of patients with uncomplicated gonorrhoea. *Clinicaltrials.gov*: 2019.
- (336) GlaxoSmithKline. A phase III, randomized, multicenter, open-label study in adolescent and adult participants comparing the efficacy and safety of gepotidacin to ceftriaxone plus azithromycin in the treatment of uncomplicated urogenital gonorrhea caused by *Neisseria gonorrhoeae*. *ClinicalTrials.gov*: 2019.
- (337) Global Antibiotics Research and Development Partnership. *Positive results announced in largest pivotal phase 3 trial of a first-in-class oral antibiotic to treat uncomplicated gonorrhoea*. 2023. <https://gardp.org/positive-results-announced-in-largest-pivotal-phase-3-trial-of-a-first-in-class-oral-antibiotic-to-treat-uncomplicated-gonorrhoea/> (accessed 2023 November 10).
- (338) Wagenlehner, F.; Perry, C. R.; Hooton, T. M.; Scangarella-Oman, N. E.; Millns, H.; Powell, M.; Jarvis, E.; Dennison, J.; Sheets, A.; Butler, D.; Breton, J.; Janmohamed, S. Oral gepotidacin versus nitrofurantoin in patients with uncomplicated urinary tract infection (EAGLE-2 and EAGLE-3): two randomised, controlled, double-blind, double-dummy, phase 3, non-inferiority trials. *Lancet* **2024**. DOI: 10.1016/S0140-6736(23)02196-7.
- (339) Wiener, J. J.; Gomez, L.; Venkatesan, H.; Santillan, A., Jr.; Allison, B. D.; Schwarz, K. L.; Shinde, S.; Tang, L.; Hack, M. D.; Morrow, B. J.; Motley, S. T.; Goldschmidt, R. M.; Shaw, K. J.; Jones, T. K.; Grice, C. A. Tetrahydroindazole inhibitors of bacterial type II topoisomerases. Part 2: SAR development and potency against multidrug-resistant strains. *Bioorg. Med. Chem. Lett.* **2007**, 17 (10), 2718-2722. DOI: 10.1016/j.bmcl.2007.03.004.

- (340) Gomez, L.; Hack, M. D.; Wu, J.; Wiener, J. J.; Venkatesan, H.; Santillan, A., Jr.; Pippel, D. J.; Mani, N.; Morrow, B. J.; Motley, S. T.; Shaw, K. J.; Wolin, R.; Grice, C. A.; Jones, T. K. Novel pyrazole derivatives as potent inhibitors of type II topoisomerases. Part 1: synthesis and preliminary SAR analysis. *Bioorg. Med. Chem. Lett.* **2007**, *17* (10), 2723-2727. DOI: 10.1016/j.bmcl.2007.03.003.
- (341) Kolaric, A.; Anderluh, M.; Minovski, N. Two decades of successful SAR-grounded stories of the novel bacterial topoisomerase inhibitors (NBTIs). *J. Med. Chem.* **2020**, *63* (11), 5664-5674. DOI: 10.1021/acs.jmedchem.9b01738.
- (342) Kokot, M.; Anderluh, M.; Hrast, M.; Minovski, N. The structural features of novel bacterial topoisomerase inhibitors that define their activity on topoisomerase IV. *J. Med. Chem.* **2022**, *65* (9), 6431-6440. DOI: 10.1021/acs.jmedchem.2c00039.
- (343) Black, M. T.; Stachyra, T.; Platel, D.; Girard, A. M.; Claudon, M.; Bruneau, J. M.; Miossec, C. Mechanism of action of the antibiotic NXL101, a novel nonfluoroquinolone inhibitor of bacterial type II topoisomerases. *Antimicrob. Agents Chemother.* **2008**, *52* (9), 3339-3349. DOI: 10.1128/AAC.00496-08.
- (344) Li, L. S.; Okumu, A.; Dellos-Nolan, S.; Li, Z.; Karmahapatra, S.; English, A.; Yalowich, J. C.; Wozniak, D. J.; Mitton-Fry, M. J. Synthesis and anti-staphylococcal activity of novel bacterial topoisomerase inhibitors with a 5-amino-1,3-dioxane linker moiety. *Bioorg. Med. Chem. Lett.* **2018**, *28* (14), 2477-2480. DOI: 10.1016/j.bmcl.2018.06.003.
- (345) Lu, Y.; Papa, J. L.; Nolan, S.; English, A.; Seffernick, J. T.; Shkolnikov, N.; Powell, J.; Lindert, S.; Wozniak, D. J.; Yalowich, J.; Mitton-Fry, M. J. Dioxane-linked amide derivatives as novel bacterial topoisomerase inhibitors against gram-positive *Staphylococcus aureus*. *ACS Med. Chem. Lett.* **2020**, *11* (12), 2446-2454. DOI: 10.1021/acsmedchemlett.0c00428.
- (346) Surivet, J. P.; Zumbrunn, C.; Rueedi, G.; Hubschwerlen, C.; Bur, D.; Bruyere, T.; Locher, H.; Ritz, D.; Keck, W.; Seiler, P.; Kohl, C.; Gauvin, J. C.; Mirre, A.; Kaegi, V.; Dos Santos, M.; Gaertner, M.; Delers, J.; Enderlin-Paput, M.; Boehme, M. Design, synthesis, and characterization of novel tetrahydropyran-based bacterial topoisomerase inhibitors with potent anti-gram-positive activity. *J. Med. Chem.* **2013**, *56* (18), 7396-7415. DOI: 10.1021/jm400963y.
- (347) Singh, S. B.; Kaelin, D. E.; Wu, J.; Miesel, L.; Tan, C. M.; Meinke, P. T.; Olsen, D.; Lagrutta, A.; Bradley, P.; Lu, J.; Patel, S.; Rickert, K. W.; Smith, R. F.; Soisson, S.; Wei, C.; Fukuda, H.; Kishii, R.; Takei, M.; Fukuda, Y. Oxabicyclooctane-linked novel bacterial topoisomerase inhibitors as broad spectrum antibacterial agents. *ACS Med. Chem. Lett.* **2014**, *5* (5), 609-614. DOI: 10.1021/ml500069w.
- (348) Dougherty, T. J.; Nayar, A.; Newman, J. V.; Hopkins, S.; Stone, G. G.; Johnstone, M.; Shapiro, A. B.; Cronin, M.; Reck, F.; Ehmann, D. E. NBTI 5463 is a novel bacterial type II topoisomerase inhibitor with activity against gram-negative bacteria and *in vivo* efficacy. *Antimicrob. Agents Chemother.* **2014**, *58* (5), 2657-2664. DOI: 10.1128/AAC.02778-13.
- (349) Charrier, C.; Salisbury, A. M.; Savage, V. J.; Duffy, T.; Moyo, E.; Chaffer-Malam, N.; Ooi, N.; Newman, R.; Cheung, J.; Metzger, R.; McGarry, D.; Pichowicz, M.; Sigerson, R.; Cooper, I. R.; Nelson, G.; Butler, H. S.; Craighead, M.; Ratcliffe, A. J.; Best, S. A.; Stokes, N. R. Novel bacterial topoisomerase inhibitors with potent broad-spectrum activity against drug-resistant bacteria. *Antimicrob. Agents Chemother.* **2017**, *61* (5), e02100-02116. DOI: 10.1128/AAC.02100-16.
- (350) Mitton-Fry, M. J.; Brickner, S. J.; Hamel, J. C.; Barham, R.; Brennan, L.; Casavant, J. M.; Ding, X.; Finegan, S.; Hardink, J.; Hoang, T.; Huband, M. D.; Maloney, M.; Marfat, A.; McCurdy, S. P.; McLeod, D.; Subramanyam, C.; Plotkin, M.; Reilly, U.; Schafer, J.; Stone, G. G.; Uccello, D. P.; Wisialowski, T.; Yoon, K.; Zaniewski, R.; Zook, C. Novel 3-fluoro-6-methoxyquinoline derivatives as inhibitors of bacterial DNA gyrase and topoisomerase IV. *Bioorg. Med. Chem. Lett.* **2017**, *27* (15), 3353-3358. DOI: 10.1016/j.bmcl.2017.06.009.

- (351) Blanco, D.; Perez-Herran, E.; Cacho, M.; Ballell, L.; Castro, J.; Gonzalez Del Rio, R.; Lavandera, J. L.; Remuinan, M. J.; Richards, C.; Rullas, J.; Vazquez-Muniz, M. J.; Woldu, E.; Zapatero-Gonzalez, M. C.; Angulo-Barturen, I.; Mendoza, A.; Barros, D. *Mycobacterium tuberculosis* gyrase inhibitors as a new class of antitubercular drugs. *Antimicrob. Agents Chemother.* **2015**, *59* (4), 1868-1875. DOI: 10.1128/AAC.03913-14.
- (352) Gibson, E. G.; Blower, T. R.; Cacho, M.; Bax, B.; Berger, J. M.; Osheroff, N. Mechanism of action of *Mycobacterium tuberculosis* gyrase inhibitors: a novel class of gyrase poisons. *ACS Infect. Dis.* **2018**, *4* (8), 1211-1222. DOI: 10.1021/acsinfecdis.8b00035.
- (353) Kolaric, A.; Minovski, N. Novel bacterial topoisomerase inhibitors: challenges and perspectives in reducing hERG toxicity. *Future Med. Chem.* **2018**, *10* (19), 2241-2244. DOI: 10.4155/fmc-2018-0272.
- (354) Kokot, M.; Weiss, M.; Zdovc, I.; Anderluh, M.; Hrast, M.; Minovski, N. Diminishing hERG inhibitory activity of aminopiperidine-naphthyridine linked NBTI antibacterials by structural and physicochemical optimizations. *Bioorg. Chem.* **2022**, *128*, 106087. DOI: 10.1016/j.bioorg.2022.106087.
- (355) GlaxoSmithKline. A phase III, randomized, multicenter, parallel-group, double-blind, double-dummy study in adolescent and adult female participants comparing the efficacy and safety of gepotidacin to nitrofurantoin in the treatment of uncomplicated urinary tract infection (acute cystitis). ClinicalTrials.gov: 2021.
- (356) GlaxoSmithKline. A phase III, randomized, multicenter, open-label study in adolescent and adult participants comparing the efficacy and safety of gepotidacin to ceftriaxone plus azithromycin in the treatment of uncomplicated urogenital gonorrhoea caused by *Neisseria gonorrhoeae*. ClinicalTrials.gov: 2022.
- (357) Hackel, M. A.; Karlowsky, J. A.; Canino, M. A.; Sahn, D. F.; Scangarella-Oman, N. E. *In vitro* activity of gepotidacin against Gram-negative and Gram-positive anaerobes. *Antimicrob. Agents Chemother.* **2022**, *66* (2), e02165-02121. DOI: 10.1128/aac.02165-21.
- (358) Perry, C.; Hossain, M.; Powell, M.; Raychaudhuri, A.; Scangarella-Oman, N.; Tiffany, C.; Xu, S.; Dumont, E.; Janmohamed, S. Design of two phase III, randomized, multicenter studies comparing gepotidacin with nitrofurantoin for the treatment of uncomplicated urinary tract infection in female participants. *Infect. Dis. Ther.* **2022**, *11* (6), 2297-2310. DOI: 10.1007/s40121-022-00706-9.
- (359) Scangarella-Oman, N. E.; Hossain, M.; Hoover, J. L.; Perry, C. R.; Tiffany, C.; Barth, A.; Dumont, E. F. Dose selection for phase III clinical evaluation of gepotidacin (GSK2140944) in the treatment of uncomplicated urinary tract infections. *Antimicrob. Agents Chemother.* **2022**, *66* (3), e0149221. DOI: 10.1128/AAC.01492-21.
- (360) Arends, S. J. R.; Butler, D.; Scangarella-Oman, N.; Castanheira, M.; Mendes, R. E. Antimicrobial activity of gepotidacin tested against *Escherichia coli* and *Staphylococcus saprophyticus* isolates causing urinary tract infections in medical centers worldwide (2019 to 2020). *Antimicrob. Agents Chemother.* **2023**, *67* (4), e01525-01522. DOI: 10.1128/aac.01525-22.
- (361) Scangarella-Oman, N. E.; Hossain, M.; Perry, C. R.; Tiffany, C.; Powell, M.; Swift, B.; Dumont, E. F. Dose selection for a phase III study evaluating gepotidacin (GSK2140944) in the treatment of uncomplicated urogenital gonorrhoea. *Sex. Transm. Infect.* **2023**, *99* (1), 64-69. DOI: 10.1136/sextrans-2022-055518.
- (362) Watkins, R. R.; Thapaliya, D.; Lemonovich, T. L.; Bonomo, R. A. Gepotidacin: a novel, oral, 'first-in-class' triazaacenaphthylene antibiotic for the treatment of uncomplicated urinary tract infections and urogenital gonorrhoea. *J. Antimicrob. Chemother.* **2023**, *78* (5), 1137-1142. DOI: 10.1093/jac/dkad060.
- (363) Biedenbach, D. J.; Bouchillon, S. K.; Hackel, M.; Miller, L. A.; Scangarella-Oman, N. E.; Jakielaszek, C.; Sahn, D. F. *In vitro* activity of gepotidacin, a novel triazaacenaphthylene

- bacterial topoisomerase inhibitor, against a broad spectrum of bacterial pathogens. *Antimicrob. Agents Chemother.* **2016**, *60* (3), 1918-1923. DOI: 10.1128/AAC.02820-15.
- (364) Kolaric, A.; Germe, T.; Hrast, M.; Stevenson, C. E. M.; Lawson, D. M.; Burton, N. P.; Voros, J.; Maxwell, A.; Minovski, N.; Anderluh, M. Potent DNA gyrase inhibitors bind asymmetrically to their target using symmetrical bifurcated halogen bonds. *Nat. Commun.* **2021**, *12* (1), 150. DOI: 10.1038/s41467-020-20405-8.
- (365) Oviatt, A. A.; Gibson, E. G.; Huang, J.; Mattern, K.; Neuman, K.; Chan, P. F.; Osheroff, N. Interactions between gepotidacin and *Escherichia coli* gyrase and topoisomerase IV: genetic and biochemical evidence for well-balanced dual targeting. *ACS Infect. Dis.* **2024**, in press. DOI: 10.1021/acsinfectdis.3c00346.
- (366) Gibson, E. G.; Oviatt, A. A.; Cacho, M.; Neuman, K. C.; Chan, P. F.; Osheroff, N. Bimodal actions of a naphthyridone/aminopiperidine-based antibacterial that targets gyrase and topoisomerase IV. *Biochemistry* **2019**, *58* (44), 4447-4455. DOI: 10.1021/acs.biochem.9b00805.
- (367) Dauda, S. E.; Collins, J. A.; Byl, J. A. W.; Lu, Y.; Yalowich, J. C.; Mitton-Fry, M. J.; Osheroff, N. Actions of a novel bacterial topoisomerase inhibitor against *Neisseria gonorrhoeae* gyrase and topoisomerase IV: enhancement of double-stranded DNA breaks. *Int. J. Mol. Sci.* **2023**, *24* (15). DOI: 10.3390/ijms241512107.
- (368) Zorman, M.; Hrast Rambaher, M.; Kokot, M.; Minovski, N.; Anderluh, M. The overview of development of novel bacterial topoisomerase inhibitors effective against multidrug-resistant bacteria in an academic environment: From early hits to in vivo active antibacterials. *Eur. J. Pharm. Sci.* **2024**, *192*, 106632. DOI: 10.1016/j.ejps.2023.106632.
- (369) Mann, C. A.; Carvajal Moreno, J. J.; Lu, Y.; Dellos-Nolan, S.; Wozniak, D. J.; Yalowich, J. C.; Mitton-Fry, M. J. Novel bacterial topoisomerase inhibitors: unique targeting activities of amide enzyme-binding motifs for tricyclic analogs. *Antimicrob. Agents Chemother.* **2023**, *67* (10), e0048223. DOI: 10.1128/aac.00482-23.
- (370) Lu, Y. R.; Vibhute, S.; Li, L. S.; Okumu, A.; Ratigan, S. C.; Nolan, S.; Papa, J. L.; Mann, C. A.; English, A.; Chen, A. N.; Seffernick, J. T.; Koci, B.; Duncan, L. R.; Roth, B.; Cummings, J. E.; Slayden, R. A.; Lindert, S.; McElroy, C. A.; Wozniak, D. J.; Yalowich, J.; Mitton-Fry, M. J. Optimization of topoIV potency, ADMET Properties, and hERG Inhibition of 5-amino-1,3-dioxane-linked novel bacterial topoisomerase inhibitors: identification of a lead with in vivo efficacy against MRSA. *J. Med. Chem.* **2021**, *64* (20), 15214-15249. DOI: 10.1021/acs.jmedchem.1c01250.
- (371) Lahiri, S. D.; Kutschke, A.; McCormack, K.; Alm, R. A. Insights into the mechanism of inhibition of novel bacterial topoisomerase inhibitors from characterization of resistant mutants of *Staphylococcus aureus*. *Antimicrob. Agents Chemother.* **2015**, *59* (9), 5278-5287. DOI: 10.1128/AAC.00571-15.
- (372) Nyerges, A.; Csorgo, B.; Draskovits, G.; Kintses, B.; Szili, P.; Ferenc, G.; Revesz, T.; Ari, E.; Nagy, I.; Balint, B.; Vasarhelyi, B. M.; Bihari, P.; Szamel, M.; Balogh, D.; Papp, H.; Kalapis, D.; Papp, B.; Pal, C. Directed evolution of multiple genomic loci allows the prediction of antibiotic resistance. *Proc. Natl. Acad. Sci. U.S.A.* **2018**, *115* (25), E5726-E5735. DOI: 10.1073/pnas.1801646115.
- (373) Szili, P.; Draskovits, G.; Revesz, T.; Bogar, F.; Balogh, D.; Martinek, T.; Daruka, L.; Spohn, R.; Vasarhelyi, B. M.; Czikkely, M.; Kintses, B.; Grezal, G.; Ferenc, G.; Pal, C.; Nyerges, A. Rapid evolution of reduced susceptibility against a balanced dual-targeting antibiotic through stepping-stone mutations. *Antimicrob. Agents Chemother.* **2019**, *63* (9). DOI: 10.1128/AAC.00207-19.
- (374) Nayar, A. S.; Dougherty, T. J.; Reck, F.; Thresher, J.; Gao, N.; Shapiro, A. B.; Ehmann, D. E. Target-based resistance in *Pseudomonas aeruginosa* and *Escherichia coli* to NBTI 5463, a novel bacterial type II topoisomerase inhibitor. *Antimicrob. Agents Chemother.* **2015**, *59* (1), 331-337. DOI: 10.1128/AAC.04077-14.



- (375) Yang, X.; Chen, H.; Zheng, Y.; Qu, S.; Wang, H.; Yi, F. Disease burden and long-term trends of urinary tract infections: a worldwide report. *Front. Public Health* **2022**, *10*, 888205. DOI: 10.3389/fpubh.2022.888205.
- (376) Jakielaszek, C.; Hossain, M.; Qian, L.; Fishman, C.; Widdowson, K.; Hilliard, J. J.; Mannino, F.; Raychaudhuri, A.; Carniel, E.; Demons, S.; Heine, H. S.; Hershfield, J.; Russo, R.; Mega, W. M.; Revelli, D.; O'Dwyer, K. Gepotidacin is efficacious in a nonhuman primate model of pneumonic plague. *Sci. Transl. Med.* **2022**, *14* (647), eabg1787. DOI: 10.1126/scitranslmed.abg1787.
- (377) Nguyen, D.; Shaik, J. S.; Tai, G.; Tiffany, C.; Perry, C.; Dumont, E.; Gardiner, D.; Barth, A.; Singh, R.; Hossain, M. Comparison between physiologically based pharmacokinetic and population pharmacokinetic modelling to select paediatric doses of gepotidacin in plague. *Br. J. Clin. Pharmacol.* **2022**, *88* (2), 416-428. DOI: 10.1111/bcp.14996.
- (378) Jakielaszek, C.; Hilliard, J. J.; Mannino, F.; Hossain, M.; Qian, L.; Fishman, C.; Chou, Y. L.; Henning, L.; Novak, J.; Demons, S.; Hershfield, J.; O'Dwyer, K. Efficacy of intravenously administered gepotidacin in cynomolgus macaques following a *Francisella tularensis* inhalational challenge. *Antimicrob. Agents Chemother.* **2023**, *67* (5), e0138122. DOI: 10.1128/aac.01381-22.
- (379) Taylor, S. N.; Marrazzo, J.; Batteiger, B. E.; Hook, E. W., 3rd; Sena, A. C.; Long, J.; Wierzbicki, M. R.; Kwak, H.; Johnson, S. M.; Lawrence, K.; Mueller, J. Single-dose zoliflodacin (ETX0914) for treatment of urogenital gonorrhea. *N. Engl. J. Med.* **2018**, *379* (19), 1835-1845. DOI: 10.1056/NEJMoa1706988.
- (380) Bradford, P. A.; Miller, A. A.; O'Donnell, J.; Mueller, J. P. Zoliflodacin: an oral spiropyrimidinetrione antibiotic for the treatment of *Neisseria gonorrhoeae*, including multi-drug-resistant isolates. *ACS Infect. Dis.* **2020**, *6* (6), 1332-1345. DOI: 10.1021/acsinfecdis.0c00021.
- (381) Jacobsson, S.; Golparian, D.; Alm, R. A.; Huband, M.; Mueller, J.; Jensen, J. S.; Ohnishi, M.; Unemo, M. High *in vitro* activity of the novel spiropyrimidinetrione AZD0914, a DNA gyrase inhibitor, against multidrug-resistant *Neisseria gonorrhoeae* isolates suggests a new effective option for oral treatment of gonorrhea. *Antimicrob. Agents Chemother.* **2014**, *58* (9), 5585-5588. DOI: 10.1128/AAC.03090-14.
- (382) Alm, R. A.; Lahiri, S. D.; Kutschke, A.; Otterson, L. G.; McLaughlin, R. E.; Whiteaker, J. D.; Lewis, L. A.; Su, X.; Huband, M. D.; Gardner, H.; Mueller, J. P. Characterization of the novel DNA gyrase inhibitor AZD0914: low resistance potential and lack of cross-resistance in *Neisseria gonorrhoeae*. *Antimicrob. Agents Chemother.* **2015**, *59* (3), 1478-1486. DOI: 10.1128/AAC.04456-14.
- (383) Huband, M. D.; Bradford, P. A.; Otterson, L. G.; Basarab, G. S.; Kutschke, A. C.; Giacobbe, R. A.; Patey, S. A.; Alm, R. A.; Johnstone, M. R.; Potter, M. E.; Miller, P. F.; Mueller, J. P. *In vitro* antibacterial activity of AZD0914, a new spiropyrimidinetrione DNA gyrase/topoisomerase inhibitor with potent activity against Gram-positive, fastidious Gram-negative, and atypical bacteria. *Antimicrob. Agents Chemother.* **2015**, *59* (1), 467-474. DOI: 10.1128/AAC.04124-14.
- (384) Unemo, M.; Ringlander, J.; Wiggins, C.; Fredlund, H.; Jacobsson, S.; Cole, M. High *in vitro* susceptibility to the novel spiropyrimidinetrione ETX0914 (AZD0914) among 873 contemporary clinical *Neisseria gonorrhoeae* isolates from 21 European countries from 2012 to 2014. *Antimicrob. Agents Chemother.* **2015**, *59* (9), 5220-5225. DOI: 10.1128/AAC.00786-15.
- (385) Papp, J. R.; Lawrence, K.; Sharpe, S.; Mueller, J.; Kirkcaldy, R. D. *In vitro* growth of multidrug-resistant *Neisseria gonorrhoeae* isolates is inhibited by ETX0914, a novel spiropyrimidinetrione. *Int. J. Antimicrob. Agents* **2016**, *48* (3), 328-330. DOI: 10.1016/j.ijantimicag.2016.05.018.



- (386) Unemo, M.; Ahlstrand, J.; Sanchez-Buso, L.; Day, M.; Aanensen, D.; Golparian, D.; Jacobsson, S.; Cole, M. J.; European Collaborative, G. High susceptibility to zoliflodacin and conserved target (GyrB) for zoliflodacin among 1209 consecutive clinical *Neisseria gonorrhoeae* isolates from 25 European countries, 2018. *J. Antimicrob. Chemother.* **2021**, *76* (5), 1221-1228. DOI: 10.1093/jac/dkab024.
- (387) Byl, J. A. W.; Mueller, R.; Bax, B.; Basarab, G. S.; Chibale, K.; Osheroff, N. A series of spiropyrimidinetriones that enhances DNA cleavage mediated by *Mycobacterium tuberculosis* gyrase. *ACS Infect. Dis.* **2023**, *9* (3), 706-715. DOI: 10.1021/acsinfecdis.3c00012.
- (388) Basarab, G. S.; Doig, P.; Eyermann, C. J.; Galullo, V.; Kern, G.; Kimzey, A.; Kutschke, A.; Morningstar, M.; Schuck, V.; Vishwanathan, K.; Zhou, F.; Gowravaram, M.; Hauck, S. Antibacterial spiropyrimidinetriones with N-linked azole substituents on a benzisoxazole scaffold targeting DNA gyrase. *J. Med. Chem.* **2020**, *63* (20), 11882-11901. DOI: 10.1021/acs.jmedchem.0c01100.
- (389) Govender, P.; Muller, R.; Singh, K.; Reddy, V.; Eyermann, C. J.; Fienberg, S.; Ghorpade, S. R.; Koekemoer, L.; Myrick, A.; Schnappinger, D.; Engelhart, C.; Meshanni, J.; Byl, J. A. W.; Osheroff, N.; Singh, V.; Chibale, K.; Basarab, G. S. Spiropyrimidinetrione DNA gyrase inhibitors with potent and selective antituberculosis activity. *J. Med. Chem.* **2022**, *65* (9), 6903-6925. DOI: 10.1021/acs.jmedchem.2c00266.
- (390) Basarab, G. S.; Ghorpade, S.; Gibhard, L.; Mueller, R.; Njoroge, M.; Peton, N.; Govender, P.; Massoudi, L. M.; Robertson, G. T.; Lenaerts, A. J.; Boshoff, H. I.; Joerss, D.; Parish, T.; Durand-Reville, T. F.; Perros, M.; Singh, V.; Chibale, K. Spiropyrimidinetriones: a class of DNA gyrase inhibitors with activity against *Mycobacterium tuberculosis* and without cross-resistance to fluoroquinolones. *Antimicrob. Agents Chemother.* **2022**, *66* (4), e0219221. DOI: 10.1128/aac.02192-21.
- (391) Collins, J. A.; Osheroff, N. Gyrase and topoisomerase IV: recycling old enzymes for new antibacterials to overcome fluoroquinolone resistance. *ACS Infect. Dis.* **2024**, in press.
- (392) Collins, J. A.; Osheroff, N. 1,2-Naphthoquinone as a poison of human type II topoisomerases. *Chem. Res. Toxicol.* **2021**, *34* (4), 1082-1090. DOI: 10.1021/acs.chemrestox.0c00492.
- (393) Byl, J. A.; Fortune, J. M.; Burden, D. A.; Nitiss, J. L.; Utsugi, T.; Yamada, Y.; Osheroff, N. DNA topoisomerases as targets for the anticancer drug TAS-103: primary cellular target and DNA cleavage enhancement. *Biochemistry* **1999**, *38* (47), 15573-15579. DOI: 10.1021/bi991791o.
- (394) Englund, P. T. The replication of kinetoplast DNA networks in *Crithidia fasciculata*. *Cell* **1978**, *14* (1), 157-168. DOI: 10.1016/0092-8674(78)90310-0.
- (395) Malik, M.; Marks, K. R.; Mustaev, A.; Zhao, X.; Chavda, K.; Kerns, R. J.; Drlica, K. Fluoroquinolone and quinazolinone activities against wild-type and gyrase mutant strains of *Mycobacterium smegmatis*. *Antimicrob. Agents Chemother.* **2011**, *55* (5), 2335-2343. DOI: 10.1128/AAC.00033-11.
- (396) Worland, S. T.; Wang, J. C. Inducible overexpression, purification, and active site mapping of DNA topoisomerase II from the yeast *Saccharomyces cerevisiae*. *J. Biol. Chem.* **1989**, *264* (8), 4412-4416.
- (397) Kingma, P. S.; Greider, C. A.; Osheroff, N. Spontaneous DNA lesions poison human topoisomerase II $\alpha$  and stimulate cleavage proximal to leukemic 11q23 chromosomal breakpoints. *Biochemistry* **1997**, *36* (20), 5934-5939.
- (398) Biersack, H.; Jensen, S.; Gromova, I.; Nielsen, I.; Westergaard, O.; Andersen, A. Active heterodimers are formed from human DNA topoisomerase II $\alpha$  and II $\beta$  isoforms. *Proc. Natl. Acad. Sci. U.S.A.* **1996**, *93*, 8288-8293.
- (399) Fortune, J. M.; Osheroff, N. Merbarone inhibits the catalytic activity of human topoisomerase II $\alpha$  by blocking DNA cleavage. *J. Biol. Chem.* **1998**, *273* (28), 17643-17650.

- (400) Gentry, A. C.; Pitts, S. L.; Jablonsky, M. J.; Bailly, C.; Graves, D. E.; Osheroff, N. Interactions between the etoposide derivative F14512 and human type II topoisomerases: implications for the C4 spermine moiety in promoting enzyme-mediated DNA cleavage. *Biochemistry* **2011**, *50* (15), 3240-3249. DOI: 10.1021/bi200094z.
- (401) Osheroff, N.; Zechiedrich, E. L. Calcium-promoted DNA cleavage by eukaryotic topoisomerase II: trapping the covalent enzyme-DNA complex in an active form. *Biochemistry* **1987**, *26*, 4303-4309.
- (402) Osheroff, N. Effect of antineoplastic agents on the DNA cleavage/religation reaction of eukaryotic topoisomerase II: inhibition of DNA religation by etoposide. *Biochemistry* **1989**, *28* (15), 6157-6160.
- (403) Dong, S.; McPherson, S. A.; Wang, Y.; Li, M.; Wang, P.; Turnbough, C. L., Jr.; Pritchard, D. G. Characterization of the enzymes encoded by the anthrose biosynthetic operon of *Bacillus anthracis*. *J. Bacteriol.* **2010**, *192* (19), 5053-5062. DOI: 10.1128/JB.00568-10.
- (404) Babula, P.; Adam, V.; Havel, L.; Kizek, R. Noteworthy secondary metabolites naphthoquinones - their occurrence, pharmacological properties and analysis. *Curr. Pharm. Anal.* **2009**, *5* (1), 47-68. DOI: Doi 10.2174/157341209787314936.
- (405) Kumagai, Y.; Shinkai, Y.; Miura, T.; Cho, A. K. The chemical biology of naphthoquinones and its environmental implications. *Annu. Rev. Pharmacol. Toxicol.* **2012**, *52*, 221-247. DOI: 10.1146/annurev-pharmtox-010611-134517.
- (406) Soares, A. G.; Muscara, M. N.; Costa, S. K. P. Molecular mechanism and health effects of 1,2-naphthoquinone. *EXCLI J.* **2020**, *19*, 707-717. DOI: 10.17179/excli2020-2153.
- (407) Cho, A. K.; Di Stefano, E.; You, Y.; Rodriguez, C. E.; Schmitz, D. A.; Kumagai, Y.; Miguel, A. H.; Eiguren-Fernandez, A.; Kobayashi, T.; Avol, E.; Froines, J. R. Determination of four quinones in diesel exhaust particles, SRM 1649a, an atmospheric PM2.5. *Aerosol. Sci. Tech.* **2004**, *38*, 68-81. DOI: 10.1080/02786820390229471.
- (408) Chung, M. Y.; Lazaro, R. A.; Lim, D.; Jackson, J.; Lyon, J.; Rendulic, D.; Hasson, A. S. Aerosol-borne quinones and reactive oxygen species generation by particulate matter extracts. *Environ. Sci. Technol.* **2006**, *40* (16), 4880-4886. DOI: 10.1021/es0515957.
- (409) Jakober, C. A.; Robert, M. A.; Riddle, S. G.; Destailats, H.; Charles, M. J.; Green, P. G.; Kleeman, M. J. Carbonyl emissions from gasoline and diesel motor vehicles. *Environ. Sci. Technol.* **2008**, *42* (13), 4697-4703. DOI: 10.1021/es7029174.
- (410) Shinyashiki, M.; Eiguren-Fernandez, A.; Schmitz, D. A.; Di Stefano, E.; Li, N.; Linak, W. P.; Cho, S. H.; Froines, J. R.; Cho, A. K. Electrophilic and redox properties of diesel exhaust particles. *Environ. Res.* **2009**, *109* (3), 239-244. DOI: 10.1016/j.envres.2008.12.008.
- (411) Kroner, R.; Kleber, E.; Elstner, E. F. Cataract induction by 1,2-naphthoquinone. II. Mechanism of hydrogenperoxide formation and inhibition by iodide. *Z. Naturforsch. C. J. Biosci.* **1991**, *46* (3-4), 285-290. DOI: 10.1515/znc-1991-3-420.
- (412) Kleber, E.; Kroner, R.; Elstner, E. F. Cataract induction by 1,2-naphthoquinone. I. Studies on the redox properties of bovine lens proteins. *Z. Naturforsch. C. J. Biosci.* **1991**, *46* (3-4), 280-284. DOI: 10.1515/znc-1991-3-419.
- (413) Wilson, A. S.; Davis, C. D.; Williams, D. P.; Buckpitt, A. R.; Pirmohamed, M.; Park, B. K. Characterisation of the toxic metabolite(s) of naphthalene. *Toxicology* **1996**, *114* (3), 233-242. DOI: 10.1016/s0300-483x(96)03515-9.
- (414) Inoue, K.; Takano, H.; Hiyoshi, K.; Ichinose, T.; Sadakane, K.; Yanagisawa, R.; Tomura, S.; Kumagai, Y. Naphthoquinone enhances antigen-related airway inflammation in mice. *Eur. Respir. J.* **2007**, *29* (2), 259-267. DOI: 10.1183/09031936.00033106.
- (415) Inoue, K.; Takano, H.; Ichinose, T.; Tomura, S.; Yanagisawa, R.; Sakurai, M.; Sumi, D.; Cho, A. K.; Hiyoshi, K.; Kumagai, Y. Effects of naphthoquinone on airway responsiveness in the presence or absence of antigen in mice. *Arch. Toxicol.* **2007**, *81* (8), 575-581. DOI: 10.1007/s00204-007-0186-5.

- (416) Nishina, T.; Deguchi, Y.; Miura, R.; Yamazaki, S.; Shinkai, Y.; Kojima, Y.; Okumura, K.; Kumagai, Y.; Nakano, H. Critical contribution of nuclear factor erythroid 2-related factor 2 (NRF2) to electrophile-induced interleukin-11 production. *J. Biol. Chem.* **2017**, *292* (1), 205-216. DOI: 10.1074/jbc.M116.744755.
- (417) Sheng, K.; Lu, J. Typical airborne quinones modulate oxidative stress and cytokine expression in lung epithelial A549 cells. *J. Environ. Sci. Health. A Tox. Hazard Subst. Environ. Eng.* **2017**, *52* (2), 127-134. DOI: 10.1080/10934529.2016.1237127.
- (418) Frydman, B.; Marton, L. J.; Sun, J. S.; Neder, K.; Witiak, D. T.; Liu, A. A.; Wang, H. M.; Mao, Y.; Wu, H. Y.; Sanders, M. M.; Liu, L. F. Induction of DNA topoisomerase II-mediated DNA cleavage by  $\beta$ -lapachone and related naphthoquinones. *Cancer Res.* **1997**, *57* (4), 620-627.
- (419) Wang, H.; Mao, Y.; Chen, A. Y.; Zhou, N.; LaVoie, E. J.; Liu, L. F. Stimulation of topoisomerase II-mediated DNA damage *via* a mechanism involving protein thiolation. *Biochemistry* **2001**, *40* (11), 3316-3323.
- (420) Lindsey, R. H., Jr.; Bromberg, K. D.; Felix, C. A.; Osheroff, N. 1,4-Benzoquinone is a topoisomerase II poison. *Biochemistry* **2004**, *43* (23), 7563-7574.
- (421) Bender, R. P.; Lehmler, H. J.; Robertson, L. W.; Ludewig, G.; Osheroff, N. Polychlorinated biphenyl quinone metabolites poison human topoisomerase II $\alpha$ : altering enzyme function by blocking the N-terminal protein gate. *Biochemistry* **2006**, *45* (33), 10140-10152. DOI: 10.1021/bi0524666.
- (422) Bandele, O. J.; Osheroff, N. Bioflavonoids as poisons of human topoisomerase II $\alpha$  and II $\beta$ . *Biochemistry* **2007**, *46* (20), 6097-6108. DOI: 10.1021/bi7000664.
- (423) Bandele, O. J.; Clawson, S. J.; Osheroff, N. Dietary polyphenols as topoisomerase II poisons: B ring and C ring substituents determine the mechanism of enzyme-mediated DNA cleavage enhancement. *Chem. Res. Toxicol.* **2008**, *21* (6), 1253-1260. DOI: 10.1021/tx8000785.
- (424) Ketron, A. C.; Gordon, O. N.; Schneider, C.; Osheroff, N. Oxidative metabolites of curcumin poison human type II topoisomerases. *Biochemistry* **2013**, *52* (1), 221-227. DOI: 10.1021/bi3014455 (accessed 2013/10/03).
- (425) Ashley, R. E.; Osheroff, N. Natural products as topoisomerase II poisons: effects of thymoquinone on DNA cleavage mediated by human topoisomerase II $\alpha$ . *Chem. Res. Toxicol.* **2014**, *27* (5), 787-793. DOI: 10.1021/tx400453v.
- (426) Vann, K. R.; Sedgeman, C. A.; Gopas, J.; Golan-Goldhirsh, A.; Osheroff, N. Effects of olive metabolites on DNA cleavage mediated by human type II topoisomerases. *Biochemistry* **2015**, *54* (29), 4531-4541. DOI: 10.1021/acs.biochem.5b00162.
- (427) Gibson, E. G.; King, M. M.; Mercer, S. L.; Deweese, J. E. Two-mechanism model for the interaction of etoposide quinone with topoisomerase II $\alpha$ . *Chem. Res. Toxicol.* **2016**, *29* (9), 1541-1548. DOI: 10.1021/acs.chemrestox.6b00209.
- (428) Bandele, O. J.; Osheroff, N. (-)-Epigallocatechin gallate, a major constituent of green tea, poisons human type II topoisomerases. *Chem. Res. Toxicol.* **2008**, *21* (4), 936-943.
- (429) Gurbani, D.; Kukshal, V.; Laubenthal, J.; Kumar, A.; Pandey, A.; Tripathi, S.; Arora, A.; Jain, S. K.; Ramachandran, R.; Anderson, D.; Dhawan, A. Mechanism of inhibition of the ATPase domain of human topoisomerase II $\alpha$  by 1,4-benzoquinone, 1,2-naphthoquinone, 1,4-naphthoquinone, and 9,10-phenanthroquinone. *Toxicol. Sci.* **2012**, *126* (2), 372-390. DOI: 10.1093/toxsci/kfr345.
- (430) Errington, F.; Willmore, E.; Leontiou, C.; Tilby, M. J.; Austin, C. A. Differences in the longevity of topo II $\alpha$  and topo II $\beta$  drug-stabilized cleavable complexes and the relationship to drug sensitivity. *Cancer Chemother. Pharmacol.* **2004**, *53* (2), 155-162. DOI: 10.1007/s00280-003-0701-1.

- (431) Bandele, O. J.; Osheroff, N. The efficacy of topoisomerase II-targeted anticancer agents reflects the persistence of drug-induced cleavage complexes in cells. *Biochemistry* **2008**, *47* (45), 11900-11908. DOI: 10.1021/bi800981j.
- (432) Osheroff, N.; Shelton, E. R.; Brutlag, D. L. DNA topoisomerase II from *Drosophila melanogaster*. Relaxation of supercoiled DNA. *J. Biol. Chem.* **1983**, *258* (15), 9536-9543. From Nlm.
- (433) Ketron, A. C.; Osheroff, N. Phytochemicals as anticancer and chemopreventive topoisomerase II poisons. *Phytochem. Rev.* **2014**, *13* (1), 19-35. DOI: 10.1007/s11101-013-9291-7.
- (434) Bender, R. P.; Ham, A. J.; Osheroff, N. Quinone-induced enhancement of DNA cleavage by human topoisomerase II $\alpha$ : adduction of cysteine residues 392 and 405. *Biochemistry* **2007**, *46* (10), 2856-2864. DOI: 10.1021/bi062017l.
- (435) Bender, R. P.; Osheroff, N. Mutation of cysteine residue 455 to alanine in human topoisomerase II $\alpha$  confers hypersensitivity to quinones: enhancing DNA scission by closing the N-terminal protein gate. *Chem. Res. Toxicol.* **2007**, *20* (6), 975-981. DOI: 10.1021/tx700062t.
- (436) Lin, R. K.; Zhou, N.; Lyu, Y. L.; Tsai, Y. C.; Lu, C. H.; Kerrigan, J.; Chen, Y. T.; Guan, Z.; Hsieh, T. S.; Liu, L. F. Dietary isothiocyanate-induced apoptosis via thiol modification of DNA topoisomerase II $\alpha$ . *J. Biol. Chem.* **2011**, *286* (38), 33591-33600. DOI: M111.258137 [pii] 10.1074/jbc.M111.258137 [doi] From Nlm.
- (437) Mondrala, S.; Eastmond, D. A. Topoisomerase II inhibition by the bioactivated benzene metabolite hydroquinone involves multiple mechanisms. *Chemico-biological interactions* **2010**, *184* (1), 259-268. DOI: <http://dx.doi.org/10.1016/j.cbi.2009.12.023>.
- (438) Jacob, D. A.; Mercer, S. L.; Osheroff, N.; Deweese, J. E. Etoposide quinone is a redox-dependent topoisomerase II poison. *Biochemistry* **2011**, *50* (25), 5660-5667. DOI: 10.1021/bi200438m [doi] From Nlm.
- (439) Dalvie, E. D.; Gopas, J.; Golan-Goldhirsh, A.; Osheroff, N. 6,6'-Dihydroxythiobinupharidine as a poison of human type II topoisomerases. *Bioorg. Med. Chem. Lett.* **2019**, *29* (15), 1881-1885. DOI: 10.1016/j.bmcl.2019.06.003.
- (440) Bender, R. P.; Lindsey, R. H., Jr.; Burden, D. A.; Osheroff, N. N-acetyl-*p*-benzoquinone imine, the toxic metabolite of acetaminophen, is a topoisomerase II poison. *Biochemistry* **2004**, *43* (12), 3731-3739. DOI: 10.1021/bi036107r.
- (441) Lindsey, R. H., Jr.; Pendleton, M.; Ashley, R. E.; Mercer, S. L.; Deweese, J. E.; Osheroff, N. Catalytic core of human topoisomerase II $\alpha$ : insights into enzyme-DNA interactions and drug mechanism. *Biochemistry* **2014**, *53* (41), 6595-65602. DOI: 10.1021/bi5010816.
- (442) Lindsey, R. H., Jr.; Bender, R. P.; Osheroff, N. Effects of benzene metabolites on DNA cleavage mediated by human topoisomerase II $\alpha$ : 1,4-hydroquinone is a topoisomerase II poison. *Chem. Res. Toxicol.* **2005**, *18* (4), 761-770. DOI: 10.1021/tx049659z.
- (443) Leroy, D.; Kajava, A. V.; Frei, C.; Gasser, S. M. Analysis of etoposide binding to subdomains of human DNA topoisomerase II $\alpha$  in the absence of DNA. *Biochemistry* **2001**, *40* (6), 1624-1634. DOI: 10.1021/bi0019141.
- (444) Vilain, N.; Tsai-Pflugfelder, M.; Benoit, A.; Gasser, S. M.; Leroy, D. Modulation of drug sensitivity in yeast cells by the ATP-binding domain of human DNA topoisomerase II $\alpha$ . *Nucleic Acids Res.* **2003**, *31* (19), 5714-5722. DOI: 10.1093/nar/gkg737.
- (445) Montecucco, A.; Zanetta, F.; Biamonti, G. Molecular mechanisms of etoposide. *EXCLI J.* **2015**, *14*, 95-108. DOI: 10.17179/excli2015-561.
- (446) Unemo, M.; Shafer, W. M. Antimicrobial resistance in *Neisseria gonorrhoeae* in the 21st century: past, evolution, and future. *Clin. Microbiol. Rev.* **2014**, *27* (3), 587-613. DOI: 10.1128/CMR.00010-14.

- (447) Centers for Disease Control and Prevention. Sexually transmitted diseases surveillance 2021. *Neisseria gonorrhoeae* - prevalence of tetracycline penicillin or ciprofloxacin resistance or elevate., Ed.; U.S. Department of Health and Human Services: Atlanta, GA, 2023.
- (448) Centers for Disease Control and Prevention. *Antibiotic resistance threats in the United States, 2019*; U.S. Department of Health and Human Services, Atlanta, GA, 2019. DOI: 10.15620/cdc:82532.
- (449) Koebler, J. *World Health Organization warns gonorrhea could join HIV as 'uncurable'*. U.S. News and World Report, 2012. <https://www.usnews.com/news/articles/2012/06/06/world-health-organization-warns-gonorrhea-could-join-hiv-as-uncurable-> (accessed November 12, 2023).
- (450) Gransden, W. R.; Warren, C. A.; Phillips, I.; Hodges, M.; Barlow, D. Decreased susceptibility of *Neisseria gonorrhoeae* to ciprofloxacin. *Lancet* **1990**, 335 (8680), 51. DOI: 10.1016/0140-6736(90)90177-7.
- (451) Tapsall, J. W.; Shultz, T. R.; Lovett, R.; Munro, R. Failure of 500 mg ciprofloxacin therapy in male urethral gonorrhoea. *Med. J. Aust.* **1992**, 156 (2), 143. DOI: 10.5694/j.1326-5377.1992.tb126457.x.
- (452) Birley, H.; McDonald, P.; Carey, P.; Fletcher, J. High level ciprofloxacin resistance in *Neisseria gonorrhoeae*. *Genitourin. Med.* **1994**, 70 (4), 292-293. DOI: 10.1136/sti.70.4.292.
- (453) Centers for Disease Control and Prevention. Fluoroquinolone resistance in *Neisseria gonorrhoeae*--Colorado and Washington, 1995. *MMWR Morb. Mortal. Wkly Rep.* **1995**, 44 (41), 761-774.
- (454) Kam, K. M.; Wong, P. W.; Cheung, M. M.; Ho, N. K. Detection of quinolone-resistant *Neisseria gonorrhoeae*. *J. Clin. Microbiol.* **1996**, 34 (6), 1462-1464. DOI: 10.1128/jcm.34.6.1462-1464.1996.
- (455) Hooper, D. C. Emerging mechanisms of fluoroquinolone resistance. *Emerg. Infect. Dis.* **2001**, 7 (2), 337-341. DOI: 10.3201/eid0702.010239.
- (456) Deguchi, T.; Yasuda, M.; Nakano, M.; Ozeki, S.; Ezaki, T.; Saito, I.; Kawada, Y. Quinolone-resistant *Neisseria gonorrhoeae*: correlation of alterations in the GyrA subunit of DNA gyrase and the ParC subunit of topoisomerase IV with antimicrobial susceptibility profiles. *Antimicrob. Agents Chemother.* **1996**, 40 (4), 1020-1023. DOI: 10.1128/AAC.40.4.1020.
- (457) Trees, D. L.; Sandul, A. L.; Peto-Mesola, V.; Aplasca, M. R.; Leng, H. B.; Whittington, W. L.; Knapp, J. S. Alterations within the quinolone resistance-determining regions of GyrA and ParC of *Neisseria gonorrhoeae* isolated in the Far East and the United States. *Int. J. Antimicrob. Agents* **1999**, 12 (4), 325-332. DOI: 10.1016/s0924-8579(99)00081-3.
- (458) Tanaka, M.; Nakayama, H.; Haraoka, M.; Saika, T. Antimicrobial resistance of *Neisseria gonorrhoeae* and high prevalence of ciprofloxacin-resistant isolates in Japan, 1993 to 1998. *J. Clin. Microbiol.* **2000**, 38 (2), 521-525. DOI: 10.1128/JCM.38.2.521-525.2000.
- (459) Shultz, T. R.; Tapsall, J. W.; White, P. A. Correlation of in vitro susceptibilities to newer quinolones of naturally occurring quinolone-resistant *Neisseria gonorrhoeae* strains with changes in GyrA and ParC. *Antimicrob Agents Chemother* **2001**, 45 (3), 734-738. DOI: 10.1128/AAC.45.3.734-738.2001.
- (460) Kivata, M. W.; Mbuchi, M.; Eyase, F. L.; Bulimo, W. D.; Kyanya, C. K.; Oundo, V.; Muriithi, S. W.; Andagalu, B.; Mbinda, W. M.; Soge, O. O.; McClelland, R. S.; Sang, W.; Mancuso, J. D. *gyrA* and *parC* mutations in fluoroquinolone-resistant *Neisseria gonorrhoeae* isolates from Kenya. *BMC Microbiol.* **2019**, 19 (1), 76. DOI: 10.1186/s12866-019-1439-1.
- (461) Hall, C. L.; Harrison, M. A.; Pond, M. J.; Chow, C.; Harding-Esch, E. M.; Sadiq, S. T. Genotypic determinants of fluoroquinolone and macrolide resistance in *Neisseria gonorrhoeae*. *Sex. Health* **2019**, 16 (5), 479-487. DOI: 10.1071/SH18225.
- (462) Giles, J. A.; Falconio, J.; Yuenger, J. D.; Zenilman, J. M.; Dan, M.; Bash, M. C. Quinolone resistance-determining region mutations and por type of *Neisseria gonorrhoeae* isolates:

- resistance surveillance and typing by molecular methodologies. *J. Infect. Dis.* **2004**, *189* (11), 2085-2093. DOI: 10.1086/386312.
- (463) Tran, T. P.; Ellsworth, E. L.; Sanchez, J. P.; Watson, B. M.; Stier, M. A.; Showalter, H. D.; Domagala, J. M.; Shapiro, M. A.; Joannides, E. T.; Gracheck, S. J.; Nguyen, D. Q.; Bird, P.; Yip, J.; Sharadendu, A.; Ha, C.; Ramezani, S.; Wu, X.; Singh, R. Structure-activity relationships of 3-aminoquinazolinones, a new class of bacterial type-2 topoisomerase (DNA gyrase and topo IV) inhibitors. *Bioorg. Med. Chem. Lett.* **2007**, *17* (5), 1312-1320. DOI: 10.1016/j.bmcl.2006.12.005.
- (464) German, N.; Malik, M.; Rosen, J. D.; Drlica, K.; Kerns, R. J. Use of gyrase resistance mutants to guide selection of 8-methoxy-quinazoline-2,4-diones. *Antimicrob. Agents Chemother.* **2008**, *52* (11), 3915-3921. DOI: 10.1128/AAC.00330-08.
- (465) Mustaev, A.; Malik, M.; Zhao, X.; Kurepina, N.; Luan, G.; Oppegard, L. M.; Hiasa, H.; Marks, K. R.; Kerns, R. J.; Berger, J. M.; Drlica, K. Fluoroquinolone-gyrase-DNA complexes: two modes of drug binding. *J. Biol. Chem.* **2014**, *289* (18), 12300-12312. DOI: 10.1074/jbc.M113.529164.
- (466) Aldred, K. J.; Schwanz, H. A.; Li, G.; McPherson, S. A.; Turnbough, C. L.; Kerns, R. J.; Osheroff, N. Overcoming target-mediated quinolone resistance in topoisomerase IV by introducing metal-ion-independent drug-enzyme interactions. *ACS Chem. Biol.* **2013**, *2* (12), 2660-2668. DOI: 10.1021/cb400592n.
- (467) Drlica, K.; Mustaev, A.; Towle, T. R.; Luan, G.; Kerns, R. J.; Berger, J. M. Bypassing fluoroquinolone resistance with quinazolinones: studies of drug-gyrase-DNA complexes having implications for drug design. *ACS Chem. Biol.* **2014**, *9* (12), 2895-2904. DOI: 10.1021/cb500629k.
- (468) Pan, X. S.; Gould, K. A.; Fisher, L. M. Probing the differential interactions of quinazolinone PD 0305970 and quinolones with gyrase and topoisomerase IV. *Antimicrob. Agents Chemother.* **2009**, *53* (9), 3822-3831. DOI: 10.1128/AAC.00113-09.
- (469) Lindback, E.; Rahman, M.; Jalal, S.; Wretling, B. Mutations in *gyrA*, *gyrB*, *parC*, and *parE* in quinolone-resistant strains of *Neisseria gonorrhoeae*. *APMIS* **2002**, *110* (9), 651-657. DOI: 10.1034/j.1600-0463.2002.1100909.x.
- (470) Ng, L. K.; Sawatzky, P.; Martin, I. E.; Booth, S. Characterization of ciprofloxacin resistance in *Neisseria gonorrhoeae* isolates in Canada. *Sex. Transm. Dis.* **2002**, *29* (12), 780-788. DOI: 10.1097/00007435-200212000-00008.
- (471) Starnino, S.; Dal Conte, I.; Matteelli, A.; Galluppi, E.; Cusini, M.; Di Carlo, A.; Delmonte, S.; Stefanelli, P. Trend of ciprofloxacin resistance in *Neisseria gonorrhoeae* strains isolated in Italy and analysis of the molecular determinants. *Diagn. Microbiol. Infect. Dis.* **2010**, *67* (4), 350-354. DOI: 10.1016/j.diagmicrobio.2010.03.001.
- (472) Calado, J.; Castro, R.; Lopes, A.; Campos, M. J.; Rocha, M.; Pereira, F. Antimicrobial resistance and molecular characteristics of *Neisseria gonorrhoeae* isolates from men who have sex with men. *Int. J. Infect. Dis.* **2019**, *79*, 116-122. DOI: 10.1016/j.ijid.2018.10.030.
- (473) GlaxoSmithKline. EAGLE-2 and EAGLE-3 phase III trials for gepotidacin stopped early for efficacy following pre-planned interim analysis by Independent Data Monitoring Committee. 2022.
- (474) GlaxoSmithKline. GSK announces positive headline results from EAGLE-1 phase III trial for gepotidacin in uncomplicated urogenital gonorrhoea (GC). 2024. <https://www.gsk.com/en-gb/media/press-releases/gsk-announces-positive-headline-results-from-eagle-1-phase-iii-trial-for-gepotidacin-in-uncomplicated-urogenital-gonorrhoea-gc/> (accessed 2024 February 28).
- (475) Mitton-Fry, M. J.; Brickner, S. J.; Hamel, J. C.; Brennan, L.; Casavant, J. M.; Chen, M.; Chen, T.; Ding, X. Y.; Driscoll, J.; Hardink, J.; Hoang, T.; Hua, E. B.; Huband, M. D.; Maloney, M.; Marfat, A.; McCurdy, S. P.; McLeod, D.; Plotkin, M.; Reilly, U.; Robinson, S.; Schafer, J.; Shepard, R. M.; Smith, J. F.; Stone, G. G.; Subramanyam, C.; Yoon, K.; Yuan,



- W.; Zaniewski, R. P.; Zook, C. Novel quinoline derivatives as inhibitors of bacterial DNA gyrase and topoisomerase IV. *Bioorg. Med. Chem. Lett.* **2013**, 23 (10), 2955-2961. DOI: 10.1016/j.bmcl.2013.03.047.
- (476) Li, L.; Okumu, A. A.; Nolan, S.; English, A.; Vibhute, S.; Lu, Y.; Hervert-Thomas, K.; Seffernick, J. T.; Azap, L.; Cole, S. L.; Shinabarger, D.; Koeth, L. M.; Lindert, S.; Yalowich, J. C.; Wozniak, D. J.; Mitton-Fry, M. J. 1,3-dioxane-linked bacterial topoisomerase inhibitors with enhanced antibacterial activity and reduced hERG inhibition. *ACS Infect. Dis.* **2019**, 5 (7), 1115-1128. DOI: 10.1021/acsinfectdis.8b00375.
- (477) Felix, C. A.; Kolaris, C. P.; Osheroff, N. Topoisomerase II and the etiology of chromosomal translocations. *DNA Repair* **2006**, 5 (9-10), 1093-1108. DOI: 10.1016/j.dnarep.2006.05.031.
- (478) Basarab, G. S.; Brassil, P.; Doig, P.; Galullo, V.; Haimes, H. B.; Kern, G.; Kutschke, A.; McNulty, J.; Schuck, V. J.; Stone, G.; Gowravaram, M. Novel DNA gyrase inhibiting spiropyrimidinetriones with a benzisoxazole scaffold: SAR and in vivo characterization. *J. Med. Chem.* **2014**, 57 (21), 9078-9095. DOI: 10.1021/jm501174m.
- (479) Basarab, G. S.; Doig, P.; Galullo, V.; Kern, G.; Kimzey, A.; Kutschke, A.; Newman, J. P.; Morningstar, M.; Mueller, J.; Otterson, L.; Vishwanathan, K.; Zhou, F.; Gowravaram, M. Discovery of novel DNA gyrase inhibiting spiropyrimidinetriones: benzisoxazole fusion with N-linked oxazolidinone substituents leading to a clinical candidate (ETX0914). *J. Med. Chem.* **2015**, 58 (15), 6264-6282. DOI: 10.1021/acs.jmedchem.5b00863.
- (480) O'Neill, J. *Antimicrobial resistance: tackling a crisis for the health and wealth of nations*; London, 2014.
- (481) Antimicrobial Resistance Collaborators. Global burden of bacterial antimicrobial resistance in 2019: a systematic analysis. *Lancet* **2022**, 399 (10325), 629-655. DOI: 10.1016/S0140-6736(21)02724-0.
- (482) Dalhoff, A. Global fluoroquinolone resistance epidemiology and implications for clinical use. *Interdiscip. Perspect. Infect. Dis.* **2012**, 2012, 976273. DOI: 10.1155/2012/976273.
- (483) Aedo, S.; Tse-Dinh, Y.-C. Isolation and quantitation of topoisomerase complexes accumulated on *Escherichia coli* chromosomal DNA. *Antimicrob. Agents Chemother.* **2012**, 56 (11), 5458-5464. DOI: 10.1128/aac.01182-12.